Spring 5-31-1984

Mathematical modeling of unsteady state photo-polymerization

Rong-Fa Liang
New Jersey Institute of Technology

MATHEMATICAL MODELING OF
UNSTEADY STATE PHOTO-POLYMERIZATION

BY

RONG-FA LIANG

Dissertation submitted to the Faculty of the Graduate School of the New Jersey Institute of Technology in partial fulfillment of the requirements for the degree of Doctor of Engineering Science

1984

APPROVAL SHEET

Title of Thesis:

MATHEMATICAL MODELING OF
UNSTEADY STATE PHOTO-POLYMERIZATION

Name of Candidate:

RONG-FA LIANG

Doctor of Engineering Science, 1984

Thesis and Abstract Approved:

________________________________ ____________

Dr. Ching-Rong Huang Date
Professor & Assistant Chairman
Department of Chemical Engineering

________________________________ ____________

Date

________________________________ ____________

Date

________________________________ ____________

Date

________________________________ ____________

Date

VITA

Name: Rong-Fa Liang

Degree and date to be conferred: Dr. Eng. Sc., 1984

Collegiate institutions attended	Dates	Degree	Dates of Degree
New Jersey Institute of Technology	1980	Ph.D.	May, 1984
University of Maine	1978	MS.	Dec, 1979
Chung Yuan University	1972	BE.	May, 1976

Major: Chemical Engineering

ABSTRACT

Title of Dissertation:

MATHEMATICAL MODELING OF
UNSTEADY STATE PHOTO-POLYMERIZATION

Rong-Fa Liang

Doctor of Engineering Science, 1984

Dissertation directed by:

Dr. Ching-Rong Huang

Professor & Assistant Chairman

Department of Chemical Engineering & Chemistry

Mathematical modeling of unsteady state photopolymerization in an isothermal batch reactor has been investigated. An analytical solution of the distribution of active polymers as a function of reaction time has been determined. It is verified that the quasi-stationary state approximation is valid in the photopolymerization process.

The free radical polymerization of styrene is forced periodically by on-off UV light regulation to the reactor. The effect of operating condition, the ratio of light-off period to light on/off period, on the polydispersity and molecular weight distribution are theoretically and numerically investigated. Significant broadening on molecular weight distribution can be obtained during the unsteady state process.

Experimental results of polydispersity are compared to a kinetic model of a nonuniformly initiated photopolymerization, which comprises a high dose rate region and a very low dose rate region. Good agreement is obtained between the model and experiments after fitting three parameters.

ACKNOWLEDGEMENTS

I wish to express my appreciation to my thesis advisor, Professor Ching-Rong Huang for his skillful guidance and valuable comments on my research. The author is also indebted to other committee members who have given comments of the manuscript.

Gratitude is also extended to my parents, Mr. and Mrs. Yuan-Tsuen Liang, and my wife, Kai-Wan, for their constant encouragement and moral support during my graduate studies.

TABLE OF CONTENTS

LIST OF TABLES

LIST OF FIGURES

Figure | Page

Figure Page

Figure Page

Figure		Page

CHAPTER 1

INTRODUCTION

The quasi-stationary state approximation (QSSA) for the reactive intermediate species, first introduced by Bodenstein and Lutkemeyer (1), has generally led to essential simplifications in the differential equations which describe the instantaneous behavior of reacting chemical species. In many cases, the use of this approximation has resulted in closed form analytical solutions for simple kinetic schemes which otherwise are mathematically tractable only by numerical techniques.

The errors incurred in free-radical chain addition polymerizations through the use of the popular QSSA are although severe, but fairly common. Biesenberger and Capinpin (2) have concluded that the proposed criteria are reasonably accurate and that in most known free-radical polymerizations only hindered termination might possibly lead to appreciable errors through application of the QSSA. The QSSA is valid virtually over the entire practical range of interest in a chain-addition polymerization from start to finish only when criteria $\sqrt{K_t(I)_o/K_i} >> 1$ and $K_t/K_p >> 1$ are satisfied. If either one is violated, then the QSSA does not apply.

Broadening of a molecular weight distribution (MWD) is of considerable importance. Billmeyer (3) has shown that of two polymers having the same weight average molecular weight the broader distribution material has a more pronounced shear rate-apparent viscosity relation, and the broader distribution material may be easier to process. Rodriguez (4) showed that the MWD has been important in many diverse applications including flow of melts and solutions, aging and weathering behavior, adhesion, and flocculation. Because of the difficulties involved in measuring a distribution in detail, one shortcut has been to postulate a reasonable mathematical form or model for the distribution and then evaluate the parameters from number and weight-average of polymerization. In general, such a model would give w_x, the weight fraction of x-mer, as a function of x, x_w, x_n and perhaps other parameters.

Thomas and Hagan (5) investigated the effect of MWD on the processing and mechanical properties of polystyrene. With samples taken from injection-molded sheets the narrow distribution was shown to have consistently higher tensile strengths than the broad distribution material. The broad distribution material also exhibited greater anisotropy at all of the molding temperatures. This was attributed to its greater melt elasticity. They also showed that, at constant molecular weight (MW), the rupture elongation of injection-molded polystyrene sheets is increased by narrowing the MWD. They also conducted creep tests at room temperature using a tensile load 5000 psi. Two materials which had the same MW were compared. The total strain in the broad distribution samples exceeded that of the narrow distribution material over most of the test. In addition, the average rupture time of the latter specimens was twice as long as that measured on the broad distribution samples.

Pezzin (6) found a small MWD effect because broadening the distribution tended to increase n when the strain-time relationship was expressed in terms of the Nutting equation: $\epsilon = kt^n$, where n is an empirical parameter independent of the applied load. Ross (7) investigated the effects of MW and MWD on polypropylene filaments. He found that the crystalline state of undrawn fibers could be correlated with extrusion temperature and MWD; fibers produced from broad distribution resins had a monoclinic structure while the narrow distribution resins gave paracrystalline fibers.

Sato and Ishizuka (8), in an extensive study showed that broad polypropylene samples had a slightly lower melting temperature than fractions with the same viscosity. Narrowing the MWD greatly increases the tear strength when comparisons are made at constant viscosity as shown by Wallach (9). Data show small increases in the heat distortion temperature when the MW is raised and the MWD is reduced (10). Limited data (11) showed that two bimodal narrow distribution polyethylene had much higher burst strengths than a low MW comparison sample which had an unusually broad MWD. Broadening the MWD increased the tensile modulus (12) of polyethylene when comparisons were made at a constant solution viscosity. This was presumably due to the fact that broadening the MWD at constant MW increases the per cent crystallinity of a material (13). Notched izod impact strength has been measured on compression-molded polyethylene fraction (14). The results showed that impact strength increases with MW at constant density. It also appeared to increase when the MWD was reduced because the impact strength of fractions was substantially higher than that measured on whole polymers. Van Schooten et al. (15) have also related the impact strength of polypropylene to MWD. A substantial effect of MWD on the stress cracking of polystyrene was observed (10) because, when comparisons were made at the same MW, it was found that the narrow distribution specimens generally lasted 10-100 times as long as the broad distribution samples.

Most of the work indicates that MW and MWD effects on the modulus and losses of amorphous polymers are quite significant in the rubbery region. Losses normally increased and modulus decreased when low MW or broad distribution materials were tested. Most investigators (17)(18) concluded that broad distributions usually decrease the fold resistance of low MW specimens when comparisons were made between fractions and blends. An MWD effect was noted by Grohn and Friedrich (19) because, at constant viscosity, the flex life of broad distribution samples was shorter than the flex life of fractions.

The molecular weight and the nature of molecular weight distribution significantly affect the physical and rheological properties of a polymer. In a continuous stirred-tank reactor, however, the MWD breadth is fixed by the conversion and the residence time of a reactor present. The effect of widening in MWD can be gotten through mixing polymer streams from different reactors. An alternate approach is to employ an unsteady process in the reactor itself to change the MWD. Cyclic operation of polymerization reactors, where one or more process inputs are intentionally varied periodically with time, can significantly enlarge the scope of available MWD's beyond those attainable at steady state.

Ray (20) examined the effects of periodic operation of both condensation and free-radical polymerization reactor under sinusoidal perturbations in monomer feed concentration. He has reported a narrowing of the MWD for a condensation polymerization scheme and a broadening of the MWD for a free-radical polymerization scheme, when compared with the steady state. Yu (21) simulated a periodically operated continuous stirred-tank reactor (CSTR) for the thermal polymerization of styrene and found the MWD to increase at low frequencies, but all effects were damped at higher frequencies because of the limited heat transfer relative to the thermal capacitance of commercial reactors. Lawrence and Vasudevan (22) considered the performance of a polymerization reactor in a very slow sinusoidal manner for both simple addition and combination-termination mechanisms. They have observed a broadening of the MWD for variations in either monomer or initiator feed compositions. Konopnicki and Kuester (23) developed a mechanism which includes transfer to both monomer and solvent as well as termination by combination and disproportionation. They examined the influence of non-isothermal operation and viscosity effects on the MWD of the polymer produced as well as induced sinusoidal and square-wave forcing functions on initiator feed concentrations and jacket temperature. The phenomena of gel-effect using correlations valid for solutions of viscosity less than thirty poise were considered in the mechanism. The patent disclosure of Claybaugh et al. (24) reports experimental data for cyclic operation of a Ziegler catalyzed polypropylene reactor. Besides providing an increase in the polydispersity, periodic variations in the feed concentration of a chain transfer agent hydrogen produced an approximately uniform product.

Based upon the relative value of the period τ and the characteristic response time τ_c of the system, four different families of periodic operation may be distinguished (25):

a. Process Life Cycle ($\tau >> \tau_c$): Providing the full initial capacity is restored, a periodic state is established. The problems here are relatively straightforward unless the operating and maintenance intervals are of similar magnitudes.

b. Quasi-Steady Periodic Operation ($\tau >> \tau_c$): This class is distinguished from the previous one in that here cycling is intentional. In both, straightforward determination of periodic reactor performance follows by application of the quasi-steady state approximation. Thus, this class is dominated by staedy-state operating characteristics.

c. Intermediate Periodic Operation ($\tau \sim \tau_c$): When the period is of the order of the system's dynamic response time, transient behavior assumes significant importance. The analytical Capabilities available for this class are limited; it is consequently one of the most interesting, since the performance shifts caused by transient phenomena are not always expected and are occasionally quite large.

d. Relaxed Steady-State Operation ($\tau << \tau_c$): A forced oscillation with very small amplitude often results when the input varies rapidly relative to the response time. Thus, to a good approximation the state of the system may be considered time-independent.

A few investigations of the performance of photochemical reactors have been reported. To predict reactor performance, the light intensity profile throughout the reactor should be specified as well as mass balance considerations regarding the reacting species. Since the radial light model is simple in every respect, it is worthwhile to know under what conditions it may be applied. Matsuura and Smith (26) proposed a diffuse light model to represent the light intensity profile within an elliptical reactor. Harada et al. (27) also pointed out in their study of an elliptical reactor that the radial light model should be carefully employed in the calculation of the light intensity profile, and they presented a two-dimensional light distribution model. Zolner and Williams (28) proposed a three-dimensional light intensity distribution model based on an external, cylindrical sleeve radiation source, within which the reactor is centered. This model contains an adjustable parameter which is the location of the source relative to the reactor. If the emitting source is placed exactly at the reactor surface, then the model predicts an infinite radiation flux at that point.

Jacob and Dranoff (29) reported a further detailed study to determine the quantum efficiency of the photohydrolysis as a function of light intensity and reactant concentration, and analyzed the reaction data on the basis that the lamp is a normal line source. Cerdá et al. (30) presented an extensive model of the elliptical-reflector reactor light distribution which accounts for the geometric properties of lamp, reflector, and reactor. The radiation arriving at any point within the reactor is traced back to the lamp surface, either via a direct path or by means of a single reflection at the elliptical-reflector surface. Jain, Graessley, and Dranoff (31) considered the reaction of the photo-polymerization of styrene in ethylbenzene solvent. Light in the near ultraviolet was used to promote this reaction with the aid of a suitable photoinitiator. They derived an expression for the intensity as a function of position in the annulus considering radiation emanating in all directions from the lamp taken as a line source.

The complete determination of the kinetic behavior of isothermal photoreactions in the presence of strong absorption of radiation often requires a knowledge not only of chemical rates but also of rates of mixing in the distribution of radiation attenuation. The response to the non-uniform initiation resulting from strong absorption depends on the reaction mechanism and on the relative rates of mass transfer, reaction, and radiation absorption. Depth-dose curves of UV light in polymer solution show a sharp decrease in dose with increasing depth. This leads to a nonuniform distribution of dose rate in the reaction system. Thus only a part of reactor is irradiated.

Yemin and Hill (32) reported that the rate of the nonuniformly initiated photopolymerization of methylmethacrylate in bulk increases with agitation speed. Chen and Hill (33) carried out a theoretical study on effects of nonuniform initiation on reaction rate and distribution of product in continuous stirred-tank reactors. They assumed the dose rate distribution to be exponential and showed that nonuniformity of dose rate distribution and the radical life time relative to mixing time have large effects. The molecular weight distribution was calculated to be unimodal, and the position of the peak moves to the lower molecular weight with increase of the nonuniformity and/or the mixing time relative to the radical life time.

Muller et al. (34) examined the molecular weight distribution of the polymer to observe a bimodal distribution. They also found that a low molecular weight species was in appreciable relative amount at low stirring speeds, and its amount became smaller with increasing stirring speeds. Kawakami and Isbin (35) reported the effects of agitation on radiolysis of chloral hydrate aqueous solution under nonuniform dose rate distribution. They reported a simplified analysis based mainly on the intermittent irradiation of fluid elements caused by recirculating flow in a stirred-tank reactor. In radiation induced reaction, a control with a higher accuracy can be attained by the dose rate regulation, and because dose rate is easily changed and affects the rate of radical formation directly, the concentration of radical reaches a new steady-state value within a very short time. Since the heat generation is proportional to the radical concentration, the temperature control by dose rate regulation is expected to give good response.

Continuous flow chemical reactors involving exothermic reactions are often operated autothermally; that is, the operating temperature is sustained entirely by the heat generated by reaction. Van Heerden (36) studied the characteristics of such processes and showed that they may possess multiple steady states and that some steady states are unstable to small perturbations. A number of theoretical studies treating control and start-up problems as well as the general nature of steady and unsteady behavior in various reactor models followed Van Heerden's work. The majority of these were focused on the continuous flow, stirred-tank reactor for reasons of mathematical tractability.

Since all kinds of polymerization are inevitably accompanied by a rapid increase in viscosity, an explosive acceleration in rate is observed by Nishimura (37), especially in bulk polymerizations. The abnormal increases in the rate of conversion, the degree of polymerization, and the mean lifetime of polymer radicals have been inclusively recognized as the gel effect, which usually causes the multiplicity behavior in the polymerization. It is also demonstrated mathematically by Knorr and O'Driscoll (38) that steady-state mass balance solutions are possible at three levels of conversion in free-radical polymerization of a CSTR.

The overall objectives of this study are concerned with the periodic operation of continuous stirred-tank polymerization reactors in an attempt to give more flexibility in the molecular weight distribution of a polymer. The ultraviolet light on and off regulation to a CSTR is considered. Analytical studies of polydispersity and molecular weight distribution are carried out on the control of a CSTR. A mathematical model is developed to correlate the effects of mixing on nonuniformly initiated polymerization. This model is then verified by data of experiments conducted in a laboratory scale reactor. In order for the quasi-stationary state approximation to be applicable, a theoretical study of free-radical concentration history in a batch reactor must be developed. Emphasis is also placed on the reactor performance characteristics and reactor responses to perturbation from steady states.

CHAPTER 2

ACTIVE POLYMER CONCENTRATION VERSUS TIME FOR PHOTOPOLYMERIZATION IN BATCH REACTOR

For polymerization the number of reactions involved is conceptually infinite. However, for simulation work, the memory of any computer is finite so that some truncation of the number of reactions to be considered is needed. A method for the calculation of the active polymerization concentrations with respect to reaction time for the photopolymerization is developed in this chapter. The method involves the use of a generating function which reduces the infinite number of differential equations to one differential equation followed by evaluation of an integral.

Theoretical Development

All of the reactor models developed in this investigation employ the following reaction steps in styrene polymerization.

(a) Initiation

By absorption of UV light by sensitizer

$$S \xrightarrow{I_{as}} 2S\cdot$$

$$S\cdot + M \xrightarrow{K_d} R_1\cdot$$

By thermal decomposition of monomer

$$M \xrightarrow{K_i} R_1\cdot$$

(b) Propagation

$$R_j\cdot + M \longrightarrow R_{j+1}\cdot$$

(c) Termination

$$R_j\cdot + R_i\cdot \xrightarrow{K_{tc}} P_{i+j}$$

$$R_j\cdot + R_i\cdot \xrightarrow{K_{td}} P_j + P_i$$

(d) Chain Transfer To the Monomer

$$R_j\cdot + M \xrightarrow{K_f} P_j + R_1\cdot$$

where $R_{i,j}$, $P_{i,j}$, S and M are the concentrations of active polymer, dead polymer, sensitizer and monomer, respectively.

In main radical chain polymerizations it is found that the deactivation can occur by two distinct mechanisms, namely, combination and disproportionation. Termination by combination has been shown to be the predominant mechanism for polystyrene. (39) The chain transfer rate constant, K_f, can be neglected due to a very small magnitude as compared to other rate constants.

The active polymer material balances for a batch reactor yield the equations

$$\frac{dR_1\cdot}{dt} = \Omega_i - K_pMR_1\cdot - K_tR_1\cdot\sum R_i \quad (1)$$

$$\frac{dR_2\cdot}{dt} = K_pMR_1\cdot - K_pMR_2\cdot - K_tR_2\cdot\sum R_i \quad (2)$$

$$\frac{dR_3\cdot}{dt} = K_pMR_2\cdot - K_pMR_3\cdot - K_tR_3\cdot\sum R_i \quad (3)$$

$$\vdots$$

$$\frac{d\sum R_i}{dt} = \Omega_i - K_t(\sum R_i)^2 \qquad (4)$$

with the additional monomer balance

$$\frac{dM}{dt} = -\Omega_i - K_p M \sum R_i \qquad (5)$$

In our system the thermal initiation rate is negligible in comparison to the photosensitized initiation rate, i.e., $\Omega_i = 2\phi_s I_{as}$, where ϕ_s is the quantum yield of sensitizer. Also the termination rate constant can be expressed as $K_t = K_{tc} + K_{td}$.

The generating function for this system is defined as(40)(41)

$$\Phi(w,t) = \sum_{j=1}^{\infty} R_j(t) w^j \qquad (6)$$

where w is a parameter. Differentiating equation (6) partially with respect to t gives

$$\frac{\partial \Phi}{\partial t} = \frac{dR_1}{dt} w + \frac{dR_2}{dt} w^2 + \frac{dR_3}{dt} w^3 + \cdots\cdots$$

Then substitution into equations (1)——(3) yields

$$\frac{\partial \Phi}{\partial t} = \Omega_i w + (-K_p M + K_p M w - K_t \sum R_i)\Phi \qquad (7)$$

Letting

$$q_1 = K_p M - K_p M w + K_t \sum R_i$$

and

$$q_2 = \Omega_i w$$

Equation (7) then becomes

$$\frac{\partial \Phi}{\partial t} + q_1 \Phi = q_2$$

Multiplying by integrating factor

$$e^{Q_1(t)}$$

where

$$Q_1(t) = \int_{t_2=0}^{t} q_1(t_2)\, dt_2$$

The solution is found to be

$$\Phi(t) = e^{Q_1(t)} \int_{t_1=0}^{t} q_2(t_1)\, e^{Q_1(t_1)}\, dt_1$$

$$= \int_{t_1=0}^{t} q_2(t_1)\, e^{-\{Q_1(t)-Q_1(t_1)\}}\, dt_1 \qquad (8)$$

and

$$Q_1(t)-Q_1(t_1) = \int_{t_2=t_1}^{t} q_1(t_2)\, dt_2$$

By inserting the defined q_1 and q_2 into the equation (8), then it can be written

$$\Phi(t) = \int_{t_1=0}^{t} \{\Omega_i w \times e^{-\int_{t_2=t_1}^{t} (K_p M + K_t \sum R_i)\, dt_2} \times$$
$$\times\, e^{\int_{t_2=t_1}^{t} K_p M w\, dt_2} \}\, dt_1$$

Also

$$w e^{\int_{t_1}^{t} K_p M w\, dt_2} = w \sum_{j=1}^{\infty} \frac{1}{(j-1)!} \left(\int_{t_1}^{t} K_p M\, dt_2 \right)^{j-1} w^{j-1}$$

Thus, by comparing with the defined equation (6), it follows that

$$R_j(t) = \int_{t_1=0}^{t} \Omega_i e^{-\int_{t_1}^{t} (K_p M + K_t \sum R_i)\, dt_2}\, \frac{1}{(j-1)!} \times$$
$$\times \left(\int_{t_1}^{t} K_p M\, dt_2 \right)^{j-1} dt_1 \qquad (9)$$

Thus if one knows the concentration of monomer, M, and total active polymer, $\sum R_i$, as a function of the reaction time, these integrals may be evaluated and the concentration R_j of the j-th active polymer obtained.

The isothermal batch reactor is assumed to be perfectly mixed and, for the photochemical case, fully illuminated. If I_o is the flux of radiation incident upon the reactor, and the total rate of light absorption is averaged over the path length of the light (42), then

$$I_{as} = I_o \left\{ \frac{\epsilon_s s}{\epsilon_s s + \epsilon_m m + \Sigma \epsilon_{p_i} P_i} \right\} \left\{ \frac{1 - e^{-(\epsilon_s s + \epsilon_m m + \Sigma \epsilon_{p_i} p_i)L}}{L} \right\} \tag{10}$$

where ϵ_m, ϵ_s, and ϵ_{p_i} are the molar absorptivities of monomer, sensitizer, and dead polymer, respectively, and L is the total path length of the light in the reactor. Quantum yield, ϕ_s, is also estimated to be 0.072 g-moles/Einstein for styrene sensitized by benzoin methyl ether from measured polymerization rates at full illumination and perfect mixing. Assumptions employed in the use of equation (10) are: axial nonuniformities due to light attenuation are negligible, the rates of reaction are uniform throughout the reactor and that the fraction of light absorbed by the monomer and the polymer is constant. In addition, for the present case, the following assumptions are made:

(1) The light absorbed by the monomer and the polymer are negligible, i.e., $\epsilon_s s >> \epsilon_m m + \Sigma \epsilon_{p_i} p_i$

(2) The light intensity absorbed by the sensitizer is assumed to be constant and of the magnitude of order 10, hence, the exponential term in equation (10) may be neglected.

By applying the assumptions (1) and (2), the corresponding relation between the total rate of light absorption and I_o is insensitive to chemical compositions, i.e.,

$$I_{as} = \frac{I_o}{L} = \text{constant}$$

and the initiation rate via absorption of ultraviolet light is

$$\Omega_i = 2\phi_s I_{as} = \frac{2\phi_s I}{L}$$

Combining equations (4) and (5), and using the initial conditions that

$$\sum R_i(t) = 0 \qquad \text{at } t = 0$$

$$M(t) = M_o \qquad \text{at } t = 0$$

we get

$$\sum R_i(t) = \frac{\sqrt{\Omega_i/K_t}\left(e^{2\sqrt{\Omega_i K_t}\, t} - 1 \right)}{e^{2\sqrt{\Omega_i K_t}\, t} + 1}$$

Since $e^{2\sqrt{\Omega_i K_t}} >> 1$, thus $\sum R_i(t)$ is approximately given by

$$\sum R_i(t) \simeq \sqrt{\Omega_i/K_t} \tag{11}$$

And then

$$M(t) = \frac{B}{K_p}\sqrt{K_t/\Omega_i}\; e^{-K_p\sqrt{\Omega_i/K_t}\, t} - \frac{\Omega_i}{K_p}\sqrt{K_t/\Omega_i} \tag{12}$$

where we define

$$B = \Omega_i + K_p\sqrt{\Omega_i/K_t}\, M_o$$

Substituting equations (11) and (12) into (9), one gets

$$R_j(t) = \frac{\Omega_i}{(j-1)!} \int_{t_1=0}^{t} F(t)G(t)\, dt_1 \tag{13}$$

in which

$$F(t) = e^{-\int_{t_1}^{t} (K_p M + K_t \sum R_i)\, dt_2}$$

$$= H(t)\, e^{-\frac{BK_t}{\Omega_i K_p} e^{-K_p \sqrt{\Omega_i / K_t}\, t_1}}$$

$$G(t) = \left(\int_{t_1}^{t} K_p M\, dt_2 \right)^{j-1}$$

$$= \left(P(t) + \sqrt{\Omega_i K_t}\, t_1 + \frac{BK_t}{\Omega_i K_p} e^{-K_p \sqrt{\Omega_i / K_t}\, t_1} \right)^{j-1} \tag{14}$$

with

$$H(t) = e^{\frac{BK_t}{\Omega_i K_p} e^{-K_p \sqrt{\Omega_i / K_t}\, t}}$$

$$P(t) = -\frac{BK_t}{\Omega_i K_p} e^{-K_p \sqrt{\Omega_i / K_t}\, t} - \sqrt{\Omega_i K_t}\, t$$

so that the equation (13) may then be written

$$R_j(t) = \frac{\Omega_i H(t)}{(j-1)!} \int_{t_1=0}^{t} e^{-c_1 e^{-c_2 t_1}} \{c_3 t_1 + c_1 e^{-c_2 t_1} + P(t)\}^{j-1}\, dt_1 \tag{15}$$

where

$$c_1 = \frac{BK_t}{\Omega_i K_p}$$

$$c_2 = K_p \sqrt{\Omega_i / K_t}$$

$$c_3 = \sqrt{\Omega_i K_t}$$

$$H(t) = e^{c_1 e^{-c_2 t}}$$

$$P(t) = -c_1 e^{-c_2 t} - c_3 t$$

Equation (15) can be expressed with the series expansion of the exponential function

$$R_j(t) = \frac{\Omega_i H(t)}{(j-1)!} \int_{t_1=0}^{t} \{ \sum_{n=0}^{\infty} \frac{(-c_1 e^{-c_2 t_1})^n}{n!} \} \{c_3 t_1 + c_1 e^{-c_2 t_1} + P(t)\}^{j-1} dt_1 \tag{16}$$

One can use binomial series to represent equation (16):

$$R_j(t) = \frac{\Omega_i H(t)}{(j-1)!} \sum_{m=0}^{j-1} \frac{c_3^m c_1^{j-1-m} (j-1)!}{m!(j-1-m)!} \sum_{n=0}^{\infty} \frac{(-c_1)^n}{n!} \times$$

$$\times \int_{t_1=0}^{t} \{t_1 + \frac{P(t)}{c_3}\}^m e^{-c_2 (j-1-m+n) t_1} dt_1$$

Finally, the active polymer concentration can be expressed as:

$$R_j(t) = \Omega_i e^{c_1 e^{-c_2 t}} \sum_{m=0}^{j-1} \frac{c_3^m c_1^{j-1-m}}{m!(j-1-m)!} \sum_{n=0}^{\infty} \frac{(-c_1)^n}{n!} \times$$

$$\times \left[e^{-c_2 (j-1-m+n) t} \sum_{\gamma=0}^{m} (-1)^{\gamma} \frac{m! (\frac{c_1}{c_3} e^{-c_2 t})^{m-\gamma}}{(m-\gamma)! \{c_2 (m+1-n-j)\}^{\gamma+1}} - \right.$$

$$\left. - \sum_{\gamma=0}^{m} (-1)^{\gamma} \frac{m! (\frac{c_1}{c_3} e^{-c_2 t} - t)^{m-\gamma}}{(m-\gamma)! \{c_2 (m+1-n-j)\}^{\gamma+1}} \right] \text{ for } m+1-n-j \neq 0$$

or

$$\times \left[\frac{1}{m+1} \{ (\frac{c_1}{c_3} e^{-c_2 t})^{m+1} - (\frac{c_1}{c_3} e^{-c_2 t} - t)^{m+1} \} \right] \text{ for } m+1-n-j = 0$$

The use of the generating function enables one to compute the concentration of any j-mer in the photopolymerization system without calculating the concentration of all of its precursors.

The accuracy of the approximation depends on the number of exponential terms used in the equation (17). From the computational standpoint some remarks must be made. The value C_1 in the equation is very large and computation with such large value becomes very tedious and difficult on the computer. Therefore, some calculation techniques should be applied. For large degree j of polymerization, however, Stirling's formula may be used to combine with the other exponential function.

To evaluate a definite integral by formal methods is often difficult, even when the function is of a relatively simple analytical form. For these intractable case, some other approach is necessary. An obvious alternative is to find a function that is both a suitable approximation of a given function and simple to integrate formally.

An integral approximation is employed as follow: Since $K_p\sqrt{\Omega_i/K_t}\,t >> 1$ and $B\sqrt{K_t/\Omega_i} >> \sqrt{\Omega_i K_t}$, reasonable for the process, then equations (12) and (14) may be written as

$$M(t) = \frac{B}{K_p}\sqrt{K_t/\Omega_i}\,(1 - K_p\sqrt{\Omega_i/K_t}) - \frac{\Omega_i}{K_p}\sqrt{K_t/\Omega_i}$$

$$= \frac{B}{K_p}\sqrt{K_t/\Omega_i} - Bt_2 - \frac{1}{K_p}\sqrt{\Omega_i K_t}$$

$$F(t) = e^{\frac{1}{2}BK_p t^2 - B\sqrt{K_t/\Omega_i}\,t} \times e^{B\sqrt{K_t/\Omega_i}\,t_1 - \frac{1}{2}BK_p t_1^2}$$

$$G(t) = \{ (\tfrac{1}{2}BK_p t_1^2 - B\sqrt{K_t/\Omega_i}\,t_1) + (B\sqrt{K_t/\Omega_i}\,t - \tfrac{1}{2}BK_p t^2) \}^{j-1}$$

so that equation (13) becomes

$$R_j(t) = \frac{\Omega_i}{(j-1)!} \int_0^t e^{A_1 t_1 - A_2 t_1^2 + A_2 t^2 - A_1 t} (A_2 t_1^2 - A_1 t_1 + A_1 t - A_2 t^2)^{j-1} dt_1$$

where

$$A_1 = B\sqrt{K_t/\Omega_i}$$

$$A_2 = \tfrac{1}{2}BK_p$$

Let

$$y = A_1 t - A_1 t_1 + A_2 t_1^2 - A_2 t^2$$

then

$$dt_1 \approx - dy/A_1 \qquad (A_1 >> A_2)$$

The active polymer concentrations with respect to time may thus be written

$$R_j(t) = - \frac{\Omega_i}{A_1} \frac{1}{(j-1)!} \int_{A_1 t - A_2 t^2}^{0} e^{-y} y^{j-1} dy$$

Which may be integrated, and then it on rearranging becomes

$$R_j(t) = \frac{\Omega_i}{A_1} \{ 1 + e^{-(A_1 t - A_2 t^2)} \sum_{\gamma=0}^{j-1} (-1)^{\gamma} \frac{(A_1 t - A_2 t^2)^{j-1-\gamma}}{(j-1-\gamma)!\ (-1)^{\gamma+1}} \}$$

In the equation, the exponential term in the brace is very small and can be negligible in comparison to unity.

Equations (1)—(5) are integrated numerically for a time step of 10^{-3} sec. with the iteration running from t = 0 sec. to t = 2000 sec.. Table 1 gives the results of the concentrations of several active polymer species for different times with I_o = 11.7×10^{-8} Einsteins/sec-cm^2 by using the thermophysical properties data shown in Table 3 (43). In our system, on the one hand, the step size should be chosen small enough to achieve required accuracy. It must depend on the value of active polymer concentrations. On the other, it should be as large as possible in order to keep rounding error under control and to avoid spending too much time in operation. The numerical method has the disadvantage that the concentration of any particular active polymer may be calculated with calculating all of its precursors.

The active polymer concentrations have also been calculated numerically in thermal polymerization with the initiation rate, $2K_iM^3$, shown in Table 2.

<u>In CSTR</u>

Similarly for a CSTR, a term $\frac{R_i}{\theta}$ (i=1, 2, 3, · · ·), has to be substracted from the right hand side of equations (1)—(4).

$$\frac{dR_1\cdot}{dt} = \Omega_i - K_pMR_1\cdot - K_tR_1\cdot\sum R_i - \frac{R_1\cdot}{\theta}$$

$$\frac{dR_2\cdot}{dt} = K_pMR_1\cdot - K_pMR_2\cdot - K_tR_2\cdot\sum R_i - \frac{R_2\cdot}{\theta}$$

$$\frac{dR_3\cdot}{dt} = K_pMR_2\cdot - K_pMR_3\cdot - K_tR_3\cdot\sum R_i - \frac{R_3\cdot}{\theta}$$

$$\vdots$$

$$\frac{d\sum R_i}{dt} = \Omega_i - K_t(\sum R_i)^2 - \frac{\sum R_i}{\theta}$$

Here, θ is the reactor residence time. By using the same procedure of generating function used for batch reactor, eq.(9) is also modified for a CSTR by adding $\frac{1}{\theta}$ as shown below

$$R_j(t) = \int_{t_1=0}^{t} \Omega_i e^{-\int_{t_1}^{t}(K_pM + K_t\sum R_i + \frac{1}{\theta})\, dt_2} \frac{1}{(j-1)!} \times \left(\int_{t_1}^{t} K_pM\, dt_2 \right)^{j-1} dt_1$$

Since $K_pM + K_t\sum R_i >> \frac{1}{\theta}$, the concentrations of active polymers in CSTR during the transient process is nearly the same as those in batch reactor.

Data Analysis

From the results of numerical calculation with the given kinetic rate constants, the values of $\frac{dR_1}{dt}$, Ω_i, K_pMR_1, and $K_tR_1\sum R_i$ in equation (1) are the orders of 10^{-13}, 10^{-6}, 10^{-6}, and 10^{-7}, respectively. $\frac{dR_1}{dt}$ therefore, can be neglected because it is of a very small magnitude as compared to other values in the equation for the photopolymerization process. Similarly, $\frac{dR_2}{dt}$, $\frac{dR_3}{dt}$, etc. can also be set equal to zero. Furthermore, the values of

Table 1

R_1, R_2, R_3, and $\sum R_i$ Concentrations vs. Time on Batch UV-Light Photopolymerization

Time (sec)	R_1(g-mole/l) (x 10^8)	R_2(g-mole/l) (x 10^8)	R_3(g-mole/l) (x 10^8)	$\sum R_i$(g-mole/l) (x 10^6)
200	.13904108625813	.13795610829565	.13687959675419	.17700573197387
400	.14045031464019	.13934315516603	.13824472337207	.17700535899700
600	.14188806204197	.14075804101094	.13963701968698	.17700501088455
800	.14334062207170	.14218726667931	.14104319150528	.17700466277142
1000	.14480814740148	.14363097505643	.14246337219015	.17700431465760
1200	.14629083307410	.14508935069317	.14389773607905	.17700399140844
1400	.14778883617386	.14656254044636	.14534642008346	.17700369302408
1600	.14930223213050	.14805061035282	.14680948112640	.17700336977378
1800	.15082380569465	.14954646038835	.14827993310543	.17700309625384
2000	.15236093776075	.15105734001183	.14976489585467	.17700279786797

Conditions: $I_o = 11.7 \times 10^{-8}$ Einsteins/sec-cm^2

Temp. = 338°K

L = 5 cm

Table 2

R_1, R_2, R_3, and $\sum R_i$ Concentrations vs. Time on Batch Thermal Polymerization

Time (sec)	R_1(g-mole/l) (x 10^{12})	R_2(g-mole/l) (x 10^{12})	R_3(g-mole/l) (x 10^{12})	$\sum R_i$(g-mole/l) (x 10^{8})
30	.30236213308467 (max.)	.30233428895217 (max.)	.30230644738381 (max.)	
32				.20939635716963 (max.)
60	.30235271969351	.30232487664627	.30229703616304	.20939148564093
120	.30233304282606	.30230520208859	.30227736391487	.20938024116560
180	.30231336499904	.30228552657150	.30225769070746	.20936899792529
240	.30229368638226	.30226585026470	.30223801671038	.20935775406368
300	.30227373474986	.30224590097567	.30221806976446	.20934638298153
360	.30225378640968	.30222595497620	.30219812610544	.20933496683335
420	.30223374270751	.30220591362867	.30217808710628	.20932355225217
480	.30221379208572	.30218596534786	.30215814117218	.20931213806951
540	.30219599703705	.30216817238772	.30214035030035	.20930196637413

Conditions: Temp. = 338°K

$\frac{d\sum R_i}{dt}$, Ω_i, and $K_t(\sum R_i)^2$ in equation (4) are the order of -10^{-15}, 10^{-6}, and 10^{-6}, respectively. Therefore, the QSSA is valid for values of the kinetic rate constants and can be applied to our photopolymerization system.

CHAPTER 3

EXPERIMENTAL

Experimental investigation of the polymerization of styrene with initiation by photodissociation of sensitizer (benzoin methyl ether) was made in a continuous stirred-tank reactor. Experimental apparatus and procedures are described as follows: (44)

Experimental Apparatus

The experimental apparatus is shown schematically in Figure 1. The reactor is a stirred baffled stainless steel vessel (7cm ID and 6 cm height). The reactor volume is partially illuminated with a light beam through the bottom of the reactor. The reactor was maintained at a constant temperature by the use of a constant temperature bath which circulated water in the jacket. For the control system, instead of a temperature controller, an UV spectrophotometer was used to monitor the reaction conversion. By providing an upper and lower limits of conversion, shutter mechanism can be opened or closed manually. Agitation speed was measured through the use of a tachometer.

The optical system provides a parallel ultraviolet beam. A 1000 watts Mercury Xenon arc lamp is housed in an air cooled lamp housing and supplied with power by a regulated DC power supply (manufactured by Oriel Optical Co.). The housing contains a mirror which increases the effective intensity of the lamp. A focusing lens mounted in the housing collects the light and produces a collimated beam which passed through a water filter. The filtered beam is reflected upward by a mirror and passes

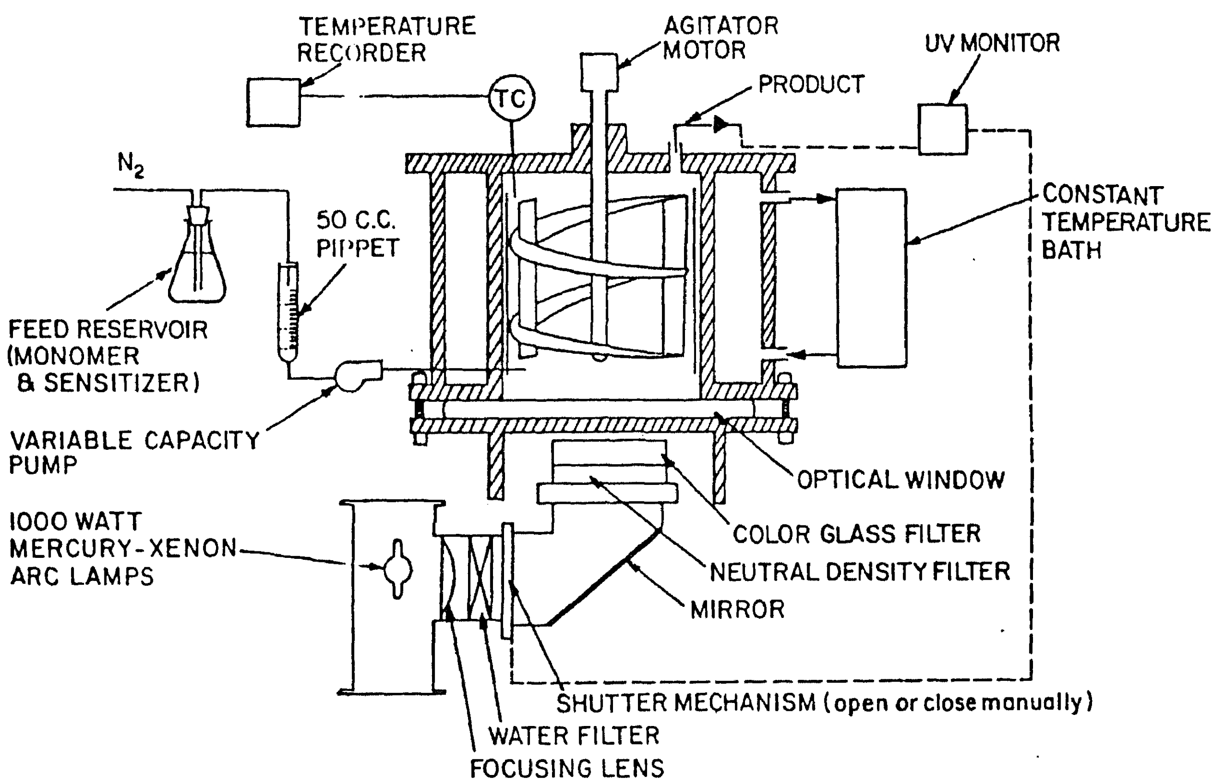

Figure 1. Arrangement of Experimental Apparatus of Isothermal CSTR

through neutral density filter to improve its cross-sectional uniformity and then through a color glass filter which transmits light with a wavelength of 310-420 nm. An iris diaphragm located under the neutral density filter is used to provide nonuniform irradiation.

The isothermal batch operation was also included in our experimental investigation. The reactor used for the batch systems is the same as the one in isothermal continuous stirred-tank reactor while the inlet and outlet were stopped.

Experimental Procedure

(1) Purification of Styrene Monomer

The styrene monomer used for this study is from Aldrich Chemical Co. of 99% purity inhibited with 10-15 ppm of p-tert-butylcatechol. Inhibitor was removed from styrene monomer by slow consecutive dropwise passage through a column (5 cm diameter and 60 cm length) packed with activated alumina. A second column packed with silica gel was connected to the first one and assigned to remove moisture from the monomer. Inhibited monomer was allowed at a flow rate about 1 c.c./min. through these two columns. The purified monomer then flew into a collection flask which was nitrogen blanketed, and nitrogen was bubbled through the monomer to remove oxygen which can react with the monomer. The sensitizer, benzoin methyl ether (manufactured by Aldrich Chemical Co.) is added immediately before the start of run. The experimental investigations involve styrene polymerization by using benzene as solvent.

Purification of benzene (99.9% purity by J.T. Baker Co.) is the same as styrene monomer purifying procedure.

(2) Measurement of Polymer Conversion

Polystyrene is insoluble in methanol while the monomer, dimers, and trimers are soluble. But, as the amounts of dimers, trimers, and impurities from the styrene present in polystyrene are relatively small, the methanol-soluble portion is principally styrene and can be taken as a measured of its presence. Conversion is determined by the gravimetric technique presented by Boundy and Boyer (16) which involves precipitating the polymer in an excess of methnol. About two to three grams of reaction mixture is collected from the reactor. The mixture is then added to 100 c.c. methyl alcohol (99.9% purity, spectrometric grade by Aldrich Chemical Co.) which is vigorously stirred to precipitate the product polymer. For more than 30% of conversion, approximate 5 c.c. of p-dioxane is required to add to the solution before precipitation. The precipitate is filtered with a buchner funnel. The polymer is then dried in a vaccum oven at 70°C for at least 12 hours to remove traces of the monomer and place it in the desiccator to cool. The conversion can thus be determined. The gravimetric method of determining the conversion by ascertaining the methanol-soluble fraction of the product gives satisfactory result, but the time involved is lengthy. An ultraviolet spectrophotometric procedure has been developed for the rapid and accurate determination of monomer in polystyrene. (45) It will reduce the time required for an analysis to approximately 10 minutes is of interest for UV light on-off regulation purposes. The procedure can be described as follows: The concentration of styrene monomer dissolved in tetrahydrofuran (THF) at the order of 0.001% wt, monomer absorbance at wave length 250 mμ varies linearly with concentration. Thus, the fraction of styrene in a mixture is:

$$g = \frac{\text{absorbance of unknown sample}}{\text{absorbance of pure styrene}}$$

and the conversion is

$$x = 1 - g$$

A Bausch and Lamb spectronic 710 spectrophotometer was used for conversion measurement.

(3) Measurement of Incident Light Intensity

The light intensity of the Mercury Xenon Arc Lamp was measured using the potassium ferrioxalate actiometer developed by Parker (46) and Hatch and Parker (47). The experiment was carried out in a acrylic reactor (3.8 cm diameter and 5 cm height) and allthe measurements were made in a dark room. The recommended procedures were as follows:

1. Solution A: Dissolve 0.006 molar of $K_3F_e(C_2O_4).3H_2O$ (2.947 g) into 100 c.c. of 1 N H_2SO_4 and then diluted to 1000 c.c.
2. Solution B: Dissolve 0.1 g of 1,10 phenathroline into 100 c.c. of H_2O (0.1% wt).
3. Solution C: 600 c.c. of 1 N sodium acetate is added to 360 c.c. of 1 N H_2SO_4 and then diluted to 1000 c.c.
4. 25 c.c. of A is added into the reactor and under exposure of ultraviolet light. In this experiment, exposing time

ranges from 3 sec. to 20 sec. for each run.

5. 1 c.c. of solution A from the reactor is then transferred to a 25 c.c. calibrated flask. Two c.c. of solution B is added followed by a volume of 0.5 c.c. of buffer solution C, and then diluted to 25 c.c.
6. After making up and mixing, the liquid was allowed to stand for one hour for complete reaction and then it was measured at 5100 Å and 9 °C with a spectrophotometer.

The incident light intensity can be varied by changing the number of neutral density filters or the opening of the iris diaphragm. Experimental results of incident light intensity is summarized in Table 3a. A plot of I_o versus time is given in Figure 2.

(4) Determination of MWD

The molecular weight distribution of product polymer was measured via gel permeation chromatography (GPC) manufactured by Water Associates model 6000Å. In the GPC process, the molecules are separated based on some measure of molecular size; the large molecules penetrate into the gel the least and hence are eluted first. The chromatograph was equipped with five μstyrgel columns. The columns were packed in series having permeability limits of 10^6, 10^5, 10^4, 10^3 and 500 Å's. If it is deemed necessary to ontain numerical data, attention must be paid to: Sample preparation, sample injection, column selection, calibration method, baseline determination, and computation.

Table 3a

Summary of Incident Light Intensity Measurements (44)

Run	No. of N.D. Filters	Reactant Volume (c.c.)	Time (sec)	Absorbance	$I_o x10^{-8}$ ($\frac{Eins}{sec\text{-}cm^2}$)
1	0	25	3	0.135	15.75
2	0	24	6	0.278	15.57
3	0	23	9	0.415	14.85
4	0	22	12	0.563	14.45
5	0	21	15	0.712	13.96
6	1	25	3	0.100	11.67
7	1	24	6	0.212	11.87
8	1	23	9	0.339	12.13
9	1	22	12	0.441	11.32
10	1	20	18	0.738	11.48
11	2	25	5	0.103	7.24
12	2	24	10	0.207	6.99
13	2	23	15	0.284	6.12
14	2	22	20	0.403	6.23
15	3	25	5	0.074	5.20
16	3	24	10	0.143	4.83
17	3	23	15	0.234	4.83
18	3	22	20	0.331	4.89

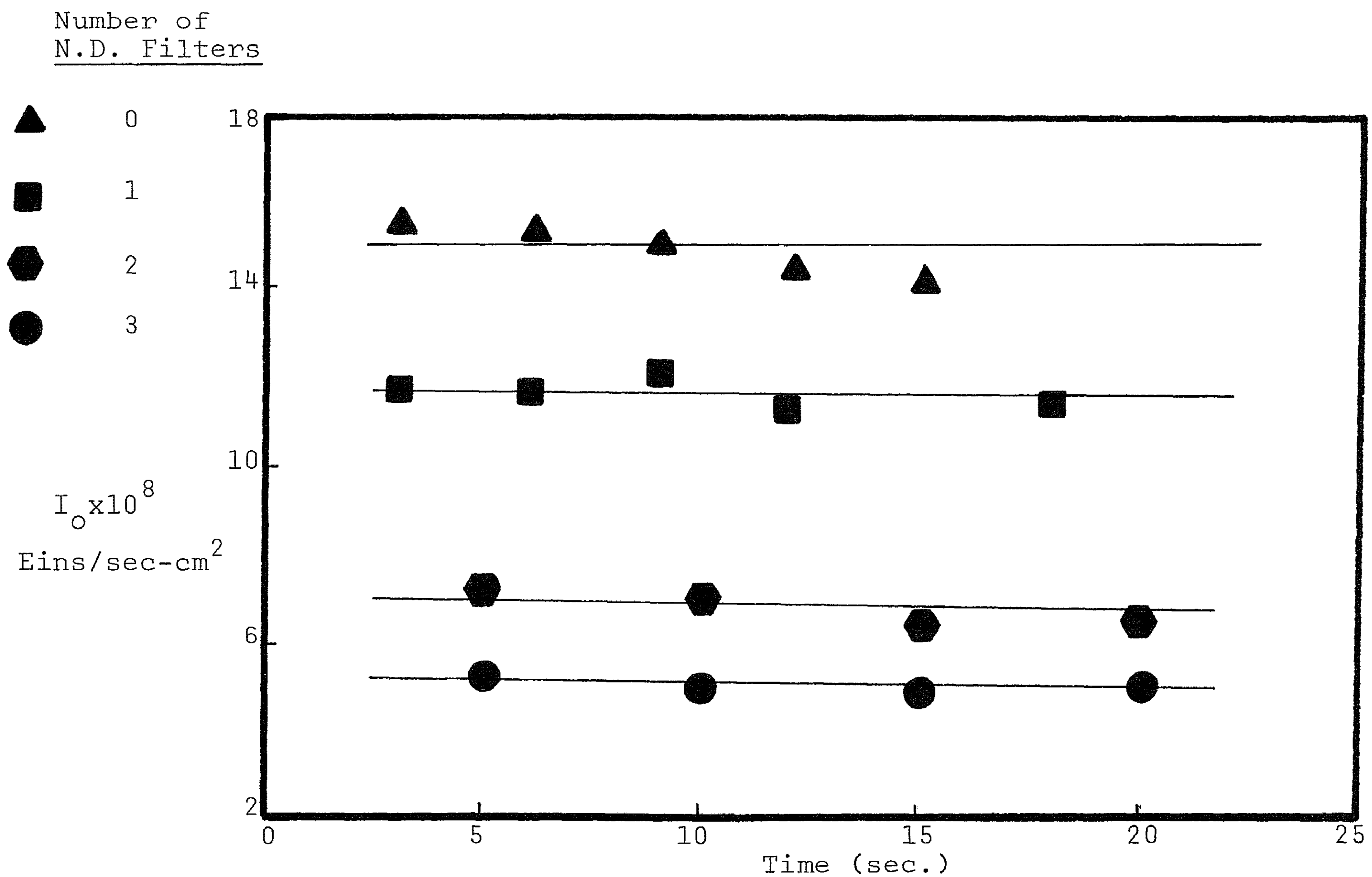

Figure 2. Experimental Measurements of Incident Light Intensity

The columns were calibrated by using six standard polystyrene samples (supplied by Water Associates) with molecular weights of $4x10^3$, $9x10^3$, $5x10^4$, $2.4x10^5$, $4.7x10^5$ and $2.7x10^6$. Calibrations were made monthly and the calibration curve was typical and over the range of interest, which is expressible as a semi-logarithmic relation of molecular weight with elution volume. A typical calibration curve is given in the Figure 3. A least-squares regression was employed to calibrate the standard curve of a quadratic equation. The polymer sample was prepared at a concentration of 0.025% wt dissolved in toluene (Aldrich-spectrophotometric grade) to minimize the possibility of viscous fingering caused by high concentrations of polymer, particularly high molecular weight polymers. Before the sample was dissolved, the solvent was filtered to remove any material likely to clog the columns. The solution was injected at a flow rate of 2.5 c.c./min. through the 30.5 cm long and 0.3 cm diameter stainless steel columns. From the GPC elution curves, marked the retention volumes for the start (V_i) and finish (V_t) of the polymer chromatogram. Drew a linear baseline from before V_i to after V_t. Once the baseline has been determined, measure peak heights to three significant figures for about 30 equally spaced points along the GPC curve. Tabulate these data under the headings shown below.

1	2	3	4	5
Retention Volume or Counts	Height (cm)	Chain Length	$\frac{\text{Column 2}}{\text{Column 3}}$	Column 2 * Column 3

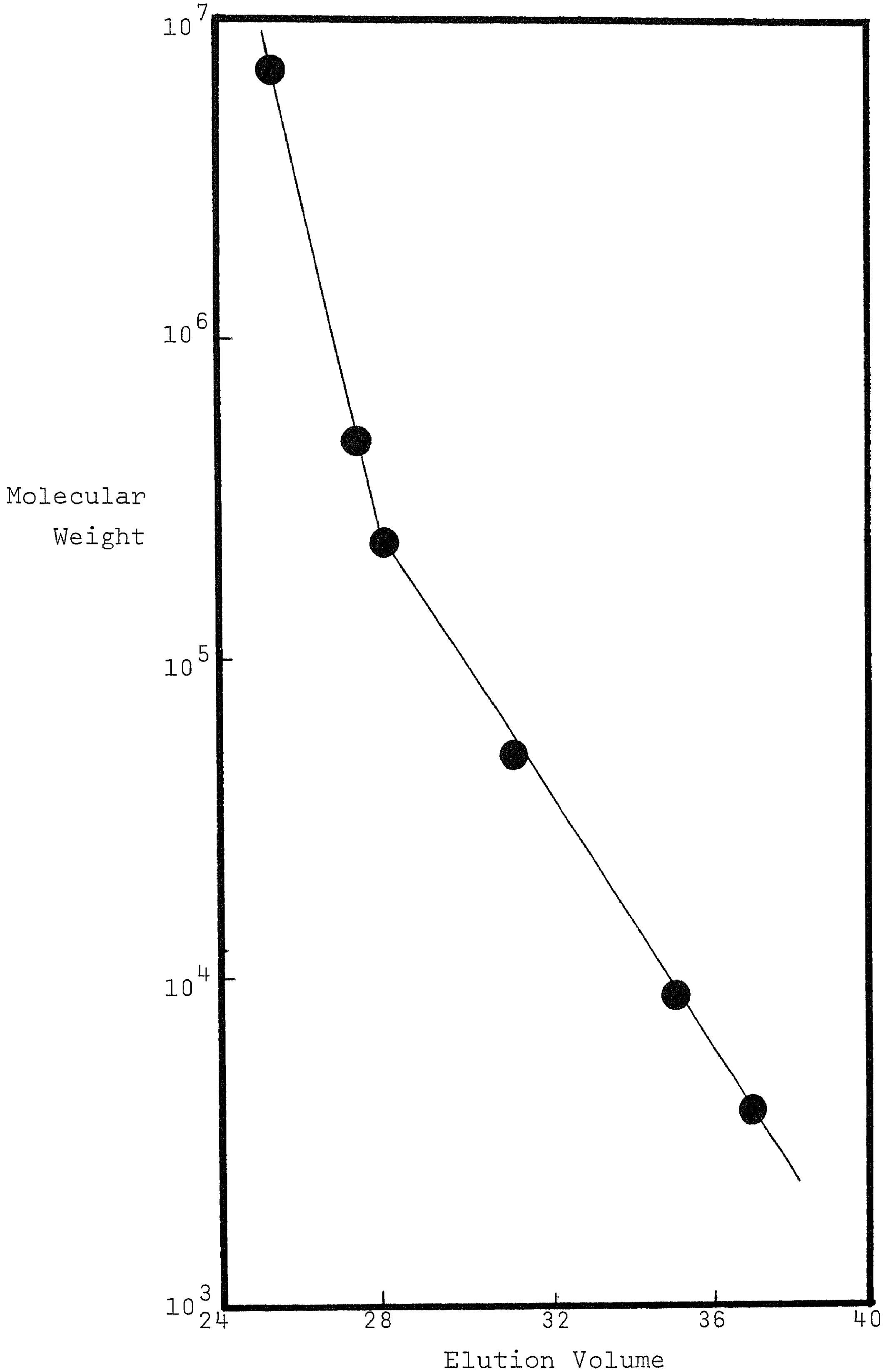

Figure 3. Molecular Weight vs. Elution Volume for GPC Calibration

After calibrating, list chain lengths in column 3 and determine chain length averages by the following equations:

X_n (Number Average Chain Length) = Σ column 2/Σ column 4

X_w (Weight Average Chain Length) = Σ column 5/Σ column 2

Polydispersity then is the ratio, X_w/X_n.

CHAPTER 4

PERIODIC OPERATION OF A PHOTOPOLYMERIZATION IN A CONTINUOUS STIRRED-TANK REACTOR

Most polymerization processes are carried out either steady state or batchwise. In this chapter a more general class of processes, the periodic process, is considered. This class exhibits some properties which may be of great practical value. The theory of periodic processes includes the theory of steady-state and batch processes, since these two types can be regarded as special cases of periodic processes. The dynamic behavior of many chemical systems can be represented by a set of differential equations:

$$\frac{dx_i}{dt} = f_i(x_1, x_2, \ldots . x_n; y_1, y_2, \ldots . y_r)$$
$$i = 1, 2, \ldots . n$$

where the x's denote state and the y's denote control variables. If the control variables are given function time, and if the initial values $x_i(0)$ of the state variables are known, the state of the system can be calculated as a function of time by integrating differential equations.

Another mode of operation is to use periodic control function y(t)- that is, functions satisfying the relations:

$$y_j(t+\tau) = y_j(t) \quad \text{for any } t$$
$$j = 1, 2, \ldots . r$$

where τ is the period for the cyclic operation

In our photopolymerization system there are five state variables (n=5) and one control variable (r=1). Here, we control either the UV light intensity incident upon the reactor or flow rate to the reactor. The UV light intensity in the process is described as

$$I_o(t) = \begin{cases} 0 & t \in (0, r\tau) \quad \text{i.e., UV light is off} \\ I_o & t \in (r\tau, \tau) \quad \text{i.e., UV light is on} \end{cases}$$

where r is a parameter restricted by

$$r \in (0,1)$$

and $I_o(t) = I_o(t+\tau)$

Owing to a course of the polymerization reactors, a typical product has a distribution of polymers with vastly varying chain length. Therefore two subjects will be presested in this study: polydispersity, which is often used as a measure of breadth of the molecular weight distribution, and molecular weight distribution itself.

Polydispersity of Periodic Operation

In the polymerization there are in principle an infinite number of reactions taking place and one could write an infinite set of differential equations representing them. Fortunately, the properties of a molecular weight distribution can usually be characterized by the polymer moments and the equations for these are quite simple. The reaction occurs in a continuous stirred-tank reactor, as shown schematically in Figure 4. The procedure is accompanied by three assumptions for a bulk

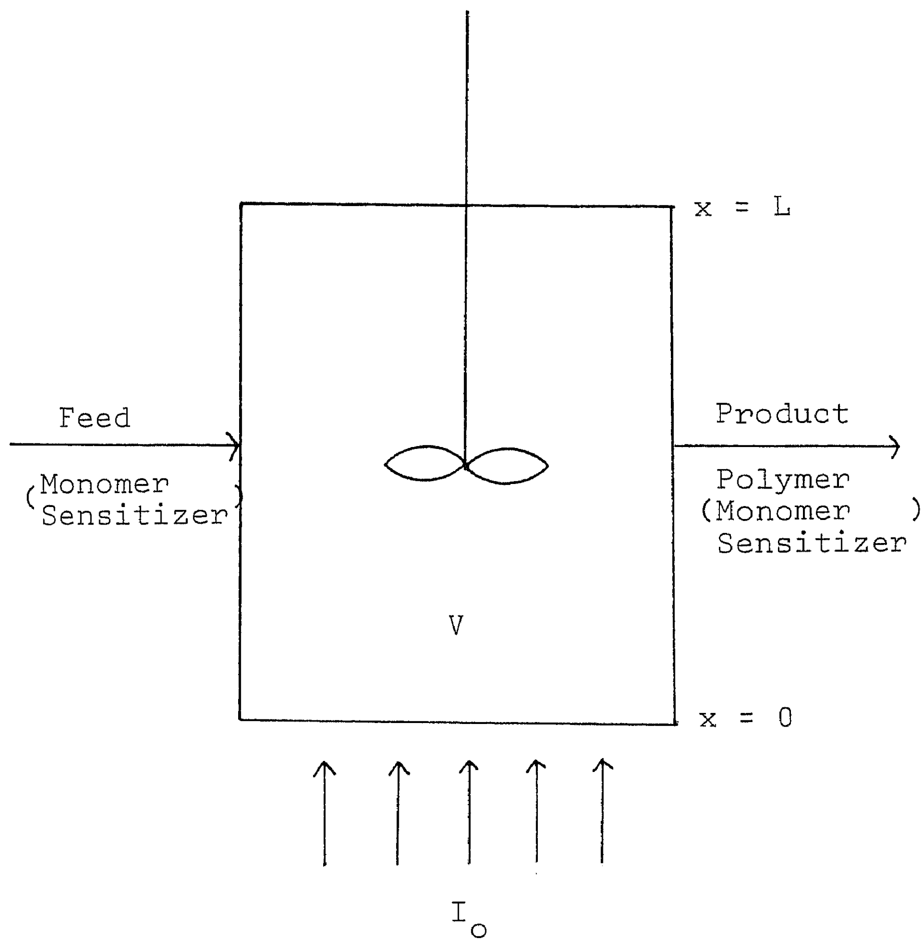

Figure 4. Schematic Diagram of Reaction Vessel

photopolymerization carried out in a CSTR:

(1) The reactor is perfectly mixed, isothermal and operated under stationary state conditions.

(2) The kinetic constants of the various reaction steps are independent from the chain length at low steady state; i.e., no gel effect occurs.

(3) No density variation occurs in the reactor; i.e., the reaction volume is constant.

Mathematical Equations for Polymer Moments

The material balance equations for the reactor are:

For total active polymer:

$$\frac{d\sum R_i}{dt} = \Omega_i - K_t(\sum R_i)^2 - \frac{\sum R_i}{\theta} \qquad (1)$$

For monomer:

$$\frac{dM}{dt} = \frac{M_o}{\theta} - \Omega_i - K_p M \sum R_i - \frac{M}{\theta} \qquad (2)$$

where θ is the residence time of reactor

The ith moment of the distribution, Q_i, is defined as

$$Q_n = \sum_{i=1}^{\infty} i^n P_i$$

The number and weight average chain length, X_n and X_w, are experimentally measurable and are related to the leading moments:

$$X_n = \frac{Q_1}{Q_0} = \frac{\sum iP_i}{\sum P_i}$$

$$X_w = \frac{Q_2}{Q_1} = \frac{\sum i^2 P_i}{\sum iP_i}$$

The distribution of chain sizes is described in terms of polydispersity, PD, which is defined as

$$PD = \frac{X_w}{X_n}$$

The $\sum P_i$, $\sum iP_i$, $\sum i^2P_i$ are, respectively, the zeroth, first, and second moments of the dead polymer size distribution in the outlet stream, and can be expressed as (33)

$$\frac{d\sum P_i}{dt} = \frac{1}{2}\Omega_i - \frac{\sum P_i}{\theta} \qquad (3)$$

$$\frac{d\sum iP_i}{dt} = M\left(\frac{K_p}{K_t^{1/2}}\right)\Omega_i - \frac{\sum iP_i}{\theta} \qquad (4)$$

$$\frac{d\sum i^2P_i}{dt} = 3M^2\frac{K_p^2}{K_t} + 5M\frac{K_p}{K_t^{1/2}}\Omega_i + 2\Omega_i - \frac{\sum i^2P_i}{\theta} \qquad (5)$$

For a steady operation of reactor by continuous irradiation at a fixed dose rate I_o, total radical concentration $\sum R_{is}$, monomer concentration M_s, and moments of the dead polymer size distribution $\sum P_{is}$, $\sum iP_{is}$, and $\sum i^2P_{is}$ are calculated by setting the derivatives equal to zero in equations (1)—(5).

UV Light Off

After several hours of steady operation, the UV light is shut off by closing the shutter while maintaining other operating conditions at its previously set value. At this time, the thermal initiation may only occur in this system, thus $\Omega_i = 2K_iM^3$ (43). Neglecting the first and third terms relative to the second term on the right of equation (1), the equation is then written as

$$\frac{d\sum R_i}{dt} = -K_t(\sum R_i)^2$$

instead of the more exact expression.

With the initial condition

$$\sum R_i(0) = \sum R_{is}$$

then the differential equation is easily integrated:

$$\sum R_i(t) = \frac{\sum R_{is}}{1 + K_t t \sum R_{is}}$$

$$\simeq \frac{1}{K_t t} \qquad (K_t t \sum R_{is} >> 1) \tag{6}$$

The monomer concentration can be solved by substituting eq. (6) into eq. (2). Also the thermal initiation rate is negligible in comparison to other terms on the right of eq. (2). The following expression is obtained

$$\frac{dM}{dt} = \frac{M_o}{\theta} - (\frac{1}{\theta} + \frac{K_p}{K_t t})M$$

with the initial condition

$$M(0) = M_s$$

Since $t^{\pm\frac{K_p}{K_t}} \to 1$, the approximate solution for M(t) is

$$M(t) \simeq C_1 + C_2 e^{-t/\theta} \tag{7}$$

where

$$C_1 = M_o$$

$$C_2 = M_s - M_o$$

Substitute equation (7) into equations (3)—(5). The three initial conditions appropriate for this system are

$$\sum P_i(0) = \sum P_{is}$$

$$\sum iP_i(0) = \sum iP_{is}$$

$$\sum i^2P_i(0) = \sum i^2P_{is}$$

By solving equations, we obtain

$$\sum P_i(t) = K_i(C_1^3\theta + 3C_1^2C_2te^{-t/\theta} - 3C_1C_2^2\theta e^{-2t/\theta} - \frac{C_2^3}{2}\theta e^{-3t/\theta}) + \{\sum P_{is} - K_i\theta(C_1^3 - 3C_1C_2^2 - \frac{C_2^3}{2})\}e^{-t/\theta} \tag{8}$$

$$\sum iP_i(t) = \sqrt{2}\, K_p\sqrt{K_i/K_t}C_1^{5/2}\theta e^{-t/\theta}\{(\sum_{\substack{n=0\\n\neq 1}}^{\infty}\binom{2.5}{n}(\frac{C_2}{C_1})^n\frac{1}{1-n}e^{(1-n)t/\theta}) + 2.5\frac{C_2}{C_1}t\} + \{\sum iP_{is} - \sqrt{2}K_p\sqrt{K_i/K_t}C_1^{5/2}\theta(\sum_{\substack{n=0\\n\neq 1}}^{\infty}\binom{2.5}{n}(\frac{C_2}{C_1})^n\frac{1}{1-n})\}e^{-t/\theta} \tag{9}$$

$$\sum i^2P_i(t) = 3\frac{K_p^2}{K_t}(C_1^2\theta + 2C_1C_2te^{-t/\theta} - C_2^2\theta e^{-2t/\theta}) + 5\sqrt{2}K_p\sqrt{K_i/K_t}C_1^{\frac{5}{2}}\theta e^{-t/\theta}\{(\sum_{\substack{n=0\\n\neq 1}}^{\infty}\binom{2.5}{n}(\frac{C_2}{C_1})^n\frac{1}{1-n}e^{(1-n)t/\theta}) + 2.5\frac{C_2}{C_1}t\} + \{\sum i^2P_{is} - 3\frac{K_p^2}{K_t}\theta(C_1^2 - C_2^2) - 5\sqrt{2}K_p\sqrt{K_i/K_t}C_1^{5/2}\theta(\sum_{\substack{n=0\\n\neq 1}}^{\infty}\binom{2.5}{n}(\frac{C_2}{C_1})^n\frac{1}{1-n})\}\times e^{-t/\theta} \tag{10}$$

Replacing t by $r\tau$ in eqs. (6)—(10), we can obtain the state values at the end of light-off period, $\sum R_{ir\tau}$, $M_{r\tau}$, $\sum P_{ir\tau}$, $\sum iP_{ir\tau}$ and $\sum i^2P_{ir\tau}$.

UV Light On

After the light-off period, the UV light is turned on by opening the shutter. Similarly, mass balances for total active polymer, monomer, and moments of dead polymer in this period are expressed as equations (1)—(5) with the initiation rate, $\Omega_i=2\phi_s I_{as}$. The five boundary conditions in this period are

$$\sum R_i(r\tau) = R_{ir\tau}$$

$$M(r\tau) = M_{r\tau}$$

$$\sum P_i(r\tau) = P_{ir\tau}$$

$$\sum iP_i(r\tau) = iP_{ir\tau}$$

$$\sum i^2P_i(r\tau) = i^2P_{ir\tau}$$

Thus, the final solutions for equations (1)—(5) are

$$\sum R_i(t) = \frac{\sqrt{\Omega_i/K_t}\left(Ce^{2\sqrt{\Omega_i K_t}(t-r\tau)} - 1\right)}{\left(1 + Ce^{2\sqrt{\Omega_i K_t}(t-r\tau)}\right)}$$

$$\simeq \sqrt{\Omega_i/K_t} \qquad \left(Ce^{2\sqrt{\Omega_i K_t}(t-r\tau)} >> 1\right) \tag{11}$$

$$M(t) = \frac{C_3}{C_4}\left(1 - e^{-C_4(t-r\tau)}\right) + M_{r\tau}e^{-C_4(t-r\tau)}$$

$$= C_5 - C_6e^{-C_4(t-r\tau)} \tag{12}$$

$$\sum P_i(t) = \frac{1}{2}\theta\Omega_i + (\sum P_{ir\tau} - \frac{1}{2}\theta\Omega_i)e^{-(t-r\tau)/\theta} \tag{13}$$

$$\sum iP_i(t) = K_p\sqrt{\Omega_i/K_t}\,\theta\Big(C_5 - \frac{C_6}{1-C_4\theta}e^{-C_4(t-r\tau)}\Big) + $$
$$+ \Big(\sum iP_{ir\tau} - K_p\sqrt{\Omega_i/K_t}\,\theta(C_5 - \frac{C_6}{1-C_4\theta})\Big)e^{-(t-r\tau)/\theta} \tag{14}$$

$$\sum i^2P_i(t) = \theta\Big(C_8 - \frac{C_9}{1-C_4\theta}e^{-C_4(t-r\tau)} + \frac{C_{10}}{1-2C_4\theta}e^{-2C_4(t-r\tau)}\Big) + $$
$$+ \Big(\sum i^2P_{ir\tau} - \theta(C_8 - \frac{C_9}{1-C_4\theta} + \frac{C_{10}}{1-2C_4\theta})\Big)e^{-(t-r\tau)/\theta} \tag{15}$$

where

$$C = (\sqrt{\Omega_i/K_t} + \sum R_{ir\tau})/(\sqrt{\Omega_i/K_t} - \sum R_{ir\tau})$$

$$C_3 = M_o/\theta - \Omega_i$$

$$C_4 = (\frac{1}{\theta} + K_p\sqrt{\Omega_i/K_t})$$

$$C_5 = C_3/C_4$$

$$C_6 = C_3/C_4 - M_{r\tau}$$

$$C_8 = 3C_5^2(K_p^2/K_t) + 5C_5K_p\sqrt{\Omega_i/K_t} + 2\Omega_i$$

$$C_9 = 6C_5C_6(K_p^2/K_t) + 5C_6K_p\sqrt{\Omega_i/K_t}$$

$$C_{10} = 3C_6^2(K_p^2/K_t)$$

Similarly replacing t by τ in equations (11)—(15), we can obtain the state values, $\sum R_{i\tau}$, M_τ, $\sum P_{i\tau}$, $\sum iP_{i\tau}$, and $\sum i^2P_{i\tau}$.

It is very often difficult to calculate and to measure the differential molecular weight distribution of a polymer but relatively easy to determine the moments of the molecular weight distribution. Therefore, these moments are often used to characterize the polymer.

Relations Among Cycles

Once the solutions of monomer concentration and polymer moments as a function of reaction time for the first cycle have been obtained analytically, an attempt to set up the cycle-variant for above properties in periodic operation is made.

For Cycle 1, where $0 \leq t \leq r\tau$

$$I_o(t) = 0 \quad \text{and} \quad M(0) = M_s$$

Thus integration of equation (2) yield,

$$M\Big|_{\substack{n=1 \\ I_o(t)=0}} = C_1 + C_2 e^{-t/\theta}$$

and

$$M\Big|_{\substack{n=1 \\ t=r\tau}} = A + BM_s$$

where

$$A = M_o(1 - e^{-r\tau/\theta})$$

$$B = e^{-r\tau/\theta}$$

Similarly, for cycle 1, where $r\tau \leq t \leq \tau$

$$I_o(t) = I_o \quad \text{and} \quad M_{r\tau} = M\Big|_{\substack{n=1 \\ t=r\tau}}$$

Thus integration of equation (2) for the new limits yields,

$$M\Big|_{\substack{n=1 \\ I_o(t)=I_o}} = C_5 - C_6 e^{-C_4(t-r\tau)}$$

and

$$M\Big|_{\substack{n=1 \\ t=\tau}} = D + EM_{r\tau}$$

$$= G + HM_s$$

where

$$D = \frac{C_3}{C_4}(1 - e^{-C_4\tau(1-r)})$$

$$E = e^{-C_4\tau(1-r)}$$

$$G = D + EA$$

$$H = BE$$

After repeating the above procedure for a number of cycles, the following relationships can be found.

$$M\Big|_{\substack{n=n \\ t=(r+n-1)\tau}} = P\sum_{\ell=0}^{\ell=n-2} H^{\ell} + H^{n-1}(A + BM_s) \tag{16}$$

and

$$M\Big|_{\substack{n=n \\ t=n\tau}} = G\sum_{\ell=0}^{\ell=n-1} H^{\ell} + H^{n}M_s \tag{17}$$

where n = cycle number; 2, 3, ... ∞

and

$$P = A + BD$$

Since H = BE < 1, so that

$$\sum_{\ell=0}^{n-1} H^{\ell} = \frac{1-H^n}{1-H}$$

which can be substituted into equations (16) and (17).

Expressions for the moments of dead polymer are similarly derived from the equations (8)—(10) and (13)—(15). For cycle 1, where $0 \leq t \leq r\tau$

$$\sum P_i\Big|_{\substack{n=1 \\ t=r\tau}} = S_1 + S_2\sum P_{is}$$

$$\sum P_i\Big|_{\substack{n=1 \\ t=\tau}} = S_3 + S_4\sum P_{ir\tau}$$

$$\sum iP_i\Big|_{\substack{n=1\\ t=r\tau}} = P_1 + P_2\sum iP_{is}$$

$$\sum iP_i\Big|_{\substack{n=1\\ t=\tau}} = P_3 + P_4\sum iP_{ir\tau}$$

$$\sum i^2P_i\Big|_{\substack{n=1\\ t=r\tau}} = X_1 + X_2\sum i^2P_{is}$$

$$\sum i^2P_i\Big|_{\substack{n=1\\ t=\tau}} = X_3 + X_4\sum i^2P_{ir\tau}$$

and for cycle n

$$\sum P_i\Big|_{\substack{n=n\\ t=(r+n-1)\tau}} = R_3\sum_{\ell=0}^{\ell=n-2} R_2^{\ell} + R_2^{n-1}(S_1 + S_2\sum P_{is})$$

$$\sum P_i\Big|_{\substack{n=n\\ t=n\tau}} = R_1\sum_{\ell=0}^{\ell=n-1} R_2^{\ell} + R_2^{n}\sum P_{is}$$

$$\sum iP_i\Big|_{\substack{n=n\\ t=(r+n-1)\tau}} = T_3\sum_{\ell=0}^{\ell=n-2} T_2^{\ell} + T_2^{n-1}(P_1 + P_2\sum iP_{is})$$

$$\sum iP_i\Big|_{\substack{n=n\\ t=n\tau}} = T_1\sum_{\ell=0}^{\ell=n-1} T_2^{\ell} + T_2^{n}\sum iP_{is}$$

$$\sum i^2P_i\Big|_{\substack{n=n\\ t=(r+n-1)\tau}} = Y_3\sum_{\ell=0}^{\ell=n-2} Y_2^{\ell} + Y_2^{n-1}(X_1 + X_2\sum i^2P_{is})$$

$$\sum i^2P_i\Big|_{\substack{n=n\\ t=n\tau}} = Y_1\sum_{\ell=0}^{\ell=n-1} Y_2^{\ell} + Y_2^{n}\sum i^2P_{is}$$

where n = cycle number; 2, 3, ... ∞

and

$$R_1 = S_3 + S_1S_4$$
$$R_2 = S_2S_4$$
$$R_3 = S_1 + S_2S_3$$
$$T_1 = P_3 + P_1P_4$$
$$T_2 = P_2P_4$$
$$T_3 = P_1 + P_2P_3$$
$$Y_1 = X_3 + X_1X_4$$
$$Y_2 = X_2X_4$$
$$Y_3 = X_1 + X_2X_3$$

Periodic Operation Experiment

Isothermal experiments were carried out at four temperatures namely, 338°K, 358°K, 373°K and 393°K. Temperatures were maintained by circulating oil through a constant temperature bath and the jacket around reactor. A tubing pump was used to maintain the feed flow into the reactor. The flow from the pump was calibrated occasionally using time flow technique. The product leaving the reactor as overflow from an opening at the top. The reaction volume, therefore can be considered to be constant irrespective of the fact that volume changes during polymerization. Three flow rates namely, 1.5, 2 and 4 c.c./min. were maintained during the experiment. UV light on/off control was carried out by manually operating a shutter in the UV path. On/off control by actually turning the UV lamp on and off was not feasible because the mercury vapor used in these experiments takes about 15-20 minutes to cool once it is turned off and can not be turned on again unless it is cooled to ambient temperature.

Reactor temperature was maintained at required level by circulating oil through its jacket. Reactants at room temperature were then fed into the reactor. When the light was turned on, the reactor temperature started to rise and the required temperature was maintained by constant temperature bath. When steady state is reached, the reaction was continued for at least one residence time in order to make sure that conversion, number average and weight average chain lengths also reach the steady state. UV on/off control was then used to continue the reaction beyond the lower steady state. The values of conversion and polydispersity at steady states are then used to compare the changes with UV on/off operation.

Results

The variation in the transient concentration of monomer and polydispersity of polymer in different cycles is shown in Figure 5. As may be seen, the cycle-invariant condition is eventually achieved where the initial and final state are equal. Analytical results of the transient behavior are shown in Figs. 6 through 9. The polydispersity becomes higher as the light is off. Because X_n does not increase as rapidly as X_w. From Figure 7 it is seen that the isothermal, unsteady state simulation is performed at conditions of several experimental runs. Good agreement is obtained between the analytical and numerical solution. The experimental results are shown in Figs. 10 through 20. The objective of the analytical and numerical solutions is to obtain a qualitative understanding of the experimental results. Experimental increases in polydispersity are less than those predictedly model. In our study, it is shown that the polydispersity increases with the value of τ_{off}/τ. Hence, wider molecular weight distribution comes from a wider range of free radical concentration existing inside the reactor with a larger value of τ_{off}/τ under unsteady state operation.

In our photopolymerization case the steady state polydispersity

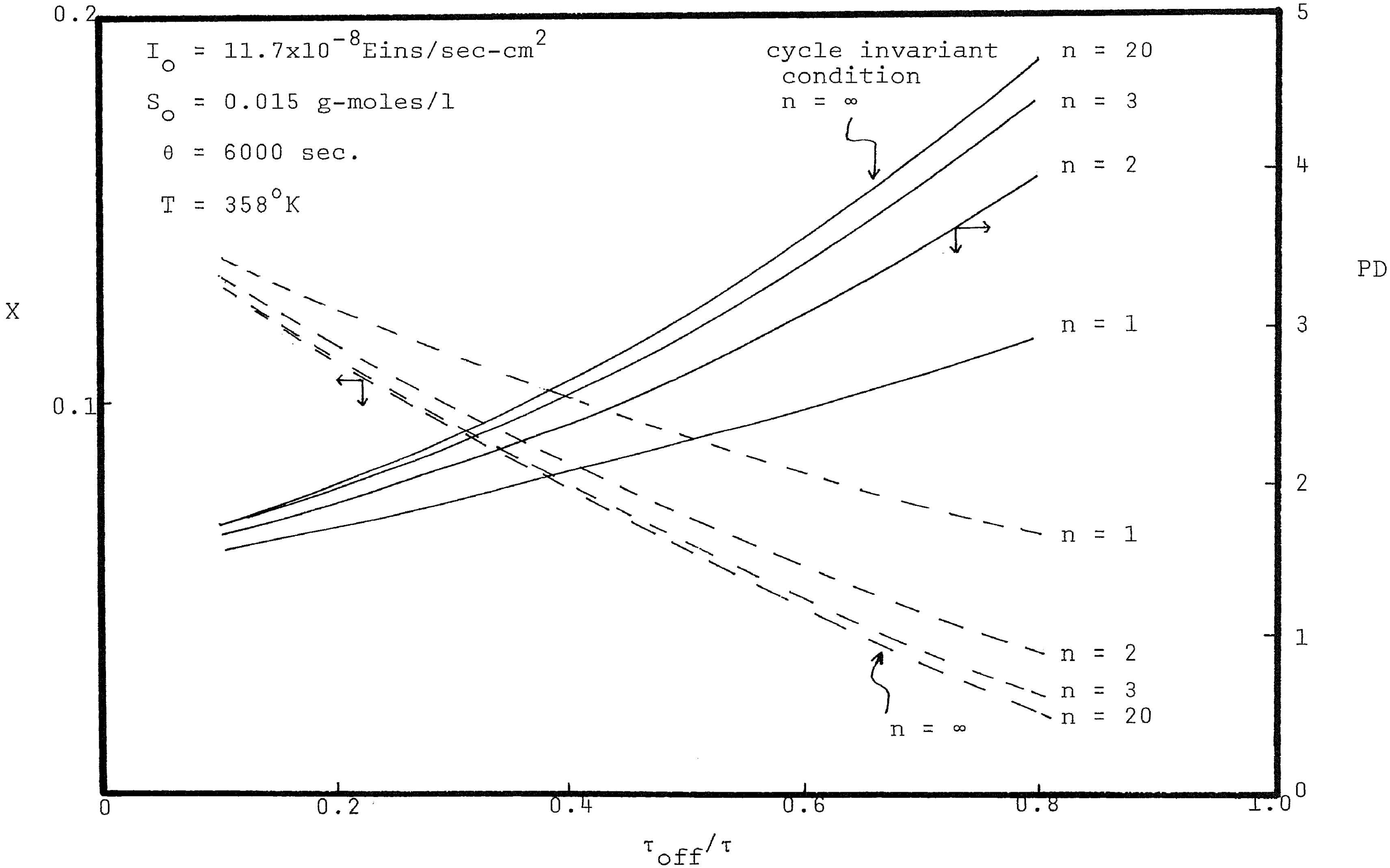

Figure 5. Time Profile of Reactor Behavior

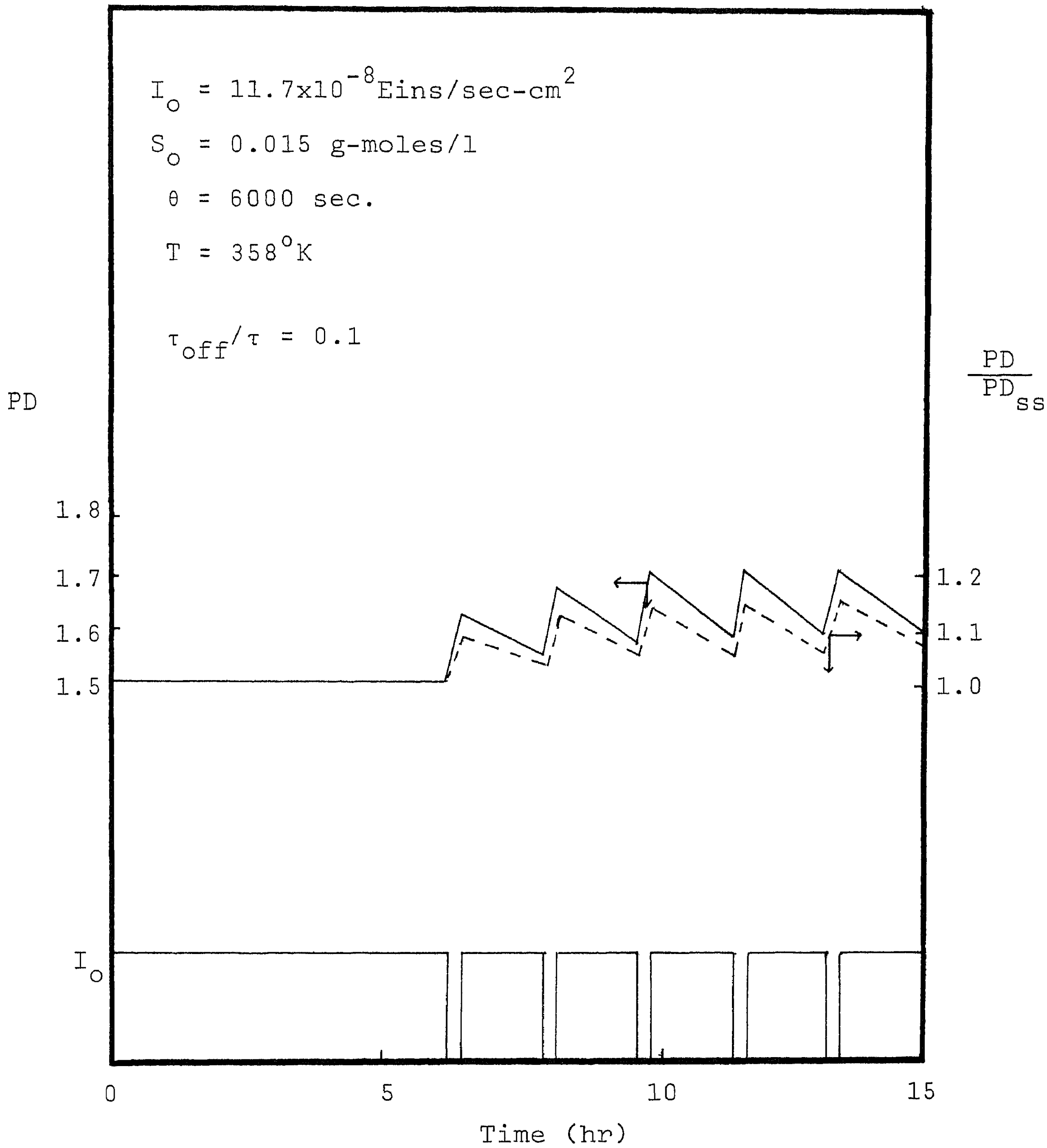

Figure 6. Transient Response to Perturbation from Stable Polydispersity at τ_{off}/τ = 0.1

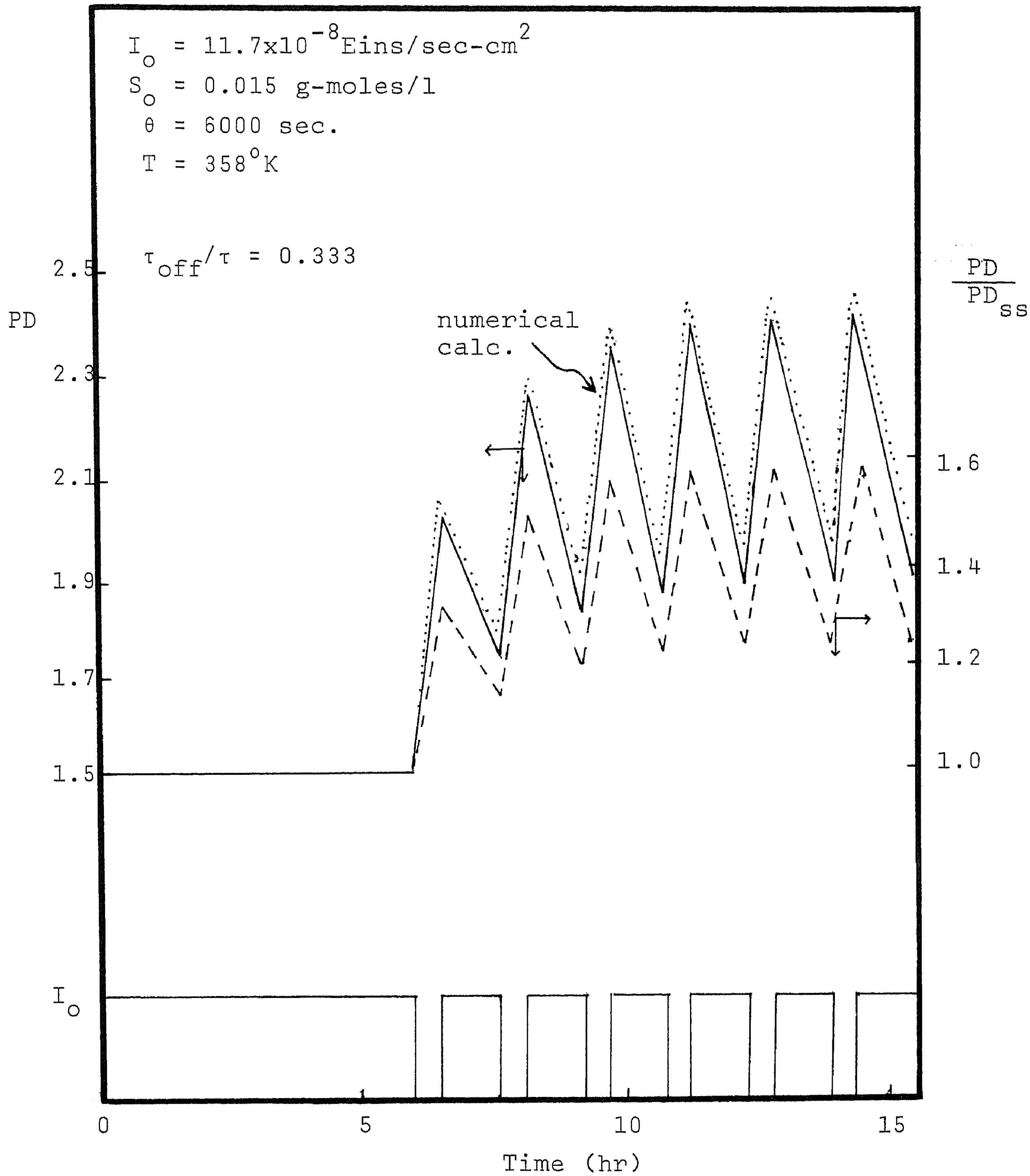

Figure 7. Transient Response to Perturbation from Stable Polydispersity at τ_{off}/τ = 0.333

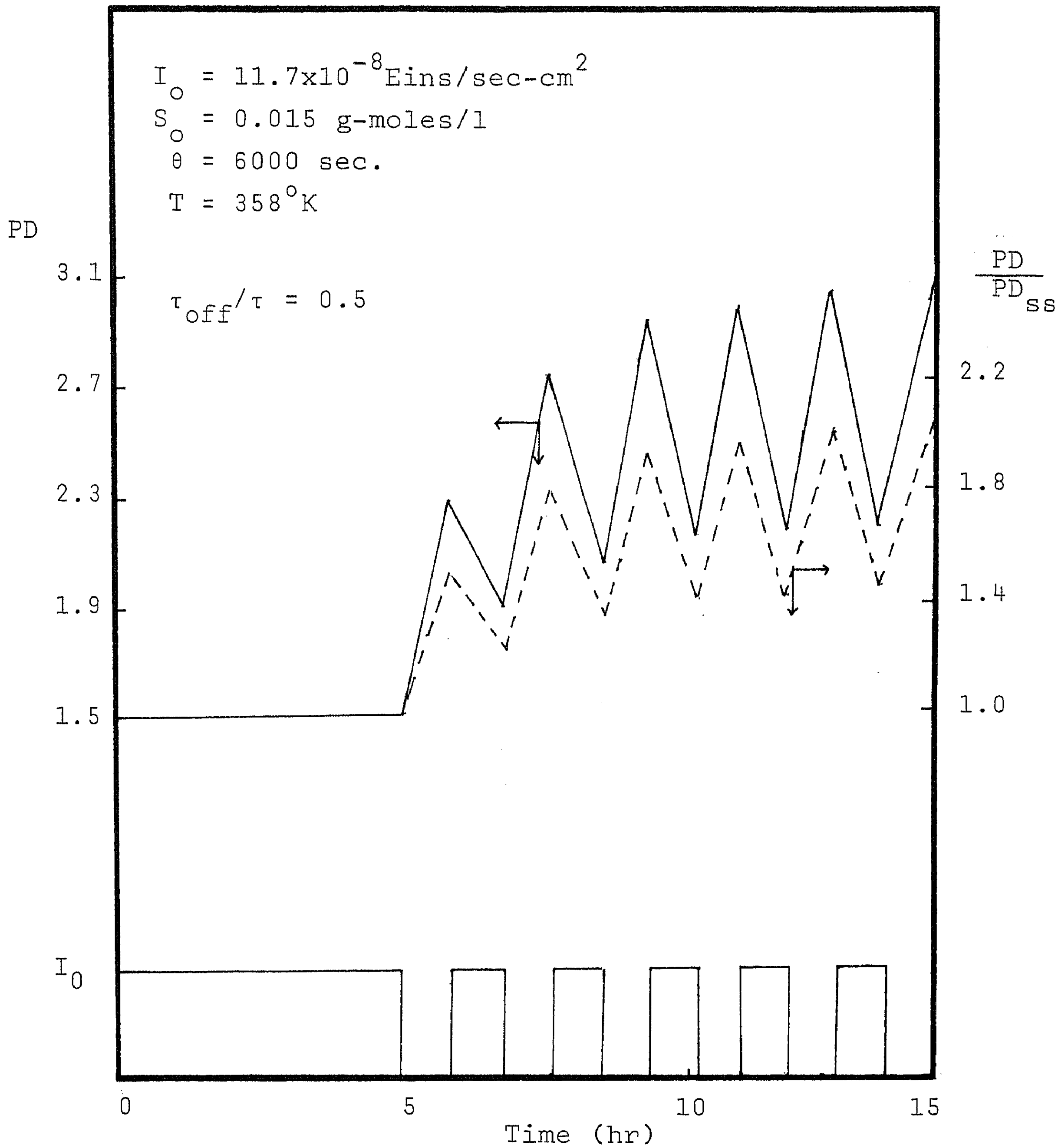

Figure 8. Transient Response to Perturbation from Stable Polydispersity at $\tau_{off}/\tau = 0.5$

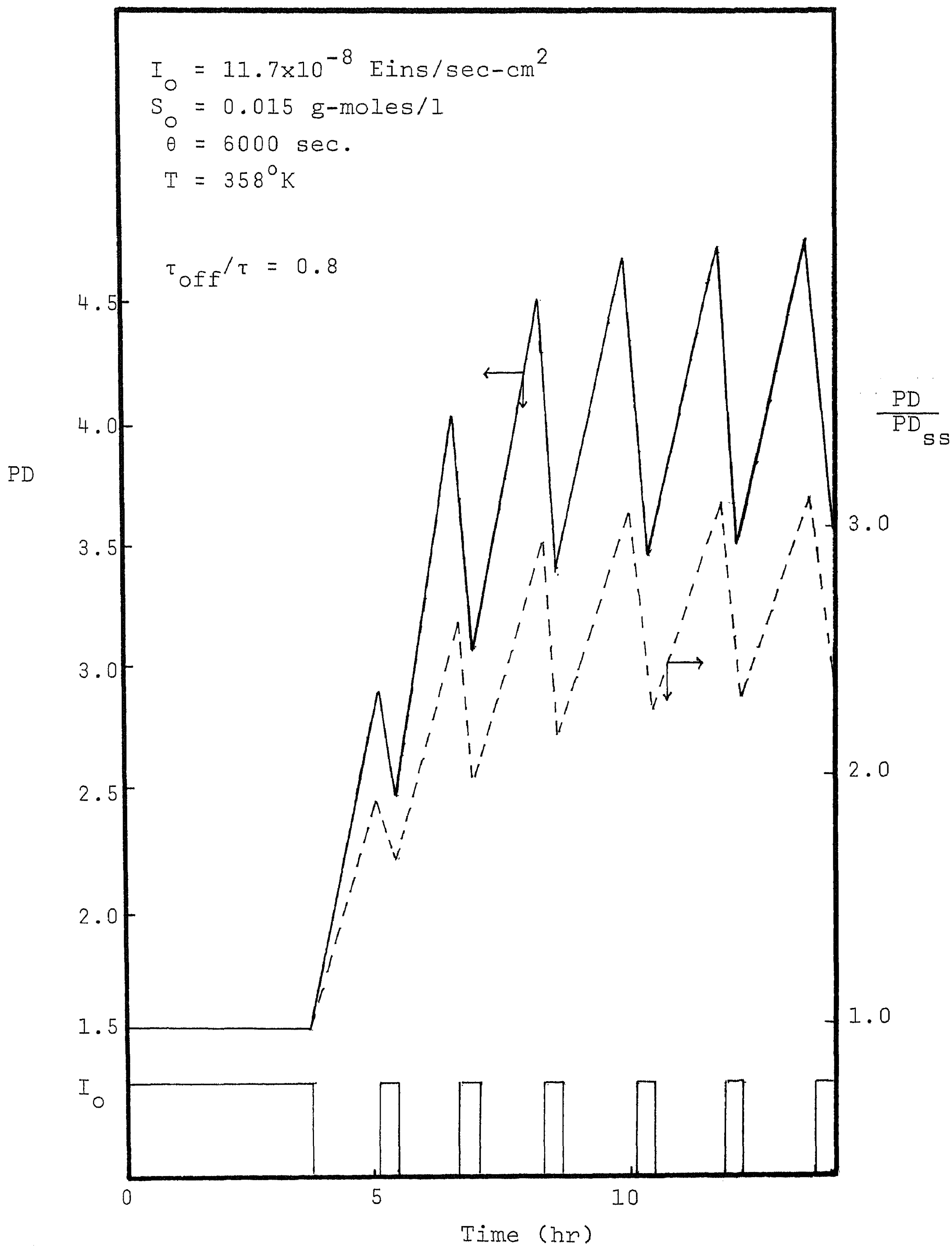

Figure 9. Transient Response to Perturbation from Stable Polydispersity at τ_{off}/τ = 0.8

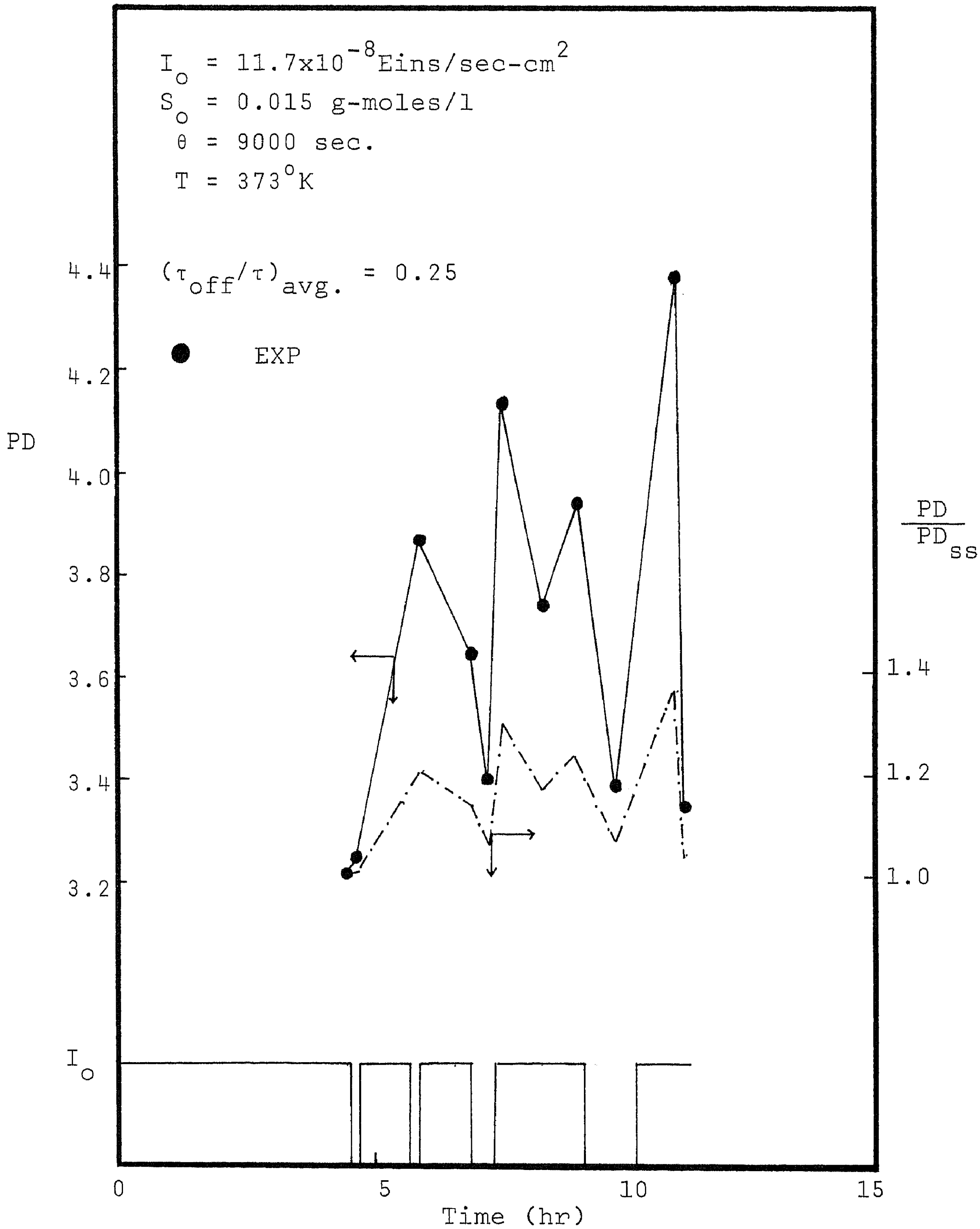

Figure 10. Experimental Data of Transient Response to Perturbation at $(\tau_{off}/\tau)_{av.} = 0.25$, $\theta = 9000$ sec and $T = 373^{o}K$

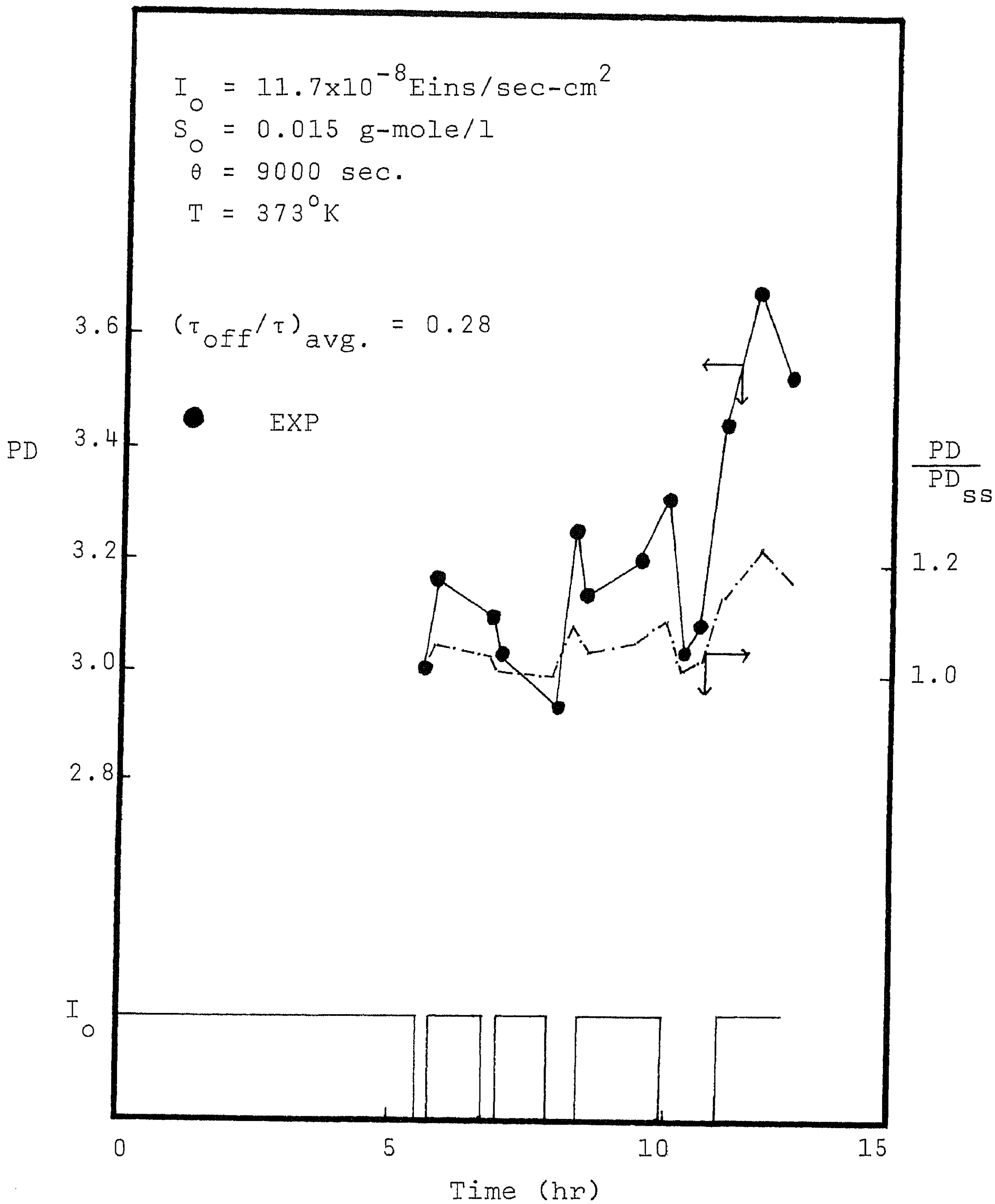

Figure 11. Experimental Data of Transient Response to Perturbation at $(\tau_{off_o}/\tau)_{av.} = 0.28$, θ = 9000 sec and T = 373^{o}K

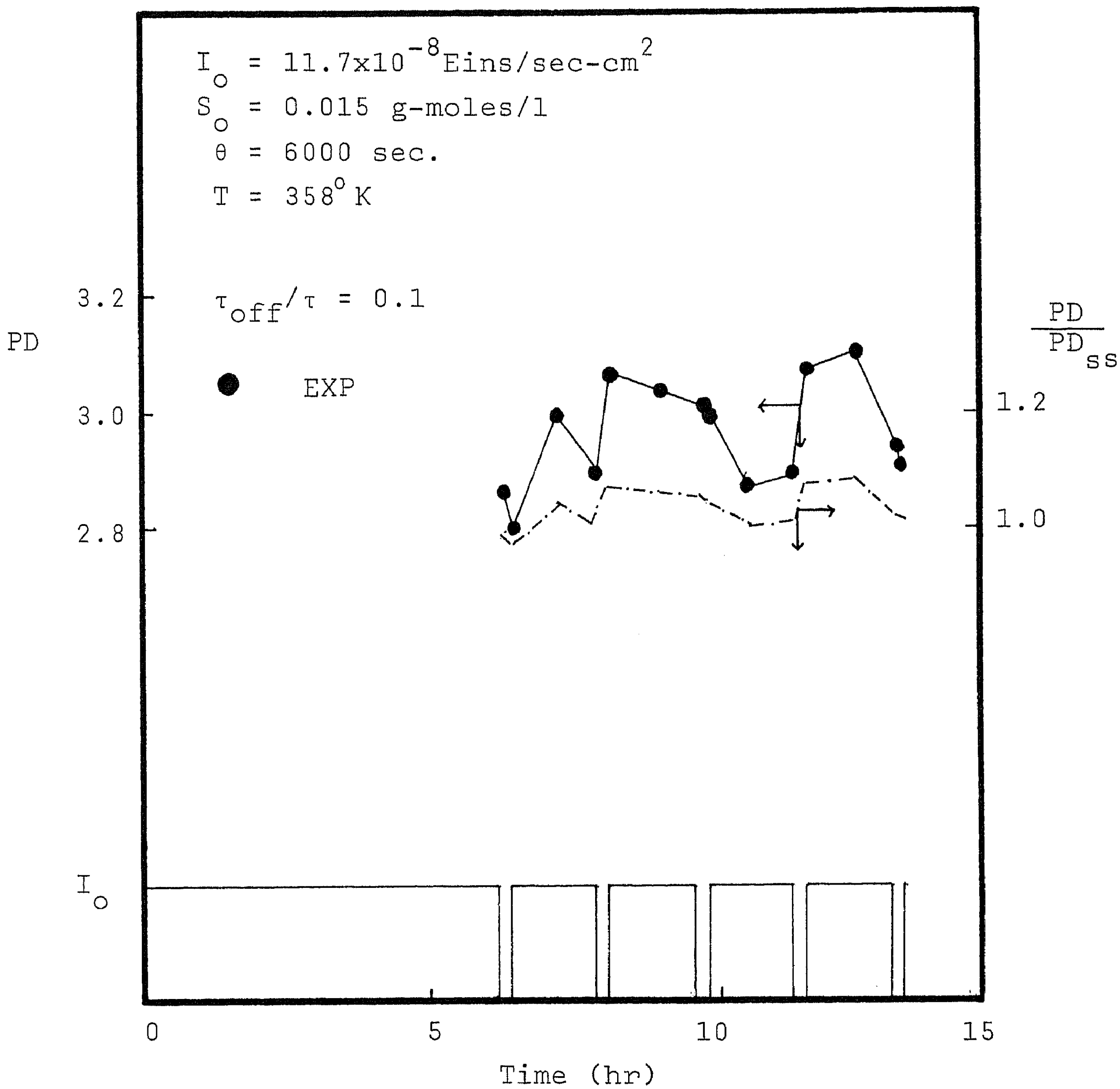

Figure 12. Experimental Data of Transient Response to Perturbation at τ_{off}/τ = 0.1, θ = 6000 sec and T = 358^{o}K

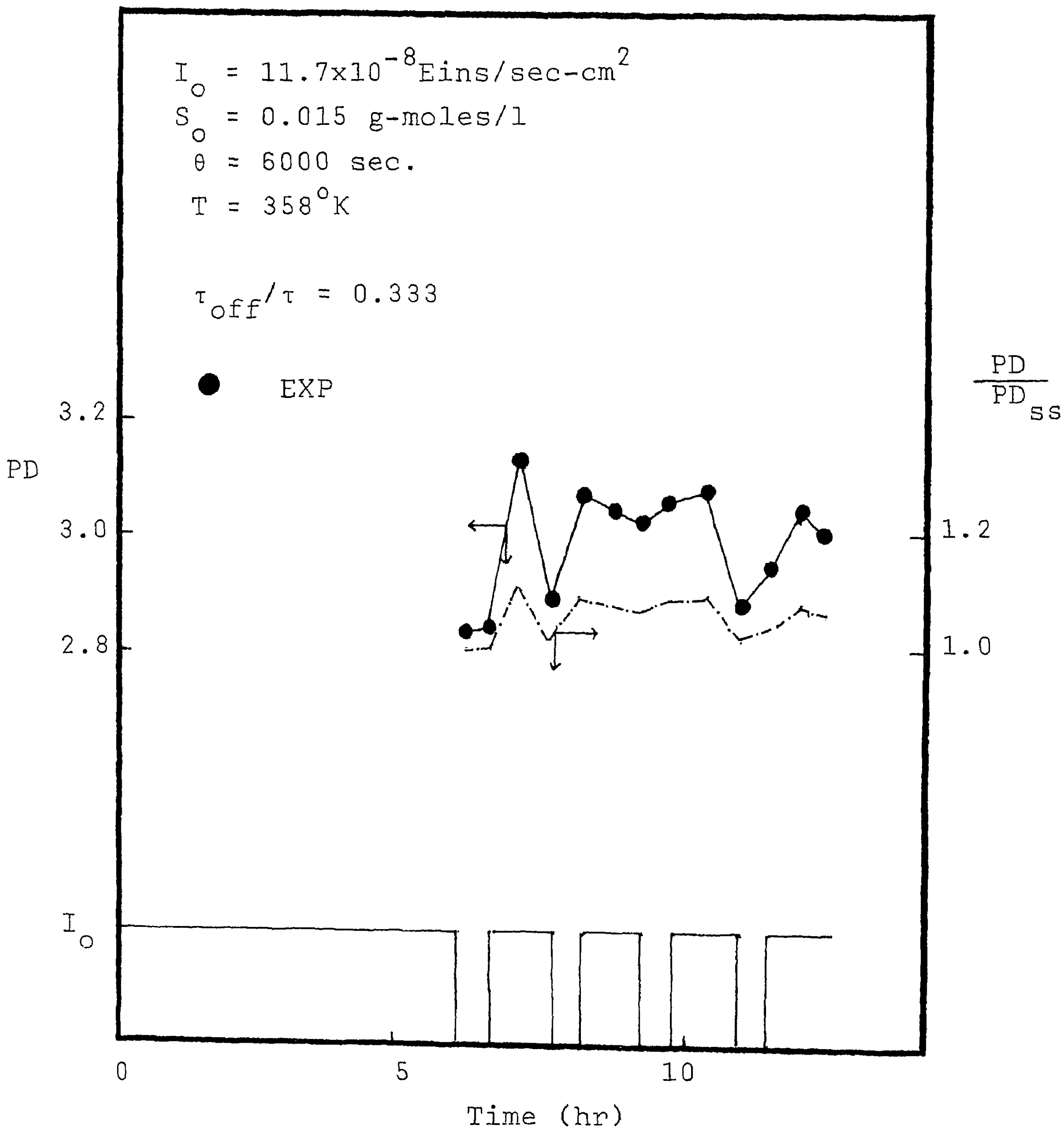

Figure 13. Experimental Data of Transient Response to Perturbation at $\tau_{off}/\tau = 0.333$, θ = 6000 sec and T = 358°K

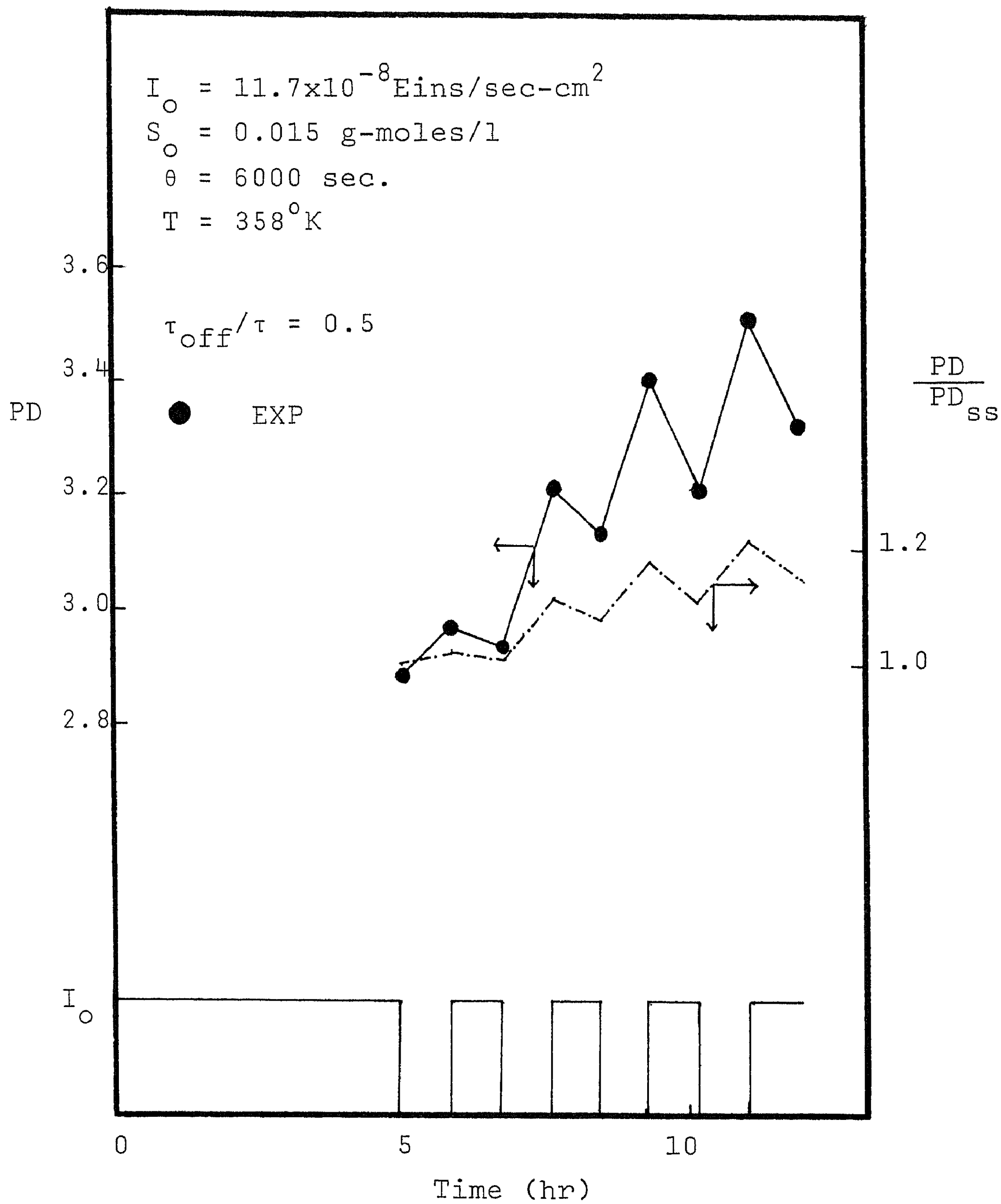

Figure 14. Experimental Data of Transient Response to Perturbation at τ_{off}/τ = 0.5, θ = 6000 sec and T = 358°K

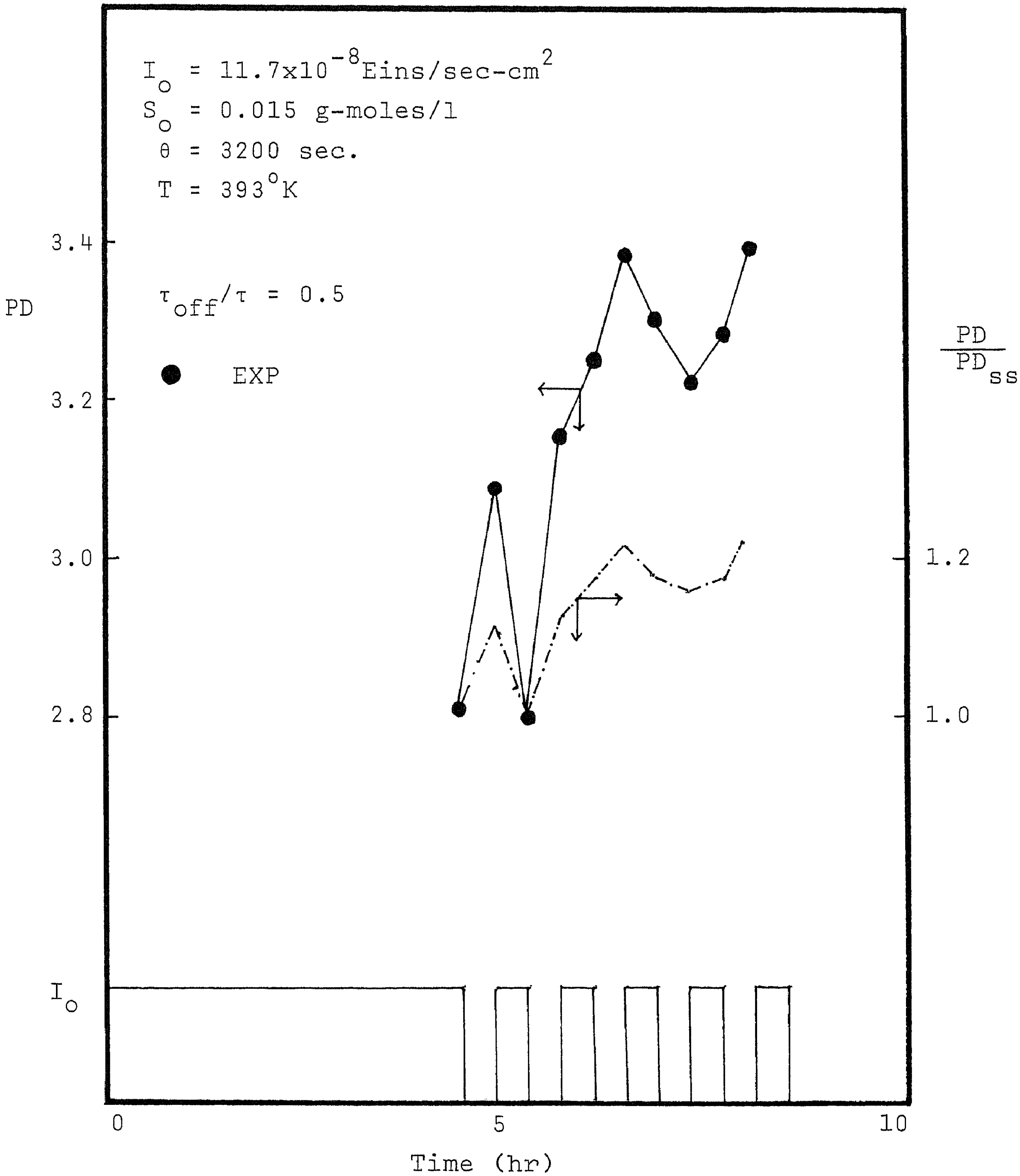

Figure 15. Experimental Data of Transient Response to Perturbation at τ_{off}/τ = 0.5, θ = 3200 sec and T = 393°K

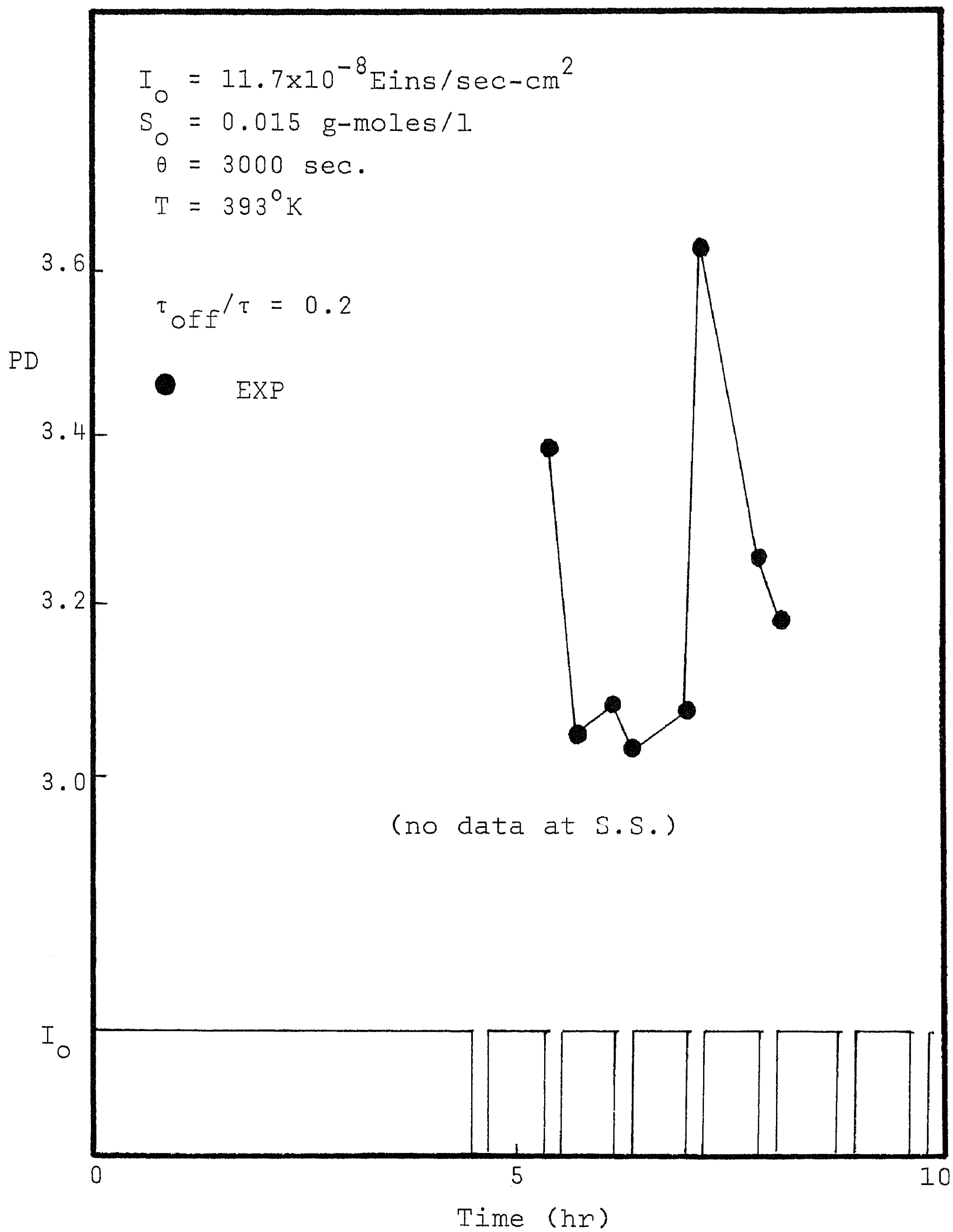

Figure 16. Experimental Data of Transient Response to Perturbation at $\tau_{off}/\tau = 0.2$, $\theta = 3000$ sec and $T = 393^{o}K$

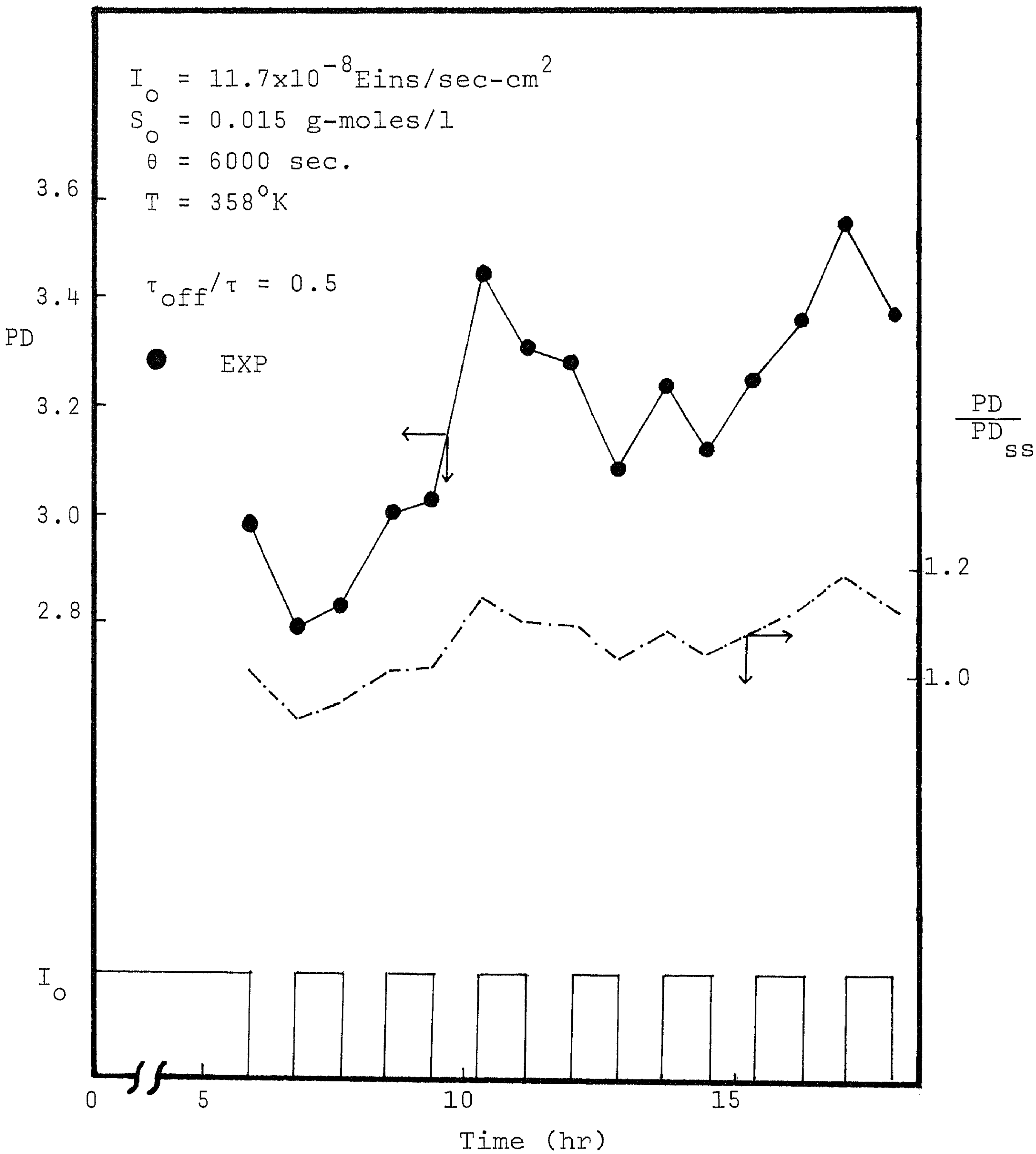

Figure 17. Experimental Data of Transient Response to Perturbation at $\tau_{off}/\tau = 0.5$, $\theta = 6000$ sec and T = 358°K

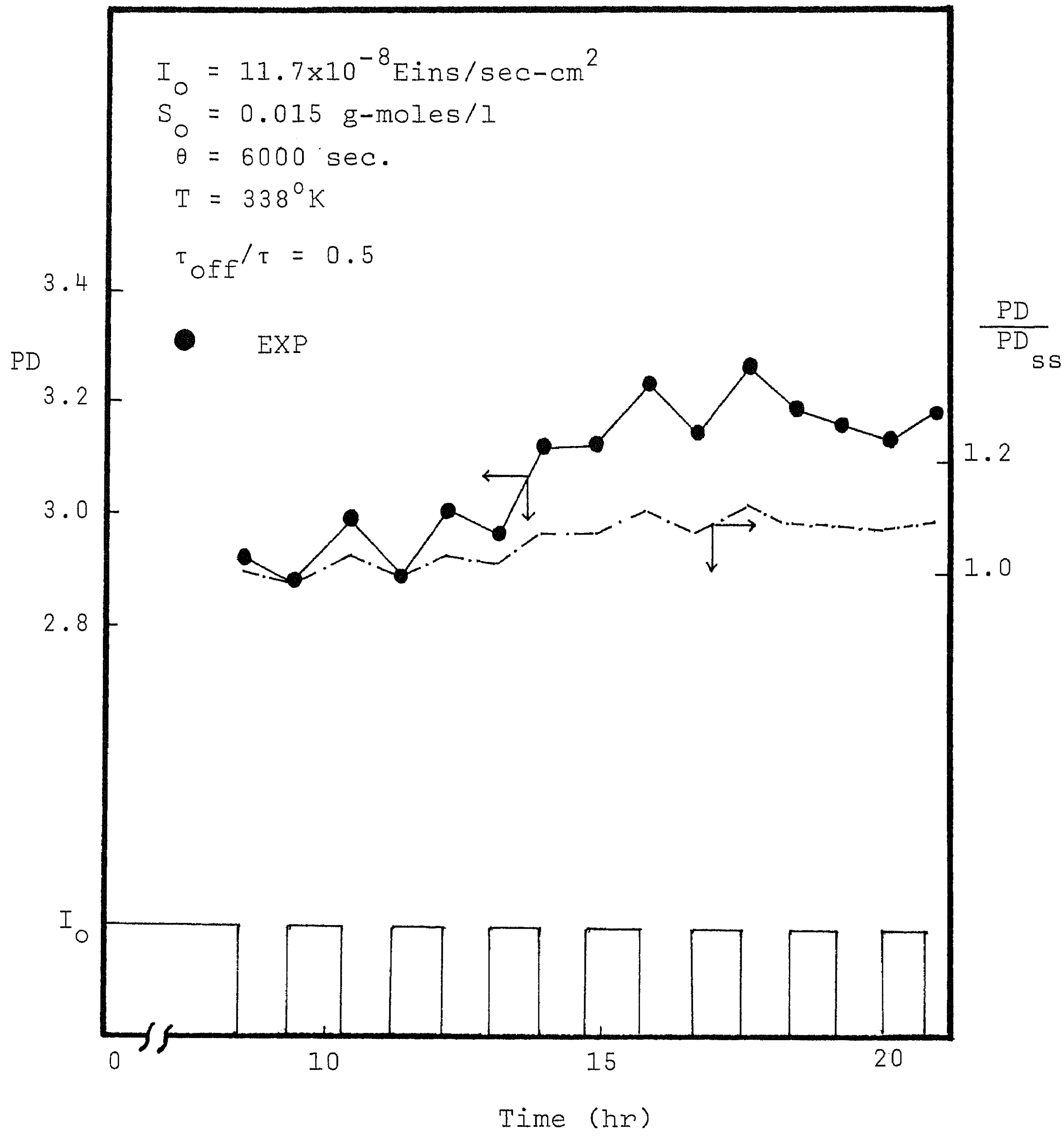

Figure 18. Experimental Data of Transient Response to Perturbation at τ_{off}/τ = 0.5, θ = 6000 sec and T = 338°K

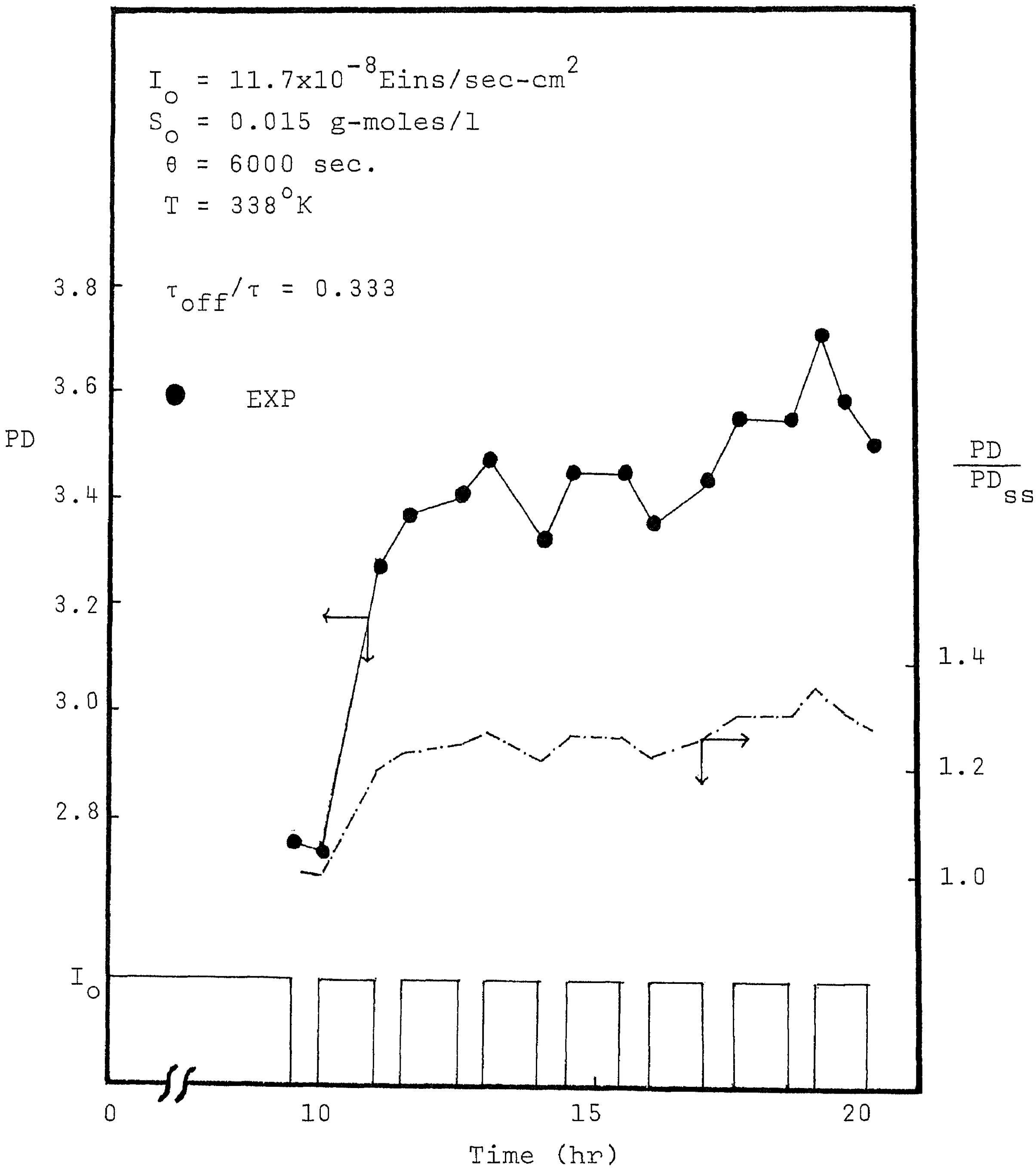

Figure 19. Experimental Data of Transient Response to Perturbation at τ_{off}/τ = 0.333, θ = 6000 sec and T = 338°K

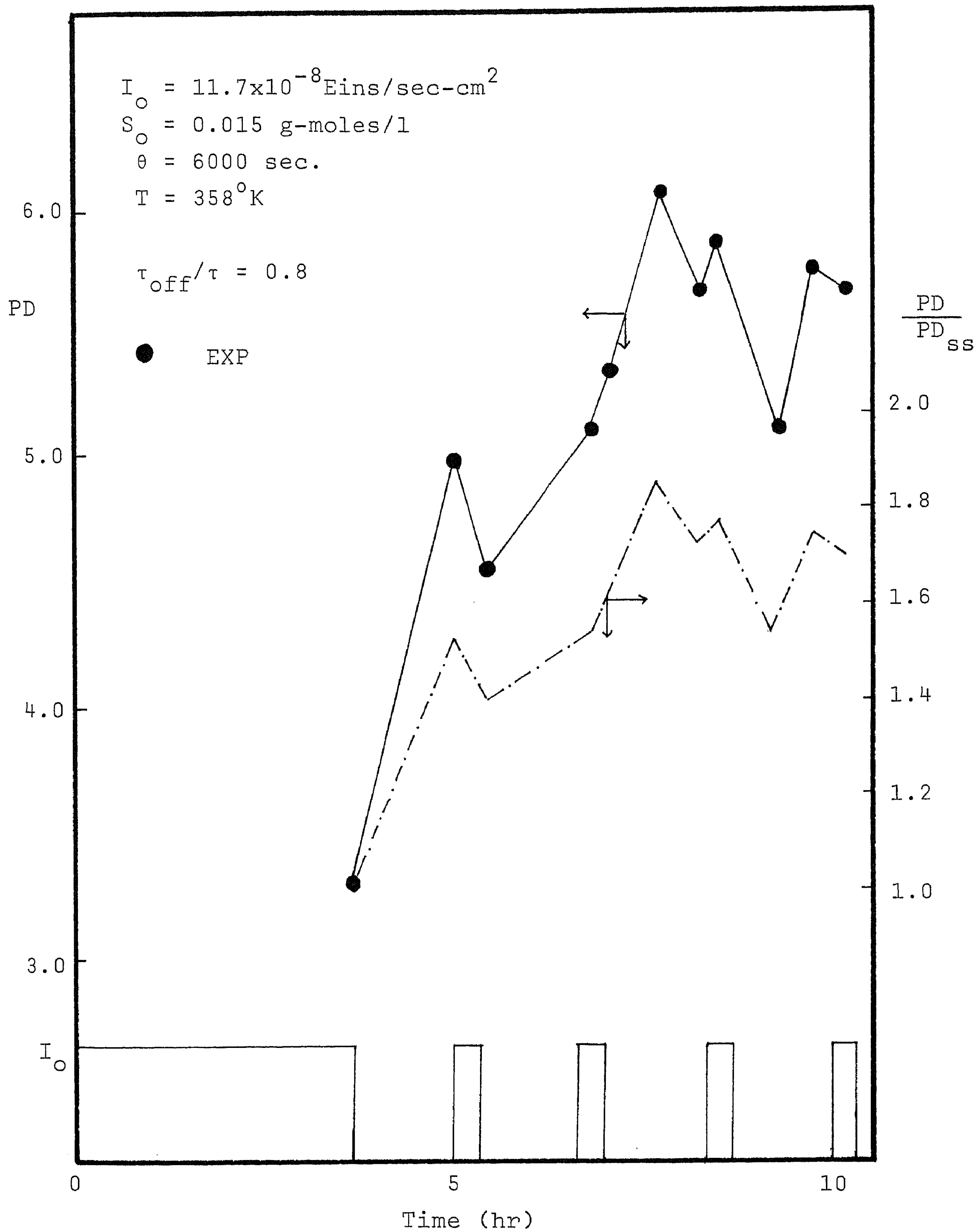

Figure 20. Experimental Data of Transient Response to Perturbation at τ_{off}/τ = 0.8, θ = 6000 sec and T = 358 °K

will always be about 1.5 analytically as shown in Appendix A. Thus, there is no possibility of molecular weight distribution width flexibility in the steady state. As to the experimental result, the polydispersity is about 3.0 and a broader molecular weight distribution is obtained at steady state. The disagreements show that the model does not describe the experimental results well. An attempt will be made on development of a mathematical model to correlate the effects of mixing on photosensitized polymerizations due to nonuniform distribution of the absorbed light intensity. The effect of temperature on polydispersity is summarized by Figure 21. The model prediction is the increase of polydispersity with decreasing temperature at a given value of τ_{off}/τ.

Molecular Weight Distribution

The distribution of molecular weights in a polymeric material may be represented as a differential distribution. A smooth curve results from the numerous points on the graph, although there are no values of P_i except for integer values of i. The weight distribution function W_i is defined by

$$W_i = \frac{\text{weight of dead polymer of length } i}{\text{total weight of dead polymer}}$$

The solution of a reactor model consisting of a very large number of non-linear algebraic equations will owing to the calculation tediousness and difficulty be possible only with the help of computers. Such a big number of equations to be solved requires theoretically an excessive need of mass storage and large computing time. In practical work however this demand

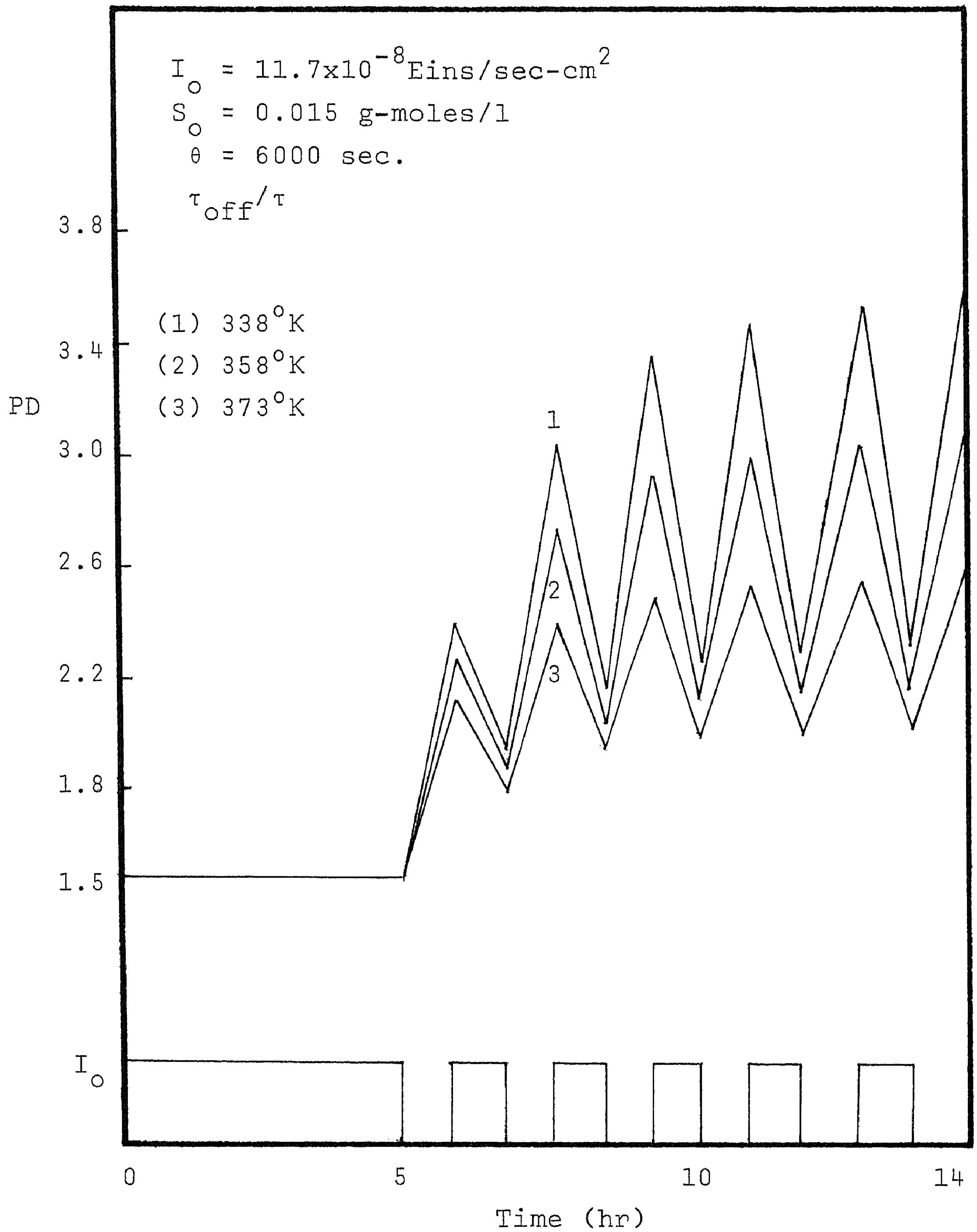

Figure 21. Effect of Temperature on the Transient Response of Polydispersity

is not particularly restrictive, because in our technical photo-polymerizations usually appears of polymerization up to 4×10^3. A problem of up to which degree of polymerization should the distribution be accounted for depends on the parameter τ_{off}/τ, the ratio of light-off period to light on-ff period, used in our system. Of course, a suitable termination criterion should be oriented on the sum of the individual weight fraction W_i. This sum must be equal to 1.0 theoretically, when all the polymers are taken into consideration. For a physical standpoint it seems more reasonable to terminate the calculation for $i=i^*$ where

$$1 - \sum_{i=1}^{i^*} W_i \leq 0.005$$

in our system. More computation time will be needed for a strong tailing of distribution to meet the criterion.

Mathematical Equations for MWD

Material balances for dead polymers are

$$\frac{dP_2}{dt} = \frac{1}{2}K_t R_1 R_1 - \frac{P_2}{\theta}$$

$$\frac{dP_3}{dt} = K_t R_1 R_2 - \frac{P_3}{\theta}$$

$$\frac{dP_4}{dt} = K_t (R_1 R_3 + \frac{1}{2} R_2 R_2) - \frac{P_4}{\theta}$$

$$\frac{dP_5}{dt} = K_t (R_1 R_4 + R_2 R_3) - \frac{P_5}{\theta}$$

$$\frac{dP_6}{dt} = K_t (R_1 R_5 + R_2 R_4 + \frac{1}{2} R_3 R_3) - \frac{P_6}{\theta}$$

.

.

.

The generalized expression will be

$$\frac{dP_i}{dt} = \frac{1}{2}K_t \sum_{j=1}^{i-1} R_j R_{i-j} - \frac{P_i}{\theta} \qquad (18)$$

$$i = 2, 3, \cdots \infty$$

For the periodic process, the rate equation (18) is solved and the effects of the system parameter on the molecular weight distribution are examined. After solving the differential equation (18), it is possible to obtain the concentration of each of a large number of polymer species during the course of polymerization. The reactor is to be operated isothermally and the volumetric change will be neglected. The rate constants are assumed to be independent of molecular size.

UV Light Off

A QSSA with respect to the concentration of free radicals for each chain length can be assumed

$$R_1 = \frac{2K_i M^3}{K_p M + K_t \Sigma R_i} \qquad (19)$$

$$R_i = \left(\frac{K_p M}{K_p M + K_t \Sigma R_i} \right)^{i-1} R_1 \qquad (20)$$

$$i = 2, 3, \cdots \infty$$

By the substitution of equations (6), (19)-(20) into equation (18), one obtains

$$\frac{dP_i}{dt} = 2(i-1)K_t K_i^2 K_p^{i-2} M^{i+4} (K_p M + \frac{1}{t})^{-i} - \frac{P_i}{\theta} \qquad (21)$$

Since $K_p M >> \frac{1}{t}$ in our system, equation (21) reduces to

$$\frac{dP_i}{dt} = 2(i-1)K_t K_i K_p^{-2} M^4 \tag{22}$$

Substituting equation (7) in equation (22), and using the initial condition that

$$P_i(0) = P_{is}$$

then the solution for the period, $0 \leq t \leq r\tau$, is given by

$$P_i(t) = A_1(C_1^4 + 4C_1^3 C_2 \frac{t}{\theta} e^{-t/\theta} - 6C_1^2 C_2^2 e^{-2t/\theta} - 2C_1 C_2^3 e^{-3t/\theta} - \frac{1}{3} C_2^4 e^{-3t/\theta})$$
$$+ \left(P_{is} - A_1(C_1^4 - 6C_1^2 C_2^2 - 2C_1 C_2^3 - \frac{1}{3} C_2^4)\right) e^{-t/\theta} \tag{23}$$
$$i = 2, 3, \cdot \cdot \cdot \cdot \infty$$

where P_{is} is the concentration of dead polymer species at steady state, and

$$A_1 = 2(i-1)K_t K_i^2 K_p^{-2} \theta$$

Replacing t by $r\tau$ in equation (23), we can obtain the concentration of dead polymer at the end of light-off period, $P_{ir\tau}$.

UV Light On

Similarly, application of the QSSA for the free radicals yields

$$R_1 = \frac{\Omega_i}{K_p M + K_t \Sigma R_i} \tag{24}$$

By substituting equations (11), (20) and (24) into equation (18), the rate of formation of dead polymer of chain length i is

$$\frac{dP_i}{dt} = D_1 K_p^{-i} M^{-2} \sum_{n=0}^{\infty} \binom{-i}{n} \left(\frac{D_2}{K_p M}\right)^n - \frac{P_i}{\theta} \tag{25}$$

where

$$D_1 = \sqrt{\Omega_i K_t}$$

$$D_2 = \frac{1}{2}(i-1) K_t K_p^{i-2} \Omega_i^2$$

and $D_2 < K_p M$ is reasinable for our system.

Substituting equation (12) into equation (25), then it can be integrated

$$P_i(t) = D_1 K_p^{-i} e^{-t/\theta} \sum_{n=0}^{\infty} \binom{-i}{n} \left(\frac{D_2}{K_p}\right)^n \int e^{t/\theta} \left(\frac{1}{C_5 - C_6 e^{-C_4(t-r\tau)}}\right)^{n+2} dt + ce^{-t/\theta} \tag{26}$$

Letting

$$x = C_5 - C_6 e^{-C_4(t-r\tau)}$$

and

$$D_3 = \frac{1}{C_4 \theta}$$

then the concentration of dead polymer of chain length i in eq. (26) is given by

$$P_i(t) = \frac{-D_1 K_p^{-i} (-C_6)^{D_3} e^{-(t-r\tau)/\theta}}{C_4} \sum_{n=0}^{\infty} \binom{-i}{n} \left(\frac{D_2}{K_p}\right)^n \int \frac{dx}{x^{n+2}(x-C_5)^{D_3+1}} + ce^{-t/\theta} \tag{27}$$

The integral in equation (27) is evaluated by

$$\int \frac{dx}{x^{n+2}(x-C_5)^{D_3+1}} = \frac{1}{x^{n+2}(x-C_5)^{D_3}} \sum_{\beta=0}^{\infty} (-1)^{\beta+1} \frac{(n+1+\beta)!(D_3-\beta-1)!}{(n+1)!D_3!} \left(\frac{x-C_5}{x}\right)^{\beta} \tag{28}$$

Substituting equation (28) into equation (27) and rearranging, then the solution for the concentration of dead polymer of chain length i, subject to the boundary condition $P_i(r\tau) = P_{ir\tau}$ for the period, $r\tau \leqq t \leqq \tau$, is

$$P_i(t) = \frac{-D_1 K_p^{-i} (-C_6)^{D_3} e^{-(t-r\tau)/\theta}}{C_4} \sum_{n=0}^{i} \binom{-i}{n} \left(\frac{D_2}{K_p}\right)^n \left(\frac{1}{C_5 - C_6 e^{-C_4(t-r\tau)}}\right)^n \times$$

$$\sum_{\beta=0}^{\infty} (-1)^{\beta+1} \frac{(n+1+\beta)!(D_3-\beta-1)!}{(n+1)!D_3!} \left(\frac{-C_6 e^{-C_4(t-r\tau)}}{C_5 - C_6 e^{-C_4(t-r\tau)}}\right)^\beta \times$$

$$\frac{1}{\left(C_5 - C_6 e^{-C_4(t-r\tau)}\right)^2 \left(-C_6 e^{-C_4(t-r\tau)}\right)^{D_3}}$$

$$+ \left\{ P_{ir\tau} + \frac{D_1 K_p^{-i} (-C_6)^{D_3}}{C_4} \sum_{n=0}^{i} \binom{-i}{n} \left(\frac{D_2}{K_p}\right)^n \left(\frac{1}{C_5 - C_6}\right)^n \times \right.$$

$$\left. \sum_{\beta=0}^{\infty} (-1)^{\beta+1} \frac{(n+1+\beta)!(D_3-\beta-1)!}{(n+1)!D_3!} \left(\frac{-C_6}{C_5-C_6}\right)^\beta \frac{1}{(C_5-C_6)^2 (-C_6)^{D_3}} \right\} \times e^{-(t-r\tau)/\theta} \qquad (29)$$

Once the concentration of dead polymer of chain length i as a function of time, $P_i(t)$ and the state value at the end of light-off period, $P_{ir\tau}$ are obtained, an expression for the P_i as a function of cycle number can be derived from the equations (23) and (29). By the same procedure as we described in the case of polydispersity, the following relationships can be found:

$$P_i\Big|_{\substack{n=1\\ t=r\tau}} = W_1 + W_2 P_{is}$$

$$P_i\Big|_{\substack{n=1\\ t=\tau}} = W_3 + W_4 P_{ir\tau}$$

and for cycle n

$$P_i\Big|_{\substack{n=n\\ t=(r+n-1)\tau}} = Q_3 \sum_{\ell=0}^{\ell=n-2} Q_2^{\ell} + Q_2^{n-1}(W_1 + W_2 P_{is})$$

$$P_i\Big|_{\substack{n=n\\ t=n\tau}} = Q_1 \sum_{\ell=0}^{\ell=n-1} Q_2^{\ell} + Q_2^{n} P_{is}$$

where n = cycle number; 2, 3, ... ∞

and

$$Q_1 = W_3 + W_1 W_4$$

$$Q_2 = W_2 W_4$$

$$Q_3 = W_1 + W_2 W_3$$

Discussion of MWD

Some advantages and disadvantages against other methods concerning the precision and expenditure, should be mentioned. The molecular weight distribution curves, which derived from the theoretical kinetics, can be obtained analytically for any location of any cycle as a function of time during the process. But if the numerical calculations are employed, the solutions should be obtained from the beginning and then continuing, and too many reaction rate equations may be needed to complete the distribution curves. Most of the molecular weight distribution is derived from the empirical formula or methodical techniques.

Here the theoretical method is introduced, which is more precise because it does not need any approximation in the calculation procedure. In contrary, the theoretical method demands more computation of the molecular weight distribution to obtain precise distribution curves. Also, it enables one to reduce an infinite number of equations to a finite number, in which a degree of polymerization step of 25 may be involved.

An outstanding effect of the parameter τ_{off}/τ, ratio of light-off period to forced period, on the molecular weight distribution is shown together with the distribution curve at a real steady state in Figures 22 through 24 at different temperatures. Broadening distribution with longer tailing is formed at controlled steady state.

Representative chromatograms are presented in Figures 25 through 28. These are the plots of the molecular weight distribution at a steady state against that of a UV light-off period perturbation about the steady state. In each case, the molecular weight distribution from the steady state and the cyclic operation are essentially not the same and the distribution from the cyclic operation gets broader.

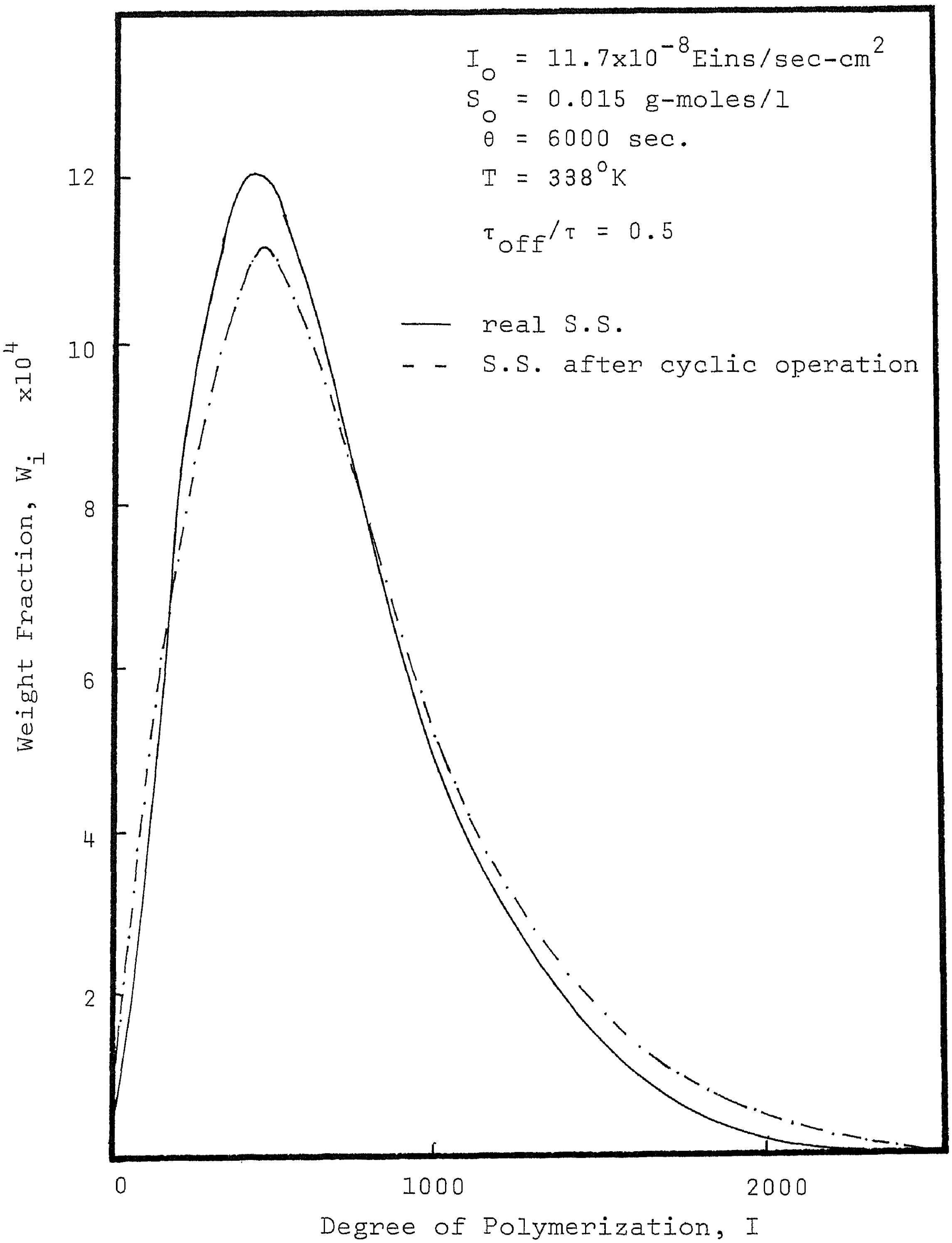

Figure 22. MWD Broadening after Periodic Operation at τ_{off}/τ = 0.5, θ = 6000 sec and T = 338^{o}K

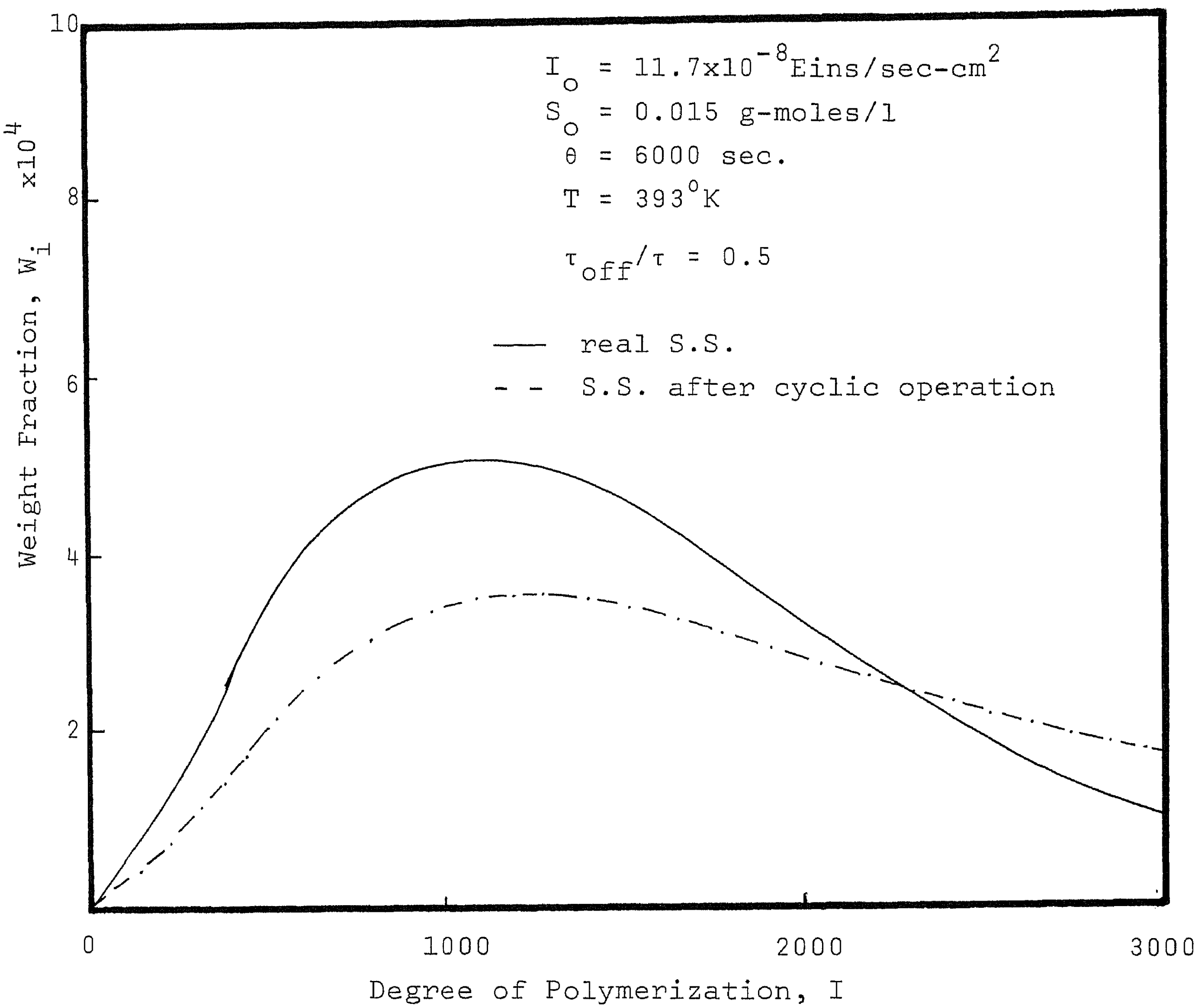

Figure 23. MWD Broadening after Periodic Operation at $\tau_{off}/\tau = 0.5$, $\theta = 6000$ sec and $T = 393^oK$

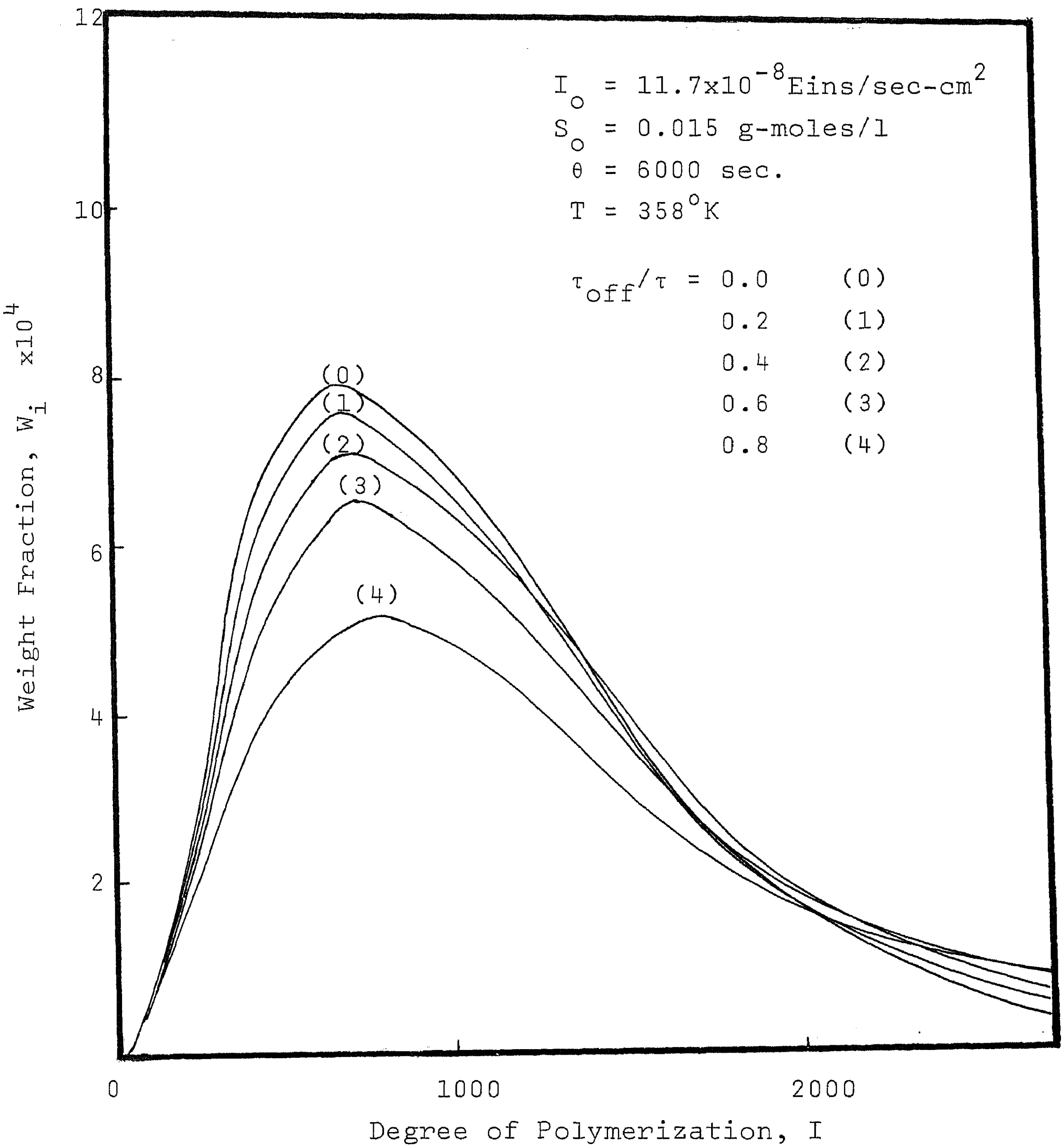

Figure 24. Effect of τ_{off}/τ on MWD Broadening

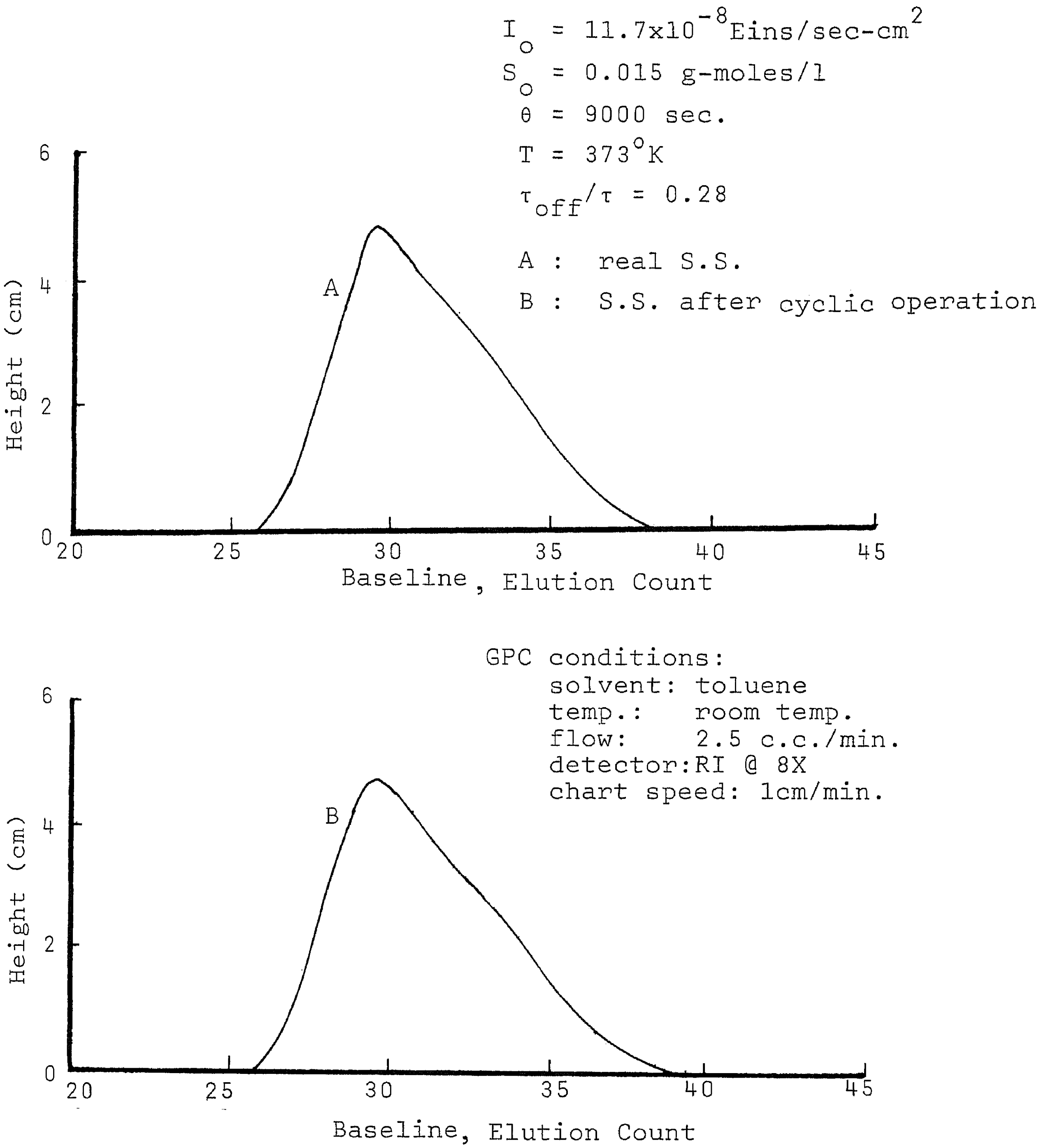

Figure 25. GPC Curves Attainable by Steady State and Periodic Operation at τ_{off}/τ = 0.28, θ = 9000 sec and T = 373^{o}K

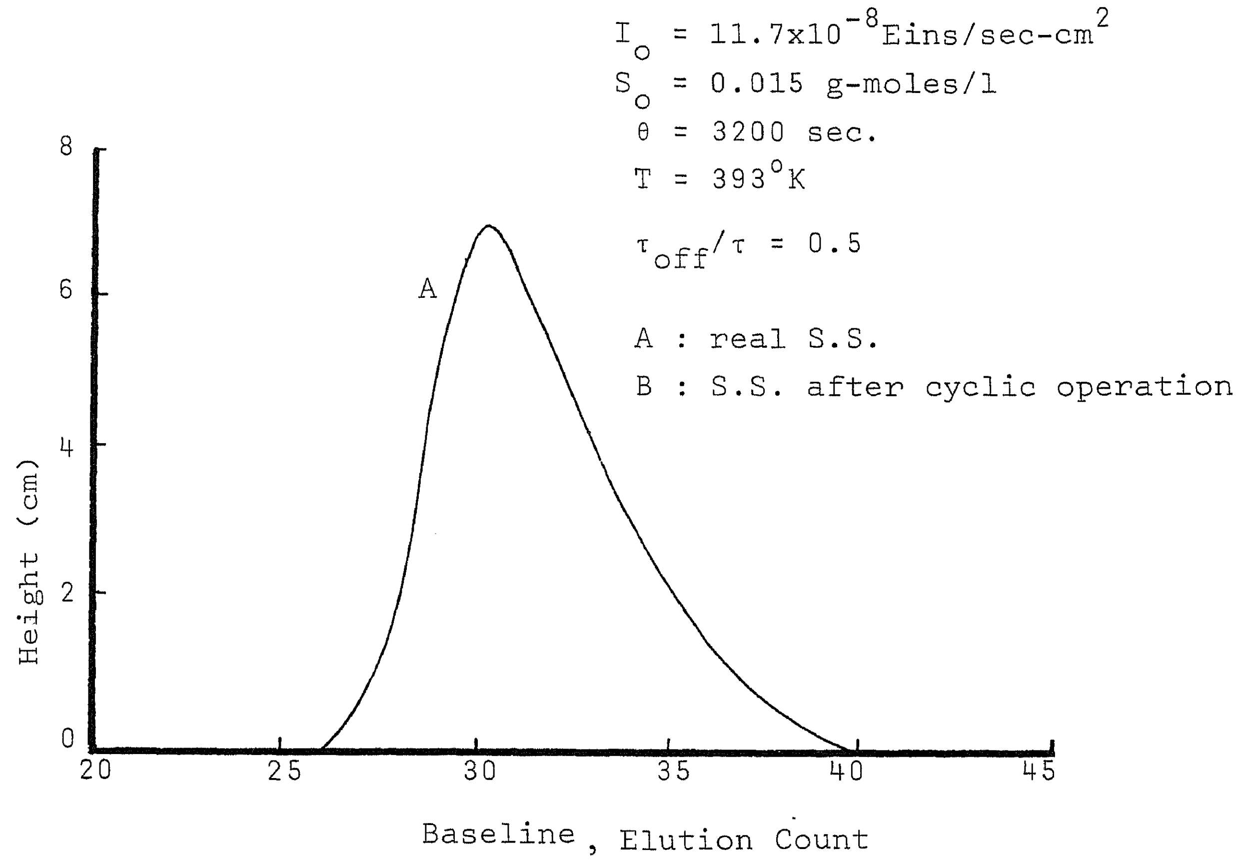

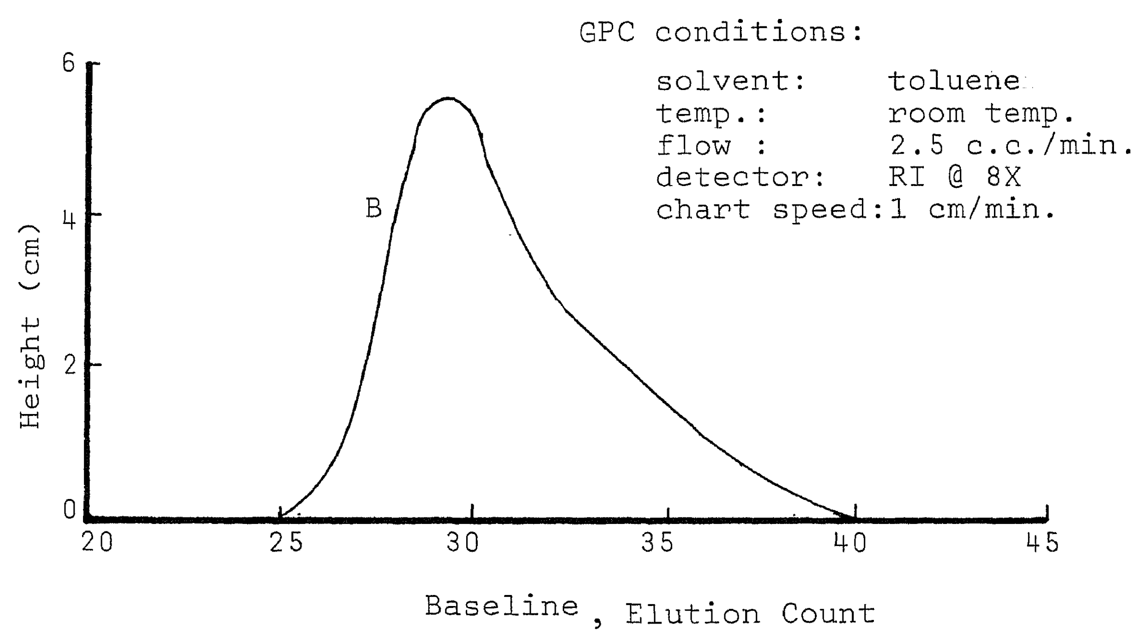

Figure 26. GPC Curves Attainable by Steady State and Periodic Operation at $\tau_{off}/\tau = 0.5$, $\theta = 3200$ sec and $T = 393^{\circ}K$

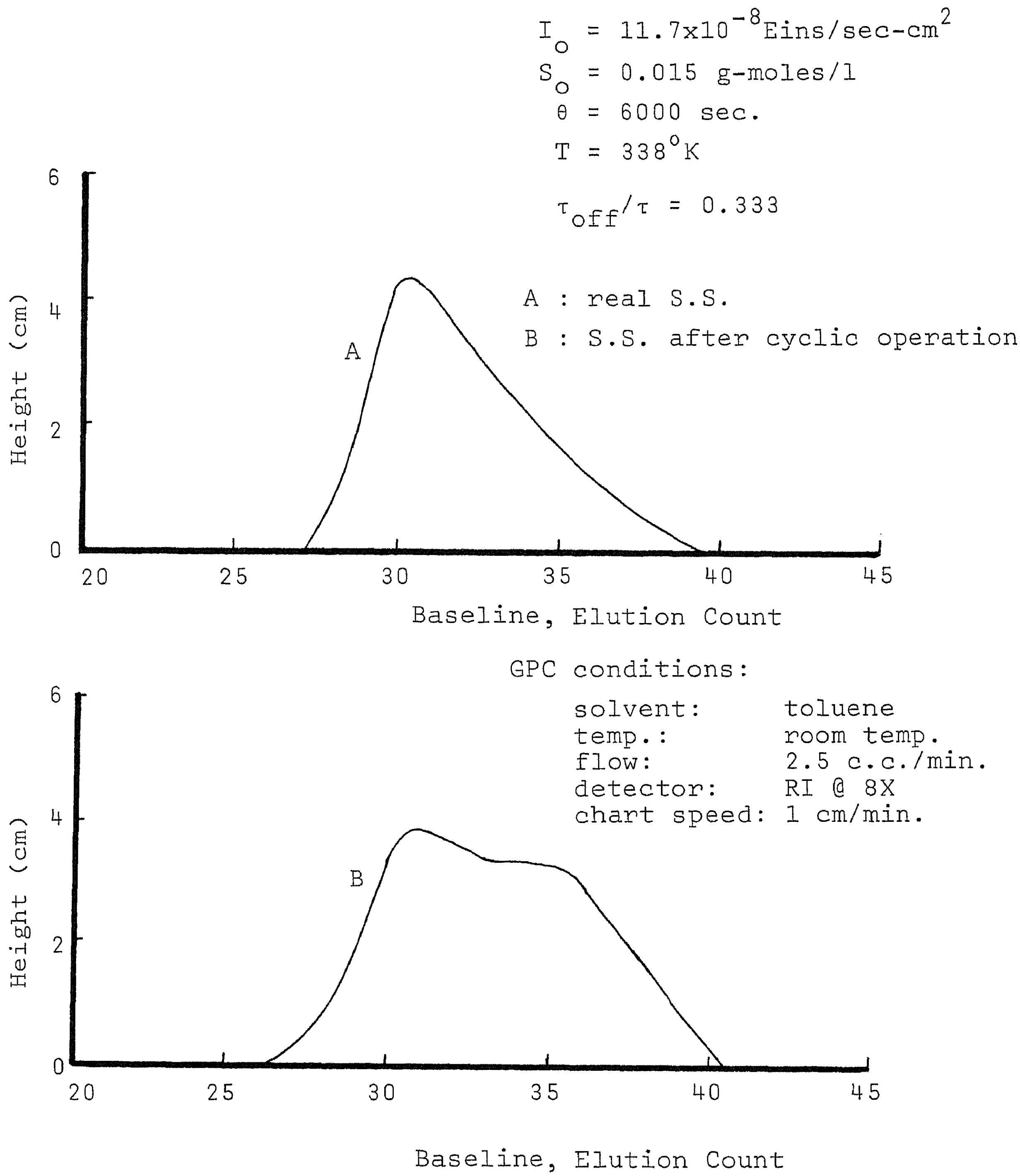

Figure 27. GPC Curves Attainable by Steady State and Periodic Operation at τ_{off}/τ = 0.333, θ = 6000 sec and T = 338°K

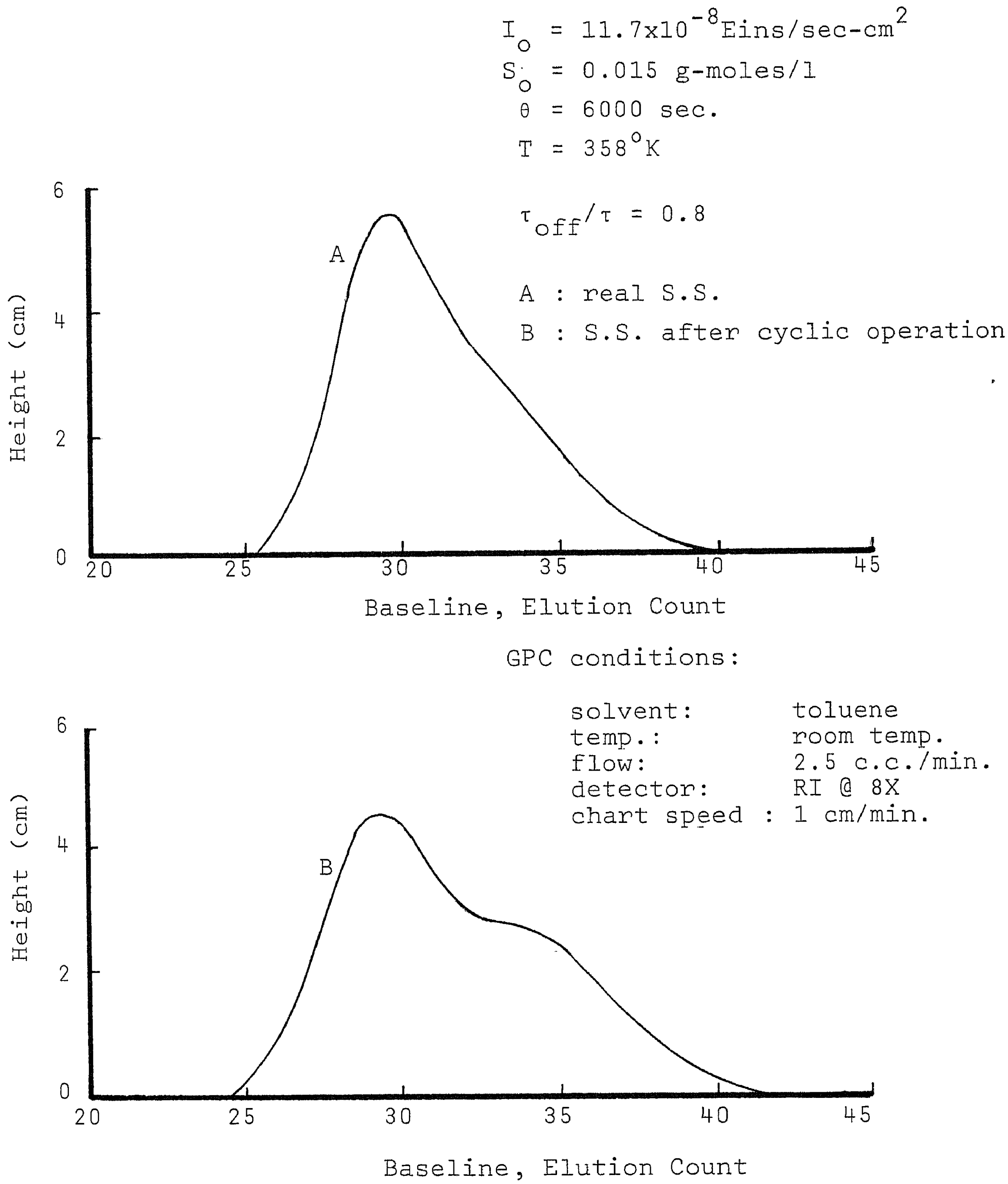

Figure 28. GPC Curves Attainable by Steady State and Periodic Operation at τ_{off}/τ = 0.8, θ = 6000 sec and T = 358^{o}K

CHAPTER 5

AN ANALYTICAL STUDY OF A NONUNIFORMLY INITIATED PHOTOPOLYMERIZATION

In this study, the analysis is based on the irradiation of chemical species circulating in a continuous stirred-tank reactor having a high dose rate region and a very low dose rate region. A schematic diagram of the reactor used is shown in Figure 29.

A volume V_L (Region I) is illuminated with a parallel, effectively uniform beam of absorbed radiation. For these conditions, and with negligible reflection, the total rate of light absorption is averaged over the path length of the light within the lighted volume. The remaining volume of the reactor, V_D (Region II), is irradiated with a very low dose rate. A stirred provides mixing between and within these two regions.

The model consists of measuring the monomer concentration, sensitizer concentration, and three moments of the dead polymer in the reactor as a function of time with three certain parameters such as the size of the lighted volume, the volumetric pumping rate between regions, and the absorbed intensity in region II. The absorbed intensity profile along the axial direction of the reactor is shown in Figure 30 at different values of sensitizer concentration and can be expressed by

$$I_{as} = I_o \epsilon_s S e^{-(\epsilon_s S + \epsilon_m M)x}$$

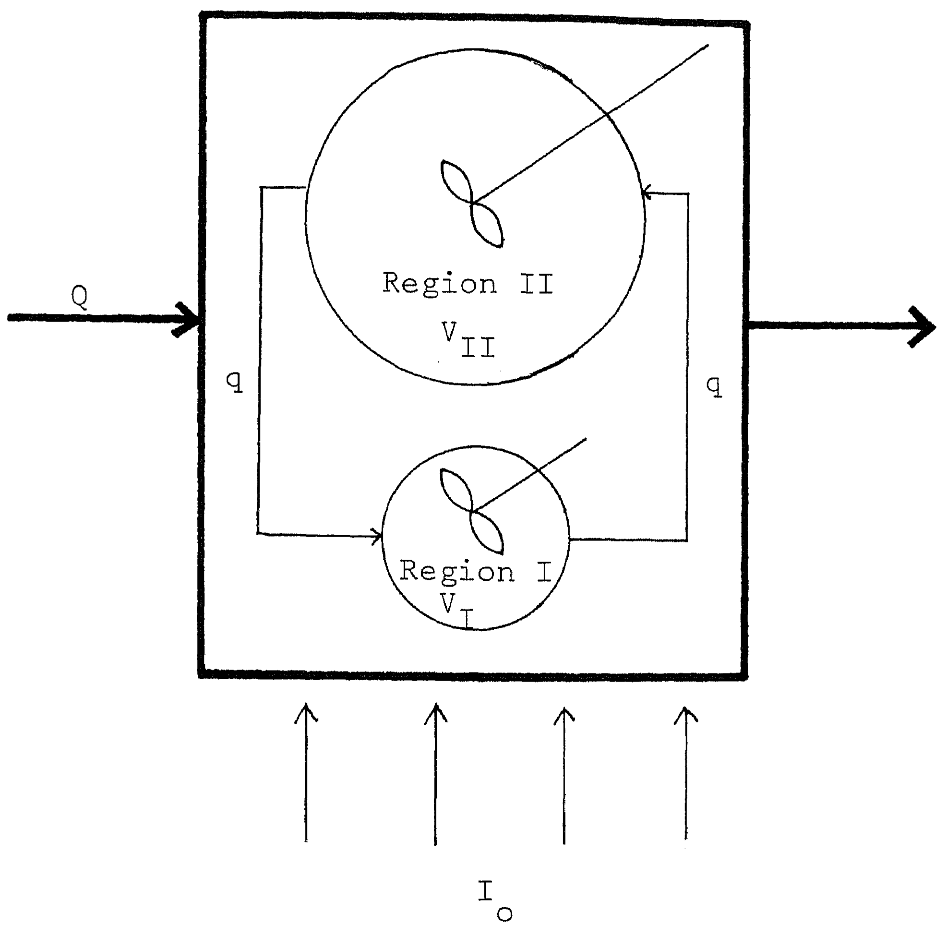

Figure 29. Schematic Flow Pattern in Reactor

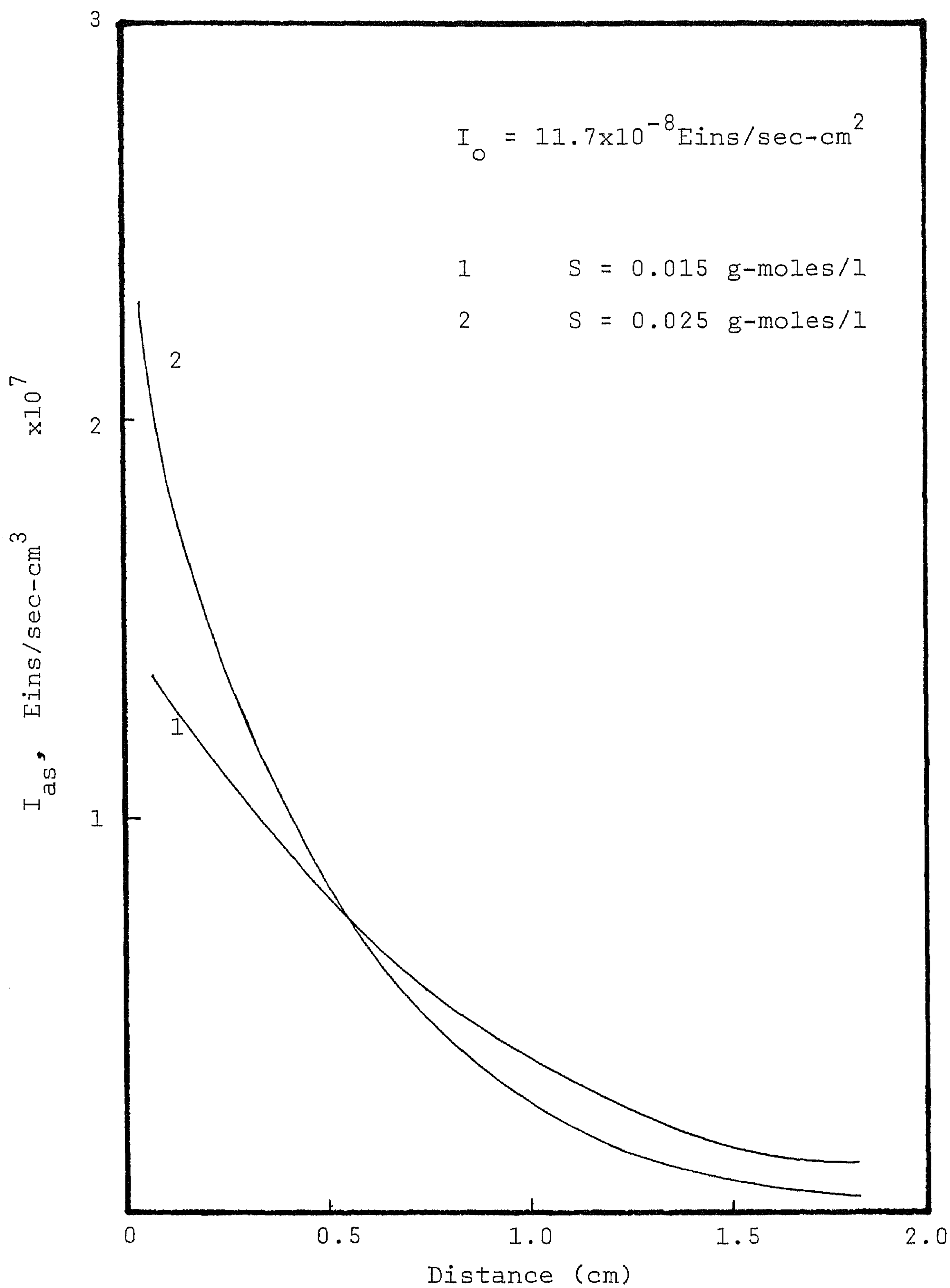

Figure 30. Rate of Absorbed Light Intensity Distribution in the Reactor

Due to the light attenuation of axial nonuniformities and the existence of agitator, the volume of the region I and the rate of light absorption in region II will be found. Mixing phenomena are important in determining the observed reaction rate and molecular weight distribution in optically dense photoreaction mixtures in our study. The accurate prediction of mixing effects requires a detailed knowledge of the mechanism of the reaction of interest, the physics of the radiation used, and the mixing pricesses themselves. The mixing process in a stirred vessel has been studied by Marr et al. (48). They found volumetric pumping rate to be dependent upon the agitator speed N, and impeller diameter D according to the equation

$$q = fND^3$$

where f is the coefficient of impeller discharge.
Since q value can not be measured experimentally, an empirical correlation will be used.

In photochemical reactions, nonuniform initiation results from radiation attenuation or from partial illumination of the reaction volume. In either case large initiation rates are found in certain regions of the reaction volume, and small rates in others. The rate of mass transfer in the direction of initiation rate variation will then be a factor determining average reactant concentration and hence the observed reaction rate.

Model Development

In region I, mass balances on the growing radicals, monomer and three moments of dead polymer in CSTR are expressed by the following equations: (44)

$$\frac{dS_I}{dt} = \frac{QS_o}{(V_I+V_{II})} + \frac{(1+\epsilon X_{II})S_{II} - (1+\epsilon X_I)S_I}{\theta_I} - \phi_s I_{asI} - \frac{QS_I}{(V_I+V_{II})} \quad (1)$$

$$\frac{dM_I}{dt} = \frac{QM_o}{(V_I+V_{II})} + \frac{(1+\epsilon X_{II})M_{II} - (1+\epsilon X_I)M_I}{\theta_I} - K_p M_I \sum R_{iI} - \frac{QM_I}{(V_I+V_{II})} \quad (2)$$

$$\frac{d\sum P_{iI}}{dt} = K_{fmI} M_I \sum R_{iI} + \frac{1}{2} K_{tI} \sum R_{iI}{}^2 + \frac{(1+\epsilon X_{II})\sum P_{iII} - (1+\epsilon X_I)\sum P_{iI}}{\theta_I} - \frac{Q\sum P_{iI}}{(V_I+V_{II})} \quad (3)$$

$$\frac{d\sum iP_{iI}}{dt} = K_{tI} \sum R_{iI} \sum iR_{iI} + K_{fmI} M_I \sum iR_{iI} + \frac{(1+\epsilon X_{II})\sum iP_{iII} - (1+\epsilon X_I)\sum iP_{iI}}{\theta_I} - \frac{Q\sum iP_{iI}}{(V_I+V_{II})} \quad (4)$$

$$\frac{d\sum i^2 P_{iI}}{dt} = K_{tI} \sum R_{iI} \sum i^2 R_{iI} + K_{tI} \sum iR_{iI}{}^2 + K_{fmI} M_I \sum i^2 R_{iI} + \frac{(1+\epsilon X_{II})\sum i^2 P_{iII} - (1+\epsilon X_I)\sum i^2 P_{iI}}{\theta_I} - \frac{Q\sum i^2 P_{iI}}{(V_I+V_{II})} \quad (5)$$

and in region II

$$\frac{dS_{II}}{dt} = \frac{QS_o}{(V_I+V_{II})} + \frac{(1+\epsilon X_I)S_I - (1+\epsilon X_{II})S_{II}}{\theta_{II}} - \phi_s I_{asII} - \frac{QS_{II}(1+\epsilon \overline{X})}{(V_I+V_{II})} \quad (6)$$

$$\frac{dM_{II}}{dt} = \frac{QM_o}{(V_I+V_{II})} + \frac{(1+\epsilon X_I)M_I - (1+\epsilon X_{II})M_{II}}{\theta_{II}} - K_p M_{II} \sum R_{iII} - \frac{QM_{II}(1+\epsilon\overline{X})}{(V_I+V_{II})} \quad (7)$$

$$\frac{d\sum P_{iII}}{dt} = K_{fmII} M_{II} \sum R_{iII} + \tfrac{1}{2} K_{tII} \sum R_{iII}{}^2 + \frac{(1+\epsilon X_I)\sum P_{iI} - (1+\epsilon X_{II})\sum P_{iII}}{\theta_{II}} - \frac{Q\sum P_{iII}(1+\epsilon\overline{X})}{(V_I+V_{II})} \quad (8)$$

$$\frac{d\sum iP_{iII}}{dt} = K_{tII}\sum R_{iII}\sum iR_{iII} + K_{fmII}M_{II}\sum iR_{iII} + \frac{(1+\epsilon X_I)\sum iP_{iI} - (1+\epsilon X_{II})\sum iP_{iII}}{\theta_{II}} - \frac{Q\sum iP_{iII}(1+\epsilon\overline{X})}{(V_I+V_{II})} \quad (9)$$

$$\frac{d\sum i^2P_{iII}}{dt} = K_{tII}\sum R_{iII}\sum i^2R_{iII} + K_{tII}\sum iR_{iII}{}^2 + K_{fmII}M_{II}\sum i^2R_{iII} + \frac{(1+\epsilon X_I)\sum i^2P_{iI} - (1+\epsilon X_{II})\sum i^2P_{iII}}{\theta_{II}} - \frac{Q\sum i^2P_{iII}(1+\epsilon\overline{X})}{(V_I+V_{II})} \quad (10)$$

where ϵ and conversion X, are defined as

$$\epsilon = \frac{V_{x=1} - V_{x=0}}{V_{x=0}}$$

$$X = \frac{M_o - M}{M_o + M}$$

and

$$\overline{X} = \frac{V_I X_I + V_{II} X_{II}}{(V_I + V_{II})}$$

For a batch reactor, the Q from the equations (1) through (10) should be set equal to zero. In order to obtain the zeroth, first and second moments of active polymer, the following material balances will be expressed as

$$\frac{dS_{\dot{I}}}{dt} = \frac{(1+\epsilon X_{II})S_{\dot{I}I} - (1+\epsilon X_{I})S_{\dot{I}}}{\theta_I} + 2\phi_s I_{asI} - K_d S_{\dot{I}} M_I - \frac{QS_{\dot{I}}}{(V_I+V_{II})} \tag{11}$$

$$\frac{dS_{\dot{I}I}}{dt} = \frac{(1+\epsilon X_{I})S_{\dot{I}} - (1+\epsilon X_{II})S_{\dot{I}I}}{\theta_{II}} + 2\phi_s I_{asII} - K_d S_{\dot{I}I} M_{II} - \frac{Q(1+\epsilon\overline{X})S_{\dot{I}I}}{(V_I+V_{II})} \tag{12}$$

$$\frac{d\sum R_{iI}}{dt} = \frac{(1+\epsilon X_{II})\sum R_{iII} - (1+\epsilon X_{I})\sum R_{iI}}{\theta_I} + \Omega_{iI} - K_{tI}\sum R_{iI}^{\;2} - \frac{Q\sum R_{iI}}{(V_I+V_{II})} \tag{13}$$

$$\frac{d\sum R_{iII}}{dt} = \frac{(1+\epsilon X_{I})\sum R_{iI} - (1+\epsilon X_{II})\sum R_{iII}}{\theta_{II}} + \Omega_{iII} - K_{tII}\sum R_{iII}^{\;2} - \frac{Q(1+\epsilon\overline{X})\sum R_{iII}}{(V_I+V_{II})} \tag{14}$$

where

$$\Omega_{iI} = 2K_i M_I^{\;3} + K_p S_{\dot{I}} M_I$$

$$\Omega_{iII} = 2K_i M_{II}^{\;3} + K_p S_{\dot{I}I} M_{II}$$

If QSSA is applied, and let $K_d = K_p$, the solutions of equations (11) and (12) will be

$$S_{\dot{I}} = \frac{(C_2/C_7 + C_5/C_3)}{(C_6/C_3 - C_1/C_7)} \tag{15}$$

$$S_{\dot{I}I} = \frac{(C_2/C_1 + C_5/C_6)}{(C_7/C_1 - C_3/C_6)} \tag{16}$$

By substituting equations (15) and (16) into equations (13) and (14), we obtain

$$\sum R_{iI} = \frac{-C_8+\sqrt{C_8^{\,2}+4\theta_I K_{tI}(\theta_I \Omega_{iI}+C_9\sum R_{iII})}}{2\theta_I K_{tI}}$$

$$\sum R_{iII} = \frac{-C_9+\sqrt{C_9^{\,2}+4\theta_{II} K_{tII}(\theta_{II} \Omega_{iII}+C_8\sum R_{iI})}}{2\theta_{II} K_{tII}}$$

where

$$C_1 = (1+\epsilon X_I) + \theta_I(K_p M_I + \frac{Q}{V_I+V_{II}})$$

$$C_2 = 2\theta_I \phi_s I_{asI}$$

$$C_3 = (1+\epsilon X_{II}) + \theta_{II}(K_p M_{II} + \frac{(1+\epsilon\overline{X})Q}{V_I+V_{II}})$$

$$C_5 = 2\theta_{II} \phi_s I_{asII}$$

$$C_6 = 1+\epsilon X_I$$

$$C_7 = 1+\epsilon X_{II}$$

$$C_8 = C_6 + \frac{\theta_I Q}{V_I+V_{II}}$$

$$C_9 = C_7 + \frac{\theta_{II}(1+\epsilon\overline{X})Q}{V_I+V_{II}}$$

The first and second moments of active polymer in both regions are obtained by applying the same procedure described above

$$\sum iR_{iI} = \frac{\frac{C_9}{\theta_I}\sum iR_{iII} + K_p M_I \sum R_{iI} + \Omega_{iI}}{\frac{C_8}{\theta_I} + K_{tI}\sum R_{iI}}$$

$$\sum iR_{iII} = \frac{\frac{C_8}{\theta_{II}}\sum iR_{iI} + K_p M_{II} \sum R_{iII} + \Omega_{iII}}{\frac{C_9}{\theta_{II}} + K_{tII}\sum R_{iII}}$$

and

$$\sum i^2 R_{iI} = \frac{\frac{C_9}{\theta_I}\sum i^2 R_{iII} + 2K_p M_I \sum iR_{iI} + \Omega_{iI} + K_p M_I \sum R_{iI}}{\frac{C_8}{\theta_I} + K_{tI}\sum R_{iI} + K_{fm} M_I}$$

$$\sum i^2 R_{iII} = \frac{\frac{C_8}{\theta_{II}}\sum i^2 R_{iI} + 2K_p M_{II} \sum iR_{iII} + \Omega_{iII} + K_p M_{II} \sum R_{iII}}{\frac{C_9}{\theta_{II}} + K_{tII}\sum R_{iII} + K_{fm} M_{II}}$$

From numerical analysis, the concentration of active sensitizer, zeroth, first, and second moments of active polymer calculated in batch reactor are approximately the same as those calculated in CSTR. Here, the rate constants of termination in both regions, K_{tI} and K_{tII}, are assumed to be equal and are independent of the chain length.

OPTIMIZATION OF BATCH POLYMERIZATION REACTOR

Now that we have a method for efficiently computing the conversion and polydispersity, then we might obtain the parameters, V_I, q (i.e., θ_I and θ_{II}), and I_{asII}. The objective of optimization is to obtain the polydispersity $\frac{X_w}{X_n}$, and conversion of the polymerization, X, as close as possible to the experimental data of batch reactor, $\frac{X_w}{X_n}^*$ and X^*, respectively, by solving the nonlinear simultaneous equations (1) through (10) of batch reactor (i.e., Q = 0), and with the appropriate parameters. The objective function to be minimized can be generally written as

$$F(t) = \sum_{i=1}^{n} \{ (\frac{X_w}{X_n} - \frac{X_w^*}{X_n})_i^2 + (X - X^*)_i^2 \} \quad (17)$$

where n is the number of data points. Now the optimization problem becomes one of minimizing the objective function F(t) defined by equation (17) subject to the following inequality constraints:

$$L \leqq X_k \leqq U \qquad k = 1, 2, 3$$

where X_k, L, and U are the parameters, the lower and upper limits of parameter, respectively.

Method

The algorithm (49) explained is based upon the automatic method proposed by Rosenbrock (50). This method is a sequential search technique to produce new constrained parameters. The procedure is then to vary the available parameters until the objective function is a minimum. The algorithm requires a starting point that satisfies the constraints and does not lie in the boundary zones which are defined as follows:

Lower Zone: $G_k \leqq X_k \leqq (G_k + (H_k - G_k) \times 10^{-4})$

Upper Zone: $H_k \leqq X_k \leqq (H_k - (H_k - G_k) \times 10^{-4})$

The algorithm proceeds as follows:

(1) Define by F^o the current best objective function value for a point where the constraints are satisfied, and F^* the current best objective function value for a point where the constraints are satisfied and in addition the boundary zones are not violated.

F^{o} and F^{*} are initially set equal to the objective function value at the starting point.

(2) If the current point objective function evaluation, F, is worse than F^{o} or if the constraints are violated, the trial is a failure and the unconstraints procedure is continued.

(3) If the current point lies within a boundary zone, the objective function is modified as follows:

$$F(new) = F(old) - (F(old) - F^{*})(3\lambda - 4\lambda^{2} + 2\lambda^{3})$$

where

$$\lambda = \frac{\text{distance into boundary zone}}{\text{width of boundary zone}}$$

$$= \frac{G_k + (H_k - G_k) \times 10^{-4} - X_k}{(H_k - G_k) \times 10^{-4}} \quad \text{(lower zone)}$$

$$= \frac{X_k - (H_k - (H_k - G_k) \times 10^{-4})}{(H_k - G_k) \times 10^{-4}} \quad \text{(upper zone)}$$

At the inner edge of the boundary zone, $\lambda = 0$, i.e., the function is unaltered (F(new) = F(old)). At the constraint, $\lambda = 1$, and thus $F(new) = F^{*}$. Thus the function value is replaced by the best current function value in the feasible region and not in a boundary zone. For a function which improves as the constraint is approached, the modified function has an optimum in the boundary zone.

(4) If an improvement in the objective function has been obtained without violating the boundary zones or constraints, F^{*} is set equal to F^{O} and the procedure continued.

(5) The search procedure is terminated when the convergence criteria is satisfied.

There are three difficulties which have to be met in developing a practical method for dealing with the problem:(1) Determining Length of Step: The principle adopted was to try a step of arbitrary length e. If e was initially so small that it made no change in objective function, it would be increased on the next attempt. (2) Determining Direction of Step: The next problem is to decide when and how to change the directions in which the steps e are taken. It was decided to work throughout with n orthogonal directions rather than choose a single direction in which to progress at each stage. (3) Inserting Limits.

Results and Analysis

The experimental results obtained from isothermal batch reactor were compared and analyzed with the numerical calculation from the procedure described above. These three parameters can be evaluated by this search technique. Figure 31 shows the experimental data of batch reactor and numerical calculation by using the searched parameters. Good agreement is obtained between solution and experiments after fitting parameters.

The result without the parameter I_{asII} (i.e., by setting $I_{asII} = 0$) is shown in Fig. 32 in which the polydispersity increases with the reaction time. The disagreement with the experimental data indicates that the light intensity absorption in low dose rate region can not be neglected when the model predicted. As I_{asII} is $5x10^{-10}$Eins/sec-cm^3, the polydispersity appears to be obtained within a certain range which is shown in Figure 33. Explanation

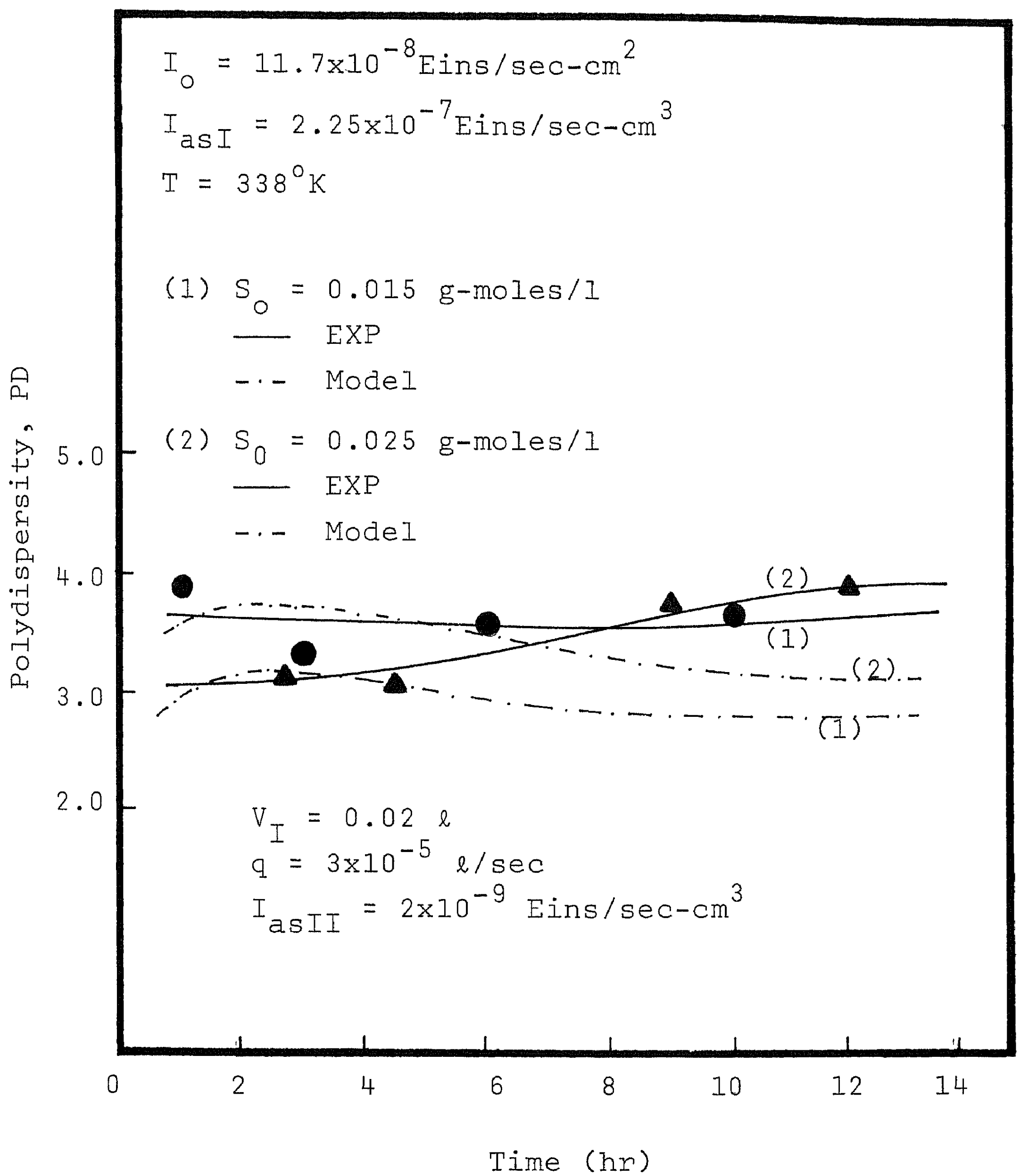

Figure 31. Polydispersity vs. Time by Batch Data and Prediction of Parameters fitting

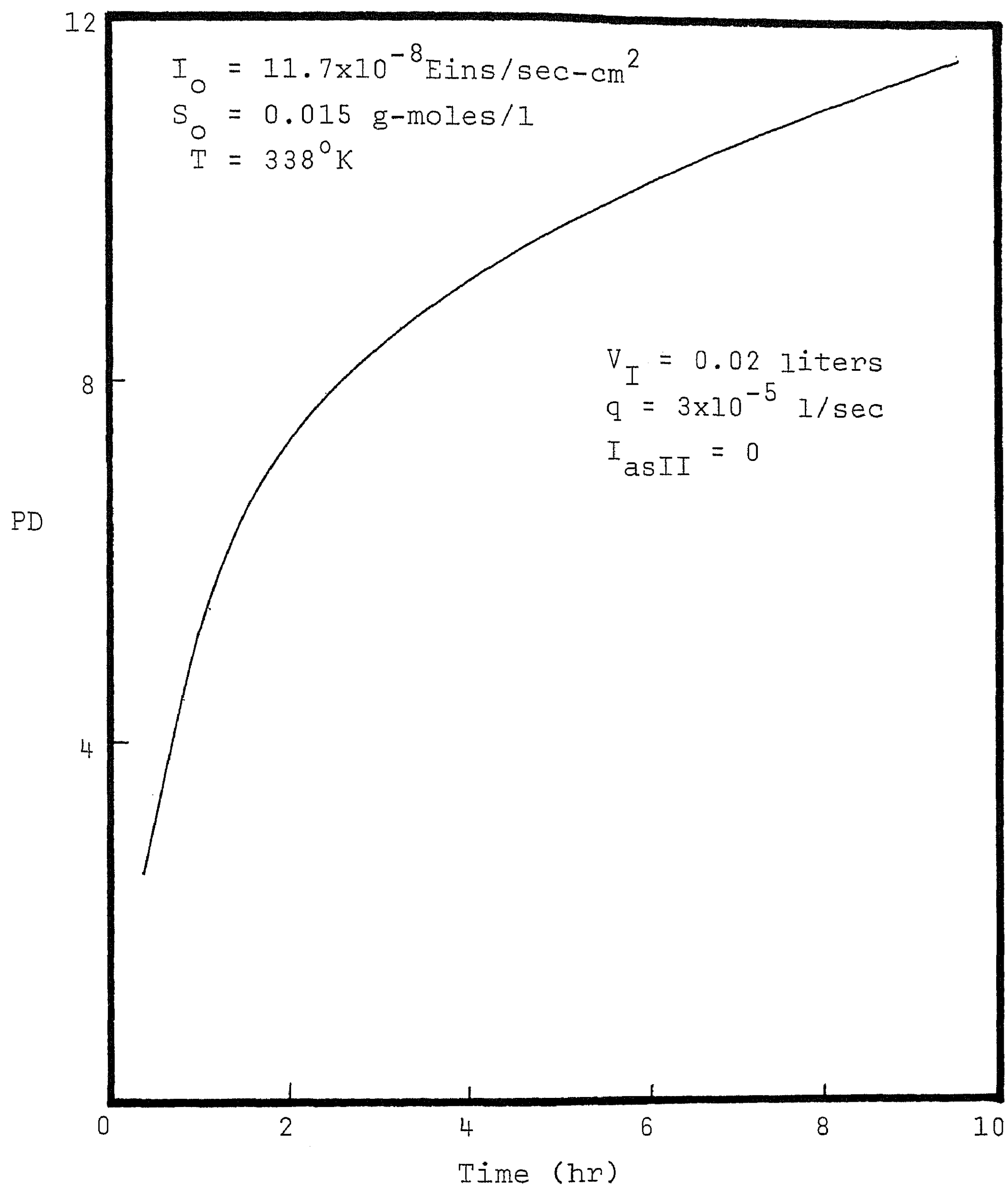

Figure 32. Effect of Initiation Without I_{asII} on Polydispersity in Two-Region Model

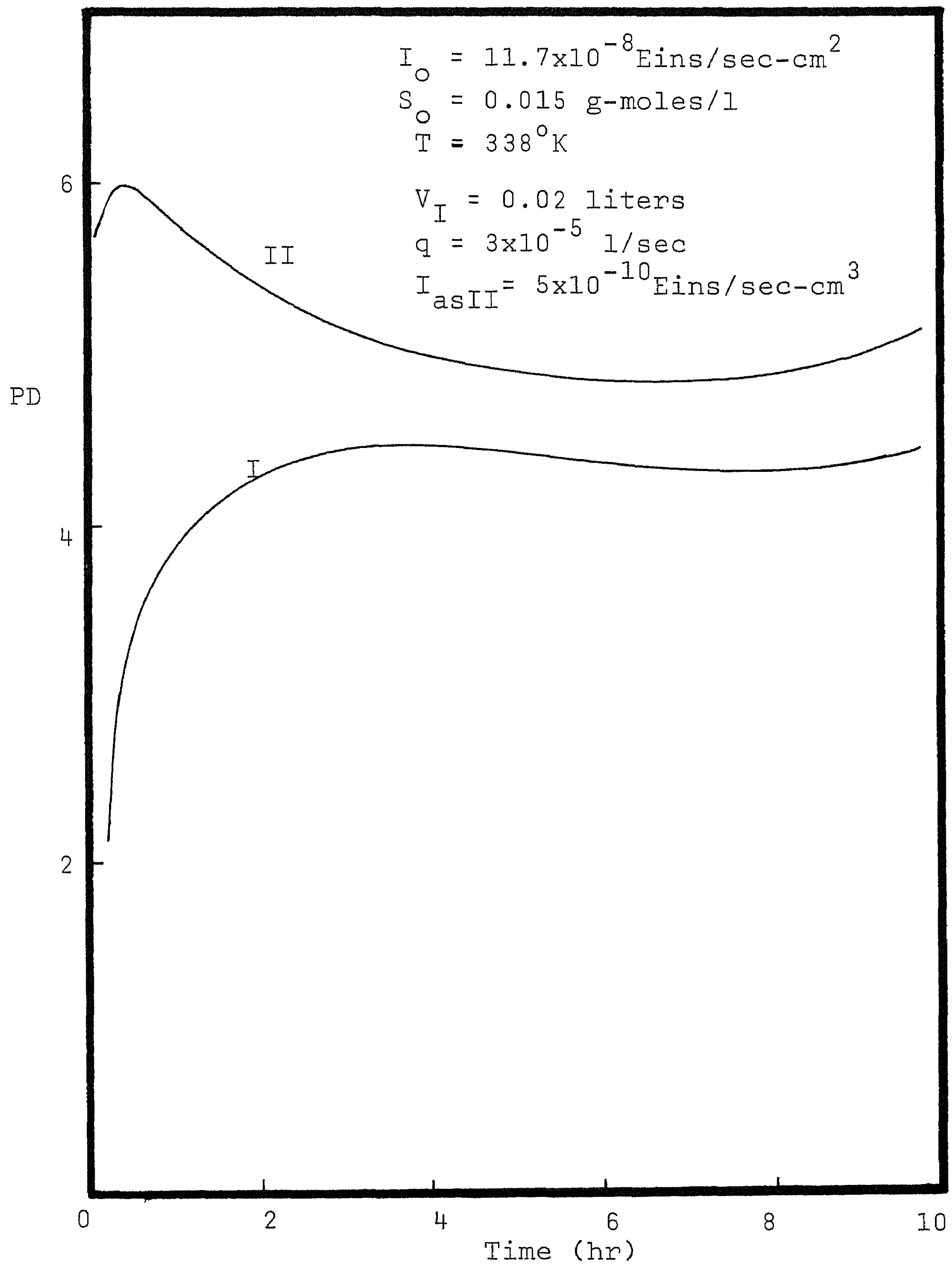

Figure 33. Effect of Small I_{asII} on Polydispersity in Two-Region Model

for this behavior is that the difference in radical concentration between two regions decreases with the small but significant initiation rate in low dose rate region. Figure 34 shows that the higher initiation rate in low dose rate region would produce a nearly uniform polydispersity. Also, Figure 35 shows uniform polydispersity can be produced by having a small volume of high dose rate region. Figure 36 shows that the similar result is achieved by increasing the speed of agitation, since the radical life time is very short and a marked difference in the initiation rates exists in these two regions. By applying the parameters to the proposed two-region model for a CSTR under UV light on-off regulation, the results show some agreements as shown in Figures 37 through 41, and the polydispersity of steady state can be increased from about 1.5 (perfect mixing) to about the range of 2.8-3.2.

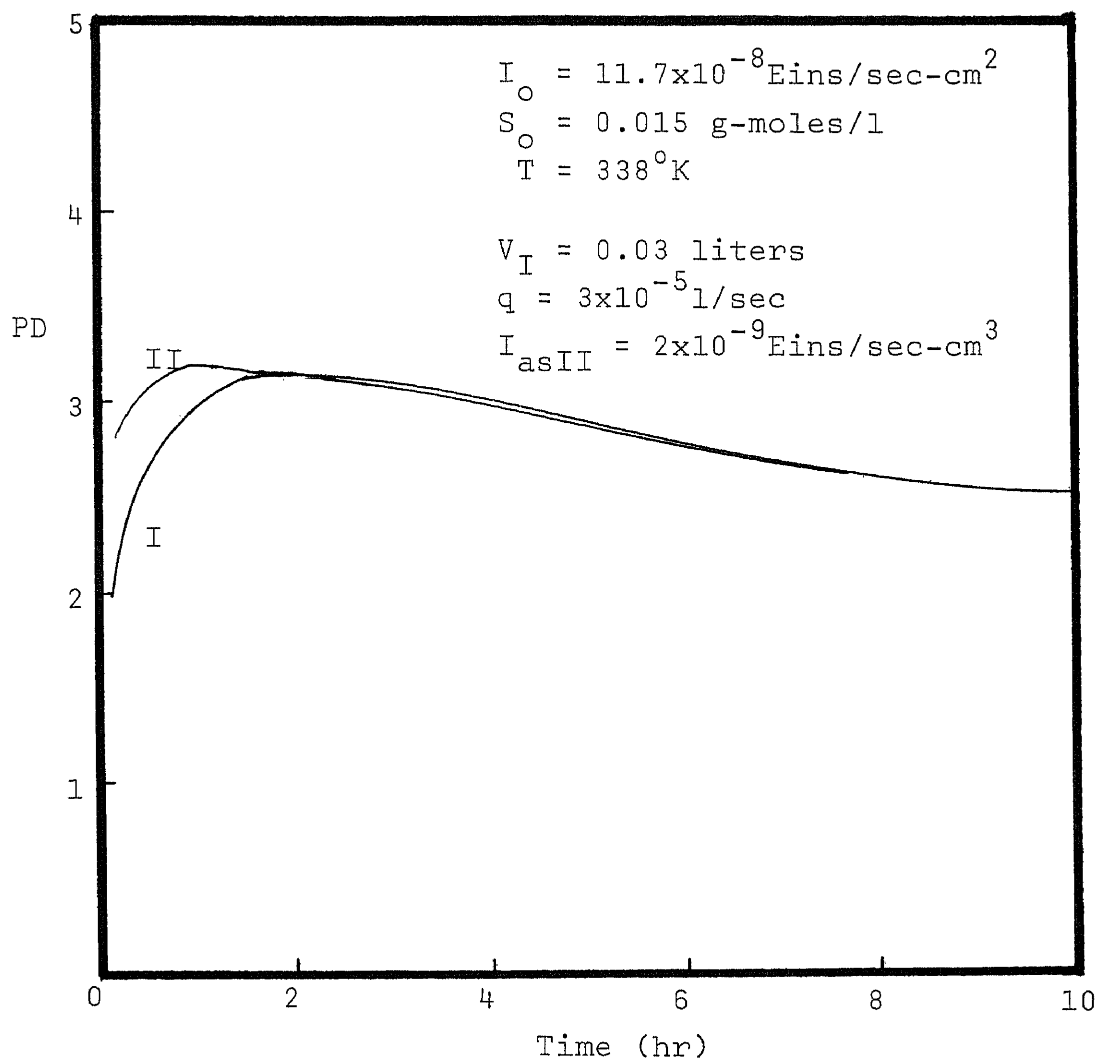

Figure 34. Effect of Large I_{asII} on Polydispersity in Two-Region Model

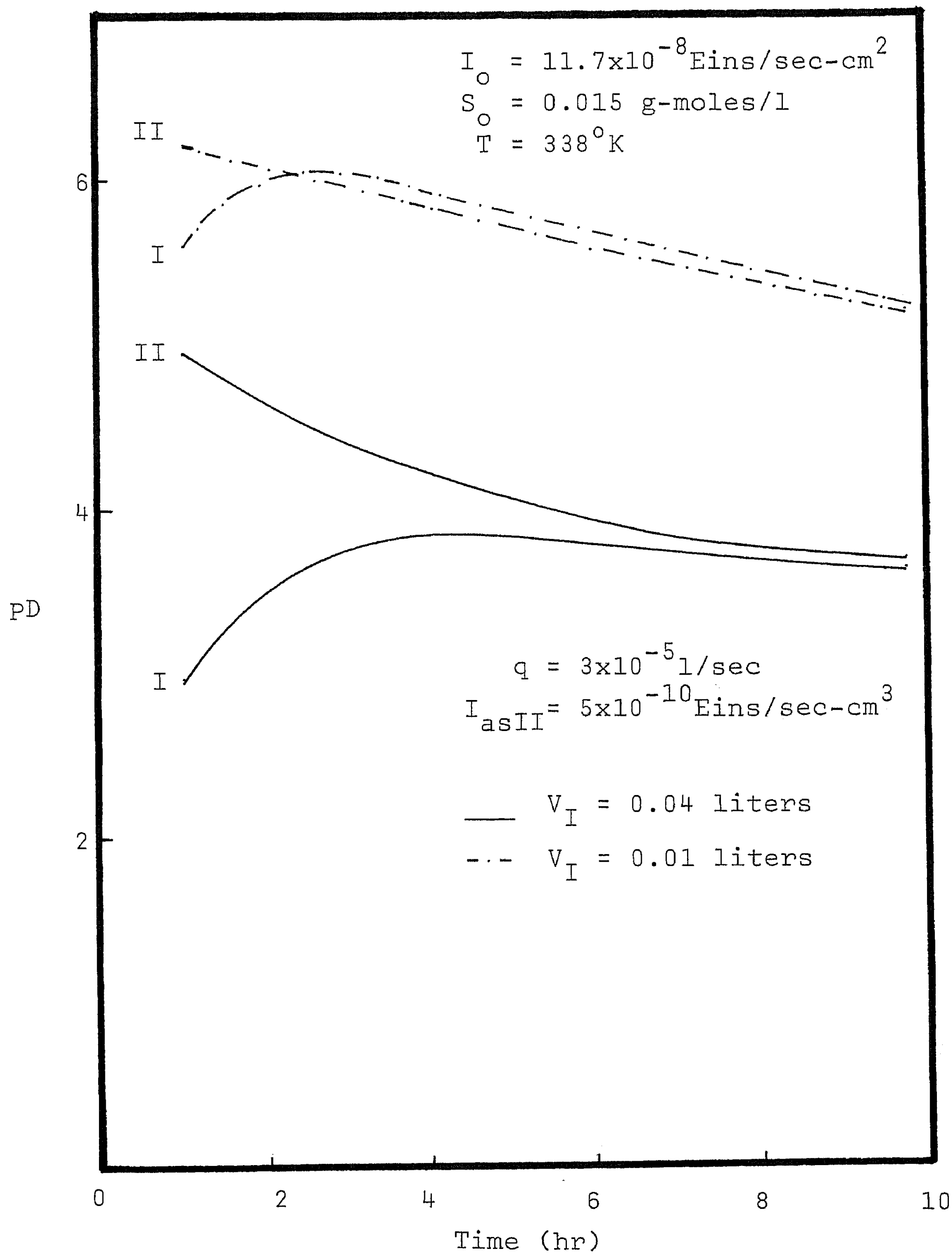

Figure 35. Effect of Lighted Volume on Polydispersity in Two-Region Model

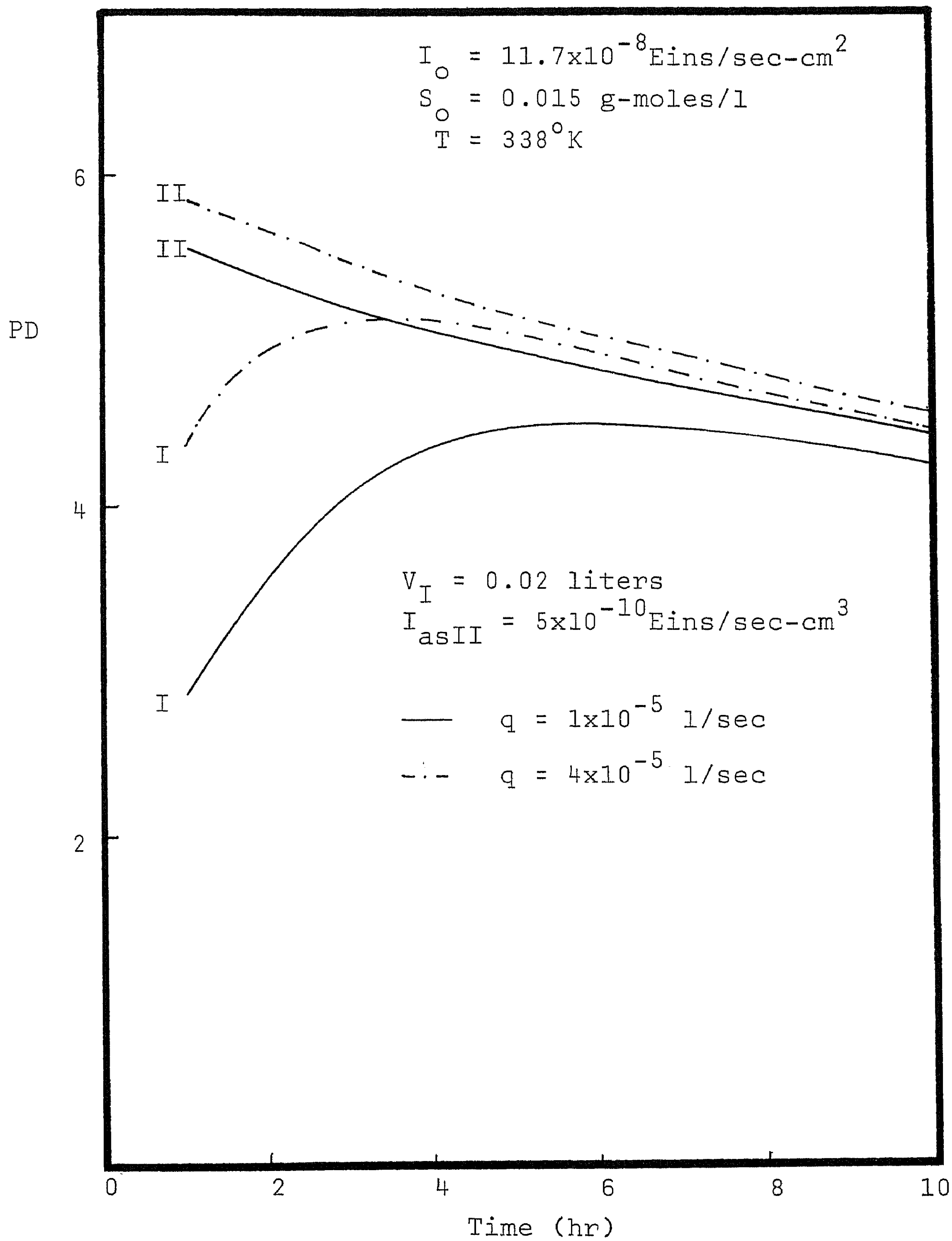

Figure 36. Effect of Volumetric Pumping Rate on Polydispersity in Two-Region Model

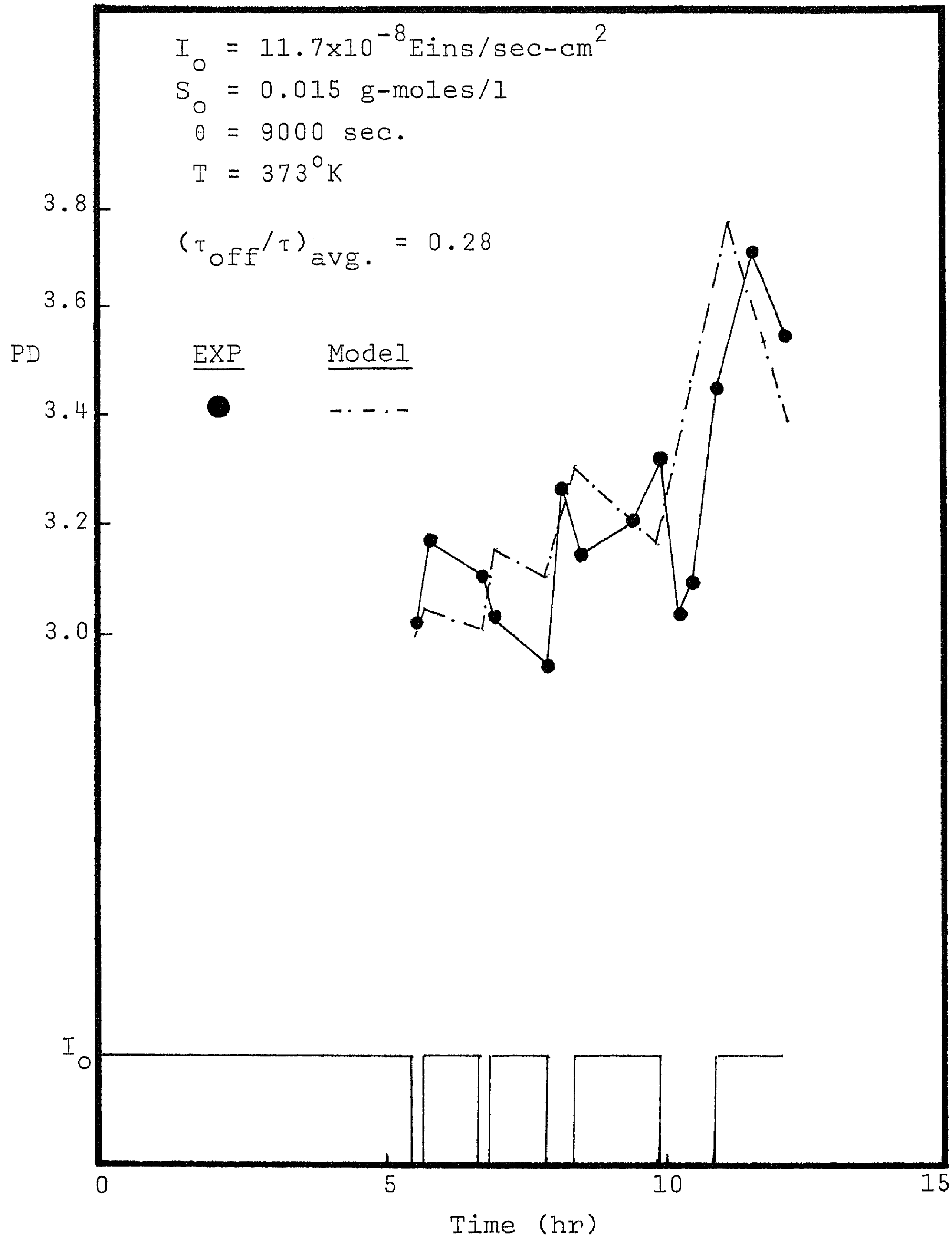

Figure 37. Experimental PD vs. Time Data and Prediction of Two-Region Model at $(\tau_{off}/\tau)_{av}$ = 0.28, θ = 9000 sec and T = 373^{o}K

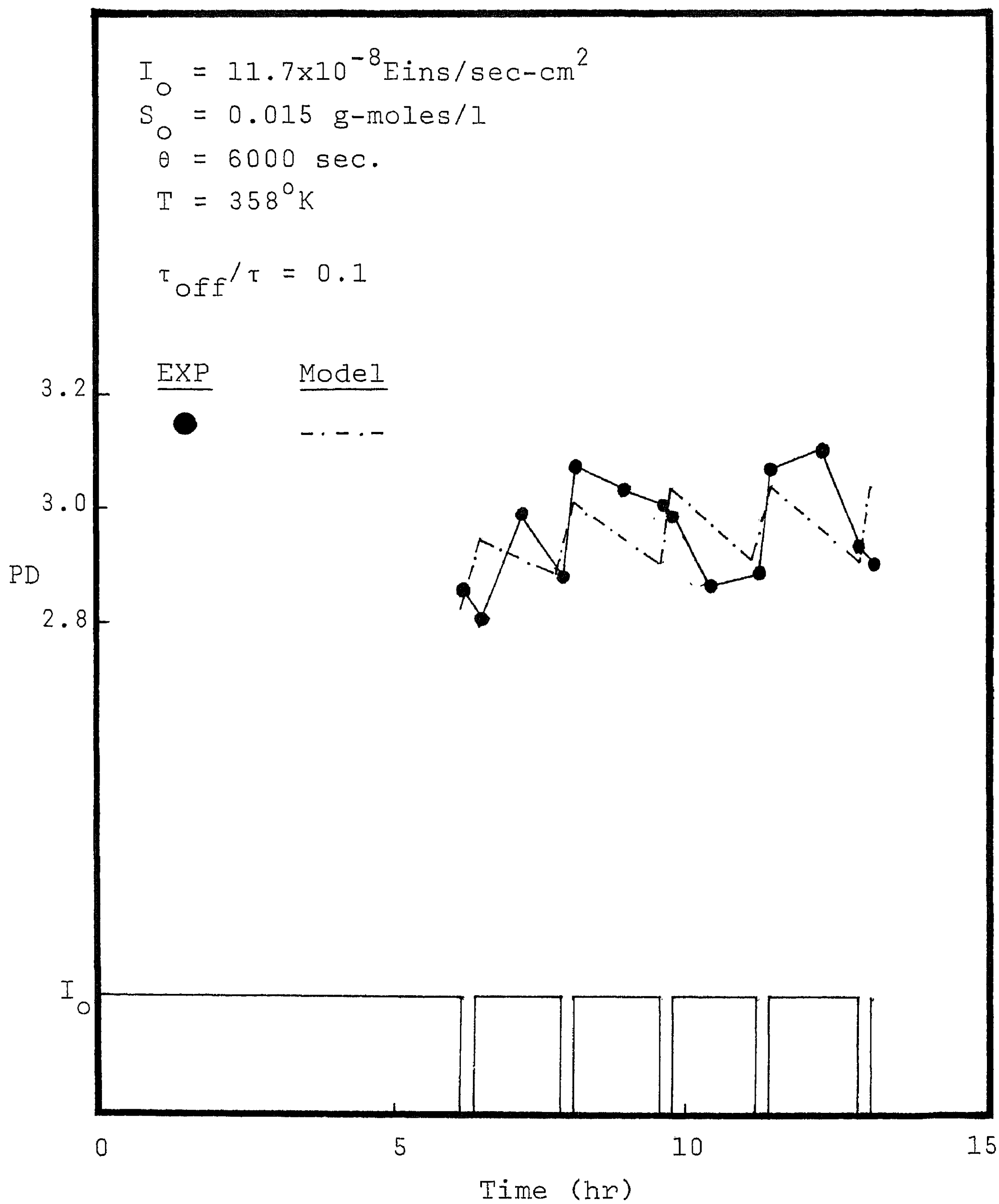

Figure 38. Experimental PD vs. Time Data and Prediction of Two-Region Model at $\tau_{off}/\tau = 0.1$, $\theta = 6000$ sec and $T = 358^{o}K$

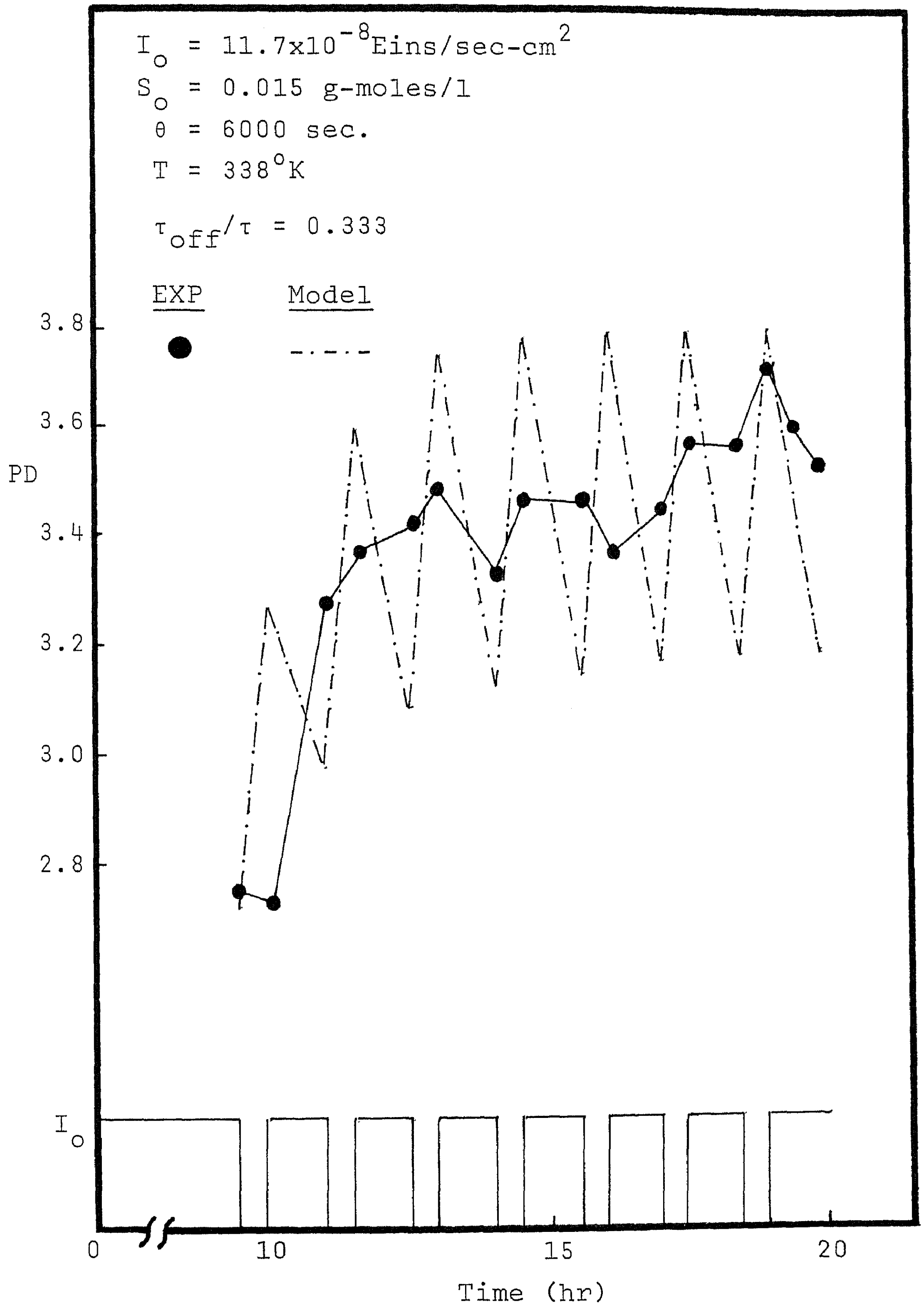

Figure 39. Experimental PD vs. Time Data and Prediction of Two-Region Model at $\tau_{off}/\tau = 0.333$, $\theta = 6000$ sec and $T = 338^{o}K$

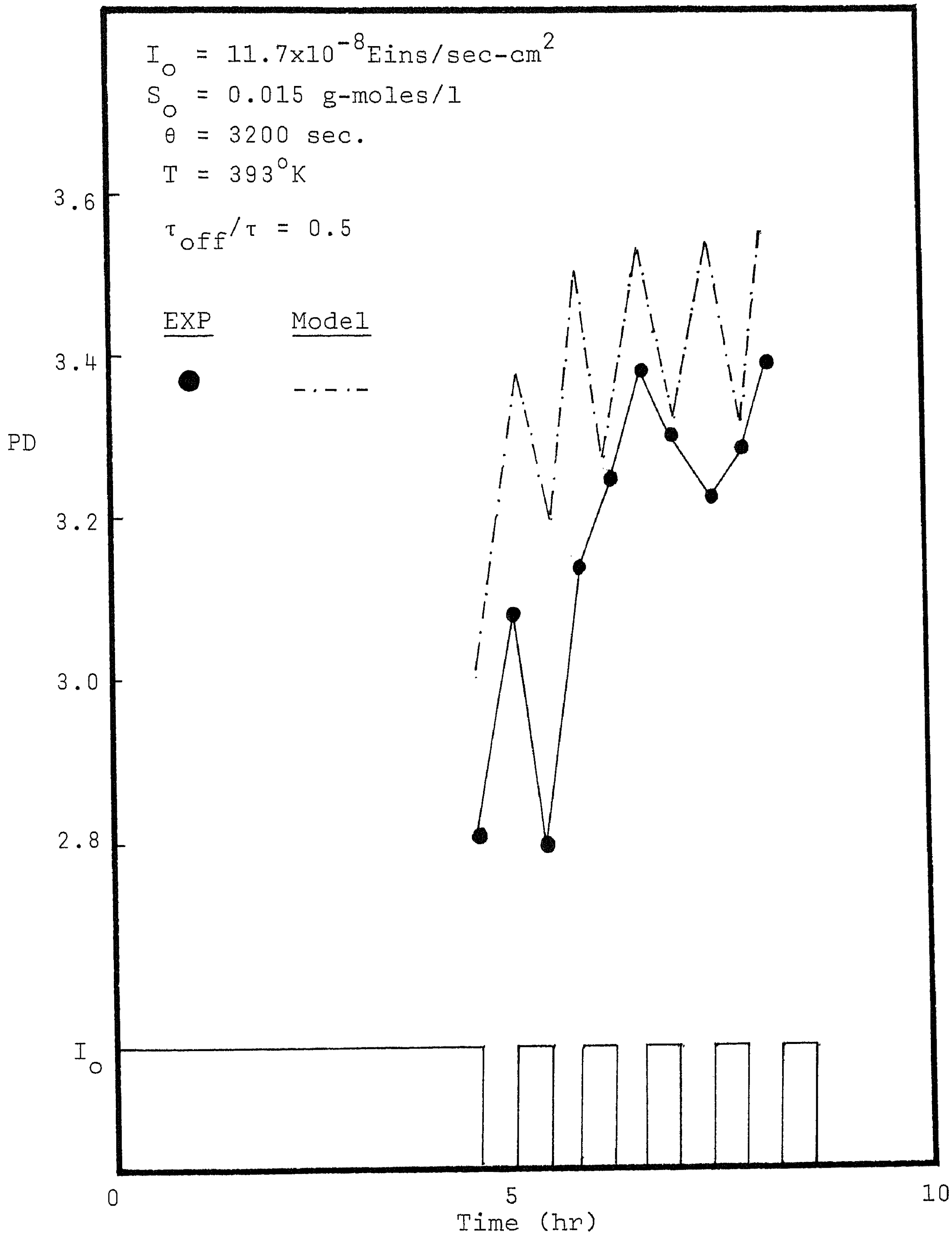

Figure 40. Experimental PD vs. Time Data and Prediction of Two-Region Model at $\tau_{off}/\tau = 0.5$, $\theta = 3200$ sec and $T = 393°K$

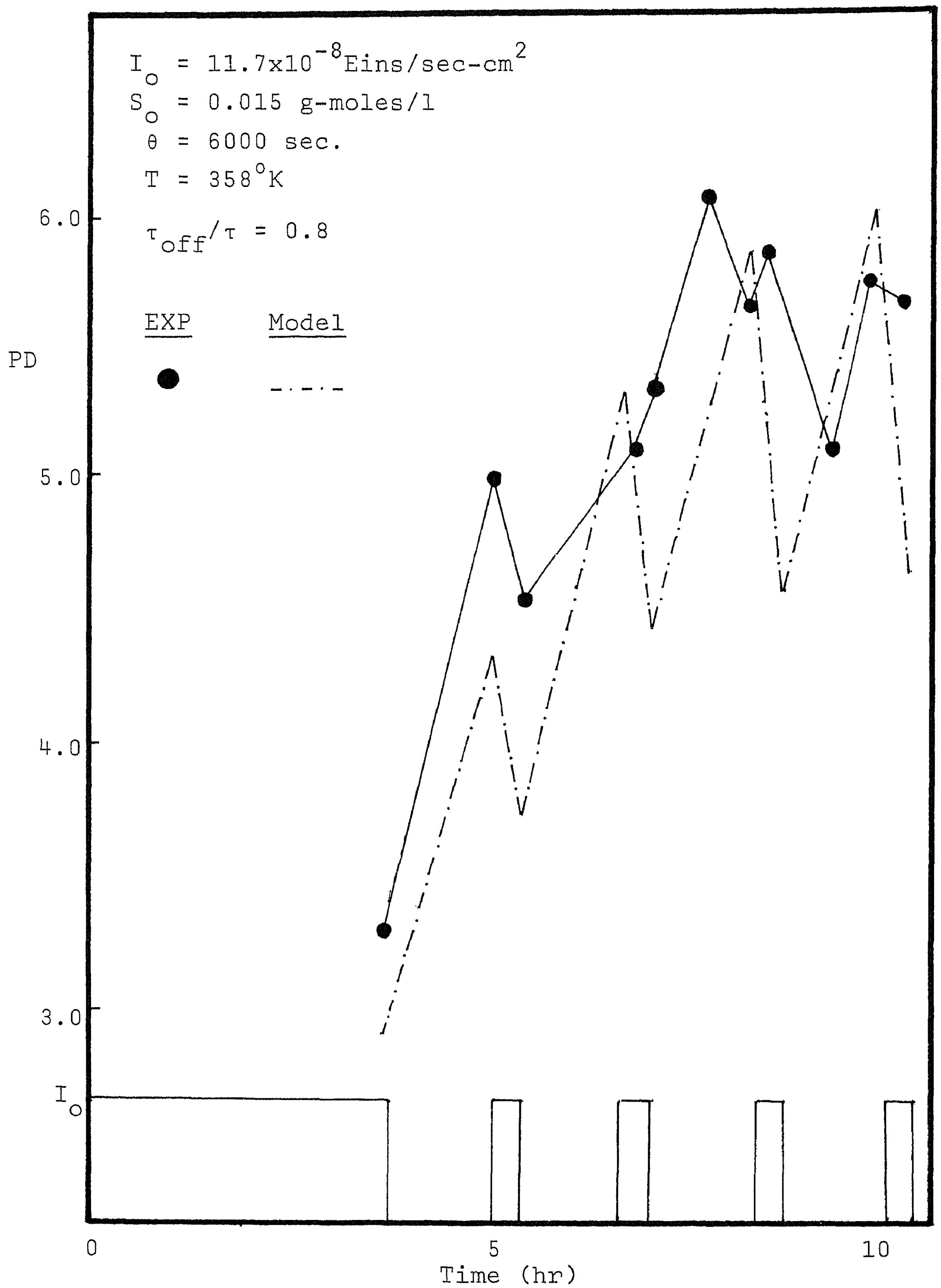

Figure 41. Experimental PD vs. Time Data and Prediction of Two-Region Model at τ_{off}/τ = 0.8 θ = 6000 sec and T = 358^{o}K

CHAPTER 6

REACTOR MULTIPLICITY, STABILITY AND CONTROLLABILITY FOR PHOTOPOLYMERIZATION IN A CSTR

A study of steady state and dynamic behavior of an isothermal CSTR has been carried out numerically. It is mathematically demonstrated that there is a clear possibility of the existence of multiple steady states induced by viscosity effects in isothermal CSTR. In solutions of high viscosity, that mass consumption rate of free-radical polymerization increases with conversion, reaching a peak at very high viscosity, then falling off rapidly. Given this sort of behavior, it is demonstrated mathematically that steady-state mass balance solutions are possible at three levels of conversion. The lower and higher steady states are stable while the metastable steady-state is shown to be necessarily unstable. This multiple steady-state problem is discussed in relation to reactor stability and control. A broader molecular weight distribution being achieved by regulating UV light on-off around the metastable steady state is investigated.

Reactor Performance Characteristics

Mass balance equations for a perfectly mixed isothermal CSTR are expressed the same as the equations (1) through (5) in Chapter 4. In which, $\frac{K_p}{K_t^{1/2}}$ is allowed to vary with conversion as follows: (43)

$$\frac{K_p}{K_t^{1/2}} = \left(\frac{K_p}{K_t^{1/2}}\right)_o e^{(A_1X + A_2X^2 + A_3X^3)}$$

The subscript o means value at zero conversion, and A_1, A_2 and A_3 and $(\frac{K_p}{K_t^{1/2}})_o$ are independent of conversion X for any temperature. In bulk radical polymerization, the viscosity of the medium increases as polymerization progresses. Such an increase decreases termination rate, which is diffusion controlled, and therefore it accelerates the polymerization rate markedly. The abnormal increases in the rate of conversion, the degree of polymerization, and the mean lifetime of polymer radicals have been inclusively recognized as the gel effect, or the Trommsdorff effect. The general solution is to separate equation (2) in Chapter 2 into two terms, Mass Supply Rate (MSR) and Mass Consumption Rate (MCR):

$$MSR = \frac{M_o - M(1+\epsilon X)}{\theta} = \frac{M_o X}{\theta}$$

$$MCR = \Omega_i^{1/2} \frac{M_o(1-X)}{1+\epsilon X} (\frac{K_p}{K_t^{1/2}}) Exp(A_1X + A_2X^2 + A_3X^3)$$

A volume change denoted by ϵ is also involved in the equations. Figure 42 shows typical solutions obtained for styrene polymerization. At steady state MSR should be equal to MCR. The Msr is a linear function of X with a slop of M_o/θ. The existence of the two steady states shown in the figure requires the supply and consumption curves be tangent at one point, a physically unlikely situation. More likely is the occurrence of one or three steady states. When three steady states are found, the central one is metastable. At this state, a decrease in X results in less mass consumption, and the monomer concentration M increases (or X decreases) until it reaches the lower steady state.

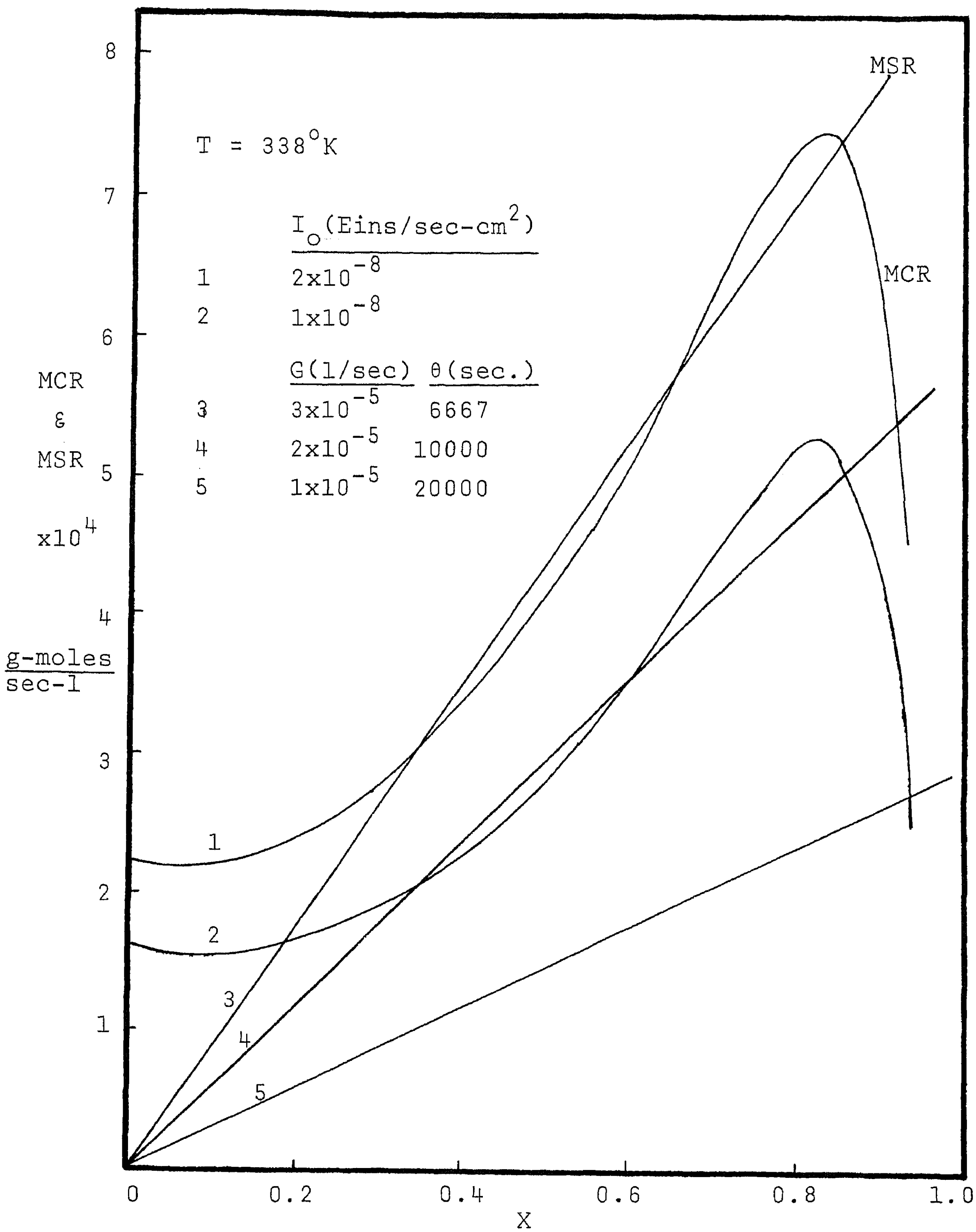

Figure 42. MSR &MCR vs. X at Different I_o's and Flow Rates

On the other hand, if the X is increased (or M is decreased) from the metastable steady state value, MCR > MSR, and the mass continues to fall (or X continues to increase) until the upper steady state is reached.

Metastable Steady State

Conversions of metastable states have been obtained by observing the effect of perturbation from stable conversions. Figure 43 shows a typical reactor conversion history for metastable steady state determination. The conversion is raised above the predicted low stable steady state by means of the batch operation and $I_o = 1.5x10^{-8}$Eins/cm^2-sec. The reactor is then operated continuously with flow rate G = $2.9x10^{-5}$ l/sec, and reaction is permitted to find its real metastable state. The conversion is then raised to the predicted metastable state by means of the batch operation. A decrease in conversion following the continuous operation indicates undershoot below the metastable point and the conversion is raised by the batch operation. Similarly, an increase in conversion indicates overshoot beyond the metastable point and the shutter is closed to lower the conversion. By means of this step-wise procedure, the metastable point is reached.

Numerical calculation has been carried on the reactor control by on-off regulation of the light intensity. The on-off operation is obtained through a shutter mechanism. This is deemed most suitable for a UV lamp which for a proper operation must be maintained at constant output. Conversion is readily controlled

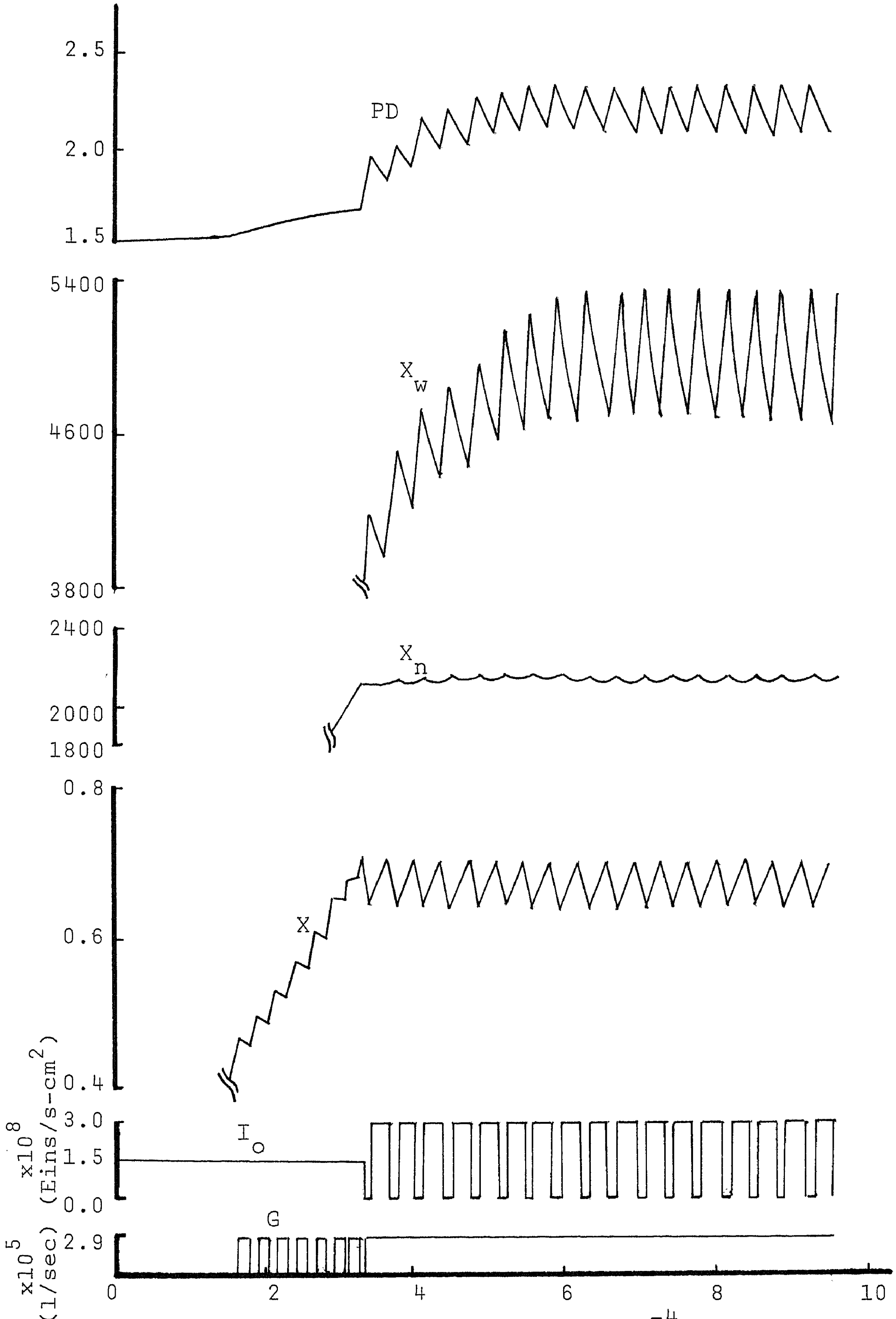

Figure 43. Light ON/OFF Regulation at Metastable S.S. with $\tau_{on}/\tau_{off} = 2.5$

with 0.025 below or above the metastable steady state. If $X \geqq X_{meta} + 0.025$, the shutter is closed manually. and vice versa ($I_o = 3x10^{-8}$Eins/sec-cm^2). From the figure, the polymer formed at the controller metastable steady state has a higher polydispersity than that obtained at the real metastable steady state.

Figure 44 illustrates the effect on the polydispersity with the same conversion range as in Figure 43 at different UV light on-off period and upper light intensity. It shows that when light on-off ratio is increased from 2.5 to 10, the upper light intensity should be decreased from $3x10^{-8}$ to $1.8x10^{-8}$Eins/sec-cm^2 in order to keep the same conversion range. In addition, the produced polydispersity decreases from 2.2 to 1.7, due to the increased number average chain length and the decreased weight average chain length.

The Control Analysis

Figure 45 shows the calculated results representing the reactor performance characteristics in terms of conversion, X and number average chain length, X_n. Note that there are three regions in Figure 45: the curve a-b(Region I, low stable), curve b-c(Region II, metastable) and curve c-d(Region III, high stable). Operation in region III may be discounted for the bulk polymerization because of high viscosity (In order to reach higher conversion, the experiments of solution photopolymerization were carried out and shown in Appendix B). With regard to Region I and II, the obvious advantage of operation in the metastable region is the significantly higher conversion and molecular weight

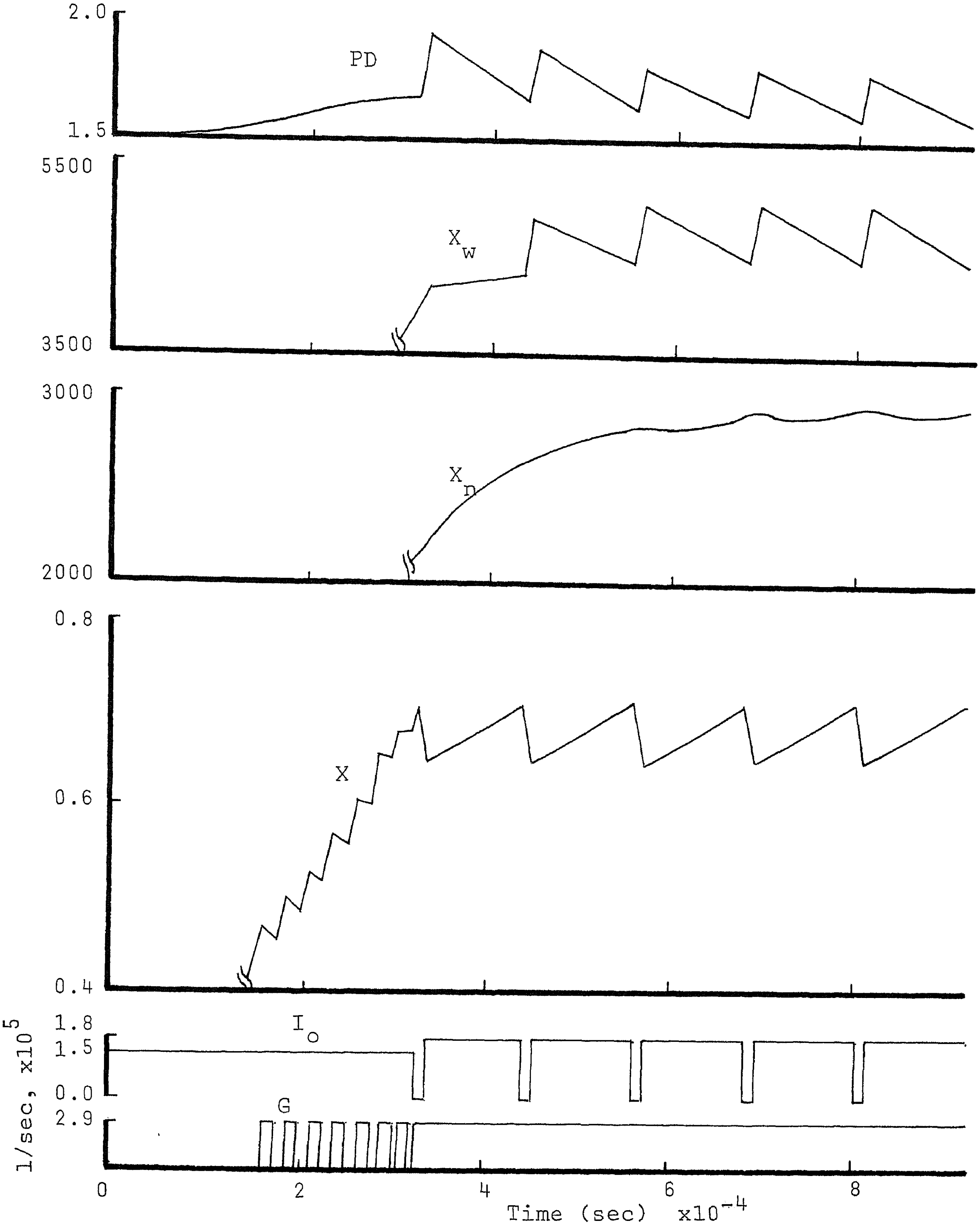

Figure 44. Light ON/OFF Regulation at Metastable S.S. with τ_{on}/τ_{off} = 10

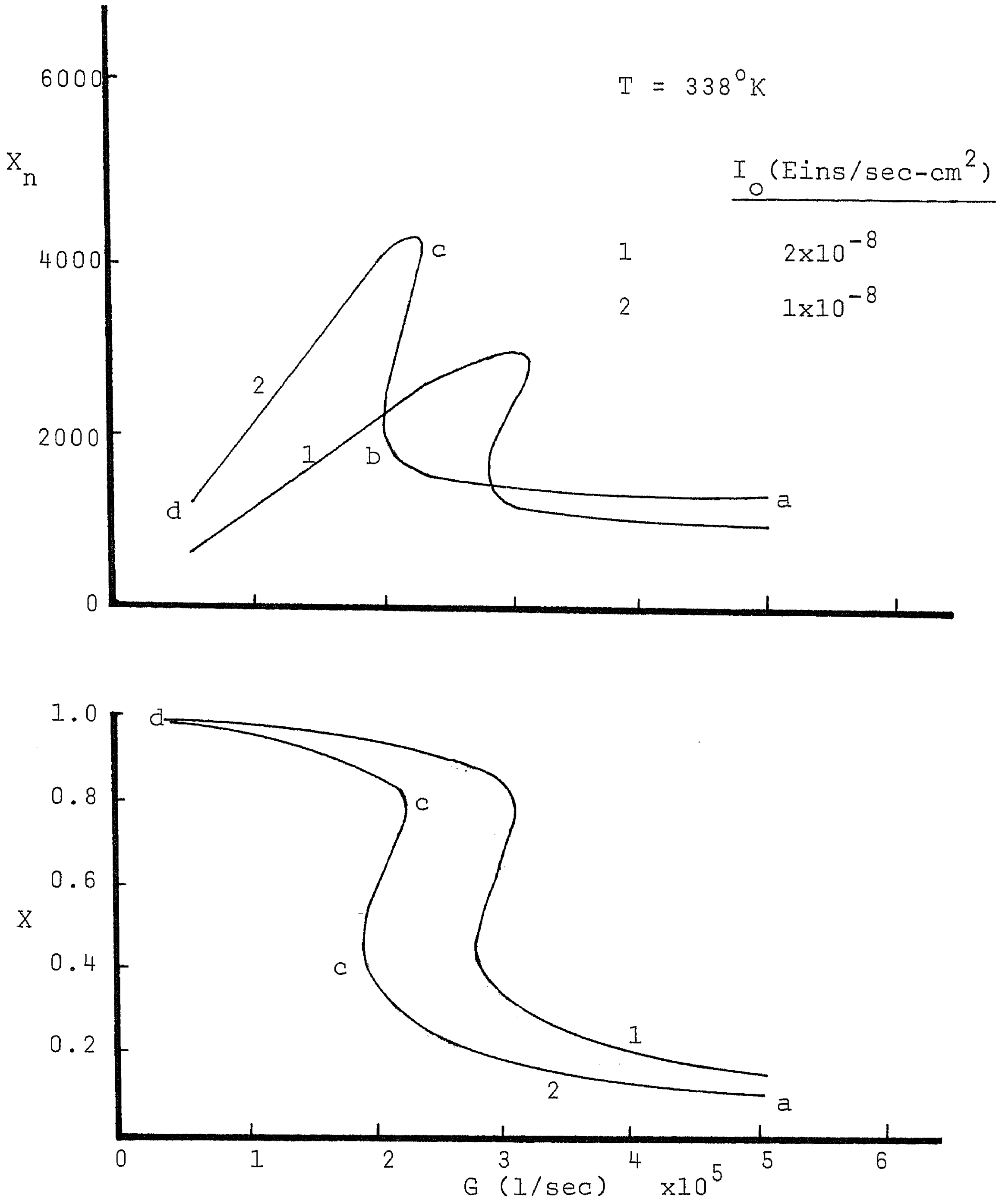

Figure 45. Reactor Performance Characteristics-
Calculated Results

attainable for the same residence time. While the reactor is operated in Region I, an increase in θ (residence time) or a decrease in G (flow rate) at a fixed I_o results in an increase in X and X_n. Also, an increase in I_o would shift the characteristics curve to lower residence time (or higher flow rate). The converse is true for Region II. The striped bands shown in Figures 46 through 48 are the range of X, X_n and X_w by on-off regulation of the light intensity on the three regions. As the light-off period is small, the bands are narrow in comparison to Figures 49—51 for which τ_{on}/τ_{off} is 4 and the band in metastable region combines with the low stable region. Having established the characteristics of operation in the metastable region, it is necessary to determine the conditions required to control a CSTR within this region. This was accomplished by means of a fourth order Runge-Kutta integration of the transient reactor equations(1)—(5) in Chapter 4. The responses obtained are to a step-change in set-point conversion X and are shown in Figures 52—55 in terms of conversion X, number average chain length X_n, weight average chain length X_w and controlled variable, flow rate, as a function of time.

The response is shown in Figure 52 with the control parameter in terms of the flow rate G. The initial point is reached over the metastable state before s step-change takes place. For this application K_c represents the change in flow rate per unit conversion. For K_c = 0.000001 l/sec the response is deemed only marginally stable on the basis that after 30000 seconds the conversion continues to increase slowly and eventually reaction

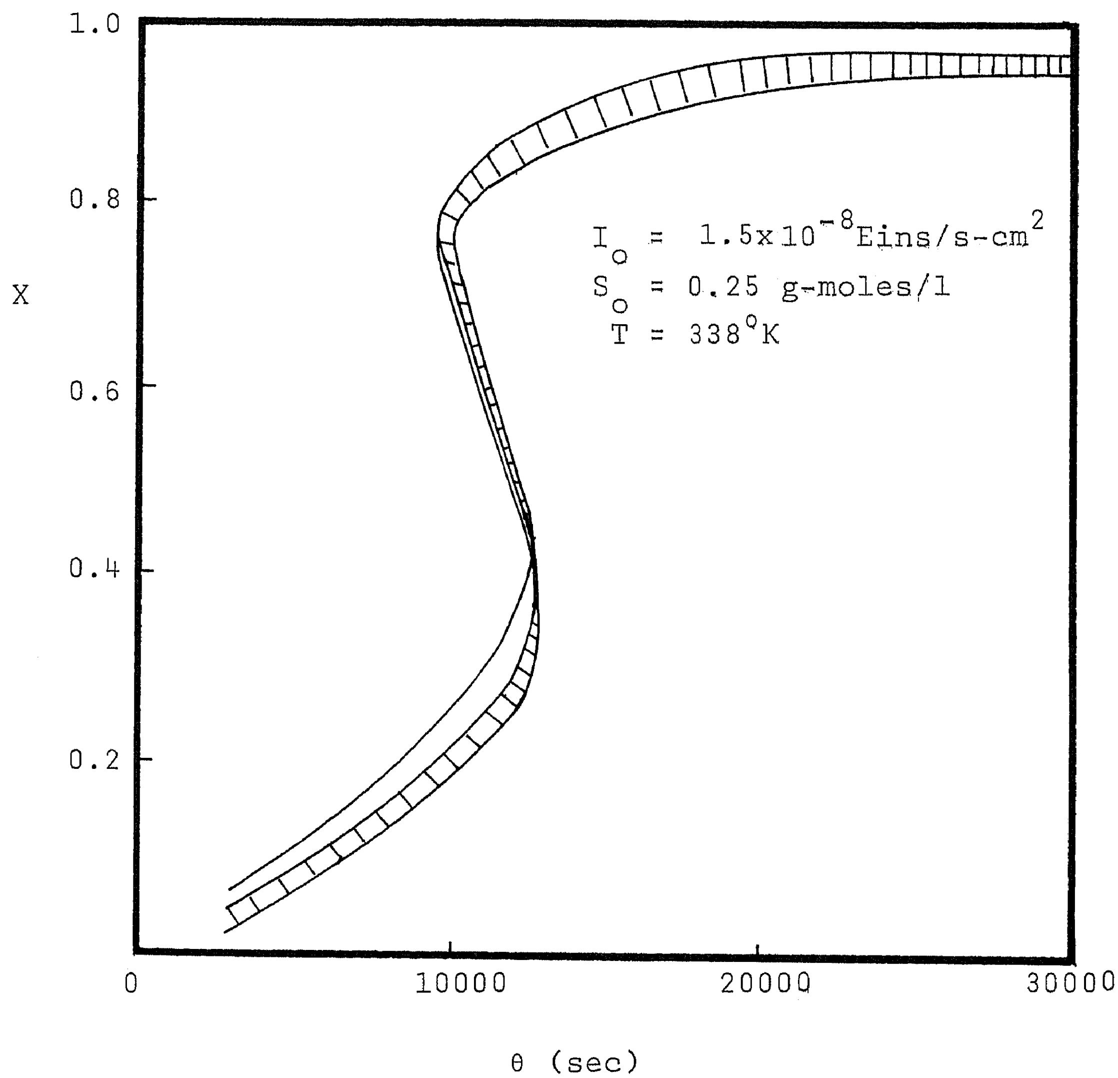

Figure 46. X vs. θ at Three Steady States Regions with τ_{off}/τ = 0.1

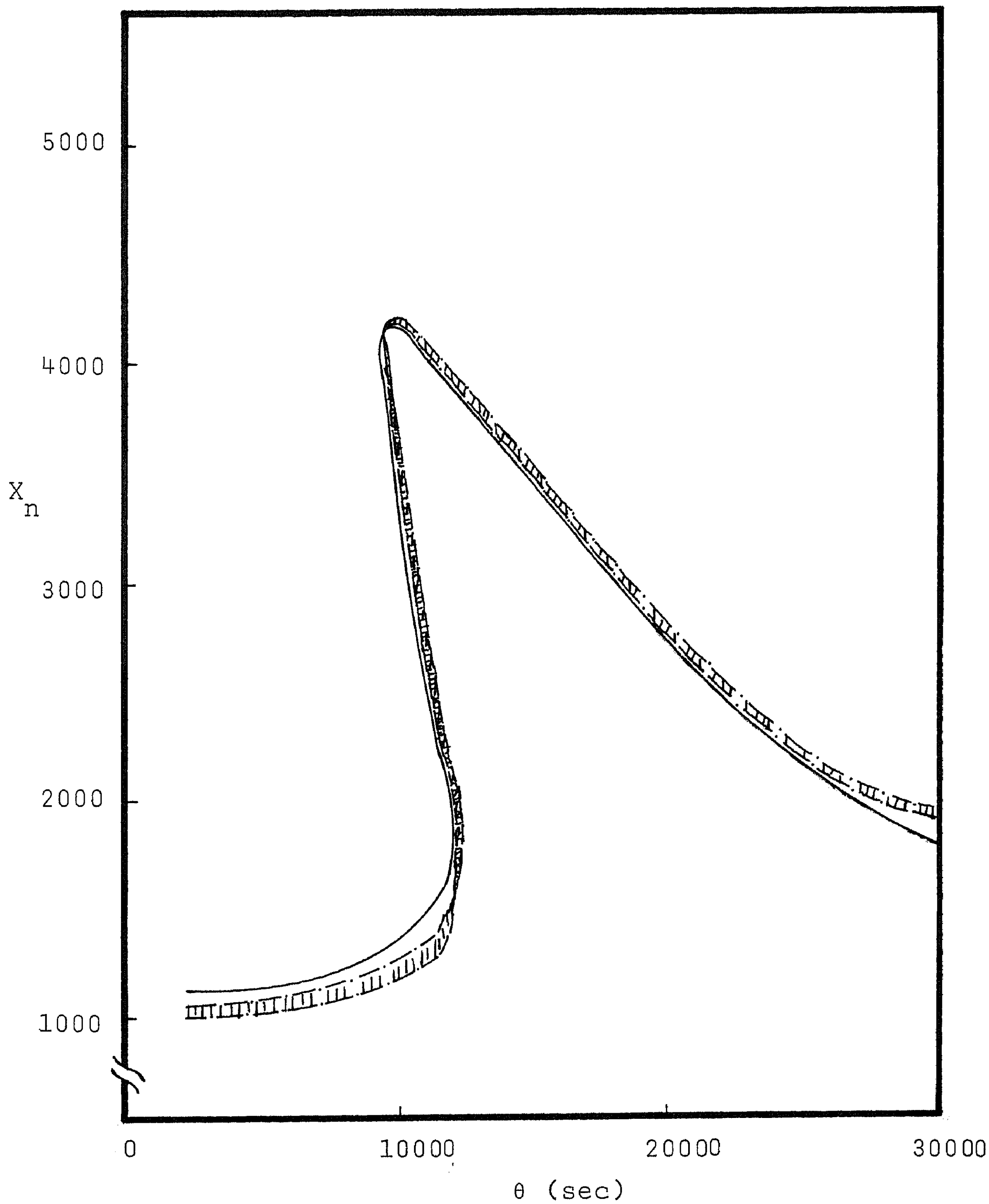

Figure 47. X_n vs. θ at Three Steady States Regions with τ_{off}/τ = 0.1

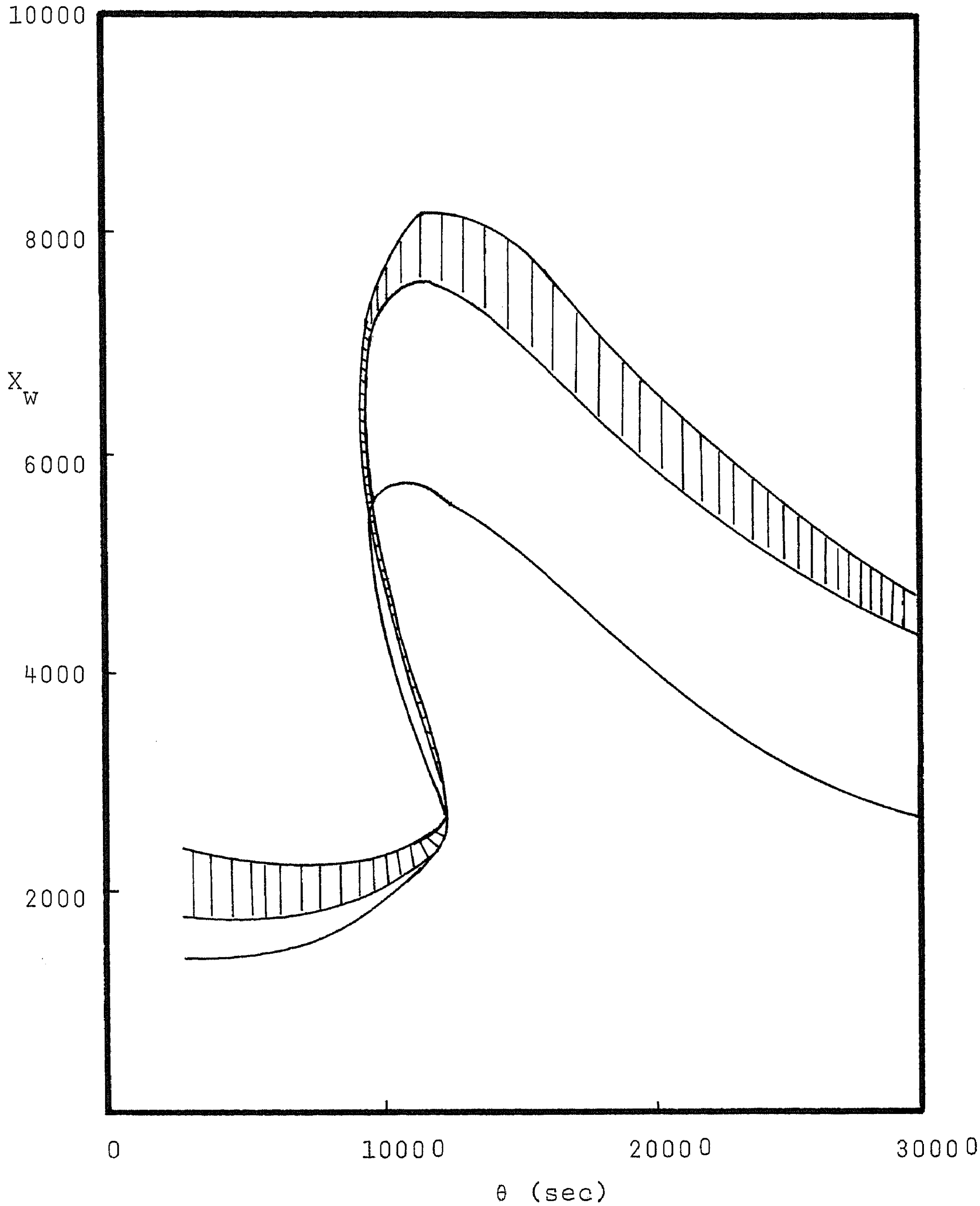

Figure 48. X_w vs. θ at Three Steady States Regions with $\tau_{off}/\tau = 0.1$

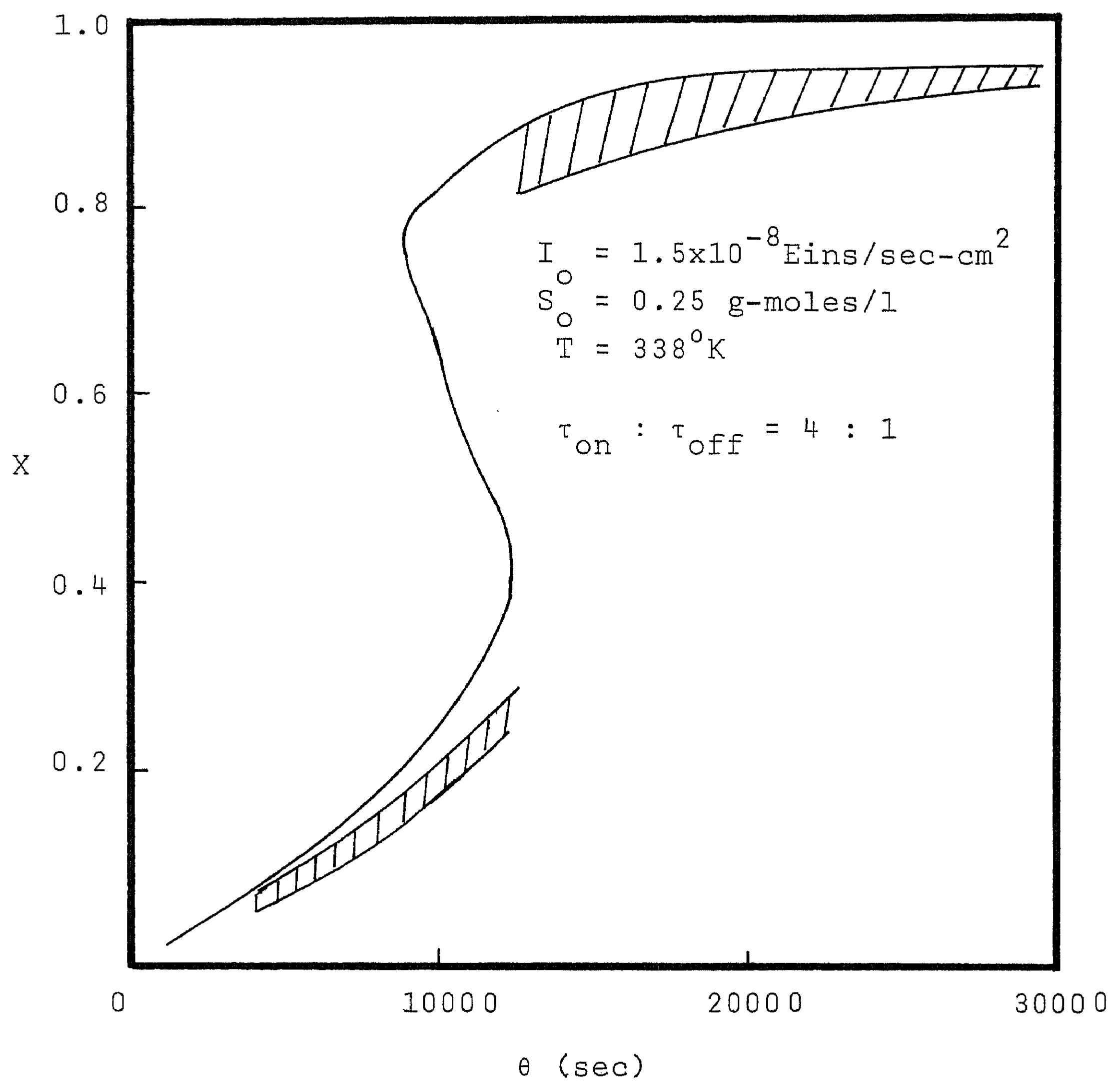

Figure 49. X vs. θ at Three Steady States Regions with τ_{off}/τ = 0.2

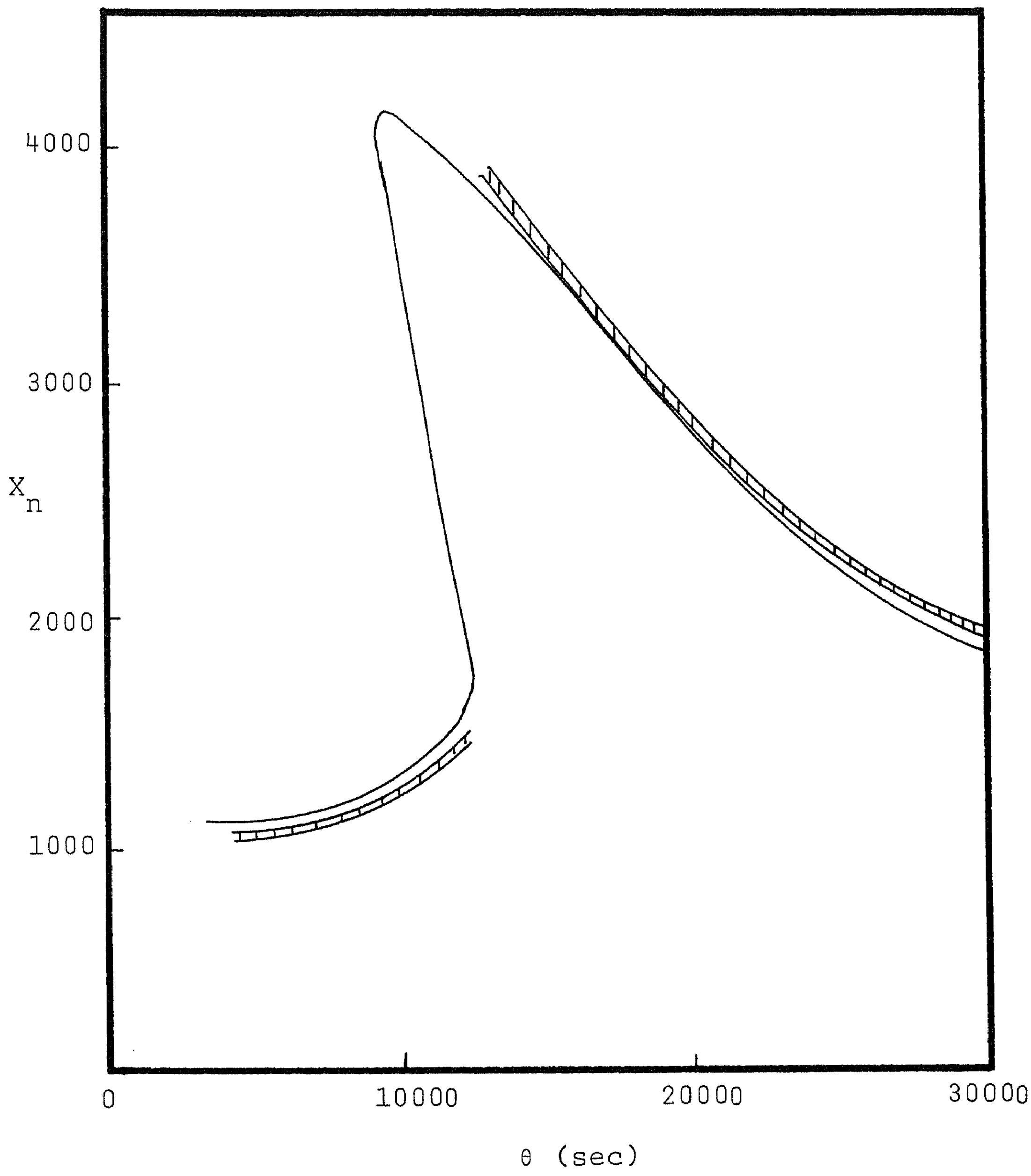

Figure 50. X_n vs. θ at Three Steady States Regions with $\tau_{off}/\tau = 0.2$

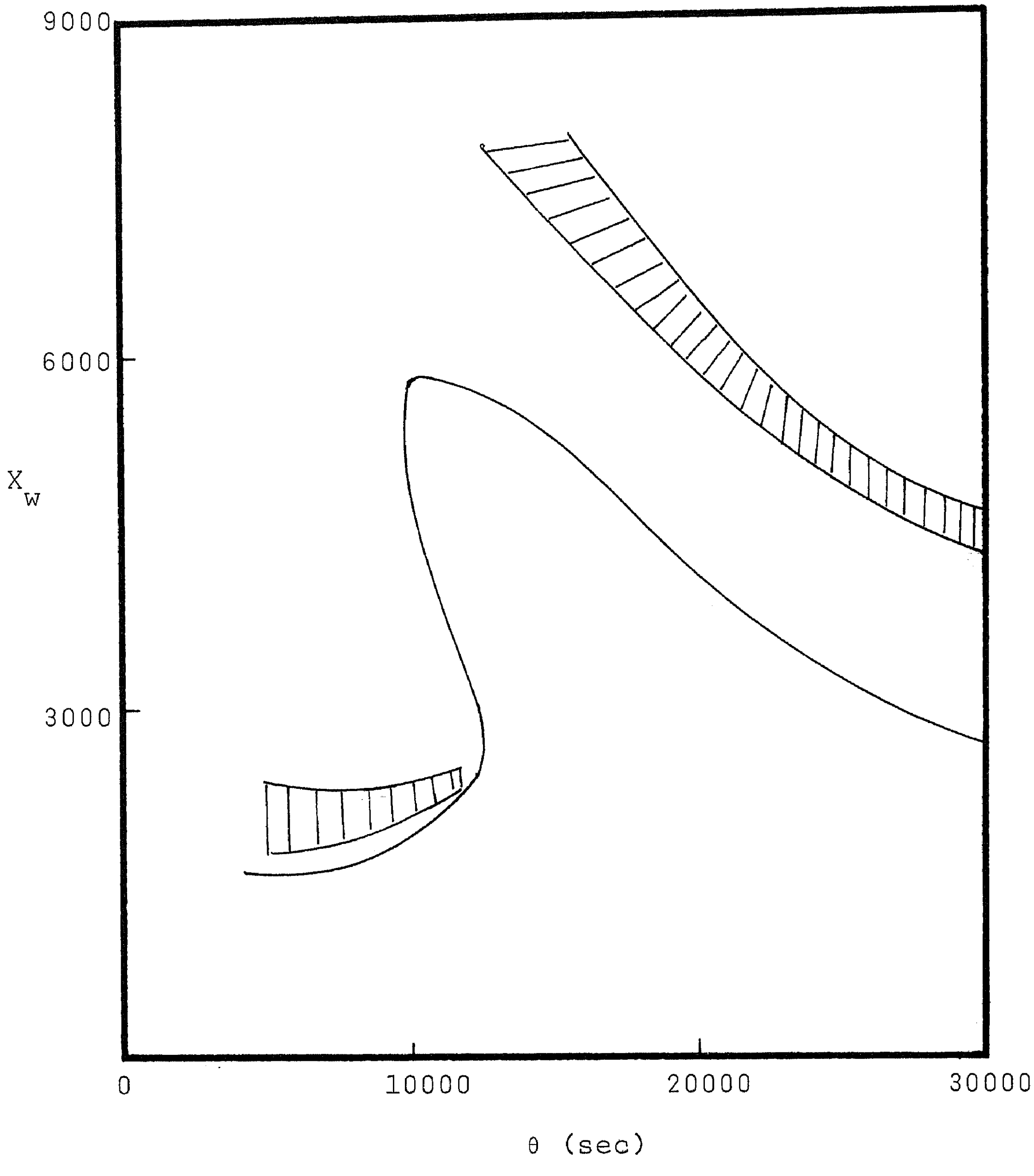

Figure 51. X_w vs. θ at Three Steady States Regions with τ_{off}/τ = 0.2

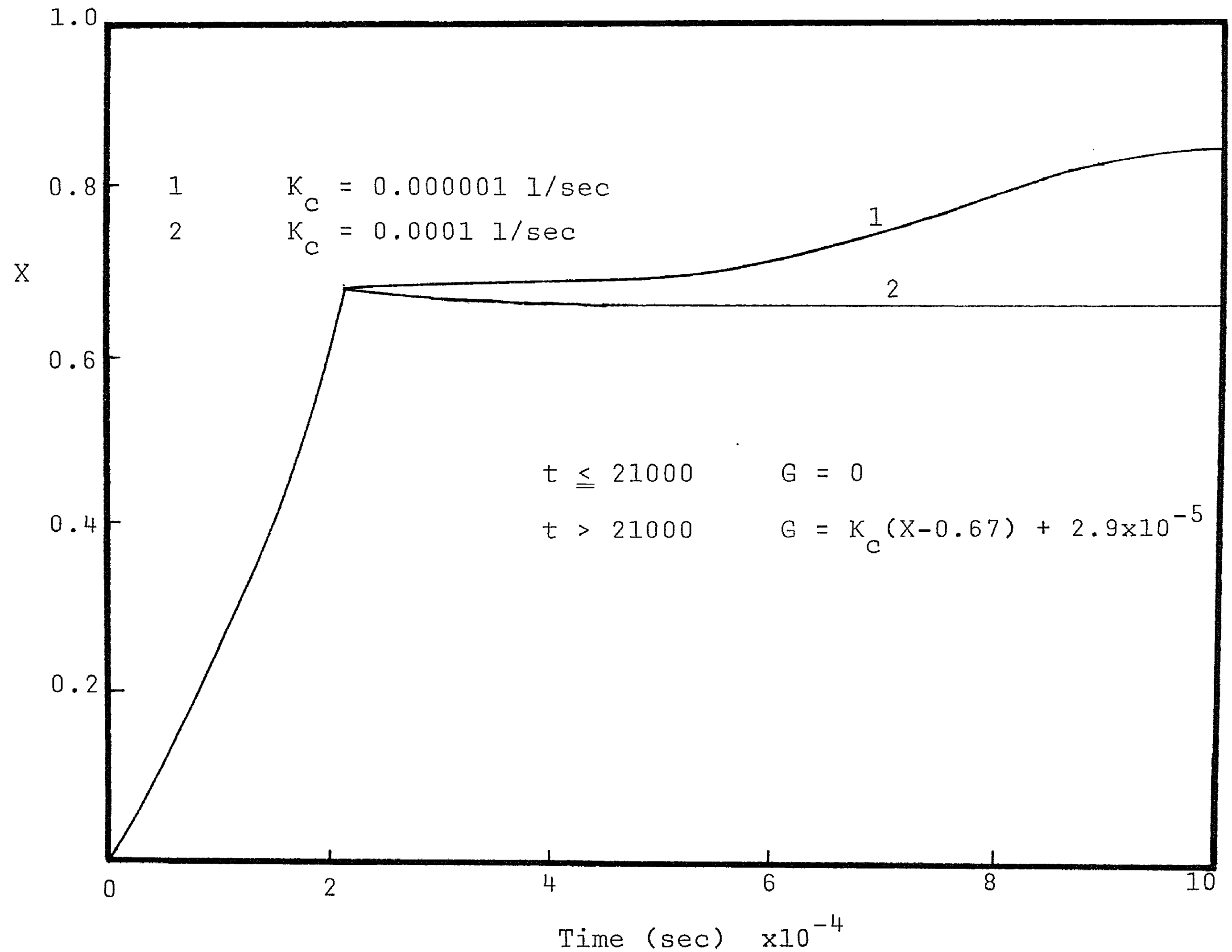

Figure 52. Proportional Control of the Flow Rate Based on Conversion at Metastable State—Initial Point Above the Steady State

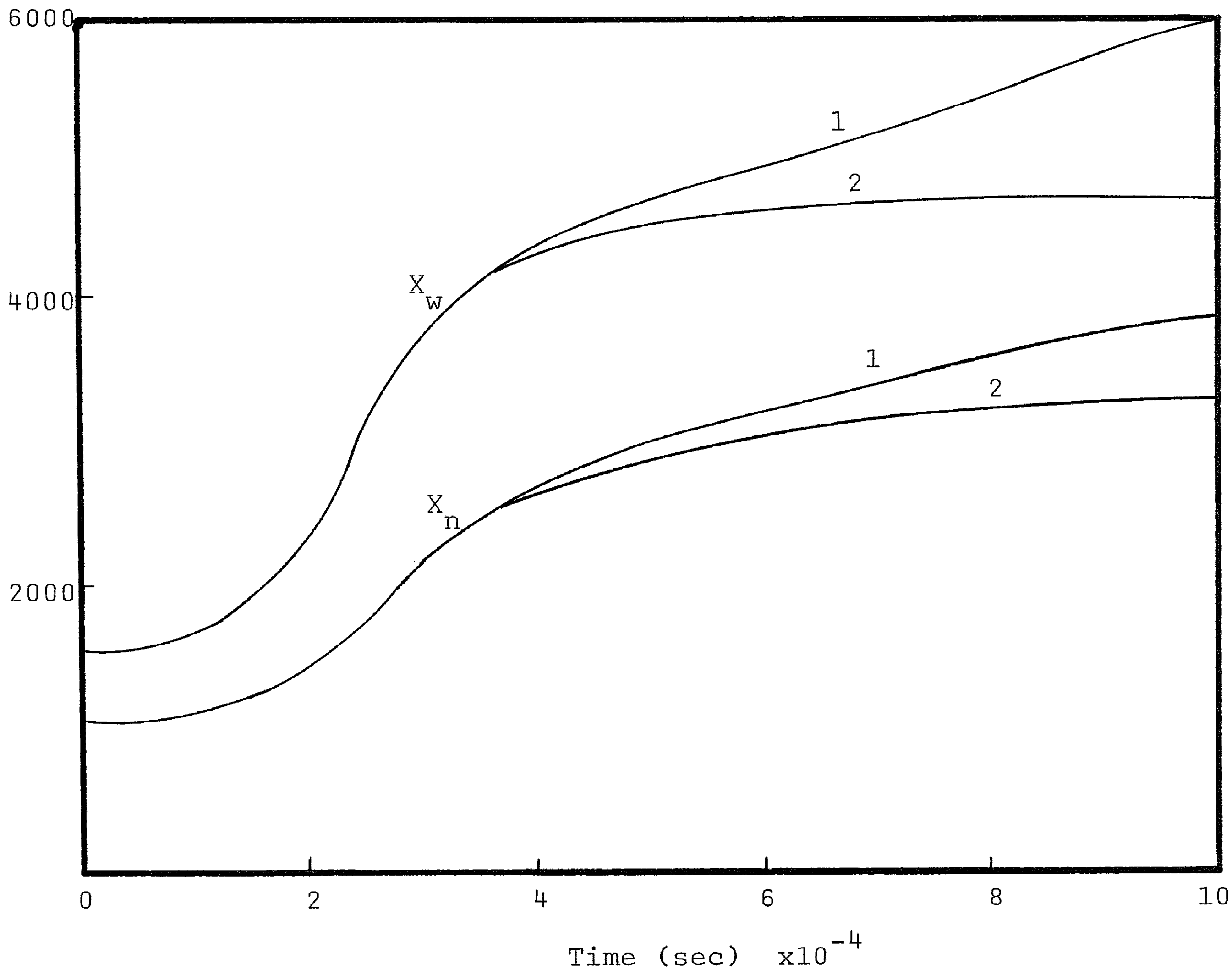

Figure 53. Control on X_n and X_w—Initial Point Above the Steady State

becomes runaway. For K_c = 0.0001 1/sec the response is stable. In Figure 54, conversely, the initial point is reached below the metastable state before a step-change takes place. For K_c= 0.00001 1/sec the response continues to creep slowly downward. The control parameter has the same effect on X_n and X_w as that on the conversion in both cases.

It is also shown in Figures 56—58 that the polydispersity is independent of flow rate with a fixed I_o. It means that the higher polydispersity can not be obtained by the regulation of reactor flow rate in any steady state.

Polymerization reactor characteristics for the no mixing state can also be represented in Appendix C.

Optimal Policies

A series of optimal light intensity policies are shown in Figure 59 with lines connecting points of constant conversion, and finally with lines connecting points of constant number average chain length. The intersection of the desired number average chain length and conversion curves determines the optimal light intensity policy. This leads to a novel development in the presentation of graphical solution for all problems, i.e., for any given conversion and number average chain length, one can locate the starting light intensity and flow rate to reach the steady state of a CSTR. If the point is at the higher steady state, the batch reactor should be started and pass the metastable region, and then the reactor will be changed to CSTR.

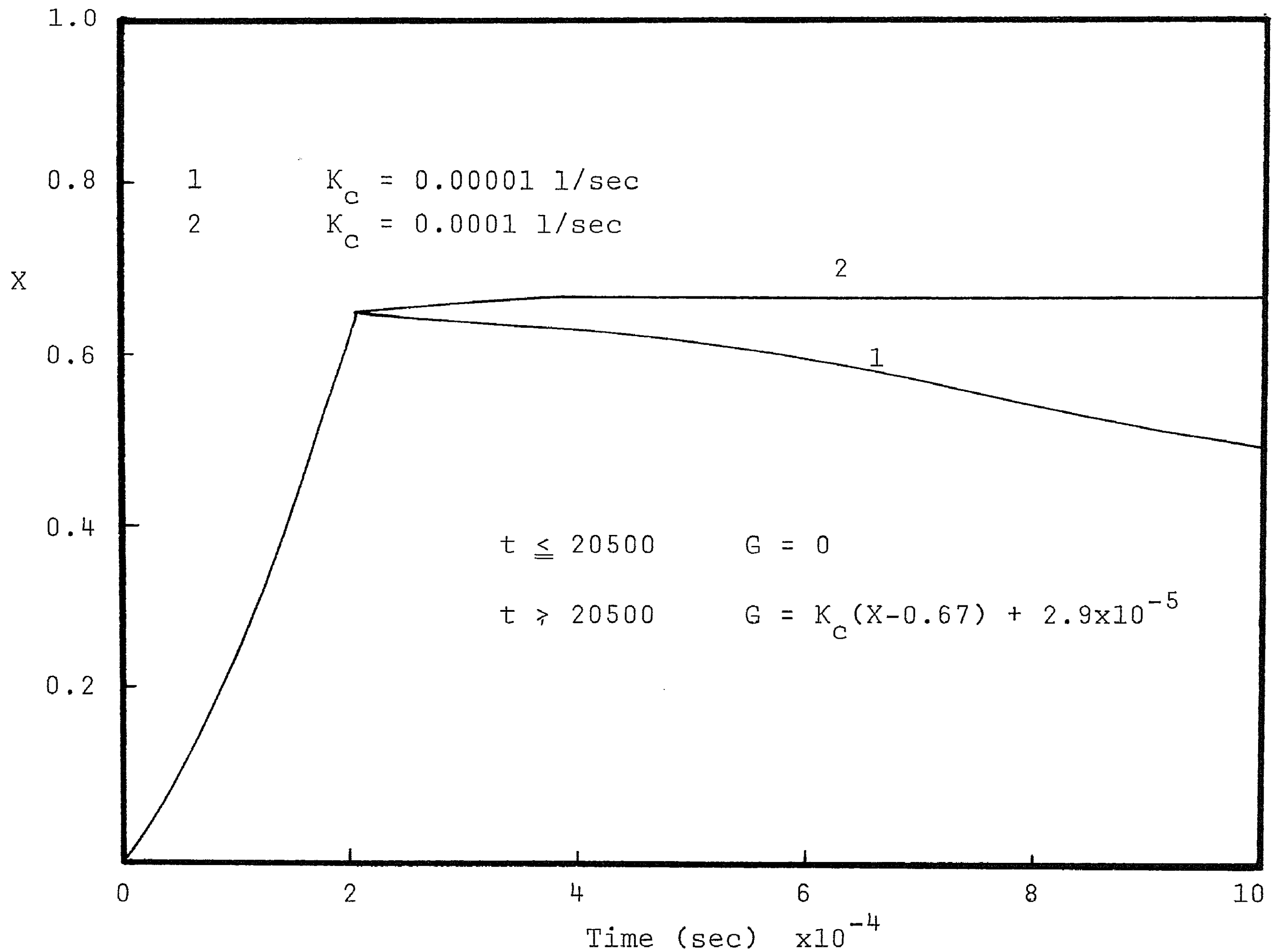

Figure 54. Proportional Control of the Flow Rate Based on Conversion at Metastable State—Initial Point Below the Steady State

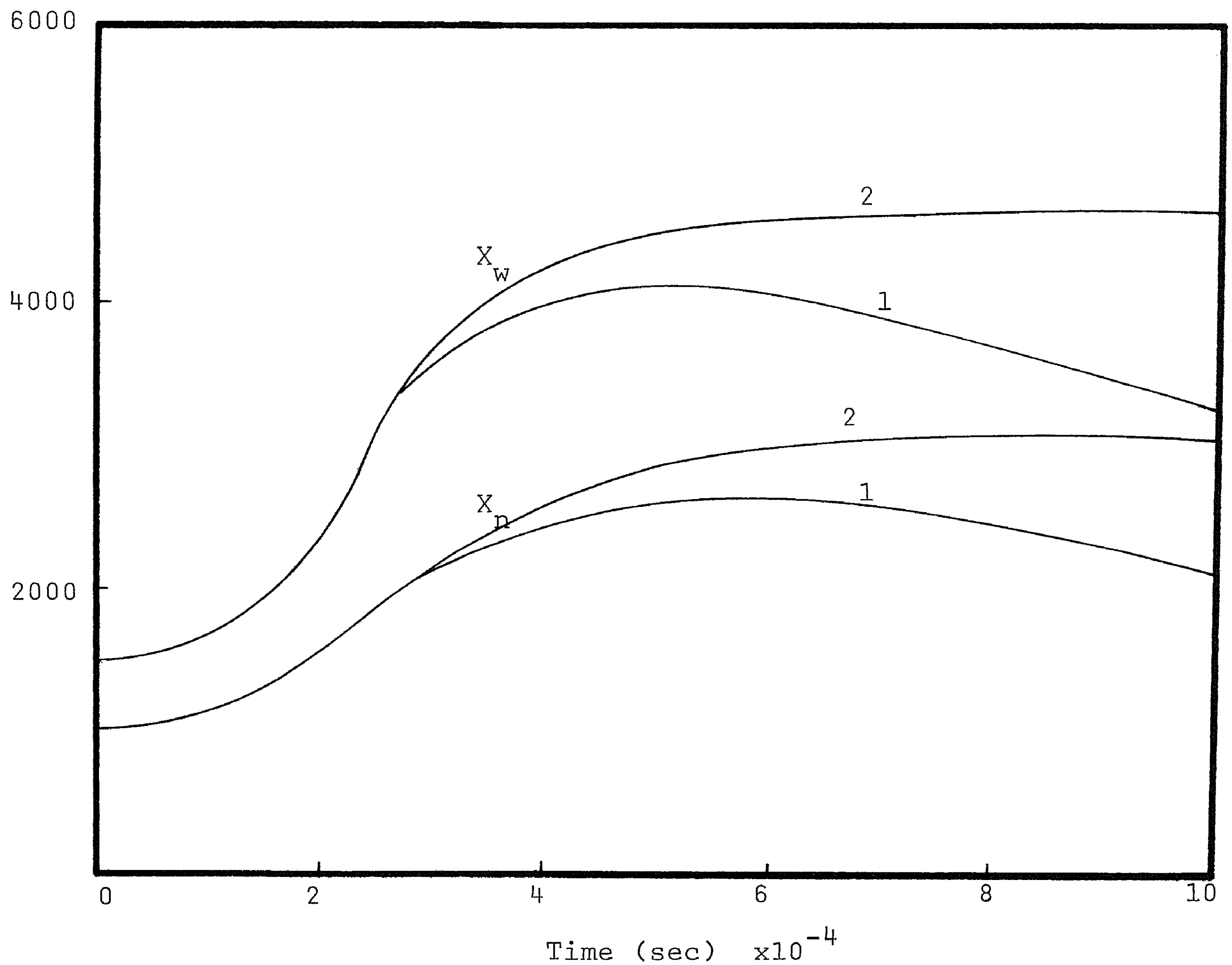

Figure 55. Control on X_n and X_w—Initial Point Below the Steady State

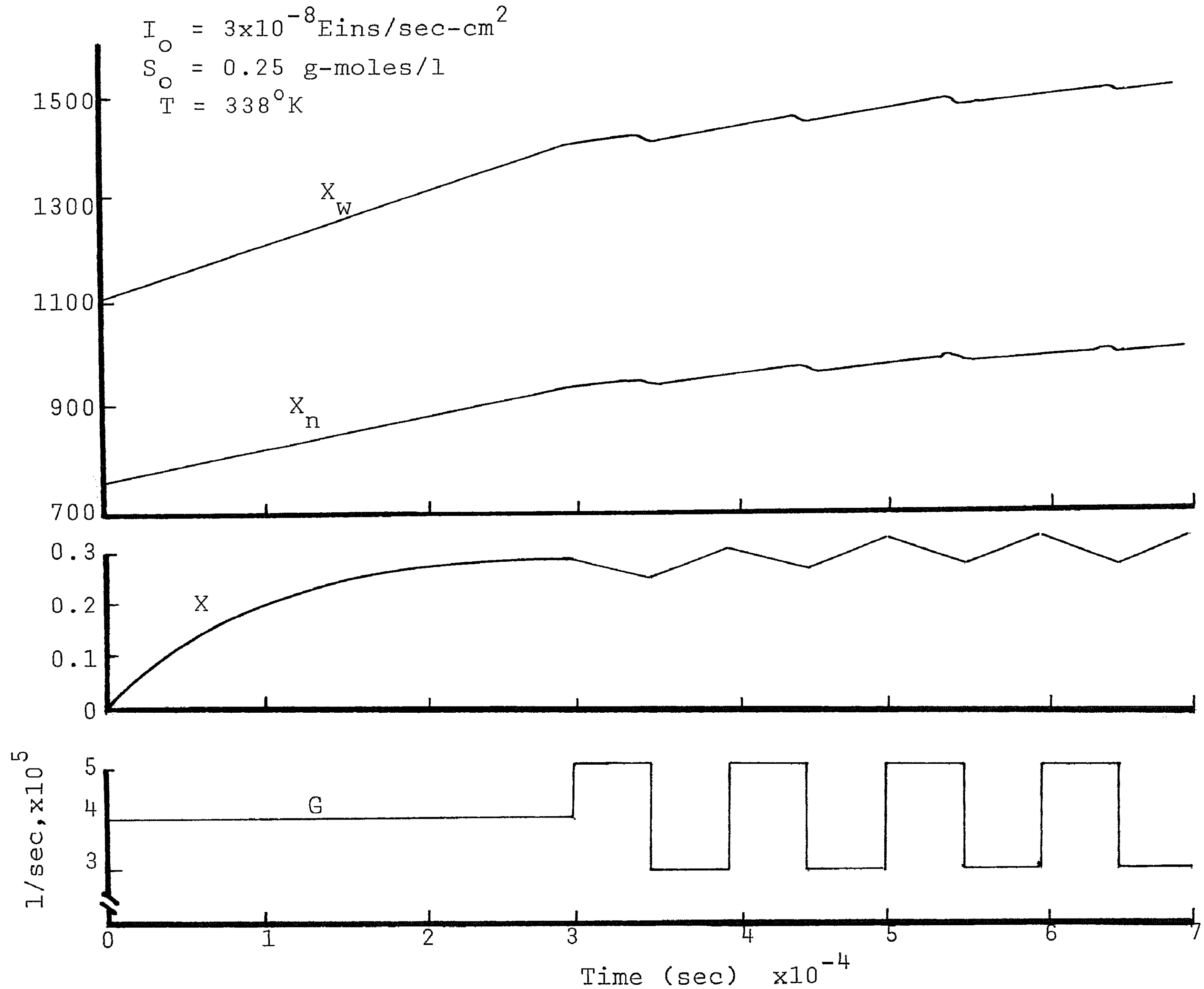

Figure 56. Flow Rate Regulation at Low Steady State

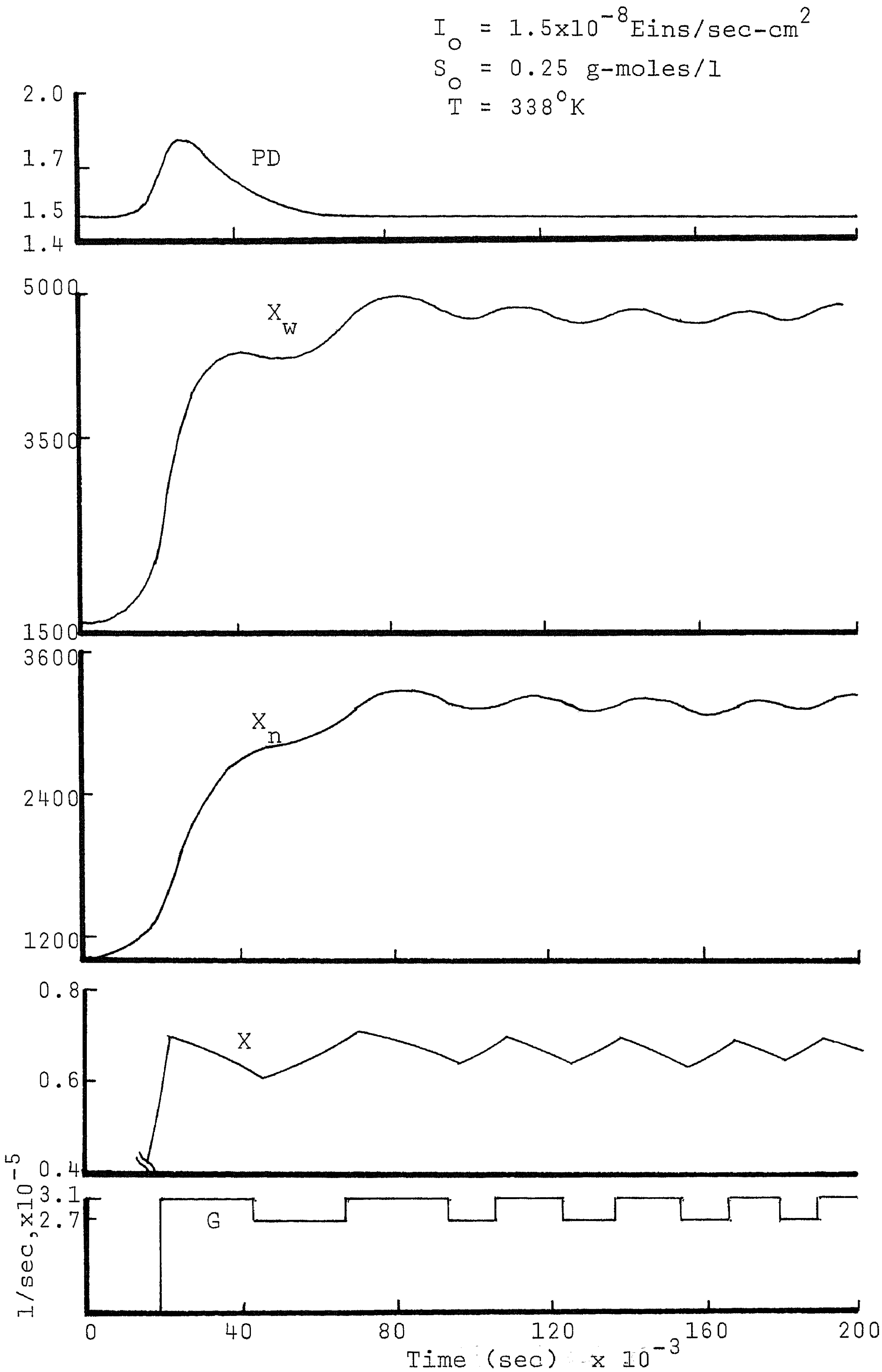

Figure 57. Flow Rate Regulation at Metastable Steady State

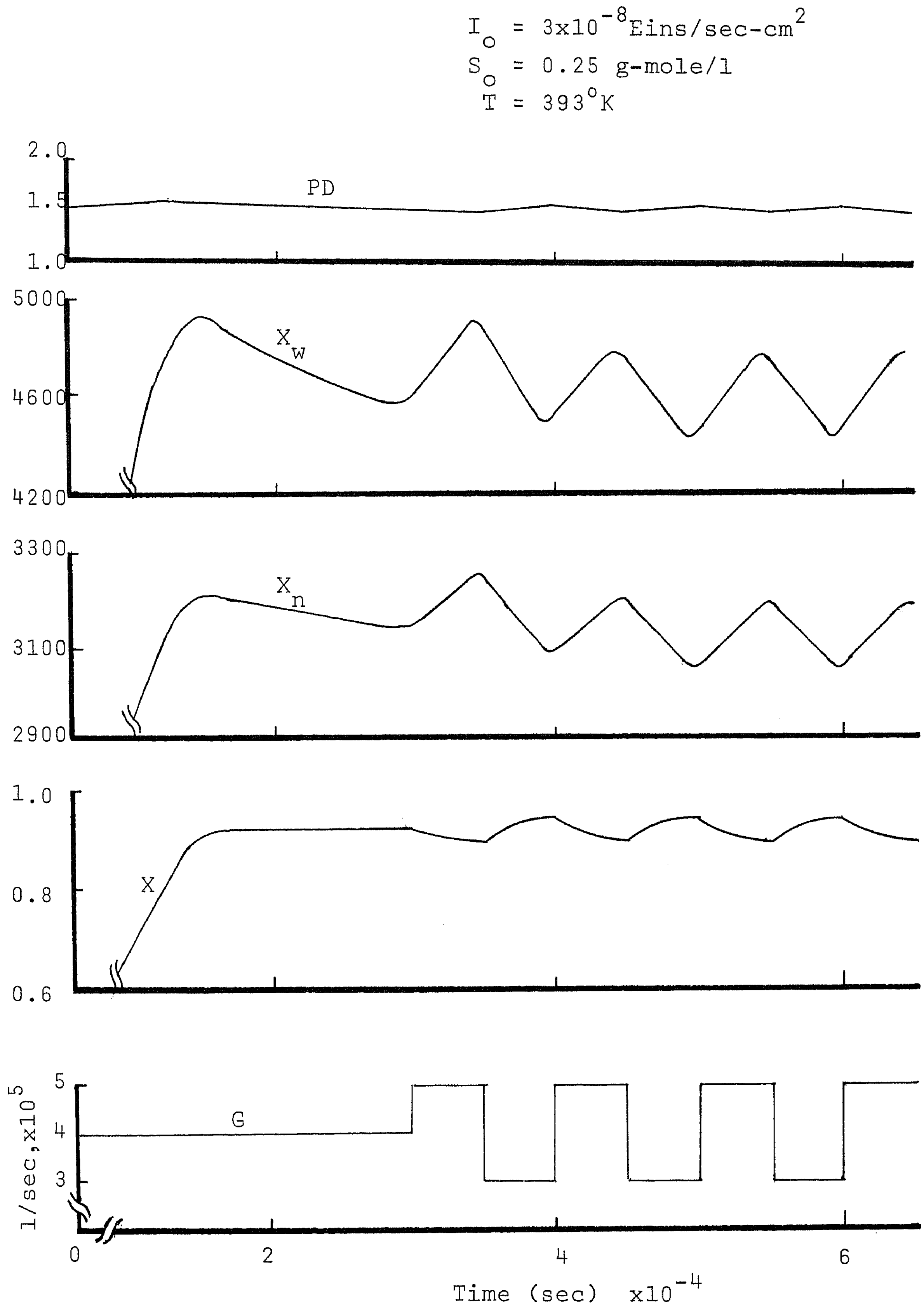

Figure 58. Flow Rate Regulation at High Steady State

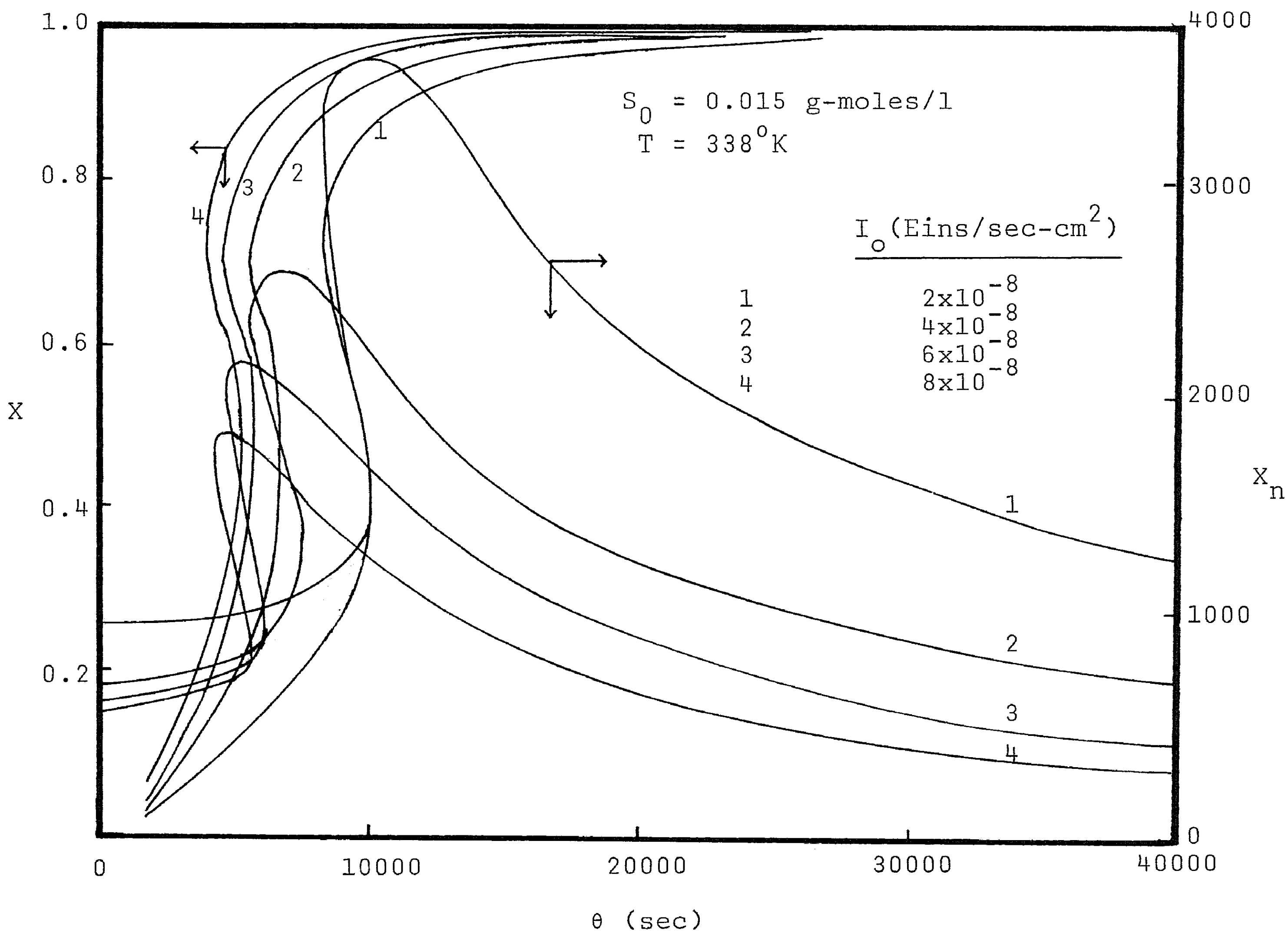

Figure 59. Reactor Performance Characteristics at Different Levels of Light Intensity

When the point is at metastable state, UV light on-off regulation should be employed. If the point is at the low stable state, the reaction can be started by using a CSTR.

In a CSTR, approximate optimization of light intensity or flow rate control to attain not only the reaction conversion but also the desired number average chain length. Figure 60 shows that the conversion, X and number average chain length, X_n with respect to reactor residence time (flow rate) for different levels of light intensity.

Note that the start-up policy of a CSTR to determine the molecular weight distribution by varying the light intensity and/or the inlet flow rate is numerically studied and shown in Appendix D.

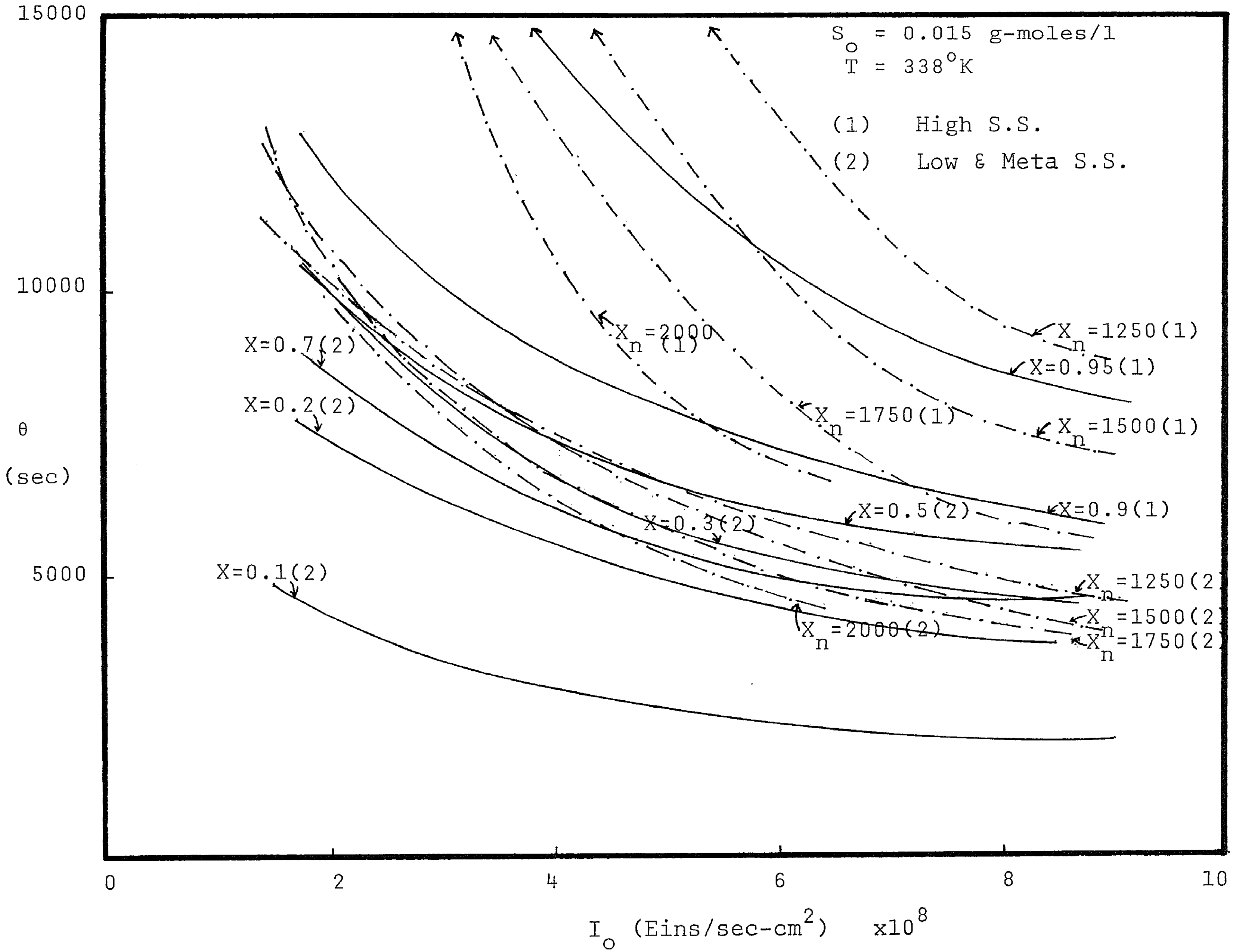

Figure 60. Model Simulation of Optimal Light Intensity and Residence Time Profiles

CHAPTER 7

CONCLUSIONS

Based on the results of this study, the following conclusions are made:

The concentration of active polymer as a function of time for addition photopolymerization has been evaluated analytically. It is verified that the quasi-stationary state approximation used for active polymers is valid for photopolymerization reactions.

It is shown that it is possible to modify appreciably the breadth of the molecular weight distribution and to increase the polydispersity by up to 80% theoretically and numerically for a free radical photopolymerization in a periodically operated in a CSTR. The broadening depends on the parameter τ_{off}/τ, the ratio of light-off period to light on/off period, when compared with steady-state operation and the conversion and number average chain length appear to be little affected by the periodic operation.

Both perfect and imperfect mixing models have been studied for free-radical polymerization reactors. It appears that the two-region model is likely to be more realistc for photopolymerization process, as it agrees well with experimental results. Disagreement between perfect mixing model and experimental data suggests the possibility of fluid elements circulating in a CSTR.

The polydispersity of molecular weight distribution of the polymer formed in batch reactor is shown to depend markedly on dose rate, fractional volume of high dose rate and rate of mass transfer between the two regions. In the process where the polydispersity is maintained within a certaon range the light absorption in low dose region is small but significant and can not be set equal to zero.

The stabilization of the metastable state in an isothermal CSTR has been examined. The photochemical reactor exhibits precise control of conversion and molecular weight for a simple on-off regulation of light intensity. As a result, it is shown that the polydispersity at the controlled steady state is higher than that at real metastable state.

On-off regulation of flow rate at low stable state and metastable state also have been investigated. The results show that no noticeable increase in polydispersity occurs at these steady states. The number average chain length changes proportionally with an increase or decrease in weight average chain length. The reason is, the flow rate regulation can not produce wide range difference in active polymer concentration which may be achieved by using light on-off regulation in photopolymerization process.

The feasibility of controlling a CSTR when operating at a metastable point is studied theoretically for the photopolymerization reaction. Stable operation of the system is dependent upon the magnitude of the proportionality constant. In the examples shown here, stability is obtained only for values of K_c approaching on-off control. For the starting point above or below the real metastable state, the smaller K_c values will cause the reaction system runaway.

The rate of initiation by ultraviolet light may be changed very rapidly and may lead to greater reactor stability and ease of reactor control. Better reactor performance is obtained as compared with other periodic polymerization reactors.

The method is described for deriving equations for the three moments and the degree of polymerization directly from the polymerization kinetics for photopolymerization in CSTRs. The determination of these moments leads to expressions for number average chain length, weight average chain length, polydispersity, and molecular weight distribution of a polymer as a function of the parameter, ratio of light-off period to the light on-off period. These results are exact, and no simplifying assumptions need to be made in their derivation.

For further study, the following recommendation is made: It is indispensable for representing I_o, $\sum R_i$ and M with discontinuities, particularly periodic phenomena, by employing the Fourier series. The Fourier coefficients can often be computed efficiently by the method of Fast Fourier transformation, which results in a considerable savings of computation time. The moments of dead polymer may be calculated by the integration of equations and lead to the expression of MWD. Emphasis is placed on the reaction time, insteady of cycle number in the unsteady state process.

NOTATION

Symbol	Definition
I_o	Incident light intensity, Eins/sec-cm^2
I_{as}	Absorbed light intensity, Eins/sec-cm^3
i,j	Number of monomer units
K_c	Controller proportional constant
K_d	Rate constant for reaction of sensitizer radical with monomer, cc/g-mole-sec
K_i	Rate constant for initiation 3rd order in monomer, cc^2/g-mole^2-sec
K_f	Rate constant for chain transfer to monomer, cc/g-mole-sec
K_p	Propagation rate constant, cc/g-mole-sec
K_{tc}	Rate constant for termination by combination, cc/g-mole-sec
K_{td}	Rate constant for termination by disproportionation, cc/g-mole-sec
K_t	$K_{tc} + K_{td}$
L	Reactor length, cm
M_o	Monomer concentration in feed, g-moles/cc
M	Monomer concentration in reactor, g-moles/cc
P_i	Concentration of dead polymer of chain length i monomer units, g-mole/cc
$\sum P_i$	Zeroth moment of dead polymer, g-moles/cc
$\sum iP_i$	First moment of dead polymer, g-moles/cc
$\sum i^2P_i$	Second moment of dead polymer, g-moles/cc
PD	Polydispersity, dimensionless
Q	Volumetric flow rate, cc/sec
q	Volumetric flow rate between two regions, cc/sec

Symbol	Definition
R_i	Concentration of free radical of chain length i monomer units, g-moles/cc
$\sum R_i$	Total active polymer or zeroth moment of active polymer, g-moles/cc
$\sum iR_i$	First moment of active polymer, g-moles/cc
$\sum i^2 R_i$	Second moment of active polymer, g-moles/cc
S_o	Sensitizer concentration in feed, g-moles/cc
S	Sensitizer concentration in reactor, g-moles/cc
t	Time, sec
T	Temperature in reactor, ^oK
V	Reactor volume, cc
W_i	Weight fraction of polymer of chain length i monomer units, dimensionless
x	Distance, cm
X	Fractional conversion, dimensionless
X_n	Number average chain length, dimensionless
X_w	Weight average chain length, dimensionless
Z	Distance, cm

Greek Symbol	Definition
Ω_i	Total initiation rate, g-moles/cc-sec
ϵ	Fractional change in volume between zero and complete conversion, dimensionless
ϵ_m	Molar absorptivity of monomer, cm^2/g-moles
ϵ_{P_i}	Molar absorptivity of dead polymer of chain length of i monomer units, cm^2/g-moles
ϵ_s	Molar absorptivity of sensitizer, cm^2/g-moles
ϕ_s	Quantum yield from sensitizer, g-moles/Eins
τ_{off}	UV light-off period, sec
τ	Forced period, UV light on/off period, sec
Φ	Generating function
θ	Reactor residence time, sec

Table 3

Summary of Kinetic Model Parameters and Thermophysical Properties Data

$(K_p)_o = 1.051 \times 10^7 \, Exp(-3557/T)$ liter/g-mole-sec

$(K_t)_o = 1.255 \times 10^9 \, Exp(-844/T)$ liter/g-mole-sec

$(K_f)_o = 2.31 \times 10^6 \, Exp(-6377/T)$ liter/g-mole-sec

$K_i = 2.19 \times 10^5 \, Exp(-13810/T)$ liter^2/g-mole^2-sec

$A_1 = 2.57 - 5.05 \times 10^{-3} T$

$A_2 = 9.56 - 1.76 \times 10^{-2} T$

$A_3 = -3.03 + 7.85 \times 10^{-3} T$

$\epsilon_m = 0.0155$ liter/g-mole-cm

$\epsilon_s = 88.5$ liter/g-mole-cm

$\epsilon_{P_i} = 76.2$ liter/g-mole-cm

$\phi_s = 0.072$ g-mole/Eins

$\rho_m = 924 - 0.918 \times (T-273.1)$ g/liter

$\rho_p = 1084.8 - 0.605 \times (T-273.1)$ g/liter

APPENDIX A

CALCULATION OF MWD AT STEADY STATE IN CSTR

For addition polymers produced in continuous stirred-tank reactors, a method is described for deriving equations for the degree of polymerization directly from the equations for the polymerization kinetics. Several investigators (51) (52) have solved the kinetic equations for free radical polymerization in CSTR to obtain expressions for the polymerization size distribution as a function of reactor operating conditions. The purpose of this study is to present relationships from which the moments, number average chain length X_n, and weight average chain length X_w may be calculated and to illustrate the derivation of these quantities from the photopolymerization system.

Mass-balance equations of monomer and free radical from the reaction mechanism expressed in Chapter 2

$$\frac{dM}{dt} = \frac{M_o}{\theta} - \Omega_i - \frac{M}{\theta} \qquad \Omega_i = K_p M \sum R_i + K_d (S\cdot) M$$

$$\frac{dS\cdot}{dt} = 2\phi_s I_{as} - K_d (S\cdot) M - \frac{S\cdot}{\theta}$$

$$\frac{dR_1}{dt} = K_d (S\cdot) M - K_p M R_1 - K_t R_1 \sum R_i - \frac{R_1}{\theta}$$

$$\frac{dR_2}{dt} = K_p M R_1 - K_p M R_2 - K_t R_2 \sum R_i - \frac{R_2}{\theta}$$

$$\vdots$$

$$\frac{dR_j}{dt} = K_p M R_{j-1} - K_p M R_j - K_t R_j \sum R_i - \frac{R_j}{\theta}$$

Similarly for the dead polymers the mass-balance is given by

$$\frac{dP_2}{dt} = \frac{1}{2} K_t R_1 R_1 - \frac{P_2}{\theta} \qquad (1)$$

$$\frac{dP_3}{dt} = K_t R_1 R_2 - \frac{P_3}{\theta} \tag{2}$$

$$\frac{dP_4}{dt} = K_t (R_1 R_3 + \frac{1}{2} R_2 R_2) - \frac{P_4}{\theta} \tag{3}$$

$$\frac{dP_5}{dt} = K_t (R_1 R_4 + R_2 R_3) - \frac{P_5}{\theta} \tag{4}$$

$$\frac{dP_6}{dt} = K_t (R_1 R_5 + R_2 R_4 + \frac{1}{2} R_3 R_3) - \frac{P_6}{\theta} \tag{5}$$

.
.
.
.

$$\frac{dP_j}{dt} = \frac{1}{2} K_t \sum_{i=1}^{j-1} R_i R_{j-i} - \frac{P_j}{\theta} \tag{6}$$

At steady state, all the derivatives are set equal to zero. Therefore

$$S\cdot = \frac{2\phi_s I_{as}}{\frac{1}{\theta} + K_d M}$$

$$M = \frac{M_o}{1 + K_p \sum R_i + K_d S\cdot}$$

$$= \frac{M_o - (2\phi_s I_{as})}{1 + K_p \sum R_i}$$

$$R_1 = \frac{K_p M}{K_p M + K_t \sum R_i + \frac{1}{\theta}} \frac{2\phi_s I_{as}}{\frac{1}{\theta} + K_d M}$$

$$R_2 = \frac{K_p M R_1}{K_p M + K_t \Sigma R_i + \frac{1}{\theta}}$$

$$= \frac{K_d K_p M^2}{(K_p M + K_t \Sigma R_i + \frac{1}{\theta})^2} \frac{2\phi_s I_{as}}{\frac{1}{\theta} + K_d M}$$

$$\vdots$$

$$R_j = \frac{K_d K_p^{\,j-1} M^j}{(K_p M + K_t \Sigma R_i + \frac{1}{\theta})^j} \frac{2\phi_s I_{as}}{\frac{1}{\theta} + K_d M}$$

The sum of equations of active polymer to infinity gives

$$\sum R_i = K_d \frac{2\phi_s I_{as}}{\frac{1}{\theta} + K_d M} \sum_{i=1}^{\infty} \frac{K_p^{\,i-1} M^i}{(K_p M + K_t \Sigma R_i + \frac{1}{\theta})^i}$$

$$= \frac{K_d}{K_p} \frac{2\phi_s I_{as}}{\frac{1}{\theta} + K_d M} \sum_{i=1}^{\infty} \left(\frac{K_p M}{K_p M + K_t \Sigma R_1 + \frac{1}{\theta}} \right)^i \qquad (7)$$

Since

$$\frac{K_p M}{K_p M + K_t \Sigma R_i + \frac{1}{\theta}} < 1$$

and

$$K_d M >> \frac{1}{\theta}$$

also it can be assumed that

$$K_d = K_p$$

then equation (7) reduces to

$$\sum R_i = \frac{2\phi_s I_{as}}{\frac{1}{\theta} + K_d M} \left(\frac{K_p M}{K_t \Sigma R_i}\right)$$

$$= \frac{2\phi_s I_{as}}{K_t \Sigma R_i}$$

So that the total active polymer can be expressed as

$$\sum R_i = \left(\frac{2\phi_s I_{as}}{K_t} \right)^{1/2}$$

Substituting the solved concentrations of active polymers, total polymer and monomer into the equations (1) through (6), finally one obtains

$$P_j = \theta K_t \left(\frac{2\phi_s I_{as}}{K_p M} \right)^2 \left(\frac{j-1}{2} \right) \left(\frac{K_p M}{K_p M + K_t \Sigma R_i} \right)^j$$

$$= A \left(\frac{j-1}{2} \right) B^j \qquad (8)$$

where

$$A = \theta K_t \left(\frac{2\phi_s I_{as}}{K_p M} \right)^2$$

$$B = \frac{K_p M}{K_p M + K_t \Sigma R_i}$$

and use of equation (8) to obtain expressions for the moments gives

$$\sum P_j = \frac{1}{2} AB^2 (1 + 2B + 3B^2 + 4B^3 + \cdots\cdots)$$

$$= \frac{1}{2} AB^2 \frac{1}{(1-B)^2}$$

$$\sum jP_j = AB^2 (1 + 3B + 6B^2 + 10B^3 + 15B^4 + 21B^5 + \cdots\cdots)$$

$$= AB^2 \frac{1}{(1-B)^3}$$

$$\sum j^2 P_j = AB^2 (3 + 12B + 30B^2 + 60B^3 + 105B^4 + \cdots\cdots)$$
$$-AB^2 (1 + 3B + 6B^2 + 10B^3 + 15B^4 + \cdots\cdots)$$

$$= AB^2 \left(\frac{3}{(1-B)^4} - \frac{1}{(1-B)^3} \right)$$

Finally, the number average and weight average chain length can be obtained

$$X_w = \frac{\sum j^2 P_j}{\sum j P_j}$$

$$= \frac{3}{1-B} - 1$$

$$X_n = \frac{\sum j P_j}{\sum P_j}$$

$$= \frac{2}{1-B}$$

Since $B \simeq 1$, $X_w \simeq \frac{3}{1-B}$, and the ratio, polydispersity, is

$$\frac{X_w}{X_n} \simeq 1.5$$

Thus a sequence of steady state concentrations of monomer and the molecular weight distribution of polymer from reactor can be calculated.

Also

$$K_p = f_1(\text{temp.})$$

$$K_t = f_2(\text{temp.})$$

$$\sum R_i = f_3(I_o, \text{temp.})$$

$$M = f_4(I_o, \text{temp.})$$

so that

$$B = \frac{K_p M}{K_p M + K_t \Sigma R_i}$$

$$= f_5(I_o, \text{temp.})$$

where f_i is a function

Since X_n and X_w are very strongly dependent upon the value of B which is very close to unity, the values of X_n and X_w will depend upon the I_o and temperature. The effects of I_o and/or temperatures on X_n, X_w and molecular weight distribution are shown in Figures 61 through 64. The distribution curve may shift to the higher molecular weight once the temperature increases at a given I_o. The X_n increases proportionally with X_w due to the term, 1-B. Also, the same effect is observed in the decrease of I_o at a given temperature. Figure 65 shows that the polydispersity and X_n behavior have been calculated numerically by UV light on and off using the equations (1)—(5) in Chapter 4. It is verified that the polydispersity, although sharply rising, can be reached steady state again and X_n can be reached to a higher location which is the steady state of thermal polymerization.

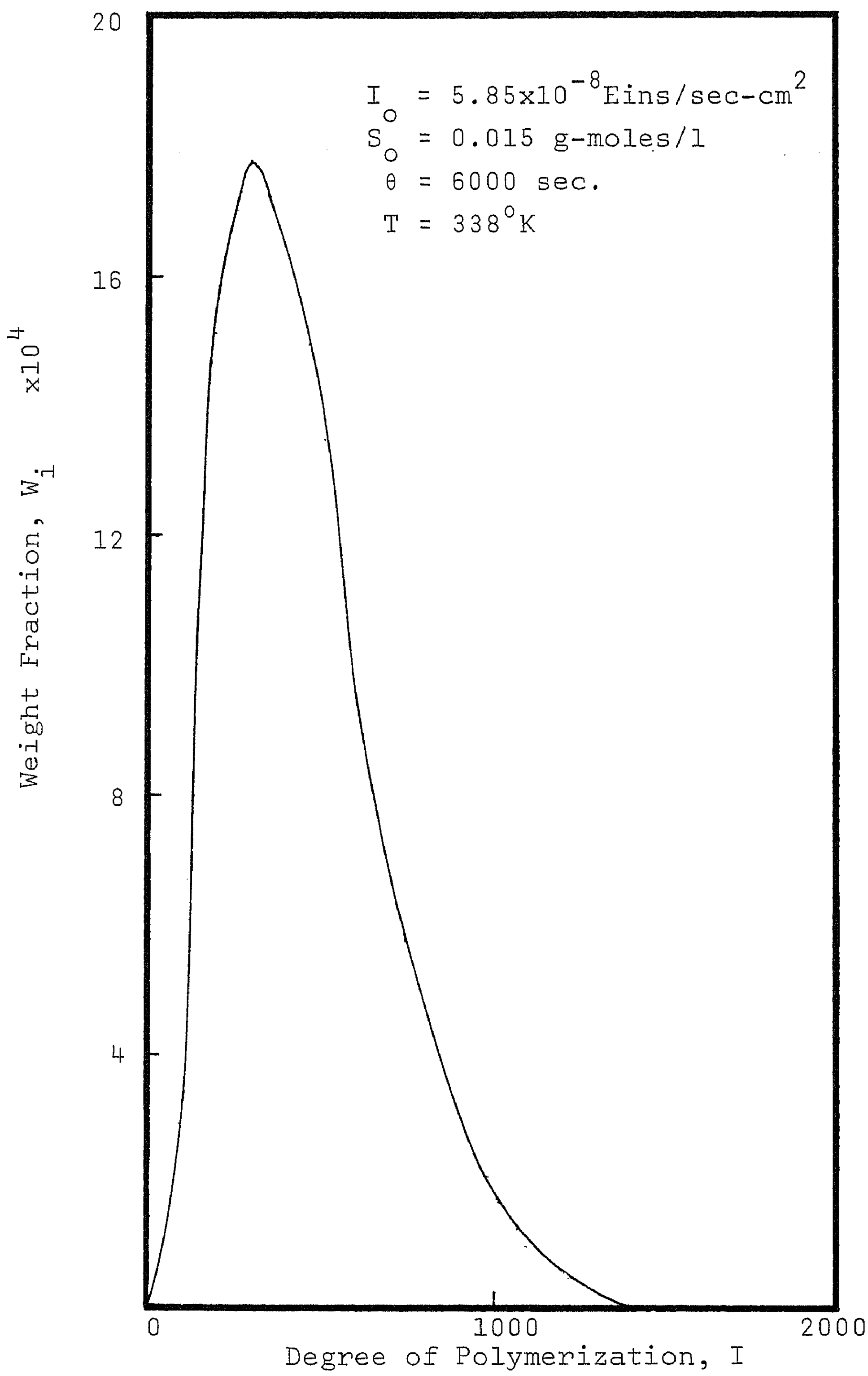

Figure 61. MWD at Steady State

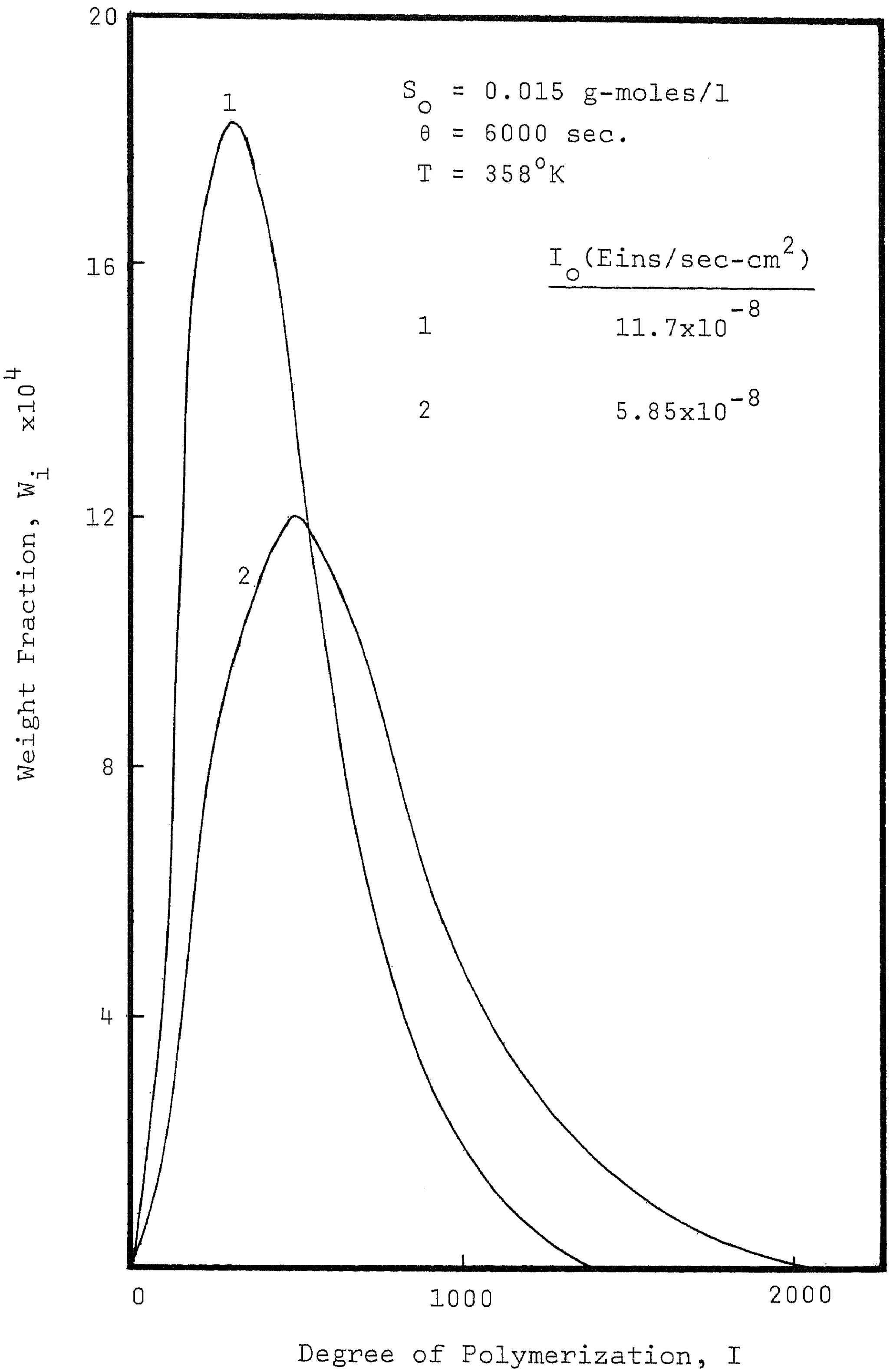

Figure 62. Effect of I_o on MWD at Steady State with T = 358°K

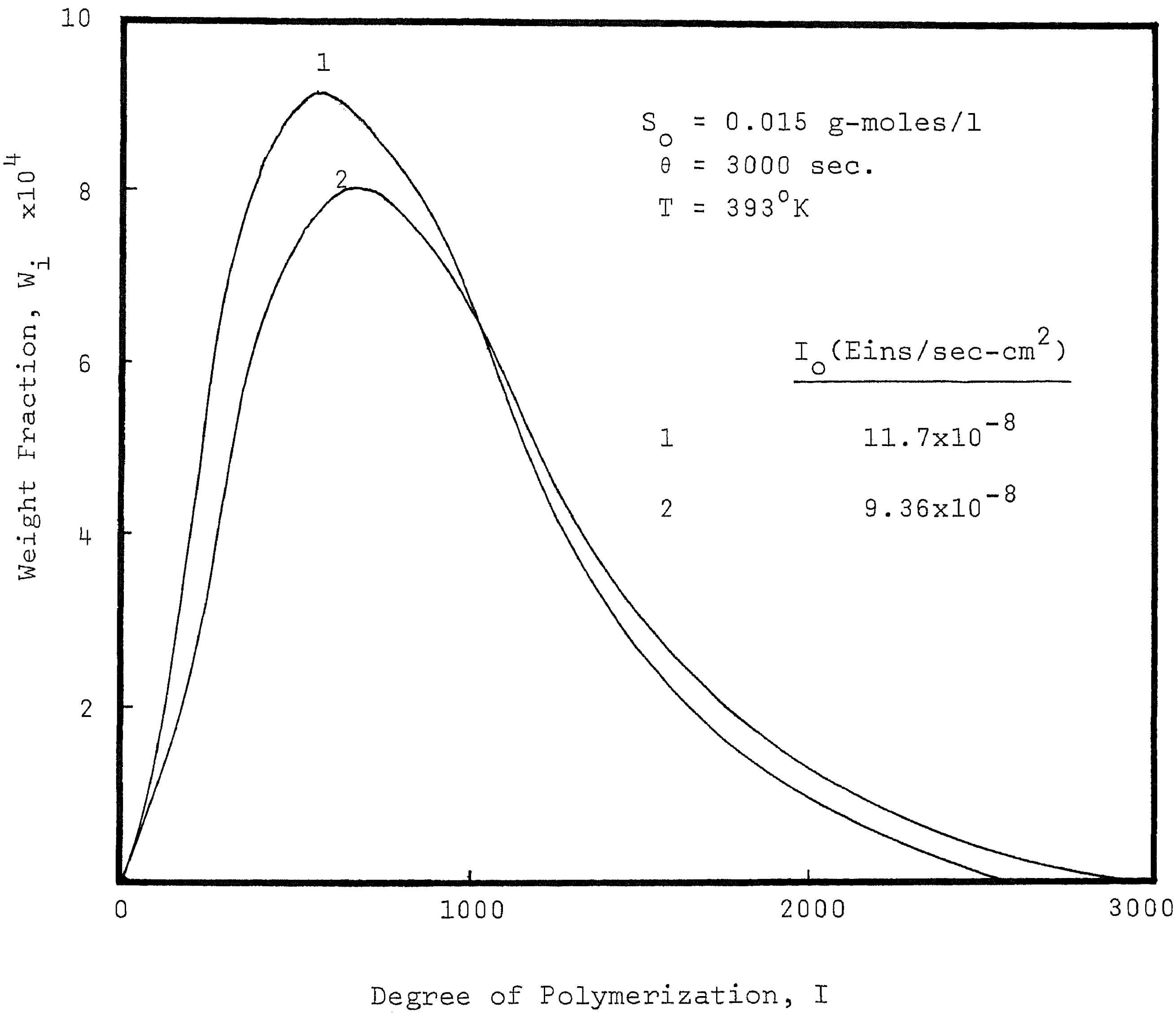

Figure 63. Effect of I_o on MWD at Steady State with T = 393°K

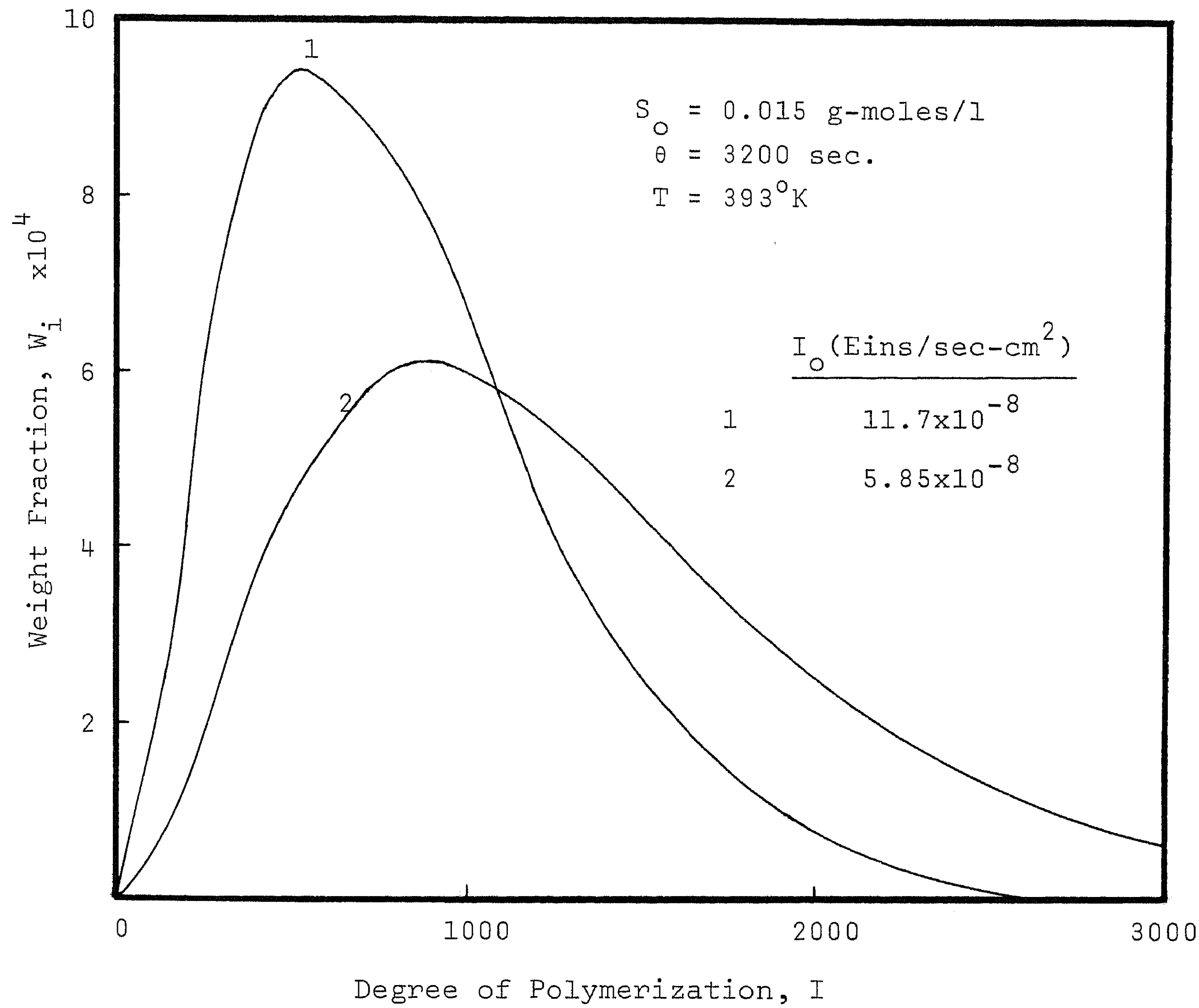

Figure 64. Effect of I_o on MWD at Steady State with T = 393°K

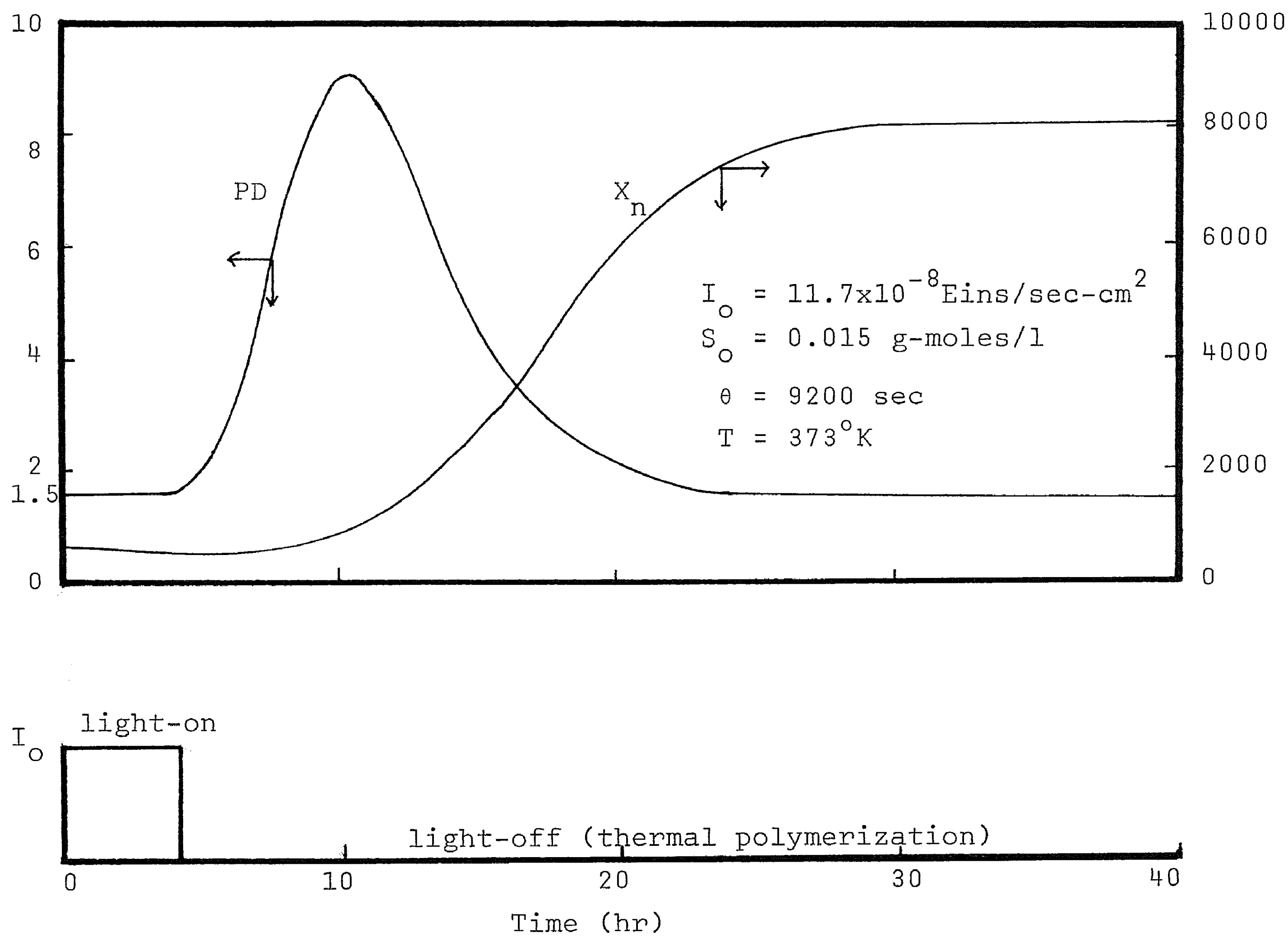

Figure 65. Transient Response of Polydispersity by the UV Light ON and OFF

APPENDIX B

SOLUTION PHOTO-POLYMERIZATION OF BATCH REACTOR

In solution polymerization the viscosity of the reaction mass is much lower than in bulk polymerization, and heat transfer is thereby improved. The choice of solvent is important as it may affect both the properties of the polymer and the rate of reaction (53). Here, the experimental investigation of the solution polymerization of styrene with initiation by photo-dissociation of sensitizer was made in batch reactor. Also, the comparison between bulk and solution photopolymerization will be made.

Figure 66 shows experimental results obtained at four different sensitizer concentrations and three different solvent concentrations. For the two runs at 50% of benzene (0.1 ℓ benzene and 0.1 ℓ styrene), the results show that if a higher sensitizer concentration is used, a longer reaction time is needed to consume all the sensitizer, and the conversion will increase. For the runs at 30% benzene (0.06 ℓ benzene and 0.14 ℓ styrene) and 25% benzene (0.05 ℓ benzene and 0.15 ℓ styrene), the results show that higher conversions (75% and 90% respectively) are reached when more concentrated solutions of styrene and sensitizer are used. Figure 66 also shows that the X_n values are approximately 75 and do not vary appreciably for all the runs. The measured X_w values are slightly higher than the low S_o runs and are about 200.

As compared to the result of Figure 67, the reaction rate is lower in solution polymerization, and the molecular weight is lower than that obtained by bulk polymerization. This means

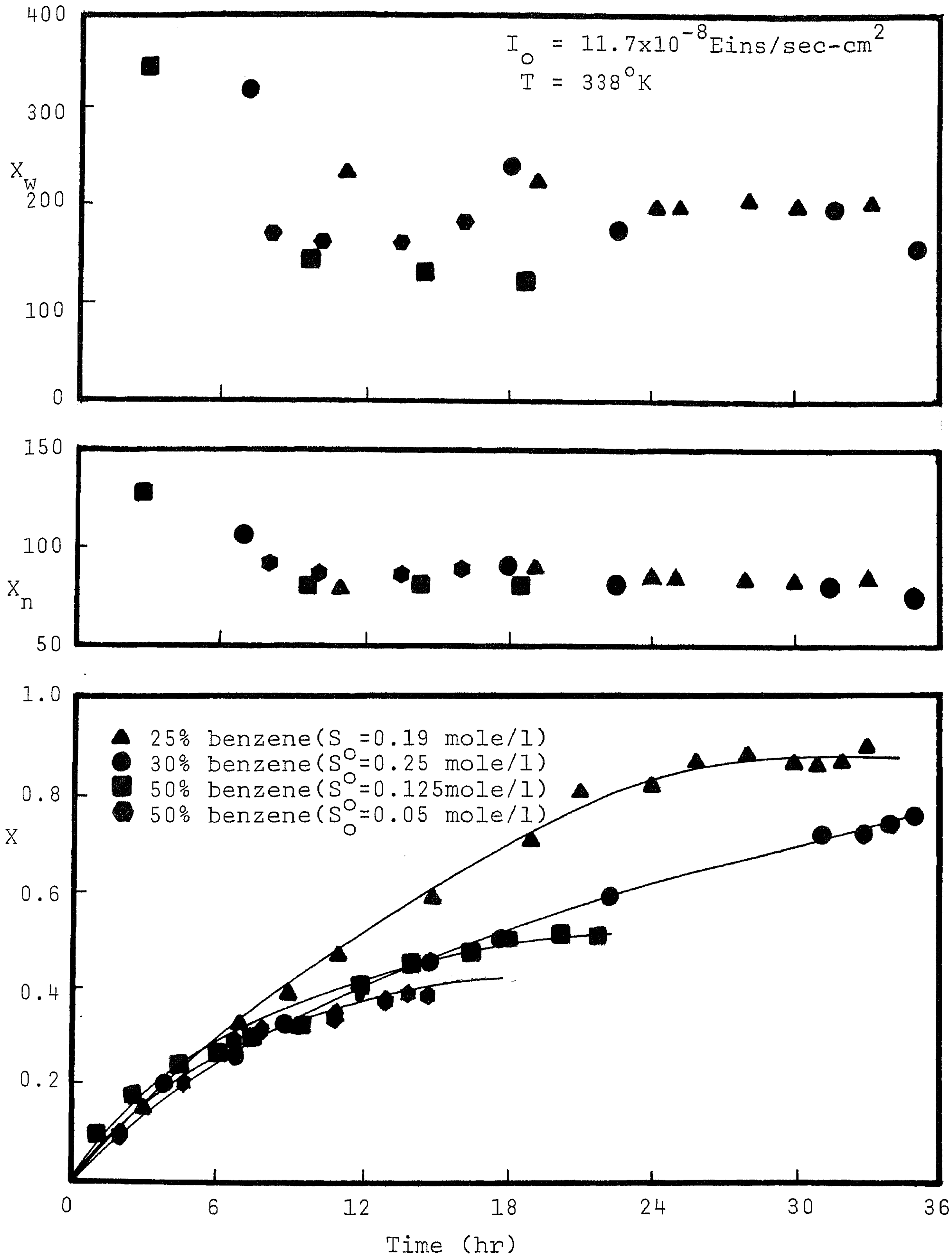

Figure 66. Experimental Data of Photopolymerization at Different Concentrations of Sensitizer and Solvent

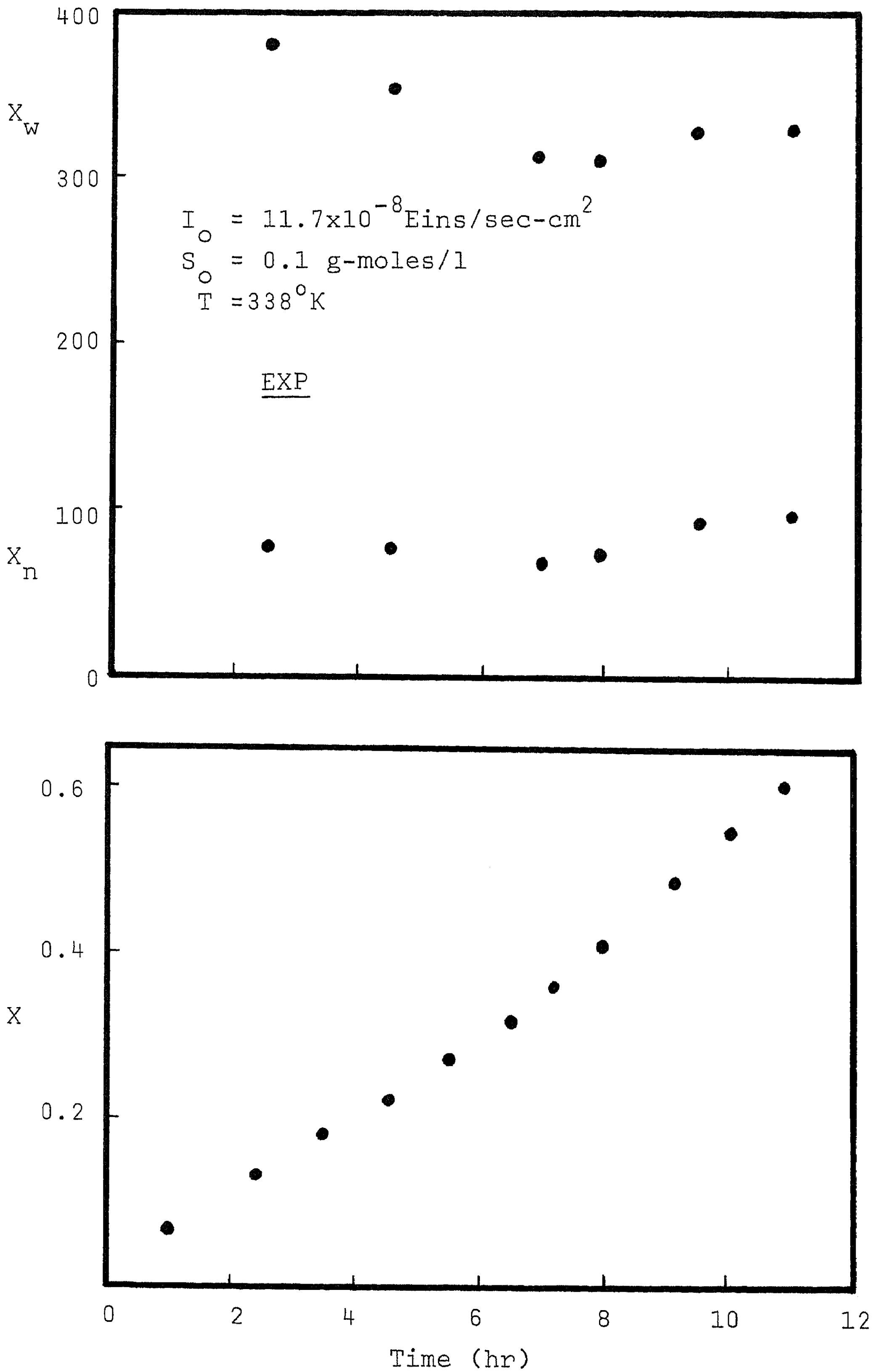

Figure 67. Experimental Data of Bulk Polymerization

the lower polydispersity will be obtained with the batch process of solution polymerization.

APPENDIX C

EFFECT OF NO MIXING ON REACTOR PERFORMANCE

The perfect mixing (PM) state with respect to chain centers, which are uniformly mixed throughout the reactor, has been considered in Chapter 6. The mean chain lifetime is long compared with the mixing time in the reactor, and the effective initiation rate is the average rate. For the opposite extreme mixing state, the no mixing (NM) state, the chain centers are born and die at the same location, subject to the local initiation rate. The mean chain lifetime is short compared with the mixing time. (33) In our study, the mass consumption rate and reactor performance characteristics in a CSTR at no mixing will be investigated and compared with perfect mixing state.

For sensitized initiation and thermal decomposition of monomer, the local initiation rate in the absence of mixing is given by

$$\begin{aligned}\Omega_i(Z) &= 2K_i M^3 + 2\phi_s I_{as} \\ &= 2K_i M^3 + 2\phi_s I_o \epsilon_s S e^{-(\epsilon_s S + \epsilon_m M_o)Z} \\ &= A + Be^{-CZ}\end{aligned}$$

where

$$A = 2K_i M^3$$

$$B = 2\phi_s I_o \epsilon_s S$$

$$C = \epsilon_s S + \epsilon_m M_o$$

The sensitizer and monomer are assumed to be perfectly mixed. Thus the concentrations of the sensitizer and the monomer are uniform throughout the reactor and are independent of distance, Z.

The averaged square root of initiation rate is integrated over the reactor length

$$\overline{\Omega_i^{1/2}} = \frac{1}{L}\int_0^L (A + Be^{-CZ})^{1/2}\, dZ$$

$$= -\frac{1}{CL}\int_1^D \frac{(A + Bx)^{1/2}}{x}\, dx \qquad (1)$$

where

$$x = e^{-CZ}$$

$$D = e^{-CL}$$

Equation (1) can be integrated, and becomes

$$\overline{\Omega_i^{1/2}} = -\frac{1}{CL}\left\{ 2(E-F) + \sqrt{A}\, \ell n \frac{(E-\sqrt{A})(F+\sqrt{A})}{(E+\sqrt{A})(F-\sqrt{A})} \right\}$$

where

$$E = \sqrt{A+BD}$$

$$F = \sqrt{A+B}$$

The resulting equation of $\overline{\Omega_i^{1/2}}$ are used in the calculation of mass consumption rate in CSTR

$$MCR = \overline{\Omega_i^{1/2}}\, M \frac{K_p}{K_t^{1/2}} e^{(A_1X + A_2X^2 + A_3X^3)}$$

Therefore the MCR of no mixing is strongly dependent upon the light absorption compared with that of perfect mixing. The effect of sensitizer concentration on the MCR for both no mixing and perfect mixing states is shown in Figure 68. It shows that the sensitizer concentration, S_o has appreciable effect on the

MCR of no mixing state. Also, the MCR curves of different temperatures are presented in Figure 69. It is verified that both perfect mixing and no mixing have the same effect on MCR at temperatures 85 ^{o}C and 100 ^{o}C. Figure 70 shows the calculated results representing the reactor performance characteristics in terms of fractional conversion X. An increase in θ at a fixed I_o results in the transition from the perfect mixing state to no mixing state.

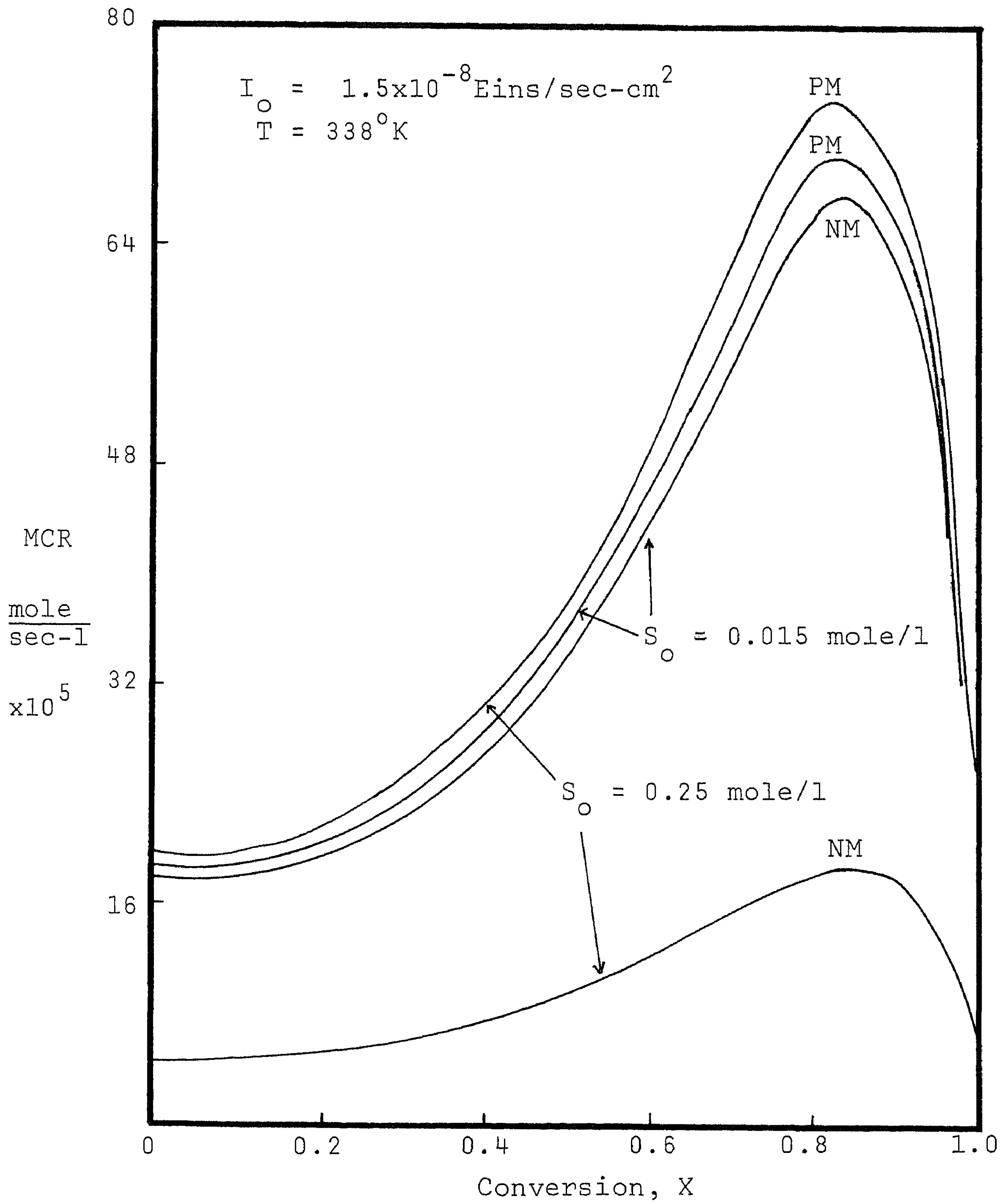

Figure 68. Effect of Sensitizer Concentration on MCR of Perfect and No Mixing

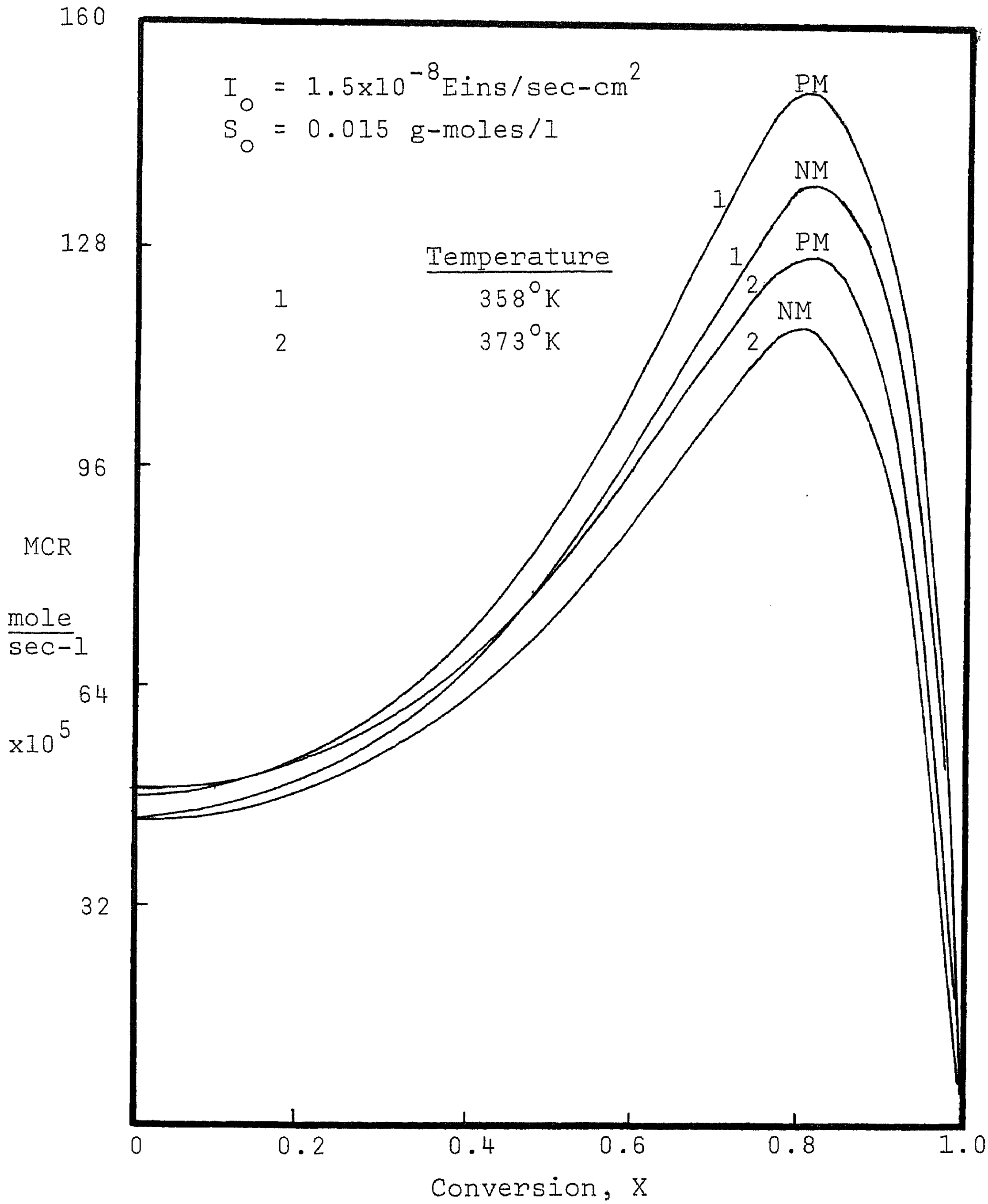

Figure 69. Effect of Temperature on MCR of Perfect and No Mixing

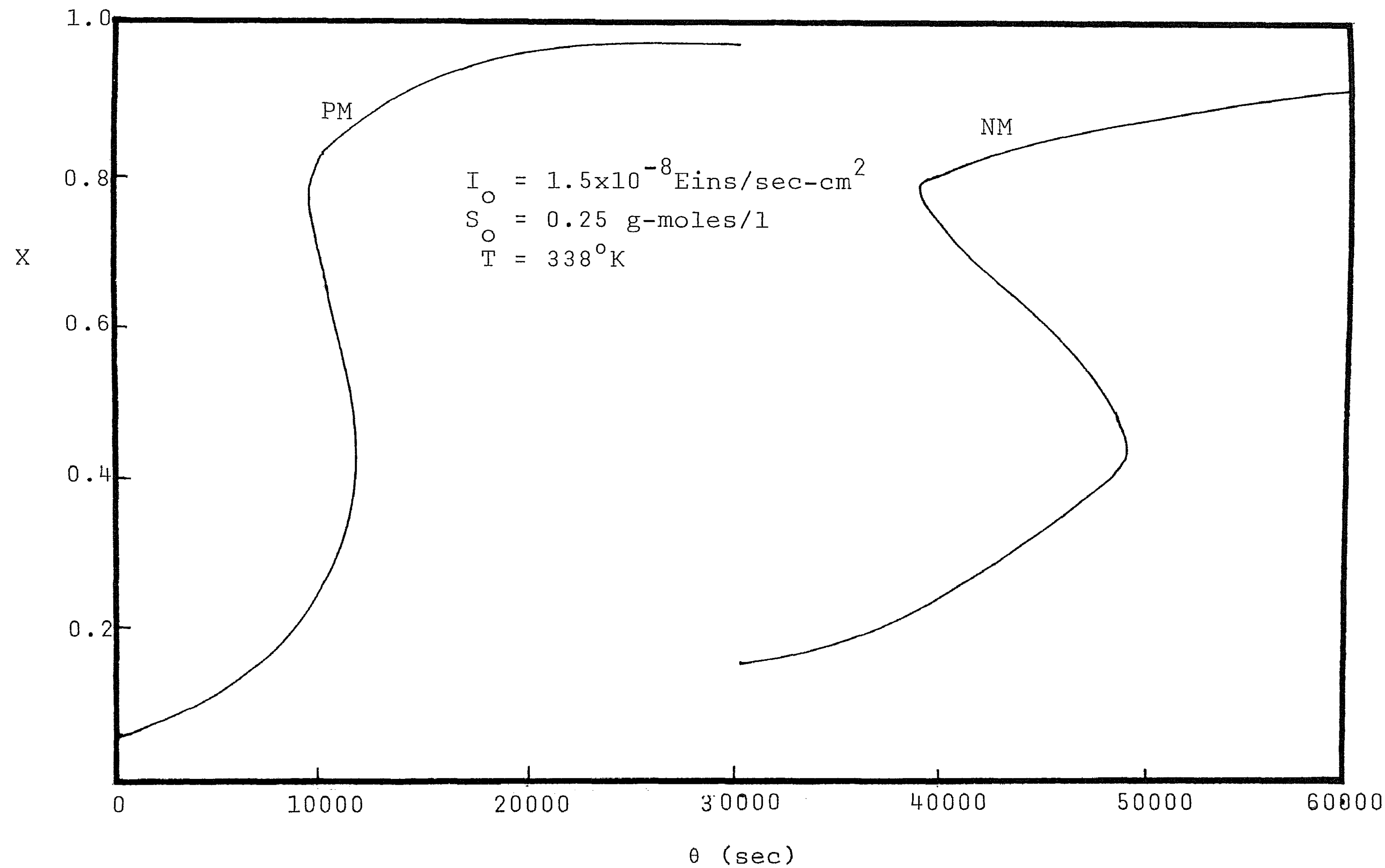

Figure 70. Effect of No Mixing on Reactor Performance Characteristics

APPENDIX D

START-UP AND DYNAMIC BEHAVIOR OF A CSTR

This study is concerned with the dynamics of CSTR during the start-up period. Predictions of dynamic behavior are realistic only when allowance is made for changes which occur in either the light intensity incident upon the reactor or the flow rate to the reactor.

The objective function to be reduced to zero as the process reaches to the steady state might be

$$F = \left(\frac{X_n}{X_{ns}} - 1\right)^2 + \left(\frac{P}{P_s} - 1\right)^2 + \left(\frac{X}{X_s} - 1\right)^2$$

where X_{ns}, P_s and X_s are the values of number average chain length, polydispersity and conversion, respectively at steady state. Material balances for a CSTR are described as in Appendix 1. The properties of X, X_n, X_w/X_n and F can be found as a function of time by numerical treatment of the differential equations. The form of the solutions depends on the start-up procedures which determine the initial values. A fourth-order Runge-Kutta method is used in this work. If the reactor I_o is linearly increased from 0 to 1.5×10^{-8} Eins/sec-cm^2 and then kept constant, the changes in conversion X, number average chain length X_n, polydispersity X_w/X_n and objective function F with time are shown by curve A in Figure 71. Sharp decline in X_n and F soon after start-up would, in this particular process, be accompanied by catastrophic events and this region would not be attained. The behavior of a real reactor is not as violent as this. If the flow is not started until the I_o reaches the predicted steady-state value the changes in X, X_n, X_w/X_n and F are altered. This is shown by curve B. Also, the curve C shows that I_o is linearly

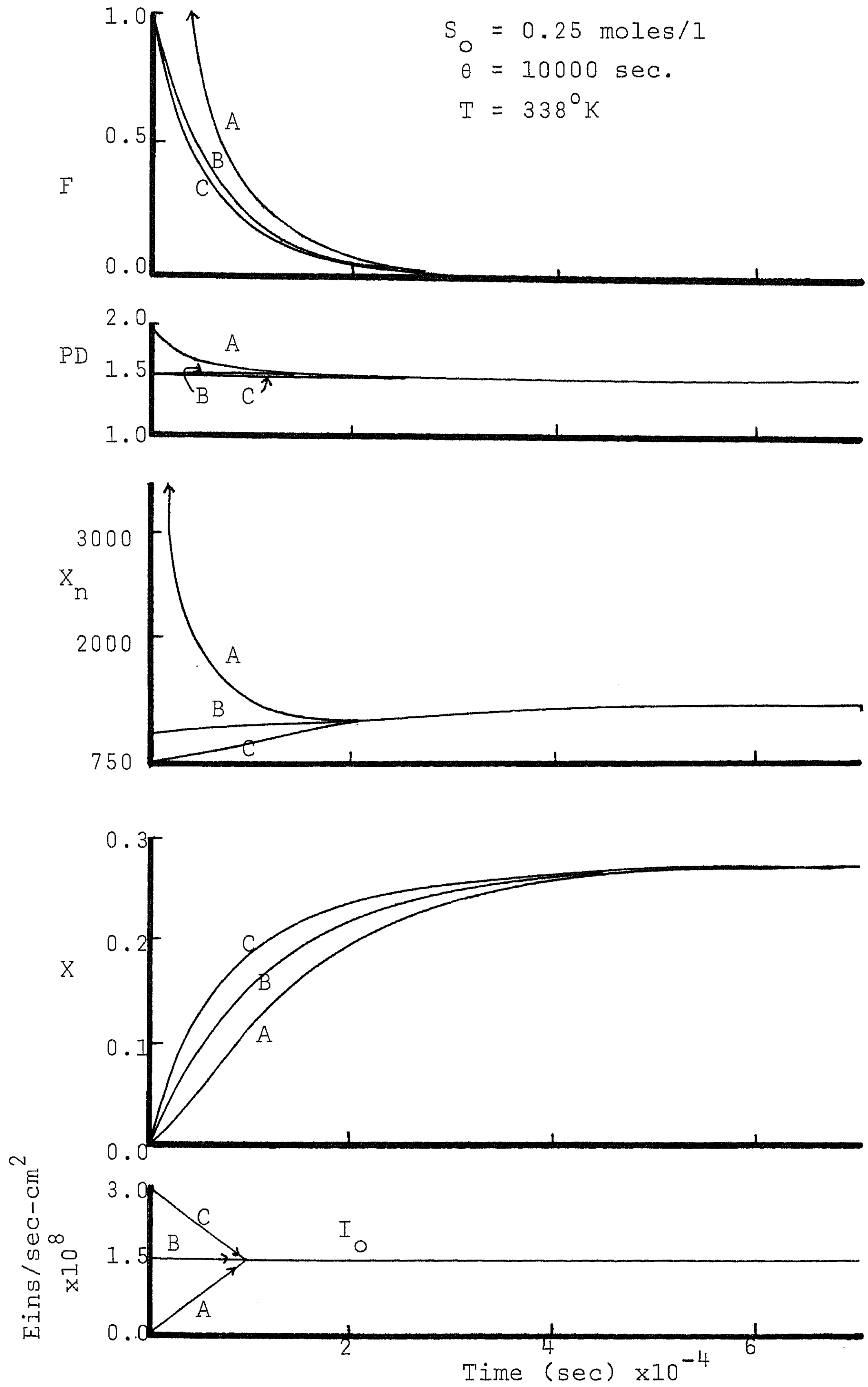

Figure 71. X, X_n and PD Changes with Different I_o Paths

decreased from 3.0×10^{-8} to 1.5×10^{-8} Eins/sec-cm^2 and then kept constant, the changes in X, X_n, X_w/X_n and F are approximately the same as those in curve B. The location of the steady state is not affected by the variations of I_o and the flow rate with X, X_n, X_w/X_n and F whereas the approach to the steady state is affected greatly. The approach to the steady state depends on start-up procedure.

Figure 72 shows the changes in X, X_n, X_w/X_n and F that occur when the flow rates are stepwise increased from zero to 3.0×10^{-5} ℓ/sec, then maintained at 3.0×10^{-5} ℓ/sec and stepwise decreased from 6.0×10^{-5} ℓ/sec to 3.0×10^{-5} ℓ/sec. It is shown that such variations, although small, can be expected to have a noticeable effect on reactor performance.

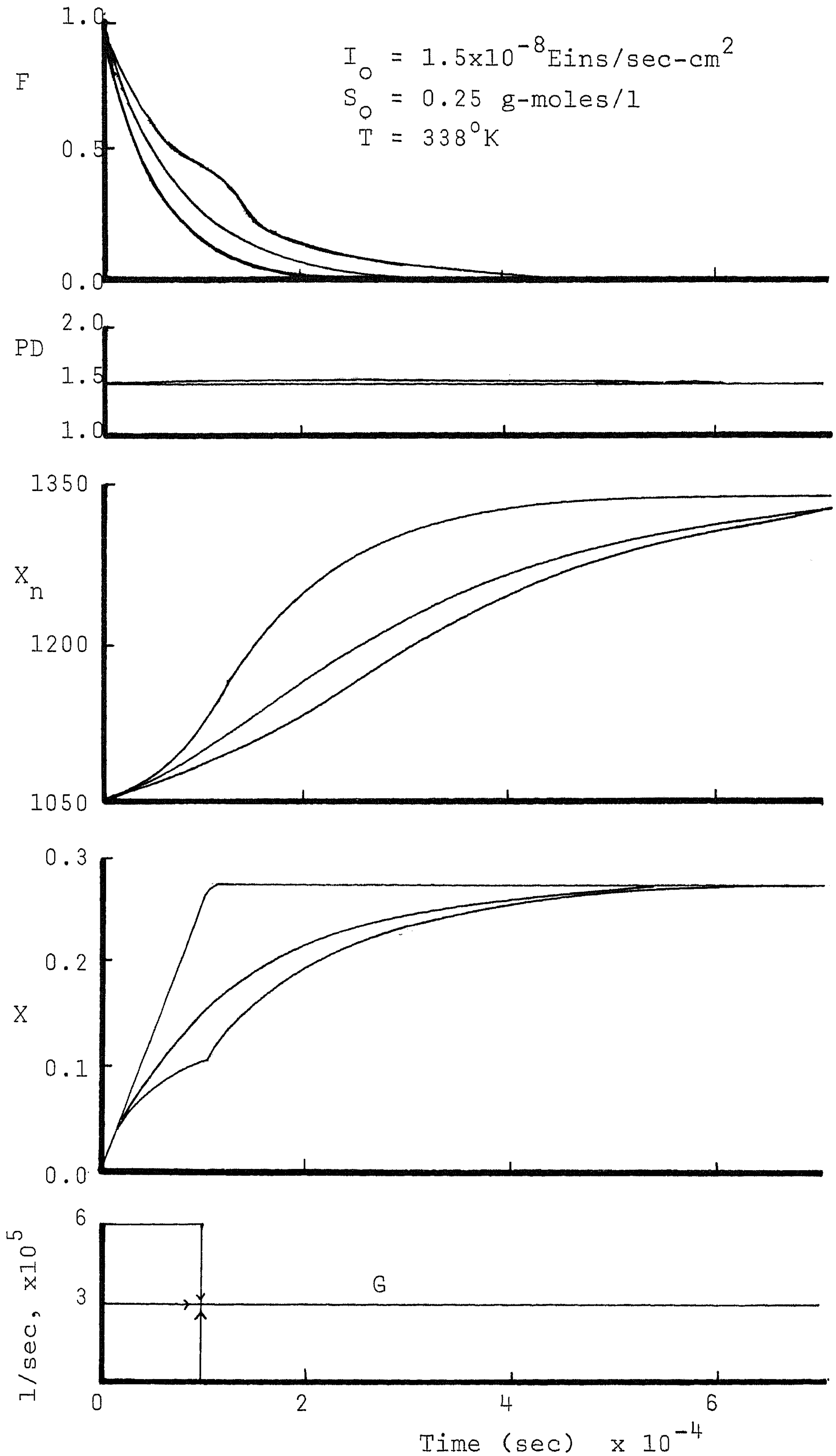

Figure 72. X, X_n and PD Changes with Different Flow Rate Paths

APPENDIX E

SUMMARY OF EXPERIMENTAL RESULTS—
PERIODIC OPERATION IN A CSTR

TABLE 4

PERIODIC OPERATION EXPERIMENT 1

I_o = 11.7x10^{-8}Eins/sec-cm^2

S_o = 0.015 g-moles/l

θ = 9000 sec.

T = 373^{o}K

$(\tau_{off}/\tau)_{av.}$ = 0.25

Sample	X	X_n	X_w	PD	
1	0.366	123	461	3.75	
2	0.357	120	445	3.71	
3	0.392	149	506	3.40	
4	0.370	191	612	3.20	*
5	0.394	210	677	3.23	
6	0.406	119	458	3.85	
7	0.431	123	447	3.63	
8	0.414	158	533	3.37	
9	0.377	117	482	4.13	
10	0.408	133	495	3.72	
11	0.442	126	498	3.94	
12	0.380	178	602	3.38	
13	0.367	115	503	4.37	
14	0.395	197	656	3.33	

* steady state reached, periodic operation started

TABLE 5

PERIODIC OPERATION EXPERIMENT 2

$I_o = 11.7 \times 10^{-8}$ Eins/sec-cm^2

$S_o = 0.015$ g-moles/l

$\theta = 9000$ sec.

$T = 373^oK$

$(\tau_{off}/\tau)_{av.} = 0.28$

Sample	X	X_n	X_w	PD	
1	0.362	238	773	3.24	
2	0.383	274	856	3.12	
3	0.368	242	816	3.37	
4	0.413	284	855	3.01	*
5	0.400	251	794	3.17	
6	0.424	270	833	3.10	
7	0.408	275	834	3.03	
8	0.419	285	835	2.94	
9	0.423	314	1028	3.27	
10	0.383	294	923	3.14	
11	0.417	260	834	3.20	
12	0.430	265	880	3.32	
13	0.396	309	938	3.03	
14	0.363	311	961	3.09	
15	0.333	281	970	3.45	
16	0.364	254	939	3.70	
17	0.391	259	918	3.54	

* steady state reached, periodic operation started

TABLE 6

PERIODIC OPERATION EXPERIMENT 3

$I_o = 11.7 \times 10^{-8}$ Eins/sec-cm^2

$S_o = 0.015$ g-moles/l

$\theta = 6000$ sec.

$T = 358^oK$

$\tau_{off}/\tau = 0.1$

Sample	X	X_n	X_w	PD	
1	0.254	-	-	-	
2	0.243	156	475	3.05	
3	0.263	178	521	2.92	
4	0.264	188	540	2.87	*
5	0.248	172	482	2.79	
6	0.249	154	461	2.99	
7	0.244	158	458	2.88	
8	0.233	159	489	3.08	
9	0.219	149	454	3.04	
10	0.248	155	469	3.02	
11	0.236	164	492	3.00	
12	0.266	170	488	2.87	
13	0.271	168	488	2.89	
14	0.236	208	642	3.08	
15	0.237	151	471	3.11	
16	0.262	169	497	2.94	
17	0.231	162	471	2.91	

* staedy state reached, periodic operation started

TABLE 7

PERIODIC OPERATION EXPERIMENT 4

I_o = 11.7x10^{-8}Eins/sec-cm^2

S_o = 0.015 g-moles/l

θ = 6000 sec.

T = 358^{o}K

τ_{off}/τ = 0.333

Sample	X	X_n	X_w	PD	
1	0.250	188	523	2.78	
2	0.250	184	523	2.84	
3	0.252	175	495	2.83	*
4	0.198	189	536	2.84	
5	0.217	181	568	3.14	
6	0.231	186	535	2.88	
7	0.182	177	546	3.08	
8	0.211	176	537	3.05	
9	0.226	176	533	3.02	
10	0.185	194	593	3.06	
11	0.210	179	551	3.08	
12	0.231	189	543	2.87	
13	0.189	191	562	2.95	
14	0.203	184	561	3.05	
15	0.224	180	543	3.01	

* steady state reached, periodic operation started

TABLE 8

PERIODIC OPERATION EXPERIMENT 5

I_o = 11.7x10^{-8}Eins/sec-cm^2

S_o = 0.015 g-moles/l

θ = 6000 sec.

T = 358^{o}K

τ_{off}/τ = 0.5

Sample	X	X_n	X_w	PD	
1	0.218	200	581	2.91	
2	0.222	196	584	2.97	
3	0.229	200	578	2.88	*
4	0.161	198	588	2.98	
5	0.195	207	605	2.93	
6	0.140	219	706	3.22	
7	0.184	185	578	3.13	
8	0.130	207	705	3.41	
9	0.179	193	618	3.20	
10	0.129	182	641	3.52	
11	0.181	184	613	3.32	

* steady state reached, periodic operation started

TABLE 9

PERIODIC OPERATION EXPERIMENT 6

I_o = 11.7x10^{-8}Eins/sec-cm^2

S_o = 0.015 g-moles/l

θ = 3200 sec.

T = 393^{o}K

τ_{off}/τ = 0.5

Sample	X	X_n	X_w	PD	
1	0.396	359	1027	2.86	
2	0.396	335	914	2.73	
3	0.381	259	725	2.80	*
4	0.288	283	874	3.09	
5	0.343	334	930	2.79	
6	0.263	376	1181	3.14	
7	0.316	330	1073	3.24	
8	0.255	341	1154	3.38	
9	0.321	317	1046	3.29	
10	0.234	358	1153	3.22	
11	0.289	286	936	3.28	
12	0.227	320	1084	3.39	

* steady state reached, periodic operation started

TABLE 10

PERIODIC OPERATION EXPERIMENT 7

$I_o = 11.7 \times 10^{-8}$ Eins/sec-cm^2

$S_o = 0.015$ g-moles/l

$\theta = 3000$ sec.

$T = 393^oK$

$\tau_{off}/\tau = 0.2$

Sample	X	X_n	X_w	PD	
1	0.329	-	-	-	
2	0.332	-	-	-	
3	0.327	-	-	-	*
4	0.301	-	-	-	
5	0.300	360	1219	3.38	
6	0.272	375	1142	3.05	
7	0.283	374	1152	3.08	
8	0.262	371	1122	3.03	
9	0.284	365	1122	3.07	
10	0.251	309	1123	3.63	
11	0.282	317	1033	3.25	
12	0.259	376	1197	3.18	

* steady state reached, periodic operation started

TABLE 11

PERIODIC OPERATION EXPERIMENT 8

I_o = 11.7x10^{-8}Eins/sec-cm^2

S_o = 0.015 g-moles/l

θ = 6000 sec.

T = 358^{o}K

τ_{off}/τ = 0.5 (the same condintion as in exp. 5)

Sample	X	X_n	X_w	PD	
1	0.228	130	371	2.85	
2	-	128	380	2.97	
3	0.230	149	426	3.19	*
4	0.158	176	514	2.92	
5	0.185	160	485	3.03	
6	0.134	157	502	3.20	
7	0.174	158	511	3.22	
8	0.129	157	573	3.66	
9	0.177	213	749	3.51	
10	0.136	151	528	3.49	
11	0.175	157	517	3.29	
12	0.123	155	536	3.45	
13	0.169	154	512	3.32	
14	0.123	152	526	3.45	
15	0.155	165	590	3.57	
16	0.125	170	637	3.75	
17	0.174	155	550	3.58	

* steady state reached, periodic operation started

TABLE 12

PERIODIC OPERATION EXPERIMENT 9

I_o = 11.7x10^{-8}Eins/sec-cm^2

S_o = 0.015 g-moles/l

θ = 6000 sec.

T = 338^{o}K

τ_{off}/τ = 0.5

Sample	X	X_n	X_w	PD	
1	0.152	129	382	2.96	
2	0.153	126	363	2.88	
3	-	110	318	2.89	
4	-	102	297	2.92	*
5	0.106	111	321	2.88	
6	0.118	94	282	2.99	
7	0.078	109	316	2.89	
8	0.130	106	319	3.01	
9	0.071	100	295	2.96	
10	0.098	86	271	3.13	
11	0.065	91	284	3.13	
12	0.095	85	276	3.25	
13	0.064	84	265	3.16	
14	0.094	85	281	3.29	
15	0.067	83	266	3.20	
16	0.093	88	279	3.17	
17	0.056	86	270	3.15	
18	0.095	86	276	3.20	

* steady state reached, periodic operation started

TABLE 13

PERIODIC OPERATION EXPERIMENT 10

$I_o = 11.7\times10^{-8}$ Eins/sec-cm^2

S_o = 0.015 g-moles/l

θ = 6000 sec.

T = 338^{o}K

τ_{off}/τ = 0.333

Sample	X	X_n	X_w	PD	
1	0.106	228	627	2.75	
2	0.107	216	595	2.76	
3	0.127	210	577	2.75	*
4	0.120	205	562	2.74	
5	0.123	137	448	3.27	
6	0.097	124	418	3.36	
7	0.131	117	398	3.41	
8	0.104	125	435	3.47	
9	0.135	114	377	3.32	
10	0.106	115	397	3.45	
11	0.125	113	390	3.45	
12	0.102	116	390	3.36	
13	0.125	111	382	3.44	
14	0.100	117	417	3.56	
15	0.125	111	397	3.56	
16	0.101	107	401	3.73	
17	0.119	111	398	3.59	
18	0.126	107	377	3.51	

* steady state reached, periodic operation started

TABLE 14

PERIODIC OPERATION EXPERIMENT 11

$I_o = 11.7 \times 10^{-8}$ Eins/sec-cm^2

$S_o = 0.015$ g-mole/l

$\theta = 6000$ sec.

$T = 358^oK$

$\tau_{off}/\tau = 0.8$

Sample	X	X_n	X_w	PD	
1	0.178	141	531	3.76	
2	0.239	143	516	3.60	
3	0.231	-	-	-	
4	0.248	-	-	-	
5	0.252	-	-	-	
6	0.251	290	953	3.28	*
7	0.097	301	1515	5.03	
8	0.119	307	1399	4.55	
9	0.095	244	1248	5.13	
10	0.110	212	1128	5.33	
11	0.096	222	1350	6.08	
12	0.089	160	895	5.58	
13	0.110	193	1123	5.83	
14	0.094	219	1119	5.11	
15	0.086	253	1460	5.77	
16	0.112	177	985	5.57	

* steady state reached, periodic operation started

APPENDIX F

SUMMARY OF EXPERIMENTAL RESULTS—
SOLUTION POLYMERIZATION OF BATCH REACTOR

TABLE 15

SOLUTION POLYMERIZATION EXPERIMENT 1

I_o = 11.7x10^{-8}Eins/sec-cm^2

T = 338^oK

S_o = 0.19 g-moles/l

Solution: 25% benzene

Sample	Time (min)	X	X_n	X_w	PD
1	180	0.153	-	-	-
2	300	0.227	-	-	-
3	420	0.311	-	-	-
4	540	0.379	-	-	-
5	660	0.458	60	236	3.93
6	780	0.499	-	-	-
7	900	0.579	-	-	-
8	1020	0.641	-	-	-
9	1140	0.705	78	219	2.80
10	1260	0.807	-	-	-
11	1380	0.818	-	-	-
12	1440	0.813	68	197	2.92
13	1500	0.868	70	204	2.89
14	1560	0.872	-	-	-
15	1620	0.879	-	-	-
16	1665	0.864	72	216	3.02
17	1725	0.863	-	-	-
18	1770	0.877	-	-	-
19	1815	0.879	65	199	3.06
20	1875	0.879	-	-	-
21	1935	0.861	-	-	-
22	1995	0.868	-	-	-
23	2055	0.898	73	211	2.89

TABLE 16

SOLUTION POLYMERIZATION EXPERIMENT 2

$I_o = 11.7 \times 10^{-8}$ Eins/sec-cm^2

$T = 338^oK$

$S_o = 0.25$ g-moles/l

Solution: 30% benzene

Sample	Time (min)	X	X_n	X_w	PD
1	240	0.188	-	-	-
2	420	0.250	111	322	2.90
3	540	0.312	-	-	-
4	720	0.378	-	-	-
5	900	0.436	-	-	-
6	1080	0.496	82	241	2.92
7	1260	0.542	-	-	-
8	1380	0.581	57	176	3.07
9	1920	0.723	60	197	3.26
10	2010	0.720	-	-	-
11	2070	0.745	-	-	-
12	2130	0.760	47	163	3.46

TABLE 17

SOLUTION POLYMERIZATION EXPERIMENT 3

$I_o = 11.7 \times 10^{-8}$ Eins/sec-cm^2

$T = 338^oK$

$S_o = 0.125$ g-moles/l

Solution: 50% benzene

Sample	Time (min)	X	X_n	X_w	PD
1	70	0.096	-	-	-
2	160	0.158	149	343	2.30
3	280	0.230	-	-	-
4	370	0.261	-	-	-
5	465	0.285	-	-	-
6	565	0.322	63	141	2.23
7	675	0.376	-	-	-
8	720	0.387	-	-	-
9	790	0.420	-	-	-
10	855	0.448	65	134	2.05
11	920	0.453	-	-	-
12	1000	0.471	-	-	-
13	1060	0.479	-	-	-
14	1105	0.493	61	119	1.96
15	1165	0.499	-	-	-
16	1215	0.508	-	-	-
17	1255	0.503	-	-	-
18	1285	0.501	-	-	-
19	1315	0.504	-	-	-

TABLE 18

SOLUTION POLYMERIZATION EXPERIMENT 4

$I_o = 11.7 \times 10^{-8}$ Eins/sec-cm^2

$T = 338^{o}K$

$S_o = 0.05$ g-moles/l

Solution: 50% benzene

Sample	Time (min)	X	X_n	X_w	PD
1	30	0.010	-	-	-
2	120	0.094	-	-	-
3	230	0.149	-	-	-
4	310	0.209	77	169	2.19
5	410	0.280	-	-	-
6	480	0.312	-	-	-
7	540	0.338	68	156	2.30
8	600	0.346	-	-	-
9	660	0.351	-	-	-
10	720	0.376	73	162	2.21
11	780	0.374	-	-	-
12	810	0.381	-	-	-
13	840	0.403	-	-	-
14	870	0.388	-	-	-
15	900	0.396	74	185	2.49

APPENDIX G

COMPUTER PROGRAM FOR CALCULATIONS

```
C     PROGRAM #1
C     FREE RADICAL CONCENTRATIONS CALCULATION
C     OF BATCH PHOTOPOLYMERIZATION
C     ###################################################
C
      COMMON KP,KT,KI,XK,XSR,XR1,XR2,XR3,XR4,XR5,KF
      REAL KI,KP,KT,KF,I1,IT
      DOUBLE PRECISION PM,XM0,XM,XK,XR1,XR2,XR3,XR4,XR5,XSR,
     CR1,R2,R3,R4,R5,SR,F1,F2,F3,F4,F5,FSR,F0,D1F0,D1F1,D1F2,
     CD1F3,D1F4,D1F5,D1FSR,D2F0,D2F1,D2F2,D2F3,D2F4,D2F5,D2FSR,
     CD3F0,D3F1,D3F2,D3F3,D3F4,D3F5,D3FSR,D4F0,D4F1,D4F2,D4F3,
     CD4F4,D4F5,D4FSR,DF0,DF1,DF2,DF3,DF4,DF5,DFSR
      DATA R1,R2,R3,R4,R5,SR/6*0.0/
      K=-1
      H=.001
      IT=338.
      KI=2.19E5*EXP(-13810/IT)
      KP=1.051E7*EXP(-3557/IT)
      KT=1.255E9*EXP(-844/IT)
      KF=2.31E6*EXP(-6377/IT)
      PM=924-.918*(IT-273.1)
      PP=1084.8-.605*(IT-273.1)
      E=PM/PP-1
      XMW=104
      XM0=PM/XMW
      T=0
      XM=XM0
      XC=(XM0-XM)/(XM0+E*XM)
      WRITE(6,80)
   80 FORMAT('0','BATCH POLYMERIZATION WITH UV LIGHT')
      WRITE(6,85)
   85 FORMAT('0','THE CONC. OF R1,R2,R3,R4,R5 AND SUM OF R ')
C
   99 XK=XM
      XR1=R1
      XR2=R2
      XR3=R3
      XR4=R4
      XR5=R5
      XSR=SR
      D1F0=H*F0(DUMMY)
      D1F1=H*F1(DUMMY)
      D1F2=H*F2(DUMMY)
      D1F3=H*F3(DUMMY)
      D1F4=H*F4(DUMMY)
      D1F5=H*F5(DUMMY)
      D1FSR=H*FSR(DUMMY)
      XK=XM+D1F0/2
      XR1=R1+D1F1/2
      XR2=R2+D1F2/2
      XR3=R3+D1F3/2
      XR4=R4+D1F4/2
      XR5=R5+D1F5/2
      XSR=SR+D1FSR/2
```

```
      D2F0=H*F0(DUMMY)
      D2F1=H*F1(DUMMY)
      D2F2=H*F2(DUMMY)
      D2F3=H*F3(DUMMY)
      D2F4=H*F4(DUMMY)
      D2F5=H*F5(DUMMY)
      D2FSR=H*FSR(DUMMY)
      XK=XM+D2F0/2
      XR1=R1+D2F1/2
      XR2=R2+D2F2/2
      XR3=R3+D2F3/2
      XR4=R4+D2F4/2
      XR5=R5+D2F5/2
      XSR=SR+D2FSR/2
      D3F0=H*F0(DUMMY)
      D3F1=H*F1(DUMMY)
      D3F2=H*F2(DUMMY)
      D3F3=H*F3(DUMMY)
      D3F4=H*F4(DUMMY)
      D3F5=H*F5(DUMMY)
      D3FSR=H*FSR(DUMMY)
      XK=XM+D3F0
      XR1=R1+D3F1
      XR2=R2+D3F2
      XR3=R3+D3F3
      XR4=R4+D3F4
      XR5=R5+D3F5
      XSR=SR+D3FSR
      D4F0=H*F0(DUMMY)
      D4F1=H*F1(DUMMY)
      D4F2=H*F2(DUMMY)
      D4F3=H*F3(DUMMY)
      D4F4=H*F4(DUMMY)
      D4F5=H*F5(DUMMY)
      D4FSR=H*FSR(DUMMY)
      DF0=(D1F0+2*D2F0+2*D3F0+D4F0)/6
      DF1=(D1F1+2*D2F1+2*D3F1+D4F1)/6
      DF2=(D1F2+2*D2F2+2*D3F2+D4F2)/6
      DF3=(D1F3+2*D2F3+2*D3F3+D4F3)/6
      DF4=(D1F4+2*D2F4+2*D3F4+D4F4)/6
      DF5=(D1F5+2*D2F5+2*D3F5+D4F5)/6
      DFSR=(D1FSR+2*D2FSR+2*D3FSR+D4FSR)/6
      XM=XM+DF0
      R1=R1+DF1
      R2=R2+DF2
      R3=R3+DF3
      R4=R4+DF4
      R5=R5+DF5
      SR=SR+DFSR
      T=T+H
      K=K+1
      IF(T.GT.2000) GO TO 200
      IF(K-K/1000*1000 .EQ. 0) GO TO 100
      GO TO 99
100   WRITE(6,110) T,XM
```

```
  110 FORMAT('0','TIME =',F5.1,5X,'XM =',F11.8)
      WRITE(6,120) R1,R2,R3,R4,R5,SR
  120 FORMAT(' ',6(D20.14,1X))
      GO TO 99
  200 STOP
      END
C
C
      FUNCTION F0(DUMMY)
      COMMON KP,KT,KI,XK,XSR,XR1,XR2,XR3,XR4,XR5,KF
      REAL KI,KP,KT,KF
      DOUBLE PRECISION XR1,XR2,XR3,XR4,XR5,XSR,F0,I1,XK
      I1=2*KI*XK**3+2*.072*.000117/5.2*(1-EXP(-88.5*.015*5.2))
      F0=-I1-KP*XK*XSR
      RETURN
      END
C
      FUNCTION F1(DUMMY)
      COMMON KP,KT,KI,XK,XSR,XR1,XR2,XR3,XR4,XR5,KF
      REAL KI,KP,KT,KF
      DOUBLE PRECISION XR1,XR2,XR3,XR4,XR5,XSR,F1,I1,XK
      I1=2*KI*XK**3+2*.072*.000117/5.2*(1-EXP(-88.5*.015*5.2))
      F1=I1-KP*XK*XR1+KF*XK*XSR-KT*XR1*XSR
      RETURN
      END
C
      FUNCTION F2(DUMMY)
      COMMON KP,KT,KI,XK,XSR,XR1,XR2,XR3,XR4,XR5,KF
      REAL KI,KP,KT,KF
      DOUBLE PRECISION XR1,XR2,XR3,XR4,XR5,XSR,F2,XK
      F2=KP*XK*XR1-KP*XK*XR2-KT*XR2*XSR
      RETURN
      END
C
      FUNCTION F3(DUMMY)
      COMMON KP,KT,KI,XK,XSR,XR1,XR2,XR3,XR4,XR5,KF
      REAL KI,KP,KT,KF
      DOUBLE PRECISION XR1,XR2,XR3,XR4,XR5,XSR,F3,XK
      F3=KP*XK*XR2-KP*XK*XR3-KT*XR3*XSR
      RETURN
      END
C
      FUNCTION F4(DUMMY)
      COMMON KP,KT,KI,XK,XSR,XR1,XR2,XR3,XR4,XR5,KF
      REAL KI,KP,KT,KF
      DOUBLE PRECISION XR1,XR2,XR3,XR4,XR5,XSR,F4,XK
      F4=KP*XK*XR3-KP*XK*XR4-KT*XR4*XSR
      RETURN
      END
C
      FUNCTION F5(DUMMY)
      COMMON KP,KT,KI,XK,XSR,XR1,XR2,XR3,XR4,XR5,KF
      REAL KI,KP,KT,KF
      DOUBLE PRECISION XR1,XR2,XR3,XR4,XR5,XSR,F5,XK
      F5=KP*XK*XR4-KP*XK*XR5-KT*XR5*XSR
      RETURN
      END
```

```
C
      FUNCTION FSR(DUMMY)
      COMMON KP,KT,KI,XK,XSR,XR1,XR2,XR3,XR4,XR5,KF
      REAL KI,KP,KT,KF
      DOUBLE PRECISION XR1,XR2,XR3,XR4,XR5,XSR,FSR,I1,XK
      I1=2*KI*XK**3+2*.072*.000117/5.2*(1-EXP(-88.5*.015*5.2))
      FSR=I1-KT*XSR**2
      RETURN
      END
```

```
C       PROGRAM #2
C       POLYDISPERSITY CALCULATION
C       UV LIGHT ON/OFF REGULATION AT LOW STEADY STATE
C       ##############################################
C
        DIMENSION S(2000)
        READ,SO,XIO,TEMP,SITA,R,V1
        TAU=SITA
C
        PM=924-.918*(TEMP-273.1)
        XMW=104
        XMO=PM/XMW
        XKP=1.051E7*EXP(-3557/TEMP)
        XKT=1.255E9*EXP(-844/TEMP)
        XKI=2.19E5*EXP(-13810/TEMP)
        V=0.2
        DV=V1/V
        AS=0.072
        ES=88.5
        XL=5.2
        XL1=XL*DV
        XC1=SITA*AS*XIO/XL1
        S(1)=SO
        DO 10 I=1,2000
        FS=S(I)-SO+XC1*(1-EXP(-ES*S(I)*XL1))
        DFS=1+XC1*ES*XL1*EXP(-ES*S(I)*XL1)
        XS1=S(I)-FS/DFS
        IF(ABS((S(I)-XS1)/S(I)) .LE. 0.01) GO TO 20
        N=I+1
        S(N)=XS1
   10   CONTINUE
   20   XIAS=XIO*(1-EXP(-ES*XS1*XL1))*DV/XL1
        AI=2*AS*XIAS
        SR=SQRT(AI/XKT)
        XM=(XMO-SITA*AI)/(1+SITA*XKP*SR)
        XS=XKP*XM/(XKP*XM+XKT*SR+1/SITA)
        WRITE(2,24)
   24   FORMAT('0','POLYDISPERSITY CALCULATION')
        WRITE(2,26)
   26   FORMAT('0','UV LIGHT ON/OFF REGULATION AT LOW S. S.')
        WRITE(2,28)
   28   FORMAT('0','######################################')
        WRITE(2,29) XKP,XKT
   29   FORMAT('0','KP= ',F6.1,5X,'KT= ',E10.3)
        WRITE(2,32) TEMP
   32   FORMAT('0','TEMPERATURE=',F5.1,' K')
        WRITE(2,34) XIO
   34   FORMAT('0','UV INTENSITY=',F8.6)
        WRITE(2,36) SITA
   36   FORMAT('0','RESIDENT TIME=',F7.1)
        WRITE(2,37) XMO
   37   FORMAT('0','INLET MONOMER CONC.=',F5.3)
        WRITE(2,38) SO
   38   FORMAT('0','INLET SENSITIZER CONC.=',F5.3)
```

```
      WRITE(2,39) R
   39 FORMAT('0','THE RATIO OF (OFF/(ON+OFF)) TIME=',F5.3)
      WRITE(2,42)
   42 FORMAT('0')
      WRITE(2,44)
   44 FORMAT('0','AT LOW STEADY STATE :')
      WRITE(2,45)
   45 FORMAT(' ','------------------------------')
      WRITE(2,46) SR
   46 FORMAT('0','SUM OF THE FREE RADICAL CONC.=',F15.13)
      WRITE(2,48) XM
   48 FORMAT('0','OUTLET MONOMER CONC.=',F6.4)
      WRITE(2,50) XS1
   50 FORMAT('0','OUTLET SENSITIZER CONC.=',E10.4)
      SUM=0.0
      SP=0.0
      SIP=0.0
      SIIP=0.0
      DO 100 I=2,10000
      PI=((I-1)/2.)*XS**I*AI**2*XKT*SITA/(XKP*XM)**2
      SP=SP+PI
      SIP=SIP+I*PI
      SIIP=SIIP+I**2*PI
      XMW=I*PI/(XMO-XM)
      SUM=SUM+XMW
      IF(SUM .GT. 0.995) GO TO 200
  100 CONTINUE
  200 XN=SIP/SP
      XW=SIIP/SIP
      PD=XW/XN
      WRITE(2,220) SP,SIP,SIIP
  220 FORMAT('0','SP=',F10.7,5X,'SIP=',F10.8,5X,'SIIP=',F10.5)
      WRITE(2,230) PD
  230 FORMAT('0','PD =',F7.4)
C
      RT=R*TAU
      C1=XMO
      C2=XM-XMO
      C3=XMO/SITA-AI
      C4=1/SITA+XKP*SQRT(AI/XKT)
      C5=C3/C4
      D=EXP(-C4*(1-R)*TAU)
      C=C5-C3*D/C4
      B=EXP(-RT/SITA)
      A=XMO*(1-B)
      C6=C3/C4-(A+B*XM)
      G=C+D*A
      H=B*D
      P=A+C*B
C
      D1=SITA*C1**3
      D2=3*RT*C2*C1**2*EXP(-RT/SITA)
      D3=3*C1*SITA*C2**2*EXP(-2*RT/SITA)
      D4=SITA/2*C2**3*EXP(-3*RT/SITA)
      D5=(D1-3*C1*SITA*C2**2-SITA/2*C2**3)*EXP(-RT/SITA)
```

```
      S1=XKI*(D1+D2-D3-D4-D5)
      S2=EXP(-RT/SITA)
      S3=.5*SITA*AI*(1-EXP(-(1-R)*TAU/SITA))
      S4=EXP(-(1-R)*TAU/SITA)
      R1=S3+S1*S4
      R2=S2*S4
      R3=S1+S2*S3
C
      E1=XKP*C1**2.5*SQRT(2*XKI/XKT)
      E5=SITA*C5-SITA*C6/(1-SITA*C4)*EXP(-C4*(1-R)*TAU)
      E6=(SITA*C5-SITA*C6/(1-SITA*C4))*EXP(-(1-R)*TAU/SITA)
      SUM1=EXP(RT/SITA)
      SUM2=1.
      V1=-15./8*(C2/C1)**2*EXP(-RT/SITA)
      V2=-15./8*(C2/C1)**2
      SUM1=SUM1+V1
      SUM2=SUM2+V2
      DO 235 N=2,20
      CALL BINOM(V1,V2,N,C1,C2,RT,SITA)
      SUM1=SUM1+V1
      SUM2=SUM2+V2
  235 CONTINUE
      XSUM=E1*SITA*(SUM1-SUM2)+E1*2.5*C2*RT/C1
      P1=EXP(-RT/SITA)*XSUM
      P2=EXP(-RT/SITA)
      P3=XKP*SQRT(AI/XKT)*(E5-E6)
      P4=EXP(-(1-R)*TAU/SITA)
      T1=P3+P1*P4
      T2=P2*P4
      T3=P1+P2*P3
C
      F1=SITA*C1**2+2*C1*C2*RT*EXP(-RT/SITA)
      F2=SITA*C2**2*EXP(-2*RT/SITA)
      F3=SITA*(C1**2-C2**2)*EXP(-RT/SITA)
      X1=3*XKP**2/XKT*(F1-F2-F3)+5*XSUM
      X2=EXP(-RT/SITA)
      C8=3*(XKP*C5)**2/XKT+5*XKP*C5*SQRT(AI/XKT)+2*AI
      C9=6*C5*C6*XKP**2/XKT+5*XKP*C6*SQRT(AI/XKT)
      C10=3*(XKP*C6)**2/XKT
      F4=SITA*C8
      F5=SITA*C9*EXP(-C4*(1-R)*TAU)/(1-SITA*C4)
      F6=SITA*C10*EXP(-2*C4*(1-R)*TAU)/(1-2*SITA*C4)
      F7=SITA*(-C8+C9/(1-SITA*C4)-C10/(1-2*SITA*C4))
     C*EXP(-(1-R)*TAU/SITA)
      X3=F4-F5+F6+F7
      X4=EXP(-(1-R)*TAU/SITA)
      Y1=X3+X1*X4
      Y2=X2*X4
      Y3=X1+X2*X3
C
      XMOT=XM
      XMRT=A+B*XM
      XCOT=(XMO-XMOT)/XMO
      XCRT=(XMO-XMRT)/XMO
      SPOT=SP
```

```
      SPRT=S1+S2*SP
      SIPOT=SIP
      SIPRT=P1+P2*SIP
      SIIPOT=SIIP
      SIIPRT=X1+X2*SIIP
      PD1T=SPRT*SIIPRT/SIPRT**2
      WRITE(2,240)
  240 FORMAT('0','########################################')
      WRITE(2,245)
  245 FORMAT('0')
      WRITE(2,250) XMOT,XMRT
  250 FORMAT('0','XMOT=',F7.5,5X,'XMRT=',F7.5)
      WRITE(2,260) XCOT,XCRT
  260 FORMAT(' ','XCOT=',F7.5,5X,'XCRT=',F7.5)
      WRITE(2,270) SPOT,SPRT
  270 FORMAT(' ','SPOT=',F10.7,5X,'SPRT=',F10.7)
      WRITE(2,280) SIPOT,SIPRT
  280 FORMAT(' ','SIPOT=',F10.8,5X,'SIPRT=',F10.8)
      WRITE(2,290) SIIPOT,SIIPRT
  290 FORMAT(' ','SIIPOT=',F10.5,5X,'SIIPRT=',F10.5)
      WRITE(2,295) PD,PD1T
  295 FORMAT(' ','PDT=',F10.5,5X,'PD1T=',F10.5)
C
      DO 500 N=1,20
      Q=(1-H**N)/(1-H)
      XMT=G*Q+XM*H**N
      XM1T=P*Q+(A+B*XM)*H**N
      XCT=(XMO-XMT)/XMO
      XC1T=(XMO-XM1T)/XMO
      XR=(1-R2**N)/(1-R2)
      SPT=R1*XR+SP*R2**N
      SP1T=R3*XR+(S1+S2*SP)*R2**N
      XT=(1-T2**N)/(1-T2)
      SIPT=T1*XT+SIP*T2**N
      SIP1T=T3*XT+(P1+P2*SIP)*T2**N
      XY=(1-Y2**N)/(1-Y2)
      SIIPT=Y1*XY+SIIP*Y2**N
      SIIP1T=Y3*XY+(X1+X2*SIIP)*Y2**N
      XNT=SIPT/SPT
      XN1T=SIP1T/SP1T
      XWT=SIIPT/SIPT
      XW1T=SIIP1T/SIP1T
      PDT=XWT/XNT
      PD1T=XW1T/XN1T
C
      WRITE(2,307) N
  307 FORMAT('0','N=',I2)
      WRITE(2,310) XMT,XM1T
  310 FORMAT('0','XMT=',F7.5,5X,'XM1T=',F7.5)
      WRITE(2,315) XCT,XC1T
  315 FORMAT(' ','XCT=',F7.5,5X,'XC1T=',F7.5)
      WRITE(2,370) PDT,PD1T
  370 FORMAT(' ','PDT=',F9.6,5X,'PD1T=',F9.6)
      WRITE(2,410)
  410 FORMAT('0')
```

```
  500 CONTINUE
      STOP
      END
C
C
      SUBROUTINE BINOM(V1,V2,N,C1,C2,RT,SITA)
      V1=V1*(N-1)/(N+1)*(2.5-N)*(C2/C1)*EXP(-RT/SITA)
      V2=V2*(N-1)/(N+1)*(2.5-N)*(C2/C1)
      RETURN
      END
```

```
C     PROGRAM #3
C     NUMERICAL CALCULATION FOR POLYDISPERSITY
C     UV LIGHT ON/OFF REGULATION AT LOW STAEDY STATE
C     ##############################################
C
      DIMENSION PEI(100)
      REAL KT,KP,KI,IO,I1,IAS,IT
      READ,TIMESS,TSTOP,G,IT,XSO,IO,V1
      READ,NI
      READ,(PEI(I),I=1,NI)
C
C
      XLH=5.2
      EM=.0155
      ES=88.5
      AS=.072
      H=500
      V=.2
      DV=V1/V
      SITA=V/G
      KI=2.19E5*EXP(-13810/IT)
      KP=1.051E7*EXP(-3557/IT)
      KT=1.255E9*EXP(-844/IT)
      A1=2.57-.00505*IT
      A2=9.56-.0176*IT
      A3=-3.03+.00785*IT
      PM=924-.918*(IT-273.1)
      PP=1084.8-.605*(IT-273.1)
      XMW=104
      XMO=PM/XMW
      VO=V*PM/PP
      E=(VO-V)/V
      TIME=0
      XM=XMO
      XS=XSO
      SP=0
      SIP=0
      SIIP=0
      SITA=V/G
      WRITE(2,50) IO
   50 FORMAT('-','THE UV INTENSITY =',F8.6)
      WRITE(2,60) IT
   60 FORMAT(' ','TEMPERATURE =',F4.0,' K')
      WRITE(2,70) SITA
   70 FORMAT(' ','RESIDENT TIME =',F7.1,' SEC.')
   99 ESS=ES*XS
      EMM=EM*XM
      ESM=ESS+EMM
      XC=(XMO-XM)/(XMO+E*XM)
      IAS=IO*(ESS/ESM)*(1-EXP(-ESS*XLH*DV))/XLH
      GE=1.
      GE1=(KP/KT**.5)*GE
      XIS=2*AS*IAS
      XIM=2*KI*XM**3
```

```
      THERMO=XIM
      UV=XIS+XIM
      IF(TIME .EQ. TIMESS) GO TO 120
  100 I1=UV
      N1=NI-1
      DO 102 I=1,N1,2
      IF(TIME.GE.PEI(I) .AND. TIME.LT.PEI(I+1)) GO TO 105
      IF(TIME.GE.PEI(I+1) .AND. TIME.LT.PEI(I+2)) GO TO 107
  102 CONTINUE
      GO TO 109
  105 I1=THERMO
      GO TO 109
  107 I1=UV
  109 D1F1=H*F1(XM,XS,I1,GE1,XMO,V,G,E)
      D1F2=H*F2(XM,XS,V,G,AS,IAS,XSO,XC,E)
      XK=XM+D1F1/2
      XL=XS+D1F2/2
      D2F1=H*F1(XK,XL,I1,GE1,XMO,V,G,E)
      D2F2=H*F2(XK,XL,V,G,AS,IAS,XSO,XC,E)
      XK=XM+D2F1/2
      XL=XS+D2F2/2
      D3F1=H*F1(XK,XL,I1,GE1,XMO,V,G,E)
      D3F2=H*F2(XK,XL,V,G,AS,IAS,XSO,XC,E)
      XK=XM+D3F1
      XL=XS+D3F2
      D4F1=H*F1(XK,XL,I1,GE1,XMO,V,G,E)
      D4F2=H*F2(XK,XL,V,G,AS,IAS,XSO,XC,E)
      DF1=(D1F1+2*D2F1+2*D3F1+D4F1)/6
      DF2=(D1F2+2*D2F2+2*D3F2+D4F2)/6
      XM=XM+DF1
      XS=XS+DF2
      BR=I1+GE1*XM*SQRT(I1)
      BK=KT*SQRT(I1/KT)
      B=2*GE1*XM*BR/SQRT(I1)
      SR=SQRT(I1/KT)
      SIR=BR/BK
      SIIR=(BR+B)/BK
      C1F3=H*F3(SP,SR,KT,V,G,E,XC)
      C1F4=H*F4(SIP,SR,SIR,V,G,KT,E,XC)
      C1F5=H*F5(SIIP,SR,SIR,SIIR,KT,V,G,E,XC)
      XSP=SP+C1F3/2
      XSIP=SIP+C1F4/2
      XSIIP=SIIP+C1F5/2
      C2F3=H*F3(XSP,SR,KT,V,G,E,XC)
      C2F4=H*F4(XSIP,SR,SIR,V,G,KT,E,XC)
      C2F5=H*F5(XSIIP,SR,SIR,SIIR,KT,V,G,E,XC)
      XSP=SP+C2F3/2
      XSIP=SIP+C2F4/2
      XSIIP=SIIP+C2F5/2
      C3F3=H*F3(XSP,SR,KT,V,G,E,XC)
      C3F4=H*F4(XSIP,SR,SIR,V,G,KT,E,XC)
      C3F5=H*F5(XSIIP,SR,SIR,SIIR,KT,V,G,E,XC)
      XSP=SP+C3F3
      XSIP=SIP+C3F4
      XSIIP=SIIP+C3F5
```

```
      C4F3=H*F3(XSP,SR,KT,V,G,E,XC)
      C4F4=H*F4(XSIP,SR,SIR,V,G,KT,E,XC)
      C4F5=H*F5(XSIIP,SR,SIR,SIIR,KT,V,G,E,XC)
      CF3=(C1F3+2*C2F3+2*C3F3+C4F3)/6
      CF4=(C1F4+2*C2F4+2*C3F4+C4F4)/6
      CF5=(C1F5+2*C2F5+2*C3F5+C4F5)/6
      SP=SP+CF3
      SIP=SIP+CF4
      SIIP=SIIP+CF5
      U1=SIP/SP
      U2=SIIP/SIP
      P=U2/U1
      XC=(XMO-XM)/(XMO+E*XM)
      TIME=TIME+H
      WRITE(2,110) TIME,XC,XM,XS,P
  110 FORMAT('0',F7.0,1X,1X,F6.4,1X,F4.2,1X,
     CF6.4,1X,F6.3)
      IF(TIME.GE.TSTOP) GO TO 160
      IF(TIME .GT. TIMESS) GO TO 130
      GO TO 99
  120 XCS=XC
      U1S=U1
      U2S=U2
      PS=P
      GO TO 100
  130 RXC=XC/XCS
      RP=P/PS
      WRITE(2,150) RXC,RP
  150 FORMAT(' ','RXC=',F5.3,2X,'RP=',F5.3)
      GO TO 99
  160 STOP
      END
C
C
      FUNCTION F1(XM,XS,I1,GE1,XMO,V,G,E)
      REAL KT,KP,KI,IO,IAS,I1
      XC=(XMO-XM)/(XMO+E*XM)
      F1=(XMO-XM*(1+E*XC))*G/V-I1**.5*XM*GE1
      RETURN
      END
C
C
      FUNCTION F2(XM,XS,V,G,AS,IAS,XSO,XC,E)
      REAL KT,KP,KI,IO,I1,IAS
      F2=(XSO-XS*(1+E*XC))*G/V-AS*IAS
      RETURN
      END
C
C
      FUNCTION F3(SP,SR,KT,V,G,E,XC)
      REAL KT,KP,KI,IO,I1,IAS
      F3=-SP*(1+E*XC)*G/V+.5*KT*SR**2
      RETURN
      END
```

```
      FUNCTION F4(SIP,SR,SIR,V,G,KT,E,XC)
      REAL KT,KP,KI,IO,I1,IAS
      F4=-SIP*(1+E*XC)*G/V+KT*SR*SIR
      RETURN
      END
C
C
      FUNCTION F5(SIIP,SR,SIR,SIIR,KT,V,G,E,XC)
      REAL KT,KP,KI,IO,I1,IAS
      F5=-SIIP*(1+E*XC)*G/V+KT*(SR*SIIR+SIR**2)
      RETURN
      END
```

```
C      PROGRAM #4
C      MOLECULAR WEIGHT DISTRIBUTION
C      UV LIGHT ON/OFF REGULATION AT LOW STEADY STATE
C      ##############################################
C
       DOUBLE PRECISION R1,R2,R3,V1,V3,SUM1,SUM2,FINAL1,FINAL2,
      CTOTAL1,TOTAL2,C1,C2,C3,C4,C5,C6,D2,D3,XP,XKP,XKT,XKI,AI,
      CXMT,XMRT,W1,W2,W3,W4,Q1,Q2,Q3,XQ,PIO,PIT,PIRT,XMWT,XMWRT,
      CXR,B1,B2,B3,B4,B5,B6,B7,B8,B9,B10,PM,XMO,
      CA,B,C,D,H,G,F,Q,SR,XS,SITA,XM,TOL1,TOL2,XMW0
       DIMENSION S(2000),TOL1(1000),TOL2(1000)
       READ,S0,XI0,TEMP,SITA,NP,XNI,V1
       TAU=SITA
C
       PM=924-.918*(TEMP-273.1)
       XMW=104
       XMO=PM/XMW
       XKP=1.051E7*EXP(-3557/TEMP)
       XKT=1.255E9*EXP(-844/TEMP)
       XKI=2.19E5*EXP(-13810/TEMP)
       V=0.2
       DV=V1/V
       AS=0.072
       ES=88.5
       XL=5.2
       XL1=XL*DV
       XC1=SITA*AS*XI0/XL1
       S(1)=S0
       DO 10 I=1,2000
       FS=S(I)-S0+XC1*(1-EXP(-ES*S(I)*XL1))
       DFS=1+XC1*ES*XL1*EXP(-ES*S(I)*XL1)
       XS1=S(I)-FS/DFS
       IF(ABS((S(I)-XS1)/S(I)) .LE. 0.01) GO TO 20
       N=I+1
       S(N)=XS1
   10  CONTINUE
   20  XIAS=XI0*(1-EXP(-ES*XS1*XL1))*DV/XL1
       AI=2*AS*XIAS
       SR=(AI/XKT)**.5
       XM=(XMO-SITA*AI)/(1+SITA*XKP*SR)
       XS=XKP*XM/(XKP*XM+XKT*SR+1/SITA)
       WRITE(6,24)
   24  FORMAT('0','MOLECULAR WEIGHT DISTRIBUTION')
       WRITE(6,26)
   26  FORMAT('0','UV LIGHT ON-OFF CONTROL AT LOW S. S.')
       WRITE(6,28)
   28  FORMAT('0','######################################')
       WRITE(6,29) XKP,XKT
   29  FORMAT('0','KP= ',F6.1,5X,'KT= ',E10.3)
       WRITE(6,32) TEMP
   32  FORMAT('0','TEMPERATURE=',F5.1,' K')
       WRITE(6,34) XI0
   34  FORMAT('0','UV INTENSITY=',F8.6)
       WRITE(6,36) SITA
```

```
 36   FORMAT('0','RESIDENT TIME=',F7.1)
      WRITE(6,37) XMO
 37   FORMAT('0','INLET MONOMER CONC.=',F5.3)
      WRITE(6,38) SO
 38   FORMAT('0','INLET SENSITIZER CONC.=',F5.3)
      WRITE(6,42)
 42   FORMAT('0')
      WRITE(6,44)
 44   FORMAT('0','AT LOW STEADY STATE :')
      WRITE(6,45)
 45   FORMAT(' ','-------------------------------')
      WRITE(6,46) SR
 46   FORMAT('0','SUM OF THE FREE RADICAL CONC.=',F15.13)
      WRITE(6,48) XM
 48   FORMAT('0','OUTLET MONOMER CONC.=',F6.4)
      WRITE(6,50) XS1
 50   FORMAT('0','OUTLET SENSITIZER CONC.=',E10.4)
C
C
      SIPO=0.
      DO 500 I=1,12000
      PIO=((I-1)/2.)*XS**I*AI**2*XKT*SITA/(XKP*XM)**2
      SIPO=SIPO+I*PIO
 500  CONTINUE
      WRITE(6,55) SIPO
 55   FORMAT('0','SIPO =',F10.7)
C
      DO 1000 LR=1,NP
      R=XNI*LR
      WRITE(6,60) R
 60   FORMAT('1','THE RATIO OF TIME  LENGTH (OFF/(ON+OFF)) =',
     CF5.3)
      WRITE(6,65)
 65   FORMAT(' ','-----------------------------------------------------')
      RT=R*TAU
      C1=XMO
      C2=XM-XMO
      C3=XMO/SITA-AI
      C4=1/SITA+XKP*(AI/XKT)**.5
      C5=C3/C4
      D=EXP(-C4*(1-R)*TAU)
      C=C5*(1-D)
      B=EXP(-RT/SITA)
      A=XMO*(1-B)
      C6=C3/C4-(A+B*XM)
      G=C+D*A
      H=B*D
      P=A+C*B
C
      D2=(AI*XKT)**.5
      D3=1/(C4*SITA)
      XMRT=A+B*XM
      XMT=G+H*XM
      B1=SITA*C1**4
      B2=4*C2*C1**3
```

```
      B3=6*SITA*(C1*C2)**2
      B4=2*SITA*C1*C2**3
      B5=SITA*C2**4/3
      B6=EXP(-RT/SITA)
      B7=EXP(-2*RT/SITA)
      B8=EXP(-3*RT/SITA)
      B9=EXP(-4*RT/SITA)
      B10=B1+B2*RT*B6-B3*B7-B4*B8-B5*B9
      XP1=SQRT(2*XKI/XKT)*C1**2.5*XKP
      XP2=2.5*C2/C1*RT
      XP3=15./8.*(C2/C1)**2*SITA
      XP4=SITA+XP2*B6-XP3*B7
      XP5=(SITA-XP3)*B6
      XP6=XKP*SQRT(AI/XKT)
      XP7=SITA*C5
      XP8=SITA*C6/(1-C4*SITA)
      XP9=EXP(-(1-R)*TAU/SITA)
      P1=XP1*(XP4-XP5)
      P2=B6
      P3=XP6*(XP7-XP8*D)-XP6*(XP7-XP8)*XP9
      P4=XP9
      T1=P1*P4+P3
      T2=P2*P4
      T3=P1+P2*P3
C
      DO 980 I=25,4000,25
      PIO=((I-1)/2.)*XS**I*AI**2*XKT*SITA/(XKP*XM)**2
      XB=2*XKT*(I-1)*(XKI/XKP)**2
      PIRT=XB*B10+(PIO-XB*(B1-B3-B4-B5))*B6
C
      R1=C5-C6*EXP(-C4*(1-R)*TAU)
      R2=-C6*EXP(-C4*(1-R)*TAU)
      R3=C5-C6
      XP=-.5*XKT*(I-1)*(AI/XKP)**2*(-C6)**D3/C4
C
      N=0
      V1=1
      V3=1
      SUM1=1/((-D3)*R1**2*R2**D3)
      SUM2=1/((-D3)*R3**2*(-C6)**D3)
      TOTAL1=SUM1
      TOTAL2=SUM2
C
      DO 600 K=1,60
      SUM1=SUM1*(K+1)*R2/((K-D3)*R1)
      SUM2=SUM2*(K+1)*(-C6)/((K-D3)*R3)
      TOTAL1=TOTAL1+SUM1
      TOTAL2=TOTAL2+SUM2
  600 CONTINUE
C
C
      DO 900 N=1,200
      CALL BINOM(N,I,R1,R3,XKP,D2,V1,V3)
      SUM1=1/((-D3)*R1**2*R2**D3)
      SUM2=1/((-D3)*R3**2*(-C6)**D3)
```

```
      FINAL1=SUM1
      FINAL2=SUM2
C
      DO 800 L=1,60
      SUM1=SUM1*(N+L+1)*R2/((L-D3)*R1)
      SUM2=SUM2*(N+L+1)*(-C6)/((L-D3)*R3)
      FINAL1=FINAL1+SUM1
      FINAL2=FINAL2+SUM2
  800 CONTINUE
C
      TOTAL1=TOTAL1+V1*FINAL1
      TOTAL2=TOTAL2+V3*FINAL2
  900 CONTINUE
C
      PIT=EXP(-(1-R)*TAU/SITA)*(XP*TOTAL1+PIRT-XP*TOTAL2)
      KK=I/25
      TOL1(KK)=TOTAL1
      TOL2(KK)=TOTAL2
      SIPRT=P1+P2*SIPO
      SIPT=P3+P4*SIPRT
      XMWO=I*PIO/SIPO
      XMWRT=I*PIRT/SIPRT
      XMW=I*PIT/SIPT
      WRITE(6,902) I,PIO,XMWO,PIRT,XMWRT
  902 FORMAT('0','I=',I5,3X,'PIO=',D20.14,3X,'XMWO=',D20.14,3X,
     C'PIRT=',D20.14,3X,'XMWRT=',D20.14)
  980 CONTINUE
C
C
      DO 990 NC=1,15
      WRITE(6,987)
  987 FORMAT('0')
C
      DO 985 I=25,4000,25
      PIO=((I-1)/2.)*XS**I*AI**2*XKT*SITA/(XKP*XM)**2
      XP=-.5*XKT*(I-1)*(AI/XKP)**2*(-C6)**D3/C4
      XB=2*XKT*(I-1)*(XKI/XKP)**2
      Q=(1-H**NC)/(1-H)
      XMT=G*Q+XM*H**NC
      XMRT=F*Q+(A+B*XM)*H**NC
C
      NN=I/25
      W1=XB*B10-XB*(B1-B3-B4-B5)*B6
      W2=B6
      W3=EXP(-(1-R)*TAU/SITA)*XP*(TOL1(NN)-TOL2(NN))
      W4=EXP(-(1-R)*TAU/SITA)
      Q1=W3+W1*W4
      Q2=W2*W4
      Q3=W1+W2*W3
      XQ=(1-Q2**NC)/(1-Q2)
      PIT=Q1*XQ+PIO*Q2**NC
      PIRT=Q3*XQ+(W1+W2*PIO)*Q2**NC
      XT=(1-T2**NC)/(1-T2)
      SIPT=T1*XT+SIPO*T2**NC
      SIPRT=T3*XT+(P1+P2*SIPO)*T2**NC
```

```
      SIRT=(AI+XKP*XMT*SR)/(XKT*SR)
      XMWT=I*PIT/SIPT
      XMWRT=I*PIRT/SIPRT
      WRITE(6,940) NC,I,XMWT,XMWRT
  940 FORMAT(' ','NC=',I2,3X,'I=',I5,3X,'XMWT=',D20.14,3X,
     C'XMWRT=',D20.14)
  985 CONTINUE
C
  990 CONTINUE
 1000 CONTINUE
      STOP
      END
C
C
      SUBROUTINE BINOM(N,I,R1,R3,XKP,D2,V1,V3)
      DOUBLE PRECISION R1,R2,R3,V1,V3,D2,XKP
      V1=-V1*(I+N-1)*(D2/(XKP*R1))/N
      V3=-V3*(I+N-1)*(D2/(XKP*R3))/N
      RETURN
      END
```

```
C       PROGRAM #5
C       ROSENBROCK'S SEARCHING TECHNIQUE
C       ################################
C
        DIMENSION X(3),XE(3),XV(3,3),SA(3),D(3),G(3),H(3),AL(3),
       1PH(3),A(3,3),B(3,3),BX(3),DA(1),VV(3,3),EINT(3),VM(3)
        DIMENSION XSR1(1000),XSIR1(1000),XSIIR1(1000)
        COMMON KOUNT,KT,KT1,KT2,KP,AS,E,XC1,XC2,XL1,XL2,XK1,XK2,
       CSR1,SR2,SIR1,SIR2,SIIR1,SIIR2,XSP1,XSP2,XSIP1,XSIP2,
       CXSIIP1,XSIIP2,SIDA1,SIDA2,IAS1,IAS2,V1,V2,XMO,I11,I12,
       CGE1,GE2
        INTEGER P,PR,R,C
        REAL LC,IT
        M=-1
        P=3
        L=3
        LOOPY=100
        PR=1
        ND=0
        NDATA=0
        NSTEP=0
C
        READ,X
        READ,XE
        READ,TIME1,TIME2,TIME3
        READ,UEXP1,UEXP2,UEXP3
        READ,PEXP1,PEXP2,PEXP3
        READ,XEXP1,XEXP2,XEXP3
C
        IF(ND-1) 30,20,30
   20   DA(1)=1
   30   LAP=PR-1
        LOOP=0
        ISW=0
        INIT=0
        KOUNT=0
        TERM=0
        DELY=1.0E-6
        F9=0.0
        NPAR=NDATA
        N=L
        DO 40 K=1,L
   40   AL(K)=(CH(X,DA,N,NPAR,K)-CG(X,DA,N,NPAR,K))*.0001
        DO 60 I=1,P
        DO 60 J=1,P
        XV(I,J)=0.0
        IF(I-J) 60,61,60
   61   XV(I,J)=1.0
   60   CONTINUE
        DO 65 KK=1,P
        EINT(KK)=XE(KK)
   65   CONTINUE
C
C
```

```
 1000 DO 70 J=1,P
      IF(NSTEP.EQ.0) XE(J)=EINT(J)
      SA(J)=2.0
   70 D(J)=0.0
      FBEST=F9
   80 I=1
      IF(INIT.EQ.0) GO TO 120
   90 DO 110 K=1,P
  110 X(K)=X(K)+XE(I)*XV(I,K)
      DO 50 K=1,L
   50 H(K)=F0
C
C
  120 F9=F(X,DA,N,NPAR)
      F9=M*F9
      IF(ISW.EQ.0) F0=F9
      ISW=1
      IF(ABS(F9)-DELY) 122,122,125
  122 TERM=1.0
      GO TO 450
  125 CONTINUE
C
C
      J=1
C
  130 XXC=CX(X,DA,N,NPAR,J)
      LC=CG(X,DA,N,NPAR,J)
      UC=CH(X,DA,N,NPAR,J)
      IF(XXC.LE.LC) GO TO 420
      IF(XXC.GE.UC) GO TO 420
      IF(F9.LT.F0) GO TO 420
      IF(XXC.LT.LC+AL(J)) GO TO 140
      IF(XXC.GT.UC-AL(J)) GO TO 140
      H(J)=F0
      GO TO 210
C
C
  140 CONTINUE
C
      BW=AL(J)
      IF(XXC .LE. LC .OR. UC .LE. XXC) GO TO 150
      IF(LC .LT. XXC .AND. XXC .LT. LC+BW) GO TO 160
      IF(UC-BW .LT. XXC .AND. XXC .LT. UC) GO TO 170
      PH(J)=1.0
      GO TO 210
C
C
  150 PH(J)=0.0
      GO TO 190
  160 PW=(LC+BW-XXC)/BW
      GO TO 180
  170 PW=(XXC-UC+BW)/BW
  180 PH(J)=1.0-3.0*PW+4.0*PW**2-2.0*PW**3
C
  190 F9=H(J)+(F9-H(J))*PH(J)
```

```
C
  210 CONTINUE
      IF(J.EQ.L) GO TO 220
      J=J+1
      GO TO 130
C
  220 INIT=1
      IF(F9.LT.F0) GO TO 420
      D(I)=D(I)+XE(I)
      XE(I)=3.0*XE(I)
      F0=F9
      IF(SA(I).GE.1.5) SA(I)=1.0
C
  230 DO 240 JJ=1,P
      IF(SA(JJ).GE.0.5) GO TO 440
  240 CONTINUE
C
C
      DO 250 R=1,P
      DO 250 C=1,P
  250 VV(C,R)=0.0
      DO 260 R=1,P
      KR=R
      DO 260 C=1,P
      DO 265 K=KR,P
  265 VV(R,C)=D(K)*XV(K,C)+VV(R,C)
  260 B(R,C)=VV(R,C)
      BMAG=0.0
      DO 280 C=1,P
      BMAG=BMAG+B(1,C)*B(1,C)
  280 CONTINUE
      BMAG=SQRT(BMAG)
      BX(1)=BMAG
      DO 310 C=1,P
  310 XV(1,C)=B(1,C)/BMAG
C
      DO 390 R=2,P
C
      IR=R-1
      DO 390 C=1,P
      SUMVM=0.0
      DO 320 KK=1,IR
      SUMAV=0.0
      DO 330 KJ=1,P
  330 SUMAV=SUMAV+VV(R,KJ)*XV(KK,KJ)
  320 SUMVM=SUMAV*XV(KK,C)+SUMVM
  390 B(R,C)=VV(R,C)-SUMVM
      DO 340 R=2,P
      BBMAG=0.0
      DO 350 K=1,P
  350 BBMAG=BBMAG+B(R,K)*B(R,K)
      BBMAG=SQRT(BBMAG)
      DO 340 C=1,P
  340 XV(R,C)=B(R,C)/BBMAG
      LOOP=LOOP+1
```

```
      LAP=LAP+1
      IF(LAP.EQ.PR) GO TO 450
      GO TO 1000
C
  420 IF(INIT.EQ.0) GO TO 450
      DO 430 IX=1,P
  430 X(IX)=X(IX)-XE(I)*XV(I,IX)
      XE(I)=-.5*XE(I)
      IF(SA(I).LT.1.5) SA(I)=0.0
      GO TO 230
C
  440 CONTINUE
      IF(I.EQ.P) GO TO 80
      I=I+1
      GO TO 90
C
  450 WRITE(2,455)
  455 FORMAT('-')
      WRITE(2,460) (X(JM),JM=1,P)
  460 FORMAT(3(F12.8,3X))
C
      LAP=0
      IF(TERM.EQ.1.0) GO TO 480
      IF(LOOP.GE.LOOPY) GO TO 480
      GO TO 1000
C
  480 CONTINUE
      STOP
      END
C
C
      FUNCTION F (X,DA,N,NPAR)
      DIMENSION X(N),DA(NPAR)
      DIMENSION XSR1(1000),XSIR1(1000),XSIIR1(1000)
      COMMON KOUNT,KT,KT1,KT2,KP,AS,E,XC1,XC2,XL1,XL2,XK1,XK2,
     CSR1,SR2,SIR1,SIR2,SIIR1,SIIR2,XSP1,XSP2,XSIP1,XSIP2,
     CXSIIP1,XSIIP2,SIDA1,SIDA2,IAS1,IAS2,V1,V2,XM0,I11,I12,
     CGE1,GE2
      REAL KT,KT1,KT2,KP,KI,I0,I11,I12,IT,IAS1,IAS2
      EM=.0155
      ES=88.5
      V=.2
      XS0=.015
      IT=338.
      XL=5.2*X(1)/.2
      V1=X(1)
      V2=.2-V1
      SIDA1=V1/X(2)
      SIDA2=V2/X(2)
      AS=.072
      H=500
      KI=2.19E5*EXP(-13810/IT)
      KP=1.051E7*EXP(-3557/IT)
      KT=1.255E9*EXP(-844/IT)
      PM=924-.918*(IT-273.1)
      PP=1084.8-.605*(IT-273.1)
```

```
      XMW=104
      XMO=PM/XMW
      VO=V*PM/PP
      E=(VO-V)/V
      T=0
      XM1=XMO
      XM2=XMO
      XS1=XSO
      XS2=XSO
      SP1=0
      SP2=0
      SIP1=0
      SIP2=0
      SIIP1=0
      SIIP2=0
      XC1=(XMO-XM1)/(XMO+E*XM1)
      XC2=(XMO-XM2)/(XMO+E*XM2)
   99 EMM1=EM*XM1
      ESS1=ES*XS1
      ESM1=ESS1+EMM1
      XK1=XM1
      XK2=XM2
      XL1=XS1
      XL2=XS2
      XSP1=SP1
      XSP2=SP2
      XSIP1=SIP1
      XSIP2=SIP2
      XSIIP1=SIIP1
      XSIIP2=SIIP2
      C6=1+E*XC1
      C7=1+E*XC2
      IO=.000117
      IAS1=IO*(ESS1/ESM1)*(1-EX**(-ESM1*XL))/XL
      IAS2=X(3)
      Y3=2.57-.00505*IT
      Y4=9.56-.0176*IT
      Y5=-3.03+.00785*IT
      GE1=EX**(Y3*XC1+Y4*XC1**2+Y5*XC1**3)
      GE2=EX**(Y3*XC2+Y4*XC2**2+Y5*XC2**3)
      KT1=KT/GE1**2
      KT2=KT/GE2**2
      XIS1=2*AS*IAS1
      XIS2=2*AS*IAS2
      XIM1=2*KI*XM1**3
      XIM2=2*KI*XM2**3
      I11=XIS1+XIM1
      I12=XIS2+XIM2
      SR1=(I11/KT)**.5
      SR2=(I12/KT)**.5
      XSIR1(1)=0
      DO 301 K=1,1000
      W2=(C6*XSIR1(K)/SIDA2+KP*XM2*SR2*GE2+I12)/
     C(C7/SIDA2+KT*SR2)
      SIR1=(C7*W2/SIDA1+KP*XM1*SR1*GE1+I11)/(C6/SIDA1+KT*SR1)
```

```
      YY=ABS(SIR1-XSIR1(K))/SIR1
      IF(YY.LE..001) GO TO 302
      L=K+1
      XSIR1(L)=SIR1
301   CONTINUE
302   SIR2=(C6*SIR1/SIDA2+KP*XM2*SR2*GE2+I12)/(C7/SIDA2+KT*SR2)
      XSIIR1(1)=0
      DO 401 K=1,1000
      W3=(C6*XSIIR1(K)/SIDA2+2*KP*XM2*SIR2*GE2)/
     C(C7/SIDA2+KT*SR2)
      SIIR1=(C7*W3/SIDA1+2*KP*XM1*SIR1*GE1)/(C6/SIDA1+KT*SR1)
      YW=ABS(SIIR1-XSIIR1(K))/SIIR1
      IF(YW.LE..001) GO TO 402
      L=K+1
      XSIIR1(L)=SIIR1
401   CONTINUE
402   SIIR2=(C6*SIIR1/SIDA2+2*KP*XM2*SIR2*GE2)/
     C(C7/SIDA2+KT*SR2)
      D1F11=H*F11(DUMMY)
      D1F12=H*F12(DUMMY)
      D1F21=H*F21(DUMMY)
      D1F22=H*F22(DUMMY)
      XK1=XM1+D1F11/2
      XK2=XM2+D1F12/2
      XL1=XS1+D1F21/2
      XL2=XS2+D1F22/2
      D2F11=H*F11(DUMMY)
      D2F12=H*F12(DUMMY)
      D2F21=H*F21(DUMMY)
      D2F22=H*F22(DUMMY)
      XK1=XM1+D2F11/2
      XK2=XM2+D2F12/2
      XL1=XS1+D2F21/2
      XL2=XS2+D2F22/2
      D3F11=H*F11(DUMMY)
      D3F12=H*F12(DUMMY)
      D3F21=H*F21(DUMMY)
      D3F22=H*F22(DUMMY)
      XK1=XM1+D3F11
      XK2=XM2+D3F12
      XL1=XS1+D3F21
      XL2=XS2+D3F22
      D4F11=H*F11(DUMMY)
      D4F12=H*F12(DUMMY)
      D4F21=H*F21(DUMMY)
      D4F22=H*F22(DUMMY)
      DF11=(D1F11+2*D2F11+2*D3F11+D4F11)/6
      DF12=(D1F12+2*D2F12+2*D3F12+D4F12)/6
      DF21=(D1F21+2*D2F21+2*D3F21+D4F21)/6
      DF22=(D1F22+2*D2F22+2*D3F22+D4F22)/6
      C1F31=H*F31(DUMMY)
      C1F32=H*F32(DUMMY)
      C1F41=H*F41(DUMMY)
      C1F42=H*F42(DUMMY)
      C1F51=H*F51(DUMMY)
```

```
C1F52=H*F52(DUMMY)
XSP1=SP1+C1F31/2
XSP2=SP2+C1F32/2
XSIP1=SIP1+C1F41/2
XSIP2=SIP2+C1F42/2
XSIIP1=SIIP1+C1F51/2
XSIIP2=SIIP2+C1F52/2
C2F31=H*F31(DUMMY)
C2F32=H*F32(DUMMY)
C2F41=H*F41(DUMMY)
C2F42=H*F42(DUMMY)
C2F51=H*F51(DUMMY)
C2F52=H*F52(DUMMY)
XSP1=SP1+C2F31/2
XSP2=SP2+C2F32/2
XSIP1=SIP1+C2F41/2
XSIP2=SIP2+C2F42/2
XSIIP1=SIIP1+C2F51/2
XSIIP2=SIIP2+C2F52/2
C3F31=H*F31(DUMMY)
C3F32=H*F32(DUMMY)
C3F41=H*F41(DUMMY)
C3F42=H*F42(DUMMY)
C3F51=H*F51(DUMMY)
C3F52=H*F52(DUMMY)
XSP1=SP1+C3F31
XSP2=SP2+C3F32
XSIP1=SIP1+C3F41
XSIP2=SIP2+C3F42
XSIIP1=SIIP1+C3F51
XSIIP2=SIIP2+C3F52
C4F31=H*F31(DUMMY)
C4F32=H*F32(DUMMY)
C4F41=H*F41(DUMMY)
C4F42=H*F42(DUMMY)
C4F51=H*F51(DUMMY)
C4F52=H*F52(DUMMY)
CF31=(C1F31+2*C2F31+2*C3F31+C4F31)/6
CF32=(C1F32+2*C2F32+2*C3F32+C4F32)/6
CF41=(C1F41+2*C2F41+2*C3F41+C4F41)/6
CF42=(C1F42+2*C2F42+2*C3F42+C4F42)/6
CF51=(C1F51+2*C2F51+2*C3F51+C4F51)/6
CF52=(C1F52+2*C2F52+2*C3F52+C4F52)/6
SP1=SP1+CF31
SP2=SP2+CF32
SIP1=SIP1+CF41
SIP2=SIP2+CF42
SIIP1=SIIP1+CF51
SIIP2=SIIP2+CF52
XM1=XM1+DF11
XM2=XM2+DF12
XS1=XS1+DF21
XS2=XS2+DF22
U11=SIP1/SP1
U12=SIP2/SP2
```

```
      U21=SIIP1/SIP1
      U22=SIIP2/SIP2
      P1=U21/U11
      P2=U22/U12
      XC1=(XM0-XM1)/(XM0+E*XM1)
      XC2=(XM0-XM2)/(XM0+E*XM2)
      T=T+H
      XLADA=10
      IF(T .EQ. TIME1) GO TO 104
      IF(T .EQ. TIME2) GO TO 106
      IF(T .GE. TIME3) GO TO 108
      GO TO 99
  104 FA=((U11-UEXP1)/UEXP1)**2+((P1-PEXP1)/PEXP1)**2
     C+XLADA*(XC1-XEXP1)**2
      PRINT,U11,P1,XC1
      GO TO 99
  106 FB=((U11-UEXP2)/UEXP2)**2+((P1-PEXP2)/PEXP2)**2
     C+XLADA*(XC1-XEXP2)**2
      PRINT,U11,P1,XC1
      GO TO 99
  108 FC=((U11-UEXP3)/UEXP3)**2+((P1-PEXP3)/PEXP3)**2
     C+XLADA*(XC1-XEXP3)**2
      PRINT,U11,P1,XC1
      F=FA+FB+FC
      WRITE(2,105) (X(JM),JM=1,3)
  105 FORMAT(3(F12.8,3X))
      KOUNT=KOUNT+1
      RETURN
      END
C
C
      FUNCTION F11(DUMMY)
      COMMON KOUNT,KT,KT1,KT2,KP,AS,E,XC1,XC2,XL1,XL2,XK1,XK2,
     CSR1,SR2,SIR1,SIR2,SIIR1,SIIR2,XSP1,XSP2,XSIP1,XSIP2,
     CXSIIP1,XSIIP2,SIDA1,SIDA2,IAS1,IAS2,V1,V2,XM0,I11,I12,
     CGE1,GE2
      REAL KT,KT1,KT2,KP,I11,I12
      F11=-KP*XK1*SR1*GE1+((1+E*XC2)*XK2-(1+E*XC1)*XK1)/SIDA1
      RETURN
      END
C
C
      FUNCTION F12(DUMMY)
      COMMON KOUNT,KT,KT1,KT2,KP,AS,E,XC1,XC2,XL1,XL2,XK1,XK2,
     CSR1,SR2,SIR1,SIR2,SIIR1,SIIR2,XSP1,XSP2,XSIP1,XSIP2,
     CXSIIP1,XSIIP2,SIDA1,SIDA2,IAS1,IAS2,V1,V2,XM0,I11,I12,
     CGE1,GE2
      REAL KT,KT1,KT2,KP,I11,I12
      F12=-KP*XK2*SR2*GE2+((1+E*XC1)*XK1-(1+E*XC2)*XK2)/SIDA2
     C-XK2*FV(DUMMY)/V2
      RETURN
      END
```

```
C
C
      FUNCTION F21(DUMMY)
      COMMON KOUNT,KT,KT1,KT2,KP,AS,E,XC1,XC2,XL1,XL2,XK1,XK2,
     CSR1,SR2,SIR1,SIR2,SIIR1,SIIR2,XSP1,XSP2,XSIP1,XSIP2,
     CXSIIP1,XSIIP2,SIDA1,SIDA2,IAS1,IAS2,V1,V2,XMO,I11,I12,
     CGE1,GE2
      REAL KT,KT1,KT2,KP,I11,I12,IAS1
      F21=-AS*IAS1+((1+E*XC2)*XL2-(1+E*XC1)*XL1)/SIDA1
      RETURN
      END
C
C
      FUNCTION F22(DUMMY)
      COMMON KOUNT,KT,KT1,KT2,KP,AS,E,XC1,XC2,XL1,XL2,XK1,XK2,
     CSR1,SR2,SIR1,SIR2,SIIR1,SIIR2,XSP1,XSP2,XSIP1,XSIP2,
     CXSIIP1,XSIIP2,SIDA1,SIDA2,IAS1,IAS2,V1,V2,XMO,I11,I12,
     CGE1,GE2
      REAL KT,KT1,KT2,KP,I11,I12,IAS2
      F22=-AS*IAS2+((1+E*XC1)*XL1-(1+E*XC2)*XL2)/SIDA2
     C-XL2*FV(DUMMY)/V2
      RETURN
      END
C
C
      FUNCTION F31(DUMMY)
      COMMON KOUNT,KT,KT1,KT2,KP,AS,E,XC1,XC2,XL1,XL2,XK1,XK2,
     CSR1,SR2,SIR1,SIR2,SIIR1,SIIR2,XSP1,XSP2,XSIP1,XSIP2,
     CXSIIP1,XSIIP2,SIDA1,SIDA2,IAS1,IAS2,V1,V2,XMO,I11,I12,
     CGE1,GE2
      REAL KT,KT1,KT2,KP,I11,I12
      F31=.5*KT*SR1**2+((1+E*XC2)*XSP2-(1+E*XC1)*XSP1)/SIDA1
      RETURN
      END
C
C
      FUNCTION F32(DUMMY)
      COMMON KOUNT,KT,KT1,KT2,KP,AS,E,XC1,XC2,XL1,XL2,XK1,XK2,
     CSR1,SR2,SIR1,SIR2,SIIR1,SIIR2,XSP1,XSP2,XSIP1,XSIP2,
     CXSIIP1,XSIIP2,SIDA1,SIDA2,IAS1,IAS2,V1,V2,XMO,I11,I12,
     CGE1,GE2
      REAL KT,KT1,KT2,KP,I11,I12
      F32=.5*KT*SR2**2+((1+E*XC1)*XSP1-(1+E*XC2)*XSP2)/SIDA2
     C-XSP2*FV(DUMMY)/V2
      RETURN
      END
C
C
```

```
      FUNCTION F41(DUMMY)
      COMMON KOUNT,KT,KT1,KT2,KP,AS,E,XC1,XC2,XL1,XL2,XK1,XK2,
     CSR1,SR2,SIR1,SIR2,SIIR1,SIIR2,XSP1,XSP2,XSIP1,XSIP2,
     CXSIIP1,XSIIP2,SIDA1,SIDA2,IAS1,IAS2,V1,V2,XMO,I11,I12,
     CGE1,GE2
      REAL KT,KT1,KT2,KP,I11,I12
      F41=KT*SR1*SIR1+((1+E*XC2)*XSIP2-(1+E*XC1)*XSIP1)/SIDA1
      RETURN
      END
C
C
      FUNCTION F42(DUMMY)
      COMMON KOUNT,KT,KT1,KT2,KP,AS,E,XC1,XC2,XL1,XL2,XK1,XK2,
     CSR1,SR2,SIR1,SIR2,SIIR1,SIIR2,XSP1,XSP2,XSIP1,XSIP2,
     CXSIIP1,XSIIP2,SIDA1,SIDA2,IAS1,IAS2,V1,V2,XMO,I11,I12,
     CGE1,GE2
      REAL KT,KT1,KT2,KP,I11,I12
      F42=KT*SR2*SIR2+((1+E*XC1)*XSIP1-(1+E*XC2)*XSIP2)/SIDA2
     C-XSIP2*FV(DUMMY)/V2
      RETURN
      END
C
C
      FUNCTION F51(DUMMY)
      COMMON KOUNT,KT,KT1,KT2,KP,AS,E,XC1,XC2,XL1,XL2,XK1,XK2,
     CSR1,SR2,SIR1,SIR2,SIIR1,SIIR2,XSP1,XSP2,XSIP1,XSIP2,
     CXSIIP1,XSIIP2,SIDA1,SIDA2,IAS1,IAS2,V1,V2,XMO,I11,I12,
     CGE1,GE2
      REAL KT,KT1,KT2,KP,I11,I12
      F51=KT*SR1*SIIR1+KT*SIR1**2+((1+E*XC2)*XSIIP2
     C-(1+E*XC1)*XSIIP1)/SIDA1
      RETURN
      END
C
C
      FUNCTION F52(DUMMY)
      COMMON KOUNT,KT,KT1,KT2,KP,AS,E,XC1,XC2,XL1,XL2,XK1,XK2,
     CSR1,SR2,SIR1,SIR2,SIIR1,SIIR2,XSP1,XSP2,XSIP1,XSIP2,
     CXSIIP1,XSIIP2,SIDA1,SIDA2,IAS1,IAS2,V1,V2,XMO,I11,I12,
     CGE1,GE2
      REAL KT,KT1,KT2,KP,I11,I12
      F52=KT*SR2*SIIR2+KT*SIR2**2+((1+E*XC1)*XSIIP1
     C-(1+E*XC2)*XSIIP2)/SIDA2-XSIIP2*FV(DUMMY)/V2
      RETURN
      END
C
C
```

```
      FUNCTION FV(DUMMY)
      COMMON KOUNT,KT,KT1,KT2,KP,AS,E,XC1,XC2,XL1,XL2,XK1,XK2,
     CSR1,SR2,SIR1,SIR2,SIIR1,SIIR2,XSP1,XSP2,XSIP1,XSIP2,
     CXSIIP1,XSIIP2,SIDA1,SIDA2,IAS1,IAS2,V1,V2,XMO,I11,I12,
     CGE1,GE2
      REAL KT,KT1,KT2,KP,I11,I12
      ALPHA=-KP*XK1*SR1*GE1+((1+E*XC2)*XK2-(1+E*XC1)*XK1)/SIDA1
      BETA=-KP*XK2*SR2*GE2+((1+E*XC1)*XK1-(1+E*XC2)*XK2)/SIDA2
      GAMMA=-E*V2*BETA/(XMO+E*XK2)
      THETA=-E*V1*ALPHA/(XMO+E*XK2)
      FV=(GAMMA+THETA)*(1+E*XK2/XMO)
      RETURN
      END
C
C
      FUNCTION CX (X,DA,N,NPAR,K)
      DIMENSION X(N),DA(NPAR)
      CX=X(K)
      RETURN
      END
C
C
      FUNCTION CG (X,DA,N,NPAR,K)
      DIMENSION X(N),DA(NPAR)
      GO TO (1,2,3),K
  1   CG=0.0
      GO TO 10
  2   CG=0.0
      GO TO 10
  3   CG=0.0
  10  RETURN
      END
C
C
      FUNCTION CH (X,DA,N,NPAR,K)
      DIMENSION X(N),DA(NPAR)
      GO TO (1,2,3),K
  1   CH=.05
      GO TO 10
  2   CH=.0002
      GO TO 10
  3   CH=.00001
  10  RETURN
      END
```

```
C       PROGRAM #6
C       TO CALCULATE REACTOR PERFORMANCE OF CSTR
C       AT LOW STEADY STATE
C       ########################################
C
        DIMENSION XSIR1(1000),XSIIR1(1000)
        COMMON KOUNT,KT,KT1,KT2,KP,AS,E,XC1,XC2,XL1,XL2,XK1,XK2,
       CSR1,SR2,SIR1,SIR2,SIIR1,SIIR2,XSP1,XSP2,XSIP1,XSIP2,XC,G,
       CXSIIP1,XSIIP2,SIDA1,SIDA2,IAS1,IAS2,V1,V2,XMO,I11,I12,
       CGE1,GE2,V,XS0
        REAL KT,KT1,KT2,KP,KI,IO,I11,I12,IT,IAS1,IAS2
        READ,TSTOP,X3,X4,IAS2
        READ,G,XS0,IT,IO
        V=.2
        SITA=V/G
        Q=X4
        V1=X3
        V2=V-V1
        SIDA1=V1/Q
        SIDA2=V2/Q
        EM=.0155
        ES=88.5
        GE1=1.
        GE2=1.
        AS=.072
        WRITE(2,20) SITA
   20   FORMAT(' ','RESIDENT TIME=',F7.1,' SEC')
        WRITE(2,30) IT
   30   FORMAT(' ','TEMPERATURE =',F5.0,' K')
        WRITE(2,40) XIAS2
   40   FORMAT(' ','LIGHT INTENSITY IN DARK REG. =',F10.8)
        WRITE(2,45)
   45   FORMAT('-')
        WRITE(2,50) V1
   50   FORMAT(' ','VOLUME IN LIGHT REGION =',F5.3)
        WRITE(2,60) Q
   60   FORMAT(' ','FLOW RATE BETW. TWO REGIONS =',F9.7)
        WRITE(2,70) SIDA1
   70   FORMAT(' ','RESIDENT TIME IN LIGHT REGION =',F7.1)
        WRITE(2,80) SIDA2
   80   FORMAT(' ','RESIDENT TIME IN DARK REGION =',F7.1)
        WRITE(2,90)
   90   FORMAT('-')
        XL=5.2*V1/V
        H=500
        KI=2.19E5*EXP(-13810/IT)
        KP=1.051E7*EXP(-3557/IT)
        KT=1.255E9*EXP(-844/IT)
        PM=924-.918*(IT-273.1)
        PP=1084.8-.605*(IT-273.1)
        XMW=104
        XMO=PM/XMW
        VO=V*PM/PP
        E=(VO-V)/V
```

```
      T=0
      XM1=XM0
      XM2=XM0
      XS1=XS0
      XS2=XS0
      SP1=0
      SP2=0
      SIP1=0
      SIP2=0
      SIIP1=0
      SIIP2=0
      XC1=(XM0-XM1)/(XM0+E*XM1)
      XC2=(XM0-XM2)/(XM0+E*XM2)
      XC=(V1*XC1+V2*XC2)/V
99    EMM1=EM*XM1
      ESS1=ES*XS1
      ESM1=ESS1+EMM1
      XK1=XM1
      XK2=XM2
      XL1=XS1
      XL2=XS2
      XSP1=SP1
      XSP2=SP2
      XSIP1=SIP1
      XSIP2=SIP2
      XSIIP1=SIIP1
      XSIIP2=SIIP2
      C6=1+E*XC1
      C7=1+E*XC2
      IAS1=IO*(ESS1/ESM1)*(1-EXP(-ESM1*XL))/XL
      Y3=2.57-.00505*IT
      Y4=9.56-.0176*IT
      Y5=-3.03+.00785*IT
      KT1=KT/GE1**2
      KT2=KT/GE2**2
      XIS1=2*AS*IAS1
      XIS2=2*AS*IAS2
      XIM1=2*KI*XM1**3
      XIM2=2*KI*XM2**3
      I11=XIS1+XIM1
      I12=XIS2+XIM2
      SR1=(I11/KT)**.5
      SR2=(I12/KT)**.5
      XSIR1(1)=0
      DO 301 K=1,1000
      W2=(C6*XSIR1(K)/SIDA2+KP*XM2*SR2*GE2+I12)/
     C(C7/SIDA2+KT*SR2)
      SIR1=(C7*W2/SIDA1+KP*XM1*SR1*GE1+I11)/(C6/SIDA1+KT*SR1)
      YY=ABS(SIR1-XSIR1(K))/SIR1
      IF(YY.LE..001) GO TO 302
      L=K+1
      XSIR1(L)=SIR1
301   CONTINUE
302   SIR2=(C6*SIR1/SIDA2+KP*XM2*SR2*GE2+I12)/(C7/SIDA2+KT*SR2)
      XSIIR1(1)=0
```

```
      DO 401 K=1,1000
      W3=(C6*XSIIR1(K)/SIDA2+2*KP*XM2*SIR2*GE2)/
     C(C7/SIDA2+KT*SR2)
      SIIR1=(C7*W3/SIDA1+2*KP*XM1*SIR1*GE1)/(C6/SIDA1+KT*SR1)
      YW=ABS(SIIR1-XSIIR1(K))/SIIR1
      IF(YW.LE..001) GO TO 402
      L=K+1
      XSIIR1(L)=SIIR1
  401 CONTINUE
  402 SIIR2=(C6*SIIR1/SIDA2+2*KP*XM2*SIR2*GE2)/
     C(C7/SIDA2+KT*SR2)
      D1F11=H*F11(DUMMY)
      D1F12=H*F12(DUMMY)
      D1F21=H*F21(DUMMY)
      D1F22=H*F22(DUMMY)
      XK1=XM1+D1F11/2
      XK2=XM2+D1F12/2
      XL1=XS1+D1F21/2
      XL2=XS2+D1F22/2
      D2F11=H*F11(DUMMY)
      D2F12=H*F12(DUMMY)
      D2F21=H*F21(DUMMY)
      D2F22=H*F22(DUMMY)
      XK1=XM1+D2F11/2
      XK2=XM2+D2F12/2
      XL1=XS1+D2F21/2
      XL2=XS2+D2F22/2
      D3F11=H*F11(DUMMY)
      D3F12=H*F12(DUMMY)
      D3F21=H*F21(DUMMY)
      D3F22=H*F22(DUMMY)
      XK1=XM1+D3F11
      XK2=XM2+D3F12
      XL1=XS1+D3F21
      XL2=XS2+D3F22
      D4F11=H*F11(DUMMY)
      D4F12=H*F12(DUMMY)
      D4F21=H*F21(DUMMY)
      D4F22=H*F22(DUMMY)
      DF11=(D1F11+2*D2F11+2*D3F11+D4F11)/6
      DF12=(D1F12+2*D2F12+2*D3F12+D4F12)/6
      DF21=(D1F21+2*D2F21+2*D3F21+D4F21)/6
      DF22=(D1F22+2*D2F22+2*D3F22+D4F22)/6
      C1F31=H*F31(DUMMY)
      C1F32=H*F32(DUMMY)
      C1F41=H*F41(DUMMY)
      C1F42=H*F42(DUMMY)
      C1F51=H*F51(DUMMY)
      C1F52=H*F52(DUMMY)
      XSP1=SP1+C1F31/2
      XSP2=SP2+C1F32/2
      XSIP1=SIP1+C1F41/2
      XSIP2=SIP2+C1F42/2
      XSIIP1=SIIP1+C1F51/2
      XSIIP2=SIIP2+C1F52/2
      C2F31=H*F31(DUMMY)
```

```
C2F32=H*F32(DUMMY)
C2F41=H*F41(DUMMY)
C2F42=H*F42(DUMMY)
C2F51=H*F51(DUMMY)
C2F52=H*F52(DUMMY)
XSP1=SP1+C2F31/2
XSP2=SP2+C2F32/2
XSIP1=SIP1+C2F41/2
XSIP2=SIP2+C2F42/2
XSIIP1=SIIP1+C2F51/2
XSIIP2=SIIP2+C2F52/2
C3F31=H*F31(DUMMY)
C3F32=H*F32(DUMMY)
C3F41=H*F41(DUMMY)
C3F42=H*F42(DUMMY)
C3F51=H*F51(DUMMY)
C3F52=H*F52(DUMMY)
XSP1=SP1+C3F31
XSP2=SP2+C3F32
XSIP1=SIP1+C3F41
XSIP2=SIP2+C3F42
XSIIP1=SIIP1+C3F51
XSIIP2=SIIP2+C3F52
C4F31=H*F31(DUMMY)
C4F32=H*F32(DUMMY)
C4F41=H*F41(DUMMY)
C4F42=H*F42(DUMMY)
C4F51=H*F51(DUMMY)
C4F52=H*F52(DUMMY)
CF31=(C1F31+2*C2F31+2*C3F31+C4F31)/6
CF32=(C1F32+2*C2F32+2*C3F32+C4F32)/6
CF41=(C1F41+2*C2F41+2*C3F41+C4F41)/6
CF42=(C1F42+2*C2F42+2*C3F42+C4F42)/6
CF51=(C1F51+2*C2F51+2*C3F51+C4F51)/6
CF52=(C1F52+2*C2F52+2*C3F52+C4F52)/6
SP1=SP1+CF31
SP2=SP2+CF32
SIP1=SIP1+CF41
SIP2=SIP2+CF42
SIIP1=SIIP1+CF51
SIIP2=SIIP2+CF52
XM1=XM1+DF11
XM2=XM2+DF12
XS1=XS1+DF21
XS2=XS2+DF22
U11=SIP1/SP1
U12=SIP2/SP2
U21=SIIP1/SIP1
U22=SIIP2/SIP2
P1=U21/U11
P2=U22/U12
XC1=(XMO-XM1)/(XMO+E*XM1)
XC2=(XMO-XM2)/(XMO+E*XM2)
XC=(V1*XC1+V2*XC2)/V
T=T+H
```

```
      WRITE(2,103) T,XC1,XC2,U11,U12,U21,U22,P1,P2
  103 FORMAT(' ',F6.0,2X,2(F7.4,2X),4(F7.2,1X),2(F5.2,2X))
      IF(T.GE.TSTOP) GO TO 104
      GO TO 99
  104 STOP
      END
C
C
      FUNCTION F11(DUMMY)
      COMMON KOUNT,KT,KT1,KT2,KP,AS,E,XC1,XC2,XL1,XL2,XK1,XK2,
     CSR1,SR2,SIR1,SIR2,SIIR1,SIIR2,XSP1,XSP2,XSIP1,XSIP2,XC,G,
     CXSIIP1,XSIIP2,SIDA1,SIDA2,IAS1,IAS2,V1,V2,XMO,I11,I12,
     CGE1,GE2,V,XSO
      REAL KT,KT1,KT2,KP,I11,I12,IAS1,IAS2
      F11=XMO*G/V-KP*XK1*SR1*GE1+((1+E*XC2)*XK2-(1+E*XC1)*XK1)
     C/SIDA1-XK1*(1+E*XC)*G/V
      RETURN
      END
C
C
      FUNCTION F12(DUMMY)
      COMMON KOUNT,KT,KT1,KT2,KP,AS,E,XC1,XC2,XL1,XL2,XK1,XK2,
     CSR1,SR2,SIR1,SIR2,SIIR1,SIIR2,XSP1,XSP2,XSIP1,XSIP2,XC,G,
     CXSIIP1,XSIIP2,SIDA1,SIDA2,IAS1,IAS2,V1,V2,XMO,I11,I12,
     CGE1,GE2,V,XSO
      REAL KT,KT1,KT2,KP,I11,I12,IAS1,IAS2
      F12=XMO*G/V-KP*XK2*SR2*GE2+((1+E*XC1)*XK1-(1+E*XC2)*XK2)
     C/SIDA2-XK2*(1+E*XC)*G/V
      RETURN
      END
C
C
      FUNCTION F21(DUMMY)
      COMMON KOUNT,KT,KT1,KT2,KP,AS,E,XC1,XC2,XL1,XL2,XK1,XK2,
     CSR1,SR2,SIR1,SIR2,SIIR1,SIIR2,XSP1,XSP2,XSIP1,XSIP2,XC,G,
     CXSIIP1,XSIIP2,SIDA1,SIDA2,IAS1,IAS2,V1,V2,XMO,I11,I12,
     CGE1,GE2,V,XSO
      REAL KT,KT1,KT2,KP,I11,I12,IAS1,IAS2
      F21=XSO*G/V-AS*IAS1+((1+E*XC2)*XL2-(1+E*XC1)*XL1)/SIDA1
     C-XL1*(1+E*XC)*G/V
      RETURN
      END
C
C
      FUNCTION F22(DUMMY)
      COMMON KOUNT,KT,KT1,KT2,KP,AS,E,XC1,XC2,XL1,XL2,XK1,XK2,
     CSR1,SR2,SIR1,SIR2,SIIR1,SIIR2,XSP1,XSP2,XSIP1,XSIP2,XC,G,
     CXSIIP1,XSIIP2,SIDA1,SIDA2,IAS1,IAS2,V1,V2,XMO,I11,I12,
     CGE1,GE2,V,XSO
      REAL KT,KT1,KT2,KP,I11,I12,IAS1,IAS2
      F22=XSO*G/V-AS*IAS2+((1+E*XC1)*XL1-(1+E*XC2)*XL2)/SIDA2
     C-XL2*(1+E*XC)*G/V
      RETURN
      END
```

```
      FUNCTION F31(DUMMY)
      COMMON KOUNT,KT,KT1,KT2,KP,AS,E,XC1,XC2,XL1,XL2,XK1,XK2,
     CSR1,SR2,SIR1,SIR2,SIIR1,SIIR2,XSP1,XSP2,XSIP1,XSIP2,XC,G,
     CXSIIP1,XSIIP2,SIDA1,SIDA2,IAS1,IAS2,V1,V2,XMO,I11,I12,
     CGE1,GE2,V,XSO
      REAL KT,KT1,KT2,KP,I11,I12,IAS1,IAS2
      F31=.5*KT*SR1**2+((1+E*XC2)*XSP2-(1+E*XC1)*XSP1)/SIDA1
     C-XSP1*(1+E*XC)*G/V
      RETURN
      END
C
C
      FUNCTION F32(DUMMY)
      COMMON KOUNT,KT,KT1,KT2,KP,AS,E,XC1,XC2,XL1,XL2,XK1,XK2,
     CSR1,SR2,SIR1,SIR2,SIIR1,SIIR2,XSP1,XSP2,XSIP1,XSIP2,XC,G,
     CXSIIP1,XSIIP2,SIDA1,SIDA2,IAS1,IAS2,V1,V2,XMO,I11,I12,
     CGE1,GE2,V,XSO
      REAL KT,KT1,KT2,KP,I11,I12,IAS1,IAS2
      F32=.5*KT*SR2**2+((1+E*XC1)*XSP1-(1+E*XC2)*XSP2)/SIDA2
     C-XSP2*(1+E*XC)*G/V
      RETURN
      END
C
C
      FUNCTION F41(DUMMY)
      COMMON KOUNT,KT,KT1,KT2,KP,AS,E,XC1,XC2,XL1,XL2,XK1,XK2,
     CSR1,SR2,SIR1,SIR2,SIIR1,SIIR2,XSP1,XSP2,XSIP1,XSIP2,XC,G,
     CXSIIP1,XSIIP2,SIDA1,SIDA2,IAS1,IAS2,V1,V2,XMO,I11,I12,
     CGE1,GE2,V,XSO
      REAL KT,KT1,KT2,KP,I11,I12,IAS1,IAS2
      F41=KT*SR1*SIR1+((1+E*XC2)*XSIP2-(1+E*XC1)*XSIP1)/SIDA1
     C-XSIP1*(1+E*XC)*G/V
      RETURN
      END
C
C
      FUNCTION F42(DUMMY)
      COMMON KOUNT,KT,KT1,KT2,KP,AS,E,XC1,XC2,XL1,XL2,XK1,XK2,
     CSR1,SR2,SIR1,SIR2,SIIR1,SIIR2,XSP1,XSP2,XSIP1,XSIP2,XC,G,
     CXSIIP1,XSIIP2,SIDA1,SIDA2,IAS1,IAS2,V1,V2,XMO,I11,I12,
     CGE1,GE2,V,XSO
      REAL KT,KT1,KT2,KP,I11,I12,IAS1,IAS2
      F42=KT*SR2*SIR2+((1+E*XC1)*XSIP1-(1+E*XC2)*XSIP2)/SIDA2
     C-XSIP2*(1+E*XC)*G/V
      RETURN
      END
C
C
      FUNCTION F51(DUMMY)
      COMMON KOUNT,KT,KT1,KT2,KP,AS,E,XC1,XC2,XL1,XL2,XK1,XK2,
     CSR1,SR2,SIR1,SIR2,SIIR1,SIIR2,XSP1,XSP2,XSIP1,XSIP2,XC,G,
     CXSIIP1,XSIIP2,SIDA1,SIDA2,IAS1,IAS2,V1,V2,XMO,I11,I12,
     CGE1,GE2,V,XSO
      REAL KT,KT1,KT2,KP,I11,I12,IAS1,IAS2
      F51=KT*SR1*SIIR1+KT*SIR1**2+((1+E*XC2)*XSIIP2
     C-(1+E*XC1)*XSIIP1)/SIDA1-XSIIP1*(1+E*XC)*G/V
      RETURN
      END
```

```
C
C
      FUNCTION F52(DUMMY)
      COMMON KOUNT,KT,KT1,KT2,KP,AS,E,XC1,XC2,XL1,XL2,XK1,XK2,
     CSR1,SR2,SIR1,SIR2,SIIR1,SIIR2,XSP1,XSP2,XSIP1,XSIP2,XC,G,
     CXSIIP1,XSIIP2,SIDA1,SIDA2,IAS1,IAS2,V1,V2,XMO,I11,I12,
     CGE1,GE2,V,XSO
      REAL KT,KT1,KT2,KP,I11,I12,IAS1,IAS2
      F52=KT*SR2*SIIR2+KT*SIR2**2+((1+E*XC1)*XSIIP1
     C-(1+E*XC2)*XSIIP2)/SIDA2-XSIIP2*(1+E*XC)*G/V
      RETURN
      END
```

References

1. Bodenstein, M. and Lutkemeyer, H., Z.phys. Chem. 114 208 (1924)

2. Biesenberger, J.A. and Capinpin, R., J. Appl, Polym. 16, 695 (1972)

3. Billmeyer, F.W., "Textbook of Polymer Science", 2nd Ed., Wiley-Interscience, New York (1970)

4. Rodriguez, F., "Principles of Polymer Systems", 2nd Ed., McGraw-Hill Book Company, Inc., New York (1982)

5. Thomas, D.P. and Hagan, R.S., Polym. Eng. Sci., 9, 164 (1969)

6. Pezzin, G. and Zinelli, G., J. appl. Polym. Sci., 12, 1119 (1968)

7. Ross, S.E., J. Appl. Polym. Sci., 9, 2729 (1965)

8. Sato, M. and Ishizuka, O., Kobunshi Kagaku, 23(259), 799 (1966)

9. Wallach, M.L., Amer. Chem. Soc., Div. Polym. Chem. Preprints, 8(1), 656 (1967); J. Polym. Sci., Part A-2, 6, 953 (1968)

10. Rudd, J.F., J. Polym. Sci., Part B, 1, 1 (1963)

11. Belov, G.P. et. al., Izv. Akad. Nauk SSSR, Ser. Khim., 1275 (1966)

12. Burch, G.N.G., Field, G.B., McTigue, F.H., and Spurlin, H.M., SPE J., 13, 34 (1957)

13. Kojima, H. and Yamaguchi, K., Kobunshi Kagaku, 19, 715 (1962)

14. Williamson, G.R., Wright, B., and Haward, R.N., J. Appl. Chem., 14, 131 (1964)

15. Van Schooten, J., Van Hoorn, H., and Boerma, J., Polymer, 2(2), 161 (1961)

16. Boundy, R.H., and Boyer, R.F., "Styrene, Its Polymers, Copolymers and Derivatives", Reinhold, New York (1952)

17. Scherer, P.C. and McNeer, R.D., Rayon Syn. Text., 31(2), 53 (1950); 31(4), 54 (1950)

18. Spurlin, H.M., Ind. Eng. Chem., 30, 538 (1938)

19. Grohn, H. and Friedrich, H., Plaste Kaut., 14, 795 (1967)

20. Ray, W.H., Ind. Eng. Chem., Proc. Des. & Dev., 7, 74 (1968)

21. Yu, F.C.L., "Periodic operation of a nonisothermal reactor," Master's Thesis, University of Massachusetts (1969)

22. Laurence, R.L. and Vasudevan, G., I.& E. C. Proc. Des. & Dev., 7, 427 (1968)

23. Konopnicki, D. and Kuester, J.L., J. Macromol. Sci. - Chem., A8(5), 887 (1974)

24. Claybaugh, B.E., Griffon, J.R., and Watson, A.T., U.S. Patent 3,472,829 (1969)

25. Bailey, J.E., "Chemical Reactor Theory", Chapter 12, Eds., Lapidus, L. and Amundson, N.R., Prentice Hall, NY (1977)

26. Matsuura, T. and Smith, J.M., A.I.C.H.E. J.,16, 321 (1970)

27. Harada, J., Akehata, T. and Shirai, T., Kagaku Kogaku, 35, 233 (1971)

28. Zolner, W.J., III and Williams, J.A., A.I.C.H.E. J., 17, 502 (1971)

29. Jacob, S.M. and Dranoff, J.M., Chem. Eng. Prog., Symposium Ser., No. 89, 64, 54 (1968)

30. Cerdá, J., Irazoqui, H.A., and Cassano, A.E., A.I.C.H.E. J., 19, 963 (1973)

31. Jain, R.L., Graessley, W.W., and Dranoff, J.S., paper presented at the Third Joint Meeting AICHE and Puerto Rican Inst. Chem. Eng., San Juan (1970)

32. Yemin, L., and Hill, F.B., Ind. Eng. Chem. Fundamentals, 8, 210 (1969)

33. Chen, H.T., and Hill, F.B., AICHE J., 17, 933 (1971)

34. Muller, A.C., Eichacker, J.C., and Hill, F.B., BNL-16455 (1971)

35. Kawakami, W., and Isbin, H.S., AICHE J., 16, 502 (1970)

36. Van Heerden, C., Chem. Eng. Sci., 8, 133 (1958)

37. Nishimura, N., J. Macromolecular Chem., 1(2), 257 (1966)

38. Knorr, R.S. and O'Driscoll, K.F., J. Appl. Polym. Sci., 14, 2863 (1970)

39. Braks, J.G. and Huang, R.Y.M., J. Appl. Polym. Sci., 22, 3111 (1978)

40. Edger, T.D., Hasan, S., and Anthony, R.G., Chem. Eng. Sci., 25, 1463 (1970)

41. Liu, S.L. and Amundson, N.R., Chem. Eng. Sci., 17, 797 (1962)

42. Mendiratta, S.K. and Felder, R.M., AICHE J., 21, 1115 (1975)

43. Hui, A.W. and Hamielec, A.E., J. Appl. Polym. Sci., 16, 749 (1972)

44. Kuan, C.N., "An Experimental Study of Multiple Steady States in a Photopolymerization Reactor", Ph.D Dissertation, New Jersey Inst. of Tech. (1982)

45. Newell, J.E., Anal. Chem., 23, 445 (1951)

46. Parker, C.A., Proc.Roy. Soc.,(London), A220, 104 (1953)

47. Hatchard, C.G. and Parker, C.A., Proc. Roy. Soc., (London), A235, 518 (1956)

48. Marr, G.R., and Johnson, E.F., AICHE J., 9, 383 (1963)

49. Kuester, J.L. and Mize, J.H., "Optimization Techniques with Fortran", McGraw-Hill Book Company, New York (1973)

50. Rosenbrock, H.H., "An Automatic Method for Finding the Greatest or Least Value of a Function", Computer J., 3, 175 (1960)

50. Cozewith, C., J. Appl. Polym.,15, 2855 (1971)

51. Peebles, L.H., "Molecular Weight Distributions in Polymers", Interscience, New York (1971)

52. Gippin, M., Ind. Eng. Chem., Prod. Res. Develop. 1, 32 (1962)